UNIVERSIDAD COMPLUTENSE DE MADRID

FACULTAD DE CIENCIAS QUÍMICAS

Departamento de Química Orgánica I

TESIS DOCTORAL

Development of ligands for the validation of the lysophosphatidic acid receptor LPA_1

Desarrollo de ligandos para la validación del receptor de ácido lisofosfatídico LPA_1

MEMORIA PARA OPTAR AL GRADO DE DOCTOR

PRESENTADA POR

Inés González Gil

Directoras

Mª Luz López Rodríguez
Silvia Ortega Gutiérrez
Henar Vázquez Villa

Madrid, 2014

UNIVERSIDAD COMPLUTENSE DE MADRID

FACULTAD DE CIENCIAS QUÍMICAS

Departamento de Química Orgánica I

DEVELOPMENT OF LIGANDS FOR THE VALIDATION OF THE LYSOPHOSPHATIDIC ACID RECEPTOR LPA_1

DESARROLLO DE LIGANDOS PARA LA VALIDACIÓN DEL RECEPTOR DE ÁCIDO LISOFOSFATÍDICO LPA_1

PhD candidate

Inés González Gil

Advisors:
Dra. Mª Luz López Rodríguez
Dra. Silvia Ortega Gutiérrez
Dra. Henar Vázquez Villa

MADRID, 2014

A mi familia

A. M. D. G.

El presente trabajo ha sido realizado en el laboratorio de Química Médica en el Departamento de Química Orgánica I de la Facultad de Ciencias Químicas de la Universidad Complutense de Madrid, bajo la supervisión de la **Catedrática Dra. Mª Luz López Rodríguez** y las profesoras **Dra. Silvia Ortega Gutiérrez y Dra. Henar Vázquez Villa** a quienes deseo expresar mi más profundo agradecimiento por su acogida en este grupo de investigación, por sus continuas enseñanzas a lo largo de todo este tiempo, y por todo el ánimo, apoyo y confianza depositados en este proyecto.

Asimismo, quiero expresar mi agradecimiento:

Al Profesor Jerold Chun de The Scripps Research Institute por acogerme en su grupo de investigación durante mi estancia predoctoral, y al Dr. Antonio Ferrer Montiel de la Universidad Miguel Hernández de Elche por su inestimable ayuda en la realización de los ensayos biológicos.

Al Profesor Dr. Guillermo Orellana Moraleda, por su admisión en el Departamento de Química Orgánica I de la Universidad Complutense de Madrid y a Soledad Martínez Real y Juan José Redondo Nistal, secretarios del Departamento, por su ayuda a lo largo de estos años.

A mis compañeros de laboratorio, por todos los buenos momentos que hemos pasado. A Ainoa, Ana, Ángel, Ángeles, Bellinda, Carlos, Carolina, Clara, Dani, Dulce, Gloria, Javi, Jorge, Laura, Leticia, Lidia, Mar, Marga, Marta, Moisés, Nagore, Nono, Paco, Raquel, Rocío, Sergio y Tania. A Jose por sus enseñanzas durante el proyecto de fin de carrera y muy especialmente a Debora, por su ayuda y por todo lo que hemos compartido.

A mis amigos, y a mi familia, muy especialmente a mis padres y a Jaime, porque sin su ejemplo y su apoyo jamás habría conseguido llegar hasta aquí.

TABLE OF CONTENTS

ABBREVIATIONS AND ACRONYMS

Throughout this manuscript, abbreviations and acronyms recommended by the American Chemical Society in the Organic Chemistry and Medicinal Chemistry areas have been employed (revised in the *Journal of Organic Chemistry* and *Journal of Medicinal Chemistry* on June 2014; http://pubs.acs.org/page/joceah/submission/authors.html and http://pubs.acs.org/paragonplus/submission/jmcmar/jmcmar_abbreviations.pdf). In addition, those indicated below have also been used.

ATX	Autotaxin
DAPI	4',6-Diamidino-2-phenylindole
DMEM	Dulbecco's modified Eagle medium
EGFP	Enhanced green fluorescent protein
E_{max}	Maximal receptor activation
ESI	Electrospray ionization
FACS	Fluorescence-activated cell sorting
FAF BSA	Fatty acid free bovine serum albumin
FBS	Fetal bovine serum
GPCR	G protein-coupled receptor
IRES	Internal ribosomal entry site
IUPHAR	International Union of Basic and Clinical Pharmacology
LP	Lysophospholipid
LPA	Lysophosphatidic acid
LPAAT	Lysophosphatidic acid acyltransferase
Lpar	LPA receptor mouse gene
LPAR	LPA receptor mammalian gene
LPC	Lysophosphatidylcholine
LPP1	Lipid phosphate phosphohydrolase 1
N.E.	No effect

NAEPA	*N*-acyl ethanolamide phosphoric acid or (2-[(9*Z*)-octadec-9-enoylamino]ethyl dihydrogen phosphate
NPC	Neural progenitor cell
OMPT	1-Oleoyl-2-*O*-methyl-*rac*-glycerophosphothionate or (2*S*)-2-methoxy-3-(thiophosphonooxy)propyl (9*Z*)-octadec-9-enoate
PA	Phosphatidic acid
PG	Protecting group
PS	Polystyrene supported
RA	Rheumatoid arthritis
s.e.m.	Standard error of the mean
S1P	Sphingosine 1-phosphate
SF	Synovial fibroblasts
TBAI	Tetrabutylammonium iodide
UCM	Universidad Complutense de Madrid
VEC	Vascular endothelial cell
VSMC	Vascular smooth muscle cell
VZ	Ventricular zone
vzg-1	Ventricular zone gene 1

1. INTRODUCTION AND OBJECTIVES

Lysophospholipids are lipid molecules that are receiving growing attention because, in addition to their structural function in the cell membrane, they are now regarded as important regulators for diverse biological functions through activation of specific receptors. These receptors have been characterized during the last two decades as G protein-coupled receptors (GPCRs) and, among them, two families stand out: lysophosphatidic acid (LPA_{1-6}) and sphingosine 1-phoshate ($S1P_{1-5}$) receptors. Despite their interest, the high structural similarity between them has restrained the development of selective and high affinity ligands and therefore the elucidation of the role of these receptors in the central nervous system (CNS).

This work will focus on the LPA receptors and, in particular, on the LPA_1 subtype, considering its prominent expression in the CNS and the lack of potent and selective agonists and antagonists that allow for the elucidation of its (patho)physiological roles.

1.1 Phospholipids as signalling molecules

The phospholipid superfamily has been traditionally linked to structural roles, as key constituents of biological membranes. Nevertheless, research from the last decades has associated some phospholipids with diverse signalling functions, reporting their action as extracellular signals and, moreover, their involvement in many physiological and pathological processes.[1,2]

Phospholipids are usually divided into two broad families: (i) glycerophospholipids,[3] which are structurally based on the glycerol scaffold (Figure 1A) and (ii) sphingophospholipids, which are derivatives of the amino alcohol sphingosine (Figure 1B). They present a polar head bearing a phosphate group ($-OPO_3Y^-$, Y = H, choline, ethanolamine…, Figure 1A, B) and two hydrophobic chains (R, X, Figure 1A, B). When one of the fatty acid chains is missing (X = H,

Figure 1A, B), the resulting derivatives are denominated lysophospholipids. These molecules are quantitatively minor lipid species compared to their parent compounds, the phospholipids -which have a major presence in cell membranes- but despite their low concentration they are important because of their ability to signal through GPCRs. Lysophosphatidic acid (LPA, 1-acyl-*sn*-glycerol-3-phosphate, Figure 1C) and sphingosine 1-phosphate[3] (S1P, Figure 1D), are the two most prominent molecules of this family, which are being extensively studied and whose biological activities have been shown to be extremely relevant.[4]

Although they belong to distinct signalling systems, similarities between these two lipids extend to their tissue distribution and concentration, homology and effector pathways of their cognate receptors, and the broad range of their biological roles. In contrast, the actions of other lysophospholipids have not been elucidated to such a high degree and very little is known about their endogenous receptors. However, recent *in vitro* studies suggest that they can induce various and unique cellular responses.[5]

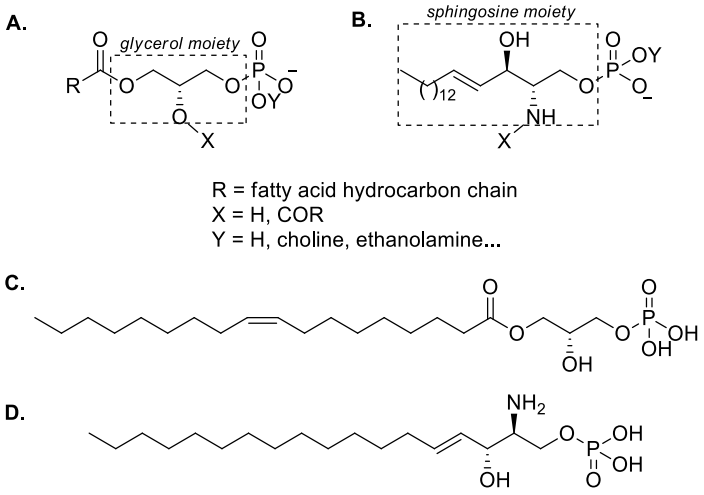

Figure 1. General structure of common glycerophospholipids (A) and sphingophospholipids (B). Structures of LPA (C) and S1P (D).

Among the bioactive phospholipids, LPA stands out as a molecule that elicits a plethora of biological effects, both in the CNS and in the periphery, by acting on at least six different receptors. Nonetheless, its therapeutic potential is still far from being established given the complexity of the system and the lack of specific ligands, agonists and antagonists, that enable the elucidation of the (patho)physiological roles played by a particular LPA subtype.

1.2 Lysophosphatidic acid receptors

LPA has a well-known structural function as precursor and metabolite in the biosynthesis of membrane phospholipids. However, it was not until the 1960s that several groups started to report biological actions mediated by LPA, such as smooth muscle contraction and platelet aggregation.[6] Nevertheless, the specific function of this intriguing molecule was still unknown.

During the mid-1980s, proliferative LPA-dependent effects in fibroblasts were described. These responses were completely inhibited with pertussis toxin pre-treatment, which specifically inactivates $G_{\alpha i/o}$-type G proteins.[7] This was followed by the description in the early 1990s of several morphological cell changes attributed to LPA, such as cell growth, cell rounding/neurite retraction[8,9] and actin stress fiber formation.[10] At the same time, S1P was reported to evoke cellular responses similar to those induced by LPA, suggesting they might even share the same GPCRs.[11]

Growing evidence was making clear that LPA was acting through a GPCR, as it was finally demonstrated by van Blitterswijkin[12] through photoaffinity labeling experiments, which revealed [^{32}P]LPA-binding membrane proteins of 38–40 kDa present in various LPA-responsive cell types and in brain. This binding protein met all the pharmacological criteria for a specific, high-affinity LPA receptor since its labelling was competitively and specifically inhibited by unlabelled LPA with an IC_{50} as low as 10 nM. In addition to the LPA responses, LPA binding was not detectable in LPA-unresponsive cells such as human neutrophils, and was blocked by suramin, a known inhibitor of LPA actions. Although similar evidences were shown independently by Clark,[13] the biophysical properties of LPA or the possibility of second messenger activities were also proposed as alternative mechanisms for LPA actions, and this ambiguity persisted in the absence of molecularly identified receptors.

Finally, in 1996, Chun and coworkers reported the discovery of the first lysophospholipid receptor gene, *ventricular zone gene 1* (*vzg-1*),[14] during their studies on mammalian neurogenesis. *Vzg-1* encoded a GPCR that had the properties of a high-affinity LPA receptor. Identification of this gene as encoding a LPA receptor was independently demonstrated by Goetzl[15] and Kiefer.[16] Definitive confirmation about the identity of this receptor was achieved by heterologous expression in mammalian cells[17] and genetic deletion of the receptor.[18]

Similar approaches allowed the identification of new receptors, like the first receptor for S1P, which was independently reported by two groups in 1998.[19,20]

Since then, several members of the orphan GPCR receptor family called "endothelial differentiation genes" (Edg) were identified as GPCRs for both LPA and S1P, including Edg4 (LPA_2),[21,22] Edg7 (LPA_3),[23] Edg5 ($S1P_2$), Edg3 ($S1P_3$), Edg6 ($S1P_4$)[24] and Edg8 ($S1P_5$).[25] Regarding the LPA receptors, another group of less similar GPCR genes have also been identified, which are GPR23 (LPA_4),[26,27] GPR92 (LPA_5),[28,29] and P2Y5 (LPA_6).[30,31] This latter group is more closely related to the family of P2Y purinergic receptor genes, indicating that LPA receptors have evolved via two distinct lineages in the rhodopsin GPCR family. Up to date, a total of eleven receptors have been described, six for LPA (LPA_{1-6}) and five for S1P ($S1P_{1-5}$). The current nomenclature includes the cognate ligand and the chronological order of identification. All LPA receptors are type I, rhodopsin-like GPCRs that differ in their tissue distribution and downstream signalling pathways[32] (see Table 1, page 9, for a summary of some relevant features).

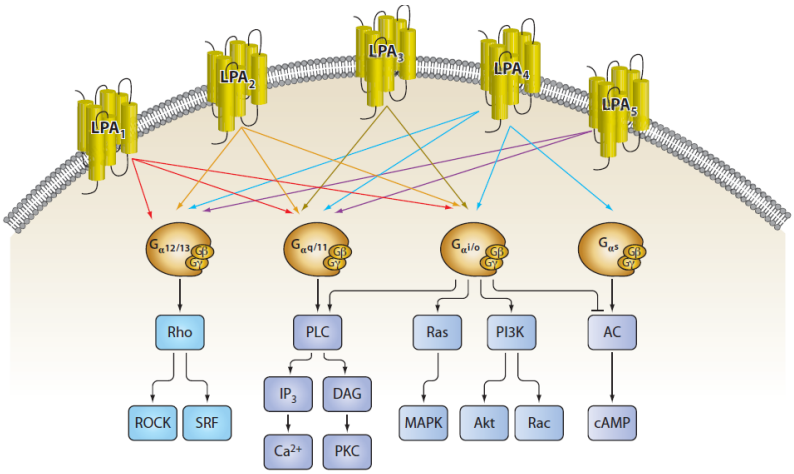

Figure 2. Schematic representation of the signalling pathways activated by the LPA_{1-5} receptors (Source: *Annu. Rev. Pharmacol. Toxicol*. **2010**, *50*, 157–186).

1.2.1 LPA_1 receptor

The mammalian *LPAR1* gene encodes an approximately 41 kDa protein consisting of 364 amino acids with seven putative transmembrane domains.

Human *LPAR1* is widely expressed in heart, brain, placenta, skeletal muscle, kidney, pancreas, spleen, prostate, testis, ovary, small intestine and colon.[33] Similar distribution is observed for the *Lpar1* mouse gene, although it is more spatially restricted during embryogenesis, where it is mainly found in the ventricular zone (VZ), a major site for neuroprogenitor cell proliferation during prenatal

developmental stages. VZ disappears prior to birth, reappearing during postnatal life within oligodendrocytes and Schwann cells that may influence myelination in central and peripheral nervous system, indicating roles for LPA signalling in cortical development.[34]

Signalling through LPA_1 receptor induces a range of cellular responses: cell proliferation and survival, cell migration and cytoskeletal changes. At the molecular level, LPA_1 receptor activation can be transduced through three types of G proteins: $G_{\alpha i/o}$, $G_{\alpha q/11}$, and $G_{\alpha 12/13}$, that are responsible of Ca^{2+} mobilization, adenylyl cyclase inhibition and activation of phospholipase C, Akt, Rho and mitogen-activated protein kinase pathways.

The targeted disruption of *Lpar1* in mice revealed unanticipated *in vivo* functions of this receptor. *Lpar1−/−* mice show 50% perinatal lethality and survivors have a reduced body size, craniofacial dysmorphism, and increased apoptosis in sciatic nerve Schwann cells.[18]

1.2.2 LPA_2 receptor

Lpar2 was identified in 1998 from GenBank searches of orphan GPCR genes because of its ~60% amino acid similarity to *Lpar1*. In humans, *LPAR2* encodes a protein that has a predicted amino acid sequence of 348 residues, with a calculated molecular mass of ~39 kDa.[21] The expression pattern of LPA_2 receptor is more spatiotemporally restricted compared to LPA_1 receptor. *Lpar2* is found in the embryonic brain, but its expression strongly attenuates one week after birth. In humans, *LPAR2* is found in testis, leukocytes, prostate, spleen, thymus and pancreas.[32] LPA_2 couples to three G proteins, $G_{\alpha i/o}$, $G_{\alpha q/11}$, and $G_{\alpha 12/13}$.

LPA_2 null mice were born normally and showed no obvious behavioural, anatomical or histological abnormalities, in contrast with LPA_1 null mice.[35] When LPA_1/LPA_2 double-null mice were generated, an aggravation of the phenotypic abnormalities was expected, as LPA_2 is coexpressed with LPA_1 in several organs and cells and thus a major loss of LPA signalling would be achieved. However, no qualitative differences in phenotypes, compared to LPA_1 null mice, were observed. Thus, LPA_1 and LPA_2 receptors may have redundant functions in LPA signalling.

1.2.3 LPA_3 receptor

LPAR3 encodes a ~40-kDa GPCR that is ~50% identical to mouse LPA_1 and LPA_2 in amino acid sequence. Expression of *LPAR3* is broad and has been observed in human heart, testis, prostate, pancreas, lung, ovary, and brain. Like

LPA_1 and LPA_2 receptors, LPA_3 can couple with $G_{\alpha i/o}$ and $G_{\alpha q/11}$ to mediate LPA-induced Ca^{2+} mobilization, adenylyl cyclase inhibition, and phospholipase C and mitogen activated protein kinase activation. Additionally, LPA_3 has a strong preference for unsaturated chains and has a relatively high affinity for 2-acyl-LPA containing unsaturated fatty acids.

Despite the fact that LPA_3 is expressed in the frontal cortex, hippocampus, and amygdala, no phenotypes related to LPA_3 loss in the nervous system have been reported to date.

1.2.4 LPA_4 receptor

LPA_4 receptor was cloned as an orphan GPCR and was found to be a specific receptor for LPA through ligand screening. LPA_4 is structurally distinct from classical LPA_{1-3} and S1P receptors that share significant homology, and is more closely related to P2Y purinergic receptors. It does not, however, respond to any nucleotide or nucleoside tested. In humans, the *LPAR4* gene encodes 370 amino acids with a calculated molecular mass of ~42 kDa. LPA_4 is ubiquitously expressed in both humans and mice and it is specifically abundant in the ovary. Its activation induces intracellular cAMP accumulation via $G_{\alpha s}$, and Ca^{2+} mobilization through $G_{\alpha q/11}$ and $G_{\alpha i/o}$.

1.2.5 LPA_5 receptor

LPA_5 (GPR92) was identified by two independent groups in 2005 from the receptor gene data bank. This receptor is structurally different to LPA_{1-3}, but shares 35% homology with LPA_4. *Lpar5* is relatively broadly expressed in murine tissues. In humans, gene expression for LPA_5 is observed in spleen, heart, small intestine, placenta, liver and colon. LPA_5 couples to $G_{\alpha 12/13}$ and to $G_{\alpha q/11}$.

1.2.6 LPA_6 receptor

The orphan receptor P2Y5, closely related to the purinergic family and sharing high homology with LPA_4 receptor, has been recently classified as the LPA_6 receptor.[31] This receptor has been found to be essential for the maintenance of hair growth.[36]

1.2.7 Other proposed receptors

GPR87 and P2Y10 are orphan GPCRs that have been described to be responsive either to LPA or to both LPA and S1P, respectively. They belong to the P2Y family and are similar to LPA_4 and LPA_5 receptors.[37]

Table 1. Summary of the most relevant LPA receptor features

IUPHAR nomenclature[a]	Gene symbol (human)	Chromosomal location (human)	Number of aminoacids (human)	Calc. mass (kDa)	Similarity to LPA_1 (%)
LPA_1	*LPAR1*	9q31.3	364	41	
LPA_2	*LPAR2*	19p12	348	39	60
LPA_3	*LPAR3*	1p22.3 p31.1	353	40	50
LPA_4	*LPAR4*	Xq13–q21.1	370	42	10
LPA_5	*LPAR5*	12p 13.31	372	41	12
LPA_6	*LPAR6*	13q14	344	39	13

[a]IUPHAR: International Union of Basic and Clinical Pharmacology

From all LPA actions, the ones elicited through LPA_{1-3} receptors have been the most studied up to date, revealing crucial roles in the nervous, vascular, immune and reproductive systems. Focusing on the CNS, LPA_1 is described as the receptor with a major expression and, even though the information is very scarce, there is evidence enough to suggest that it can contribute to the pathogenesis of several diseases and, accordingly, could be endowed with therapeutic relevance for the treatment of CNS disorders.

1.2.8 Lysophosphatidic acid receptor structure

Currently, no crystal structures have been resolved for any native LPA receptor. The only phospholipid GPCR crystal structure available is the structure of $S1P_1$,[38] which has provided valuable information about the receptor-ligand interaction of this type of receptors.[39] This is especially useful for molecular modelling of LPA receptors, because they share much higher sequence homology with this receptor than with any of the other currently available GPCR crystal structures, fact that will enable the construction of homology models of LPA_{1-3} receptors using the structure of $S1P_1$ receptor as template.[40]

Mutagenesis studies combined with computational analysis identified several important residues in $LPA_{1–3}$ receptors, most of them located in transmembrane domains.[41,42] In this regard, Arg3.28 is important for efficacy and potency for all three receptors, as it forms a salt bridge with the phosphate group while Gln3.29 interacts with the hydroxy group of LPA. Thus, this latter position is responsible of LPA/S1P selectivity, as S1P receptors bear a glutamic acid instead. These two residues are conserved over the $LPA_{1–3}$ receptors, together with Trp4.64, which, in

contrast, is only implicated in LPA_3 activation. Other aminoacids important for ligand recognition and selectivity among the $LPA_{1–3}$ and S1P receptors are found in positions 5.38 (Asp in LPA_1) and 7.36 (Lys in LPA_1), though their function is still not clear. LPA_4 and LPA_5 share less amino acid identity with $LPA_{1–3}$, and detailed models of their interaction with LPA are not available. Most of the residues described above are not present in LPA_4 and LPA_5, suggesting that these receptors have different ligand binding characteristics. Further research is needed to identify the critical residues for these receptors, and this information will need to be re-evaluated once crystal structure data become available.[43]

1.3 Biosynthesis and degradation of LPA

LPA is generally known as a mixture of various lysophospholipids with both saturated (16:0, 18:0) and unsaturated (16:1, 18:1, 18:2, 20:4) fatty acid chains. It must be noted that in the context of LPA as a signalling molecule, and thus throughout this work, LPA refers to 1-oleoyl-s*n*-glycerol-3-phosphate.

LPA is found in almost all eukaryotic tissues and biological fluids, including blood.[32] Among them, serum is the best characterized source of LPA, where it is bound to albumin and other proteins, probably preventing the molecule from rapid degradation.[44]

Autotaxin (ATX),[45,46] a secreted glycoprotein with lysophospholipase D activity, is the primary enzyme responsible for LPA production in blood. In fact, ATX heterozygote knocknout mice have a 50% reduction of circulating LPA compared to wild type mice[47] and negligible levels of LPA are detected after treatment with ATX inhibitors.[48] Outside the cell, the enzyme ATX converts lysophosphatidylcholine (LPC), produced from different membrane phospholipids, into LPA (Figure 3).

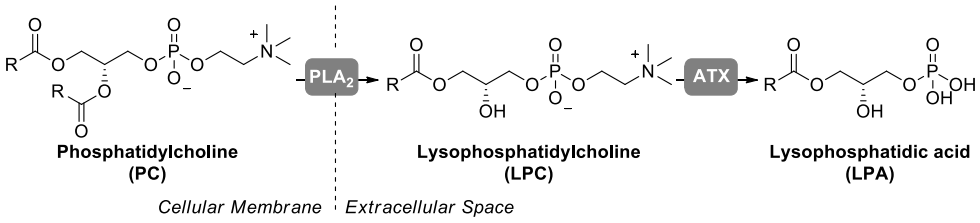

Figure 3. Pathway for LPA production.

Degradation of LPA can occur through two main routes. In the first one, LPA is irreversibly dephosphorylated to monacylglycerol by lipid phosphate phosphohydrolases, presumably LPP1. In the second route, LPA is reversibly esterified to phosphatidic acid (PA) by the enzyme LPA-acyltransferase (LPAAT).[49]

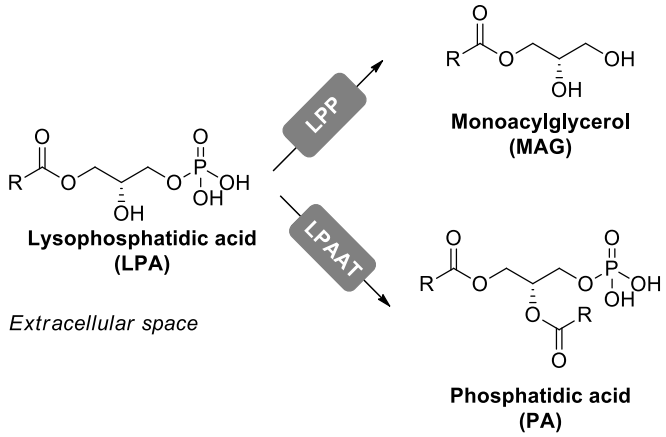

Figure 4. LPA degradation pathways.

1.4 Physiological roles of LPA_1 receptor and therapeutic potential

LPA displays a wide range of cellular effects through its receptors. Among the most important actions of LPA, those mediated by the LPA_1 receptor in the CNS stand out, fact that immediately suggests a potential for the treatment of related diseases.

1.4.1 Nervous system

As highlighted before, the nervous system is one of the major locations for LPA receptors,[34] as they are expressed in most of its cell types in physiological and pathological conditions. In addition, LPA can be found in the brain in high concentrations, influencing many developmental processes and neurological disorders.

Among the different LPA receptors, the LPA_1 subtype is the most abundant one in brain,[32] where it plays a major role in the development of the embryonic brain and thus in neurogenesis, due to its main expression in the VZ of the embryonic brain. Neural progenitor cells (NPCs) -the differentiable cells responsible for neurogenesis- express LPA_{1-3} receptors and are found in this area,

where they proliferate and sequentially differentiate into various cell types, such as neurons, astrocytes or oligodendrocytes.

Several *in vitro* and *in vivo* studies have demonstrated that LPA controls proliferation and differentiation of NPCs via LPA_1. Furthermore, LPA_1 null NPCs do not present the ability to achieve LPA-dependent neurogenesis-related changes, confirming LPA_1 as a modulator of neurogenesis. In adult neurons, LPA is known to influence neuronal survival/death processes. Moreover, it has been described that LPA_1 is related with neuroprotection, as apoptotic cell death is described in LPA_1 null mouse brains.[34]

Neuropsychiatric disorders, like schizophrenia, anxiety, memory impairment or Alzheimer's disease, have been recently linked to LPA signalling. LPA_1 null mutants share schizophrenia-type defects, such as pre-pulse inhibition, serotonin synthesis alteration or cranial dysmorphism. In addition, LPA signalling through LPA_1 in the hippocampus modulates neurogenesis, which is related with learning and emotional behaviour; and memory impairments have been reported in LPA_1 deficient mice.[34]

Two important developmental disorders are linked to LPA_1 receptor: fetal hypoxia and fetal hydrocephalus. It was shown that mouse brains exposed to LPA develop fetal hydrocephalus, and that treatment with a LPA_1 antagonist blocked this response, demonstrating the implication of the receptor.[50] Regarding fetal hypoxia, it has been described that the absence of the adequate supply of oxigen causes cortical disorganization throughout NPCs via overactivation of LPA_1 receptor.[51] Since both diseases are associated with latter development of CNS disorders, such as epilepsy, schizophrenia or autism, it is clear that LPA_1 signalling needs to be tightly regulated to ensure unaltered brain functions.

LPA_1 has also been associated with myelination because its expression in oligodendrocytes (CNS myelinating cells) correlates spatiotemporally with their maturation and myelination, and it has been shown that LPA influences several of its cellular responses. Moreover, in the peripheral nervous system (PNS) a recent study has shown that LPA, acting through LPA_1 receptor, promotes Schwann cell migration, which precedes myelination and remyelination in the PNS.[52]

It has been suggested that LPA plays a key role in the initiation of neuropathic pain, a form of chronic pain which accounts for almost the 20% of its diagnosed cases in the U.S. Neuropathic pain is the result of a combination of multiple factors, but a direct link with fiber demyelination has been reported.[53] LPA produces nerve injury via LPA_1-mediated demyelination with subsequent loss of the structural and

functional integrity of neurons. In further support of this, LPA_1 deficient mice do not show neuropathic pain behaviour or demyelination in response to intrathecal LPA injection or nerve injury. LPA_5 null mice are also protected from developing neurophatic pain, although the mechanisms involved are different to those mediated by LPA_1.[54]

1.4.2 Peripheral roles for LPA_1 receptor

The main peripheral roles of LPA characterized so far are related with the ability of this molecule to influence cellular proliferation and differentiation in several tissues and systems. In this regard, LPA performs an important role in the vascular system, where it modulates different effects in vascular smooth muscle cells (VSMCs) and vascular endothelial cells (VECs), which are involved in processes like angiogenesis (the formation of new capillary networks from pre-existing vasculature by sprouting and/or splitting of capillaries) or vascular maturation. Angiogenesis involves coordinated proliferation, migration, adhesion, differentiation, and assembly of both VECs and their surrounding VSMCs, and its dysregulation can lead to diverse pathological conditions, such as atherosclerosis,[55] cardiovascular diseases, or development of tumours.

Similarly, and related with the ability of LPA to promote cell proliferation, the LPA_1 receptor is gaining attention as a druggable target for fibrosis.[56,57] This disease consists in the formation of excessive connective tissue, and it has been found to be strongly influenced by receptor-mediated LPA signalling in lung, kidney and skin. Hence, increased epithelial cell apoptosis, migration and proliferation of lung fibroblasts, together with enhanced fibroblast resistance to apoptosis are LPA_1-mediated processes directly linked with the development of pulmonary, dermal and kidney fibrosis. In addition, results obtained with a dual LPA_1/LPA_3 antagonist suggests a possible implication of LPA_3 receptor. Supporting these data, one LPA_1 antagonist is currently in phase II clinical trials for idiopathic pulmonary fibrosis[58] and another one is still in preclinical stages, indicated for the treatment of liver, lung and kidney fibrosis.[59]

Recent research has also associated LPA_1 receptor with the initiation and development of rheumatoid arthritis (RA). It is known that synovial fibroblasts (SFs), implicated in the beginning and perpetuation of RA, express all LPA receptors and that LPA stimulates proliferation, adhesion and migration of SFs. Accordingly, LPA_1 receptor has been suggested as a possible therapeutic target in the treatment of this disease.[60,61]

LPA_1 is also the most widely expressed lysophospholipid receptor in adipose tissue, fact that makes it an interesting pharmacological target for the treatment of obesity-associated metabolic diseases. Obesity, one of the key factors leading to type II diabetes, is accompanied by an increased ATX-mediated synthesis of LPA by adipocytes, where LPA exerts different biological actions through the activation of LPA_1 receptor.[62]

Finally, it is well known that LPA signalling influences cancer-related processes,[63] especially via LPA_2. Nevertheless, there is also evidence of LPA_1 implication in cancer progression, specifically in ovarian, breast and gastrointestinal ones.

1.5 LPA_1 receptor ligands

Given the importance of LPA_1 receptor in a variety of pathologies, the need of potent and selective ligands is crucial to unravel its potential as a therapeutic target, but up to this moment there are no drugs in the market targeting any of the LPA receptors. The only commercialized drug targeting a lysophospholipid receptor is Fingolimod, (**1**, Gilenya®), a non-selective S1P antagonist approved for the treatment of multiple sclerosis.[64]

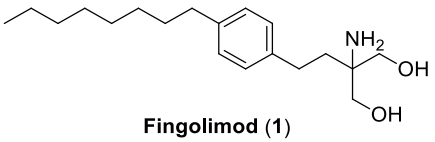

Fingolimod (**1**)

Although much research is ongoing in this field, the lack of potent and selective ligands is still an issue. Lipid-ressembling molecules encounter solubility problems and show very high protein binding with only a small percentage within plasma available to interact with receptors. Moreover, the abundant cell surface lipid phosphate phosphohydrolases may rapidly degrade them. Regarding non-lipid structures, some advances have been done in the field of antagonists, as two of them have currently reached clinical trials.[58,65,66] Still, small molecule agonists structurally different from LPA have not been described yet.

1.5.1 Agonists of LPA_1 receptor

Detailed studies have been carried out on the search for the essential patterns required to obtain selective agonism at the LPA_1 receptor.[40] The information available so far comes from LPA analogues, as no structurally different synthetic agonists have been described yet.

The first LPA-based agonist was *N*-acyl ethanolamide phosphoric acid (2-[(9*Z*)-octadec-9-enoylamino]ethyl dihydrogen phosphate or NAEPA, **2**) described by Sugiura in 1994[67] as a LPA mimetic and later confirmed as a dual LPA_1/LPA_2 agonist.[68] Several changes in its structure have led to ligands with improved activity and, in some cases, selectivity over LPA_1 receptor. Initial modifications included the introduction of different substituents in the β-carbon atom (Figure 5, left panel) and revealed a strong enantiomer preference, as well as a decrease in agonist potency when bulky substituents were introduced. Among all the synthesized compounds, **3**, **4** and **5** stand out as potent dual LPA_1/LPA_3 agonists, with stronger preference for LPA_1 and activity values similar to LPA [EC_{50} (LPA_1) = 7.9, 4.9 and 3.4 nM; EC_{50} (LPA_3) = 321.8, 683.7 and 112.6 nM, respectively].[69]

Further replacements of the phosphate group by its mimetics thiophosphate (Y = S, Z = O, Figure 5), and the metabolically stabilized phosphorothioate (Y = O, Z = S, Figure 5) and phosphonate groups (Y = C, Z = O, Figure 5) were carried out. These groups, especially phosphonates, had higher pK_a values than LPA, so α-substituted phosphonate groups with electronegative groups at the *α*- carbon were also prepared in order to maintain acidity (Figure 5, right panel). Amid them, selective compounds **7** [EC_{50} (LPA_1) = 318 nM] and **8** [EC_{50} (LPA_1) = 221 nM] kept an activity similar to NAEPA at the LPA_1 receptor (EC_{50} = 197 nM), and compound **6** [EC_{50} (LPA_1) = 40 nM; EC_{50} (LPA_2) = 108 nM] improved it. It must be noted that analogue **9**, bearing a *α*-fluorophosphonate moiety, more acid than compound **6**, was inactive at LPA_1 receptor, indicating that acidity is not the only requirement for receptor activation when modifying the phosphate moiety.[70] In fact, also LPA-derived phosphonates and analogues bearing fluoro or difluoro moieties in the *α*-carbon have led to good LPA_2 or LPA_3 agonists, but are inactive at LPA_1.[71]

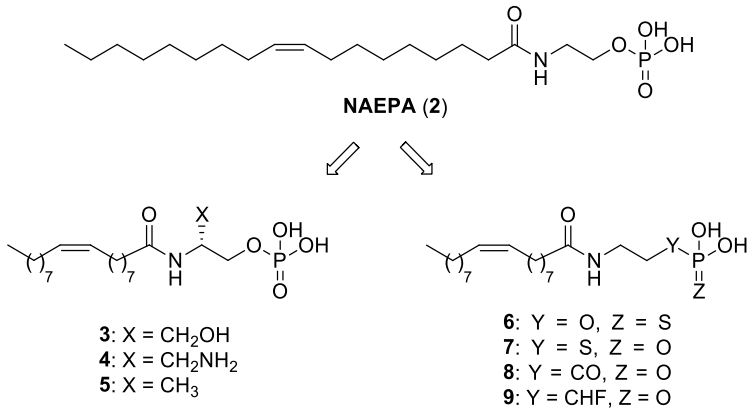

Figure 5. Structure of NAEPA and derivatives.

The LPA analogue (2*S*)-2-methoxy-3-(thiophosphonooxy)propyl (9*Z*)-octadec-9-enoate or OMPT (**10**), was one of the first LPA_3 selective agonists with an EC_{50} value of 276 nM.[72] Its modification led to diverse structures, such as the enantiomers **11** [EC_{50} (LPA_1) = 790 nM; EC_{50} (LPA_3) = 62 nM] and **12** [EC_{50} (LPA_1) = 571 nM; EC_{50} (LPA_3) = 80 nM], which turned out to be good LPA_3 agonists but also present modest activity at LPA_1.[73] In order to prevent acyl chain migration, other metabolically stabilizing modifications were carried out, leading to phosphorothioate analogues of *sn*-2 LPA (compounds **13**-**15**). These three compounds displayed weak LPA_1 agonism, but they stand out as potent LPA_3, LPA_5 and LPA_6 agonists.[74]

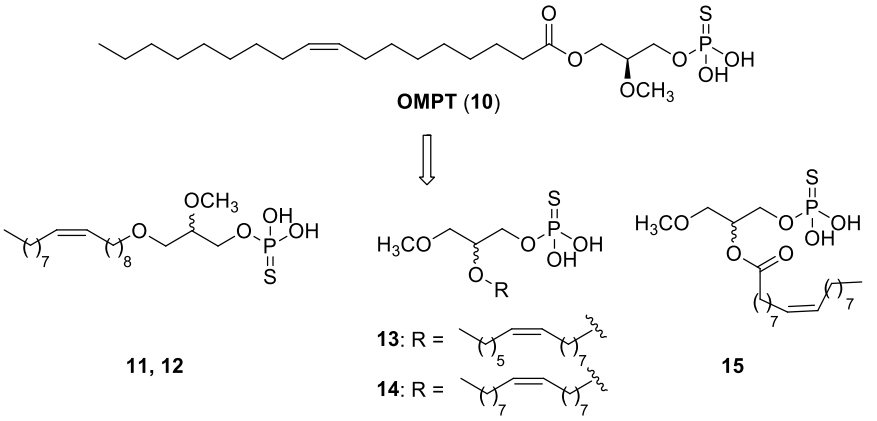

Figure 6. OMPT and derivatives.

The influence of the position of the acyl chain has been also studied. For example, *sn-2* LPA derivatives resistant to acyl migration such as 1,1-difluorinated phosphates,[75] difluoromethyl phosphates[76] or *α*-fluorinated phosphonates[77] were synthesized. Unfortunately, none of these compounds was active at the LPA_1 receptor,[71] though LPA_1 and LPA_2 receptors were reported to show no regioisomeric preference between *sn*-1 and *sn*-2 positions.

Cyclic phosphate analogues have also been described as LPA_1 agonists. The cyclic difluorophosphate **16** was reported as a weak $LPA_{1\text{-}3}$ agonist [EC_{50} (LPA_1) > 1940 nM; EC_{50} (LPA_2) > 9460 nM; EC_{50} (LPA_3) > 7030 nM].[78] In addition, some acetal phosphatidates, also known as Darmstoff analogues, have been reported as LPA mimetics. Some of these compounds are LPA pan-agonists (**17**-**20**), though with activity in the low micromolar range at LPA_1 receptor.[79] Again, small structural modifications turn the compounds into antagonists.

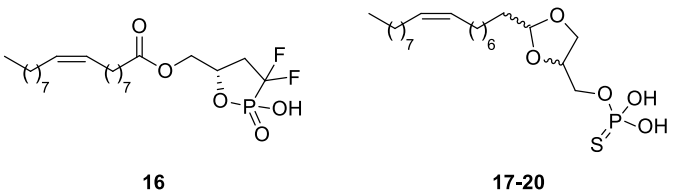

16 **17-20**

Figure 7. Structure of cyclic phosphate agonists.

In summary, around 20 years after the discovery of the first LPA_1 ligands, there is still a lack of potent and selective agonists. Nowadays, the knowledge about the features needed for activity has been somehow disclosed, but even though, the complete puzzle of the structural requirements for activating this receptor is not yet fully understood.

1.5.2 Antagonists of LPA_1 receptor

The LPA_1 antagonist field is a current focus of pharmaceutical companies. Structurally, LPA_1 antagonists can be classified into two broad classes: a family closely related with LPA and a second group formed by compounds whose structures widely differ from LPA.

Starting with LPA analogues, modification of the agonist NAEPA (**2**, page 15) with a bulky substituent in the β-carbon atom led to compound **21**, which turned out to be a dual $LPA_{1/3}$ antagonist [IC_{50} (LPA_1) = 5210 nM; IC_{50} (LPA_3) = 6450 nM],[69] and has been used *in vivo* in a model of lung fibrosis.[80] An exhaustive SAR of this structure yielded compounds **22**, a selective LPA_1 ligand with moderate activity [IC_{50} (LPA_1) = 2490 nM] and **23**, which showed increased potency [IC_{50} (LPA_1) = 109 nM; IC_{50} (LPA_3) = 175 nM] and which is five times more active than its (*S*)-enantiomer.[81] Further optimizations led to **24**, a dual $LPA_{1/3}$ antagonist with nanomolar potency [IC_{50} (LPA_1) = 84 nM; IC_{50} (LPA_3) = 48 nM].[82]

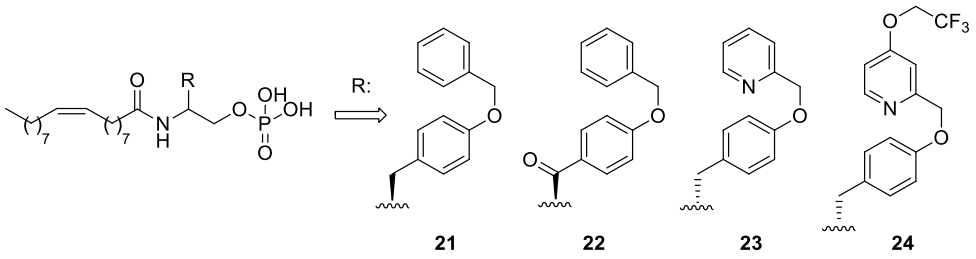

21 **22** **23** **24**

Figure 8. Structure of NAEPA-derived antagonists.

Another important LPA analogue is the bromophosphonate **25**, also known as BrP-LPA, a LPA pan-antagonist [IC_{50} (LPA_1) = 1500 nM; IC_{50} (LPA_2) = 1420 nM; IC_{50} (LPA_3) = 1160 nM; IC_{50} (LPA_4) = 266 nM] and ATX inhibitor with *in vivo* activity.[83] This molecule has contributed to elucidate the involvement of LPA receptors in the inhibition of tumour growth[84] and in the attenuation of arthritis in animal models.[85]

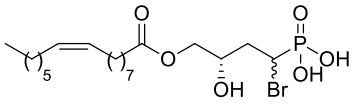

25

Figure 9. Structure of the pan-antagonist bromophosphonate BrP-LPA (**25**).

Cyclic LPA derivatives have also been described as LPA_1 antagonists. Compound **26** and cyclic phosphorothioates **27** and **28** show activity as partial LPA_1/LPA_3 antagonists with moderate potencies [IC_{50} (LPA_1) = 106-941 nM; IC_{50} (LPA_3) = 1270-7720 nM].[78]

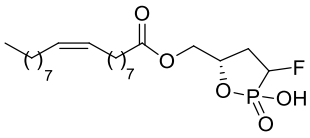

26

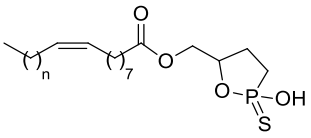

27: n = 7
28: n = 5

Figure 10. Structure of cyclic phosphate antagonists.

Overall, these series of compounds show the difficulty of discovering the requirements needed to regulate the pharmacology of LPA-derived ligands, as subtle changes in their structures convert agonists into antagonists and cause drastic changes in activity. In addition, the coexistence of a polar head and a long hydrophobic tail becomes a problem in order to obtain orally active compounds. Thus, high-throughput screening was used to discover novel hits, structurally different from LPA, followed by hit to lead processes to improve their pharmacology.

The first reported non-lipid dual $LPA_{1/3}$ antagonist was compound **29** (Ki16425)[86] [IC_{50} (LPA_1) = 130 nM; IC_{50} (LPA_3) = 2300 nM] which has been widely used as a tool compound as it displays *in vivo* activity.[50,61] Several modifications of its structure by different academic groups and pharmaceutical companies have led

to more potent and selective compounds, some of them even achieving clinical trials.

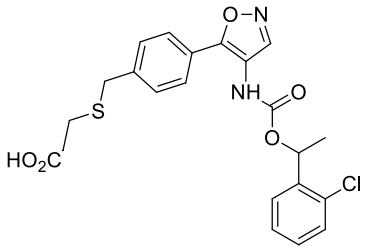

Ki16425 (**29**)

Based on this scaffold, Amira Pharmaceuticals (currently Bristol-Myers Squibb) developed a series of isoxazole derivatives. Among them, compounds **30** (AM966),[87] [IC_{50} (LPA_1) = 17 nM; IC_{50} (LPA_2) = 1700 nM; IC_{50} (LPA_3) = 1600 nM] and **31** (AM095)[88,89] [IC_{50} (LPA_1) = 25 nM; IC_{50} ($LPA_{2\text{-}5}$) > 8000 nM] stand out as potent LPA_1 antagonists with good oral bioavailability and antifibrotic *in vivo* activity. Moreover, a compound coming from this series, BMS-986020, whose structure has not been disclosed yet, is currently facing phase II trials for the treatment of idiopathic pulmonary fibrosis.[58]

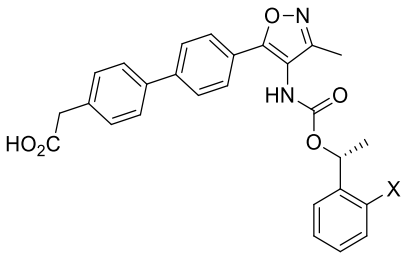

X = Cl: **AM966** (**30**)
X = H: **AM095** (**31**)

Figure 11. Isoxazole LPA_1 receptor antagonists developed by Amira Pharmaceuticals.

Hoffman-La Roche's modifications of Ki16425 involved changes in the carboxylic acid and the heterocyclic core, replacing the isoxazole moiety with pyrazole and triazole rings. The best compounds were **32**, with low nanomolar activity and good selectivity values [IC_{50} (LPA_1) = 25 nM; IC_{50} (LPA_3) > 30000 nM], and **33**, a dual LPA_1/LPA_3 antagonist [IC_{50} (LPA_1) = 24 nM; IC_{50} (LPA_3) = 65 nM].[90]

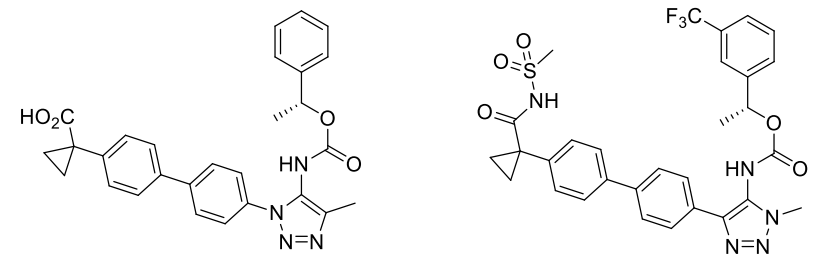

32 **33**

Figure 12. Triazole LPA_1 receptor antagonists developed by Hoffman-La Roche.

Further exploration of the central heterocycle ring by other pharmaceutical companies has led to potent antagonists of the LPA_1 receptor, with IC_{50} values in the low nanomolar range, such as compound **34**, which is a selective LPA_1 receptor antagonist [IC_{50} (LPA_1) < 50 nM; IC_{50} (LPA_3) > 500 nM).[91] Introduction of different sulfonamide groups led to LPA_1 antagonists with activities in the low nanomolar scale.[92,93] For example, compound **35** is a LPA_1 antagonist with an IC_{50} value of 6.6 nM.

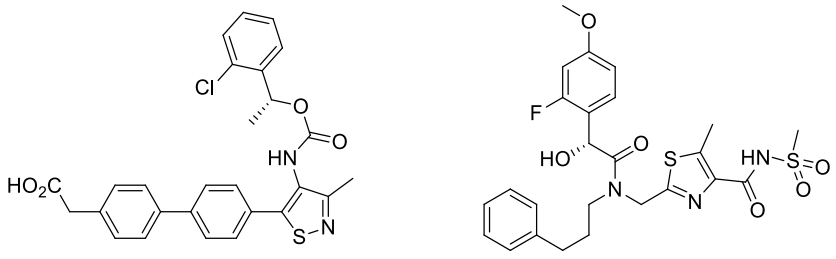

34 **35**

Figure 13. Thiazole LPA_1 receptor antagonists.

Initially inspired by Ki16425, Sanofi-Aventis synthesized a series of non-natural aminoacids, such as compound **36**, with IC_{50} values lower than 100 nM. It must be highlighted that SAR100842 (structure not yet disclosed), is a LPA_1/LPA_3 antagonist from this set of compounds which is currently undergoing phase II clinical trials for systemic sclerosis.[66]

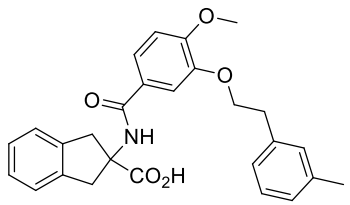

36

Figure 14. Sanofi-Aventis antagonist.

In conclusion, it is clear that LPA_1 receptor has an outstanding but yet intriguing role in physiological and pathological conditions. Thus, the discovery of potent and selective agonists and antagonists is nowadays a crucial need to achieve the validation of this receptor as a therapeutic target, which is the main goal of the present work.

This overall objective involves the following steps:

1. Design and synthesis of new ligands for the LPA_1 receptor
2. Determination of the capacity of the compounds to activate the LPA_1 receptor
3. Evaluation of LPA_1 receptor antagonism
4. Study of the selectivity of the synthesized compounds in the LPA receptor family
5. Biological evaluation of selected compound(s)

RESULTS AND DISCUSSION

2. RESULTS AND DISCUSSION

2.1 Design and synthesis of new ligands for the LPA_1 receptor

LPA receptors were discovered less than two decades ago. Thus, at the moment of starting this project, little information about this novel signalling system was available. No receptor 3D structures had been elucidated and, although several structure-activity relationship (SAR) studies had been carried out, no potent ligands for the LPA_1 receptor had been described, especially in the agonist field. In this context, we focused our efforts on finding molecular entities with activity at this receptor, using as starting point the structure of the endogenous ligand, LPA. Initially, two series of compounds were designed: series **I**, which comprised changes in the acid group, and series **II**, which included modifications in the hydrophobic unit (Figure 15).

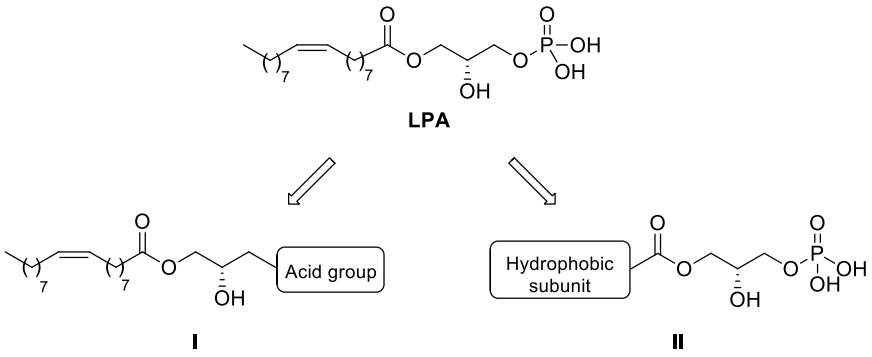

Figure 15. Design of new LPA_1 ligands.

*2.1.1 Design and synthesis of series **I***

Several SAR studies[40] suggest that changes in the polar head of LPA are poorly tolerated. In particular, it has been shown that an important requirement for activity is the presence of free acid groups that retain their negative charge under physiological conditions.[94] In fact, when the phosphate group has been modified in LPA-like structures, it has usually led to a decrease in LPA_1 activity of agonists. This is confirmed by the few potent agonists described for this receptor despite the variety of phosphate modifications tried (see Introduction).

Accordingly, phosphorous-free isosters, specifically carboxylic and boronic acids (Figure 16) were chosen as acidic subunits, as they have been described as carboxy-based phosphoryl replacements, specially malonic acid.[95,96] Furthermore, they maintain pK_a values similar to the phosphate group, which has been shown to be important for activity.

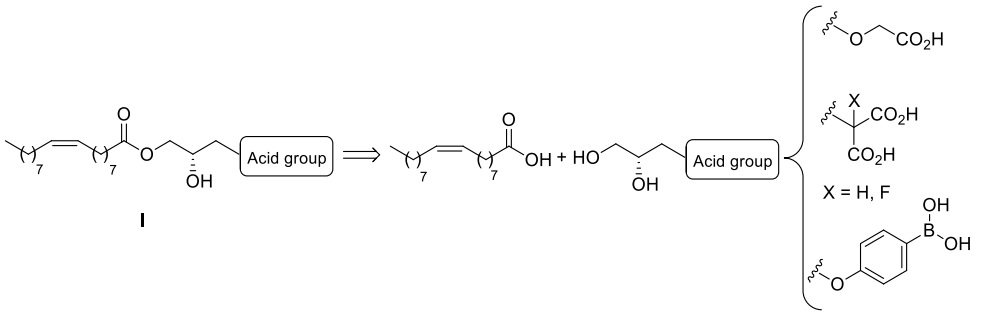

I

Figure 16. Acid groups proposed for series **I**.

The synthesis of compounds of series **I** implied the preparation of the corresponding glycerol derivatives for their subsequent regioselective coupling with the oleate moiety (Figure 16). It must be noted that in all cases the stereochemistry was conserved identical to LPA.

The preparation of the glycerol derivatives started by choosing the adequate and compatible protecting groups (PGs) for the diol and the carboxylic acid moieties present in these derivatives (Figure 17). The two groups had to be orthogonal, this is, it was required that the deprotection of the diol (PG) did not affect the protecting group of the carboxylic acid (PG_1). Additionally, the final deprotection of PG_1 had to be compatible with the presence of the oleate ester group.

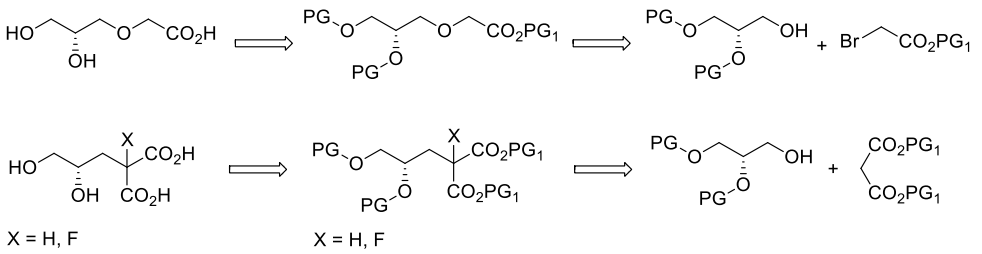

Figure 17. Retrosynthetic analysis for the glycerol moieties.

Therefore, the *tert*-butyl (*t*Bu) ester was chosen as PG_1 due to its easy cleavage in acid media which should not affect the base-labile oleate ester. Regarding the glycerol, the acetal was first considered as starting material, as it is a cheap and commercially available reagent that can be deprotected under mild conditions. However, the conditions tested (catalytic amounts of iodine in methanol at room temperature, Table 2) showed that the acetal cleavage occurred with simultaneous hydrolysis of the *tert*-butyl ester. In view of these results, the benzyl group (Bn) was finally chosen as the glycerol protecting group since its removal by hydrogenation would not affect the ester function.

Table 2. Tested conditions for acetal cleavage

Substrate	Cat. I_2 (%)	Time	Product
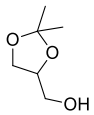	0.5	18h	Starting material
	1	4h	Starting material
	1.5	4h	Starting material
	2.5	4h	
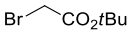	2.5	4h	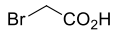
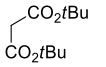	2.5	4h	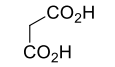

Regarding the compound bearing a boronic acid, the need of two orthogonal protecting groups (PG and PG_1) was solved by protecting the diol as an acetal (PG), whereas the boronic acid was introduced as a pinacol ester (PG_1) whose

deprotection conditions should be compatible with the presence of the oleate moiety (Figure 18).

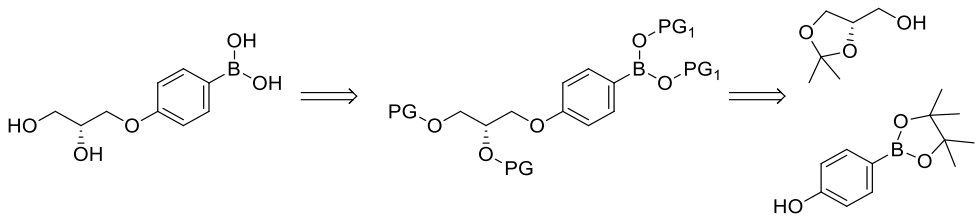

Figure 18. Retrosynthetic analysis for the boronic moiety.

Hence, for carboxylic acid derivatives, alkylation of commercially available (*S*)-(-)-2,3-bis(benzyloxy)propan-1-ol with *tert*-butyl bromoacetate in the presence of sodium hydride and tetrabutylammonium iodide (TBAI) led to the intermediate **37**, which was deprotected by catalytic hydrogenation to afford the glycerol intermediate **38** (Scheme 1).

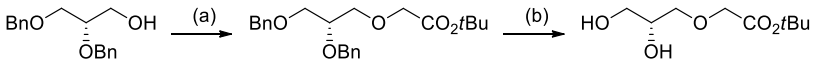

37 **38**

Reagents and conditions: (a) *tert*-Butyl bromoacetate, NaH, TBAI, THF, 0ºC to 50ºC, 16 h, 22%; (b) H_2, 10% Pd(C), EtOH, 60ºC, 95%.

Scheme 1

Next, glycerol derivatives functionalized with malonic and α-fluoromalonic acid were prepared, where the fluorine atom was introduced in order to increase the acidity of the carboxylic acids. Thus, (*S*)-(-)-2,3-bis(benzyloxy)propan-1-ol was transformed into the corresponding mesylate **39**, which was then alkylated with di-*tert*-butyl malonate using sodium hydride as base to yield intermediate **40**. For the preparation of the α-fluoromalonic derivative, intermediate **40** was treated with Selectfluor® under basic conditions. Catalytic hydrogenation of intermediates **40** and **42** afforded the glycerol derivatives **41** and **43** (Scheme 2).

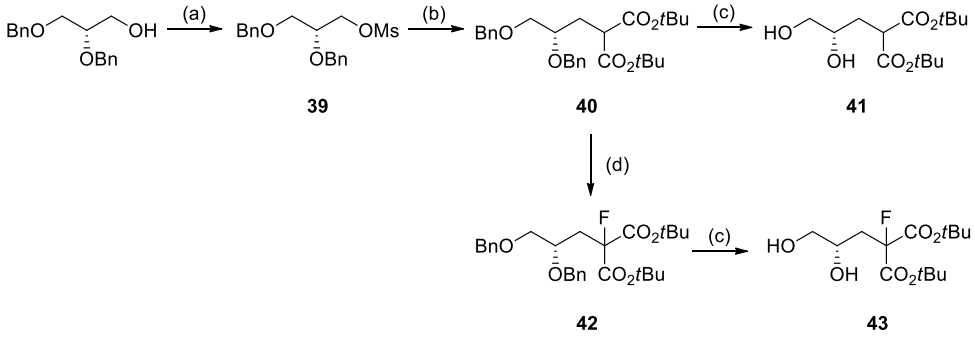

Reagents and conditions: (a) Mesyl chloride, triethylamine, DCM, 0ºC to rt, 1 h, 80%; (b) di-*tert*-butyl malonate, NaH, NaI, DMF:THF, 0ºC to 80ºC, 17 h, 76%; (c) H_2, 10% Pd(C), EtOH, 60ºC, 99%; (d) Selectfluor®, NaH, DMF:THF, 0ºC to rt, 48 h, 48%.

Scheme 2

For the glycerol derivative bearing a boronic acid moiety (**46**), the synthesis started with the tosylation of commercially available (*S*)-(+)-1,2-isopropylydeneglycerol to obtain intermediate **44**, which was further reacted with commercial 4-hydroxyphenylboronic acid pinacol ester to yield derivative **45**. Diol **46** was obtained by deprotection of the acetal using polystyrene-supported *p*-toluensulfonic acid (PS-*p*TsOH) (Scheme 3). In a first attempt, **45** was treated with HCl, but this conditions led to the cleavage of the boronate moiety.

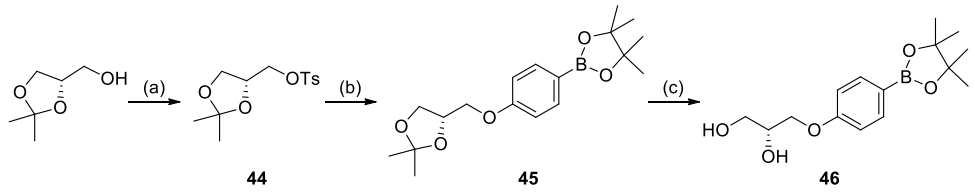

Reagents and conditions: (a) Tosyl chloride, pyridine, DCM, 0ºC to rt, 16 h, 86%; (b) 4-hydroxyphenylboronic acid pinacol ester, Cs_2CO_3, DMF, 90ºC, 16 h, 84%; (c) PS-*p*TsOH, CH_3OH, rt, 18 h, 88%.

Scheme 3

Once the functionalized glycerol derivatives **38**, **41**, **43** and **46** were synthesized, their regioselective condensation with oleic acid was carried out. Following conditions previously employed by our group,[97] a two-fold stoichiometric excess of **38** was reacted with oleic acid using *N*,*N*-dicyclohexylcarbodiimide (DCC) as coupling reagent and catalytic amounts of 4-dimethylaminopyridine (DMAP). However, the corresponding ester **47** was obtained in very low yield (Scheme 4).

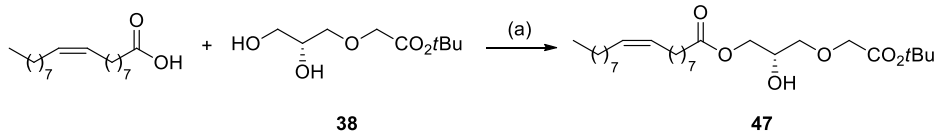

38 **47**

Reagents and conditions: (a) DCC, DMAP, DCM, 0ºC to rt, 12 h, 15%.

Scheme 4

In order to improve the yield of this reaction, **38** was coupled with the more reactive oleoyl chloride in the presence of 2,4,6-collidine at low temperature, which afforded ester **47** with better yield. The reaction was also completely regioselective, and only the acylation at *sn*-3 position of the glycerol moiety was observed. The *tert*-butyl group of intermediate **47** was removed by treatment with trifluoroacetic acid (TFA), yielding the final compound **1a** without detection of the hydrolysis of the oleate ester (Scheme 5).

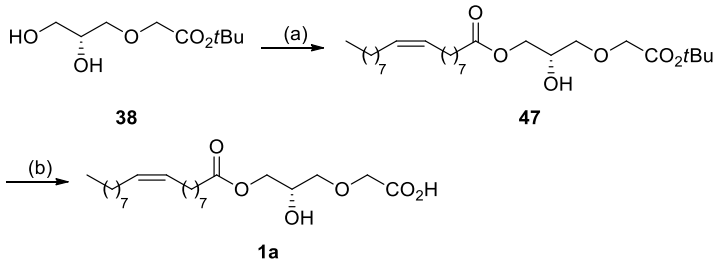

38 **47** **1a**

Reagents and conditions: (a) Oleoyl chloride, 2,4,6-collidine, DCM, -78ºC to rt, 24 h, 36%; (b) TFA, DCM, rt, 17 h, 52%.

Scheme 5

The esterification conditions were then applied to the reaction of the oleoyl chloride with the malonate derivatives **41** and **43** to yield the intermediate esters **48** and **49** which were then subjected to acid conditions to remove the *tert*-butyl group. However, treatment of derivatives **48** and **49** with TFA led to the formation of lactones **1b** and **1c** instead of the expected malonic acids (Scheme 6). These products, obtained as a mixture of diastereoisomers in 1:1 proportion, are the consequence of an intramolecular cyclization of the carboxylic acid with the hydroxy group in γ position.

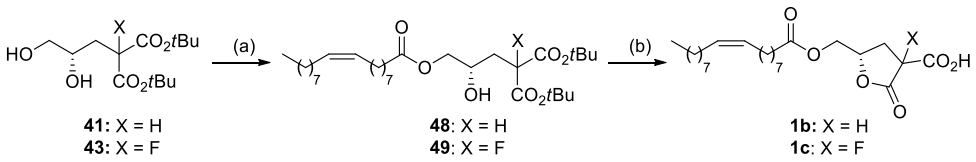

41: X = H
43: X = F

48: X = H
49: X = F

1b: X = H
1c: X = F

Reagents and conditions: (a) Oleoyl chloride, 2,4,6-collidine, DCM, -78ºC to rt, 24 h, 60-99%; (b) TFA, DCM, rt, 17-18 h, 88-99%.

Scheme 6

The optimized conditions were also used to carry out the esterification reaction of glycerol **46** with oleoyl chloride. The pinacolyl boronate ester **50** was transformed into the corresponding trifluoroborate salt **51**, following hydrolysis with trimethylsilyl chloride (TMSCl) to yield final compound **1d** (Scheme 7). Pinacolyl boronate ester **50** had been previously subjected to other deprotection conditions such as transesterification reaction with phenylboronic acid or displacement with diethanolamine followed by hydrolysis, but no reaction occurred or it was incomplete.

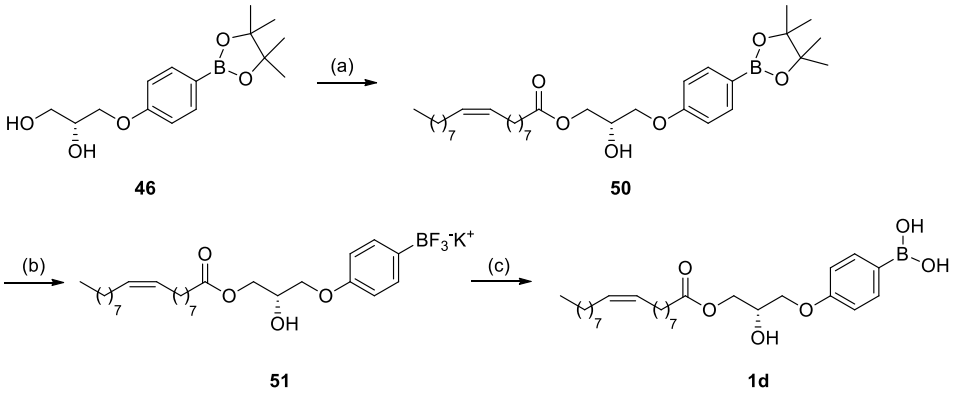

46

50

51

1d

Reagents and conditions: (a) Oleoyl chloride, 2,4,6-collidine, DCM, -78ºC to rt, 24 h, 40%; (b) KHF_2, CH_3OH:H_2O, rt, 30 min; 99%; (c) TMSCl, CH_3CN:H_2O, rt, 1 h, 60%.

Scheme 7

Once the compounds **1a**-**d** were synthesized, they were tested in a LPA_1-overexpressing cell line, in order to determine if any of the phosphate replacements carried out had allowed to obtain compounds with activity at this receptor.

2.1.2 Determination of the agonist activity at LPA_1 receptor

In order to test the synthesized compounds as LPA_1 receptor agonists, the corresponding biological assay was set up in our laboratory. The ability of the compounds to activate the receptor was determined by the measurement of calcium mobilization in RH7777 cells stably transfected with the receptor, as the binding of an LPA_1 agonist causes an increase in intracellular calcium levels,[98] which can be quantified using a fluorescence-based assay.

After some experimental optimizations, Fluo 4-NW (no-wash) was chosen as the most appropriate calcium sensor. To determine the agonist activity of the compounds, cells were preloaded with Fluo 4-NW and then incubated in the presence of the compounds under study. Fluorescence intensity was measured (excitation wavelength of 494 nm and emission wavelength of 516 nm) in a 96-well microplate reader. Ionomycin 10 µM was employed as positive control, with 10 µM LPA response being 30% of ionomycin response.[99] In order to rule out non-LPA_1 receptor mediated calcium mobilization, parallel experiments using non-transfected RH7777 cells were carried out.

The compounds were initially tested at a fixed dose of 10 µM and the maximal receptor activation (E_{max}) for each of them was expressed as a percentage, referring their response to the response induced by 10 µM LPA. The complete dose-response curve, at six or seven different concentrations of the ligand, was determined for those compounds that presented E_{max} over 30%. Data are expressed as the average and standard error (s.e.m.) obtained from two to four independent experiments carried out in triplicate.

The obtained results for compounds **1a**-**d** are shown in Table 3.

Table 3. Agonist activities of compounds **1a-d** at LPA_1 receptor

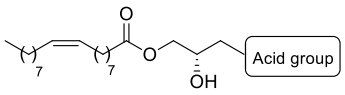

Compound	Acid group	E_{max} (%)[a]	EC_{50} (μM)[b]	pK_a[c]
1a	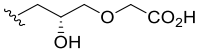	N.E.[d]	-	3.4 ± 0.1
1b	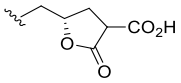	N.E.	-	2.7 ± 0.4
1c	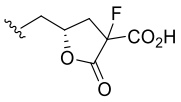	33 ± 5	1.7 ± 0.2	0.5 ± 0.4
1d	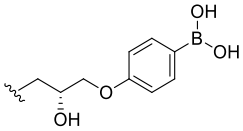	N.E.	-	8.7 ± 0.2
LPA	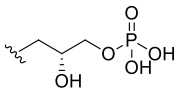	100	0.83 ± 0.02	1.8 ± 0.1

[a]E_{max} = maximal efficacy of the drug/maximal efficacy of LPA, expressed as the percentage. [b]For E_{max} > 30%, EC_{50} values are expressed as mean ± s.e.m, from a minimum of two independent experiments, performed in triplicate. [c]Values estimated with ACDLabs program. [d]No effect was observed at the highest concentration of compound tested (10 μM).

In this initial set of compounds, the influence of pK_a seems to be important for activity, as only compound **1c**, with a pK_a value lower than LPA, activates the receptor (Table 3). Accordingly, it was necessary to confirm if the non-cyclic malonic derivatives originally proposed, with two free carboxylic acids, would exhibit better activities at LPA_1 receptor. In order to avoid cyclization, the most straightforward structural modifications were either the removal of the hydroxy group (compounds **1e**, **f**) or its masking with a methyl group, as in derivative **1g** (Figure 19).

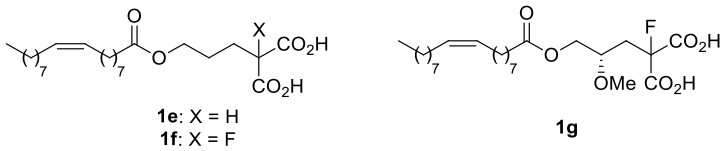

Figure 19

Hence, the commercially available 3-(benzyloxy)propan-1-ol was transformed into the corresponding mesylate **52**, which was further alkylated with di-*tert*-butyl malonate to obtain intermediate **53**. This compound was treated with Selectfluor® to yield the fluorinated derivative **55**. The obtention of the desired diols **54** and **56** involved catalytic hydrogenation to remove the benzyl group of their precursors **53** and **55** (Scheme 8).

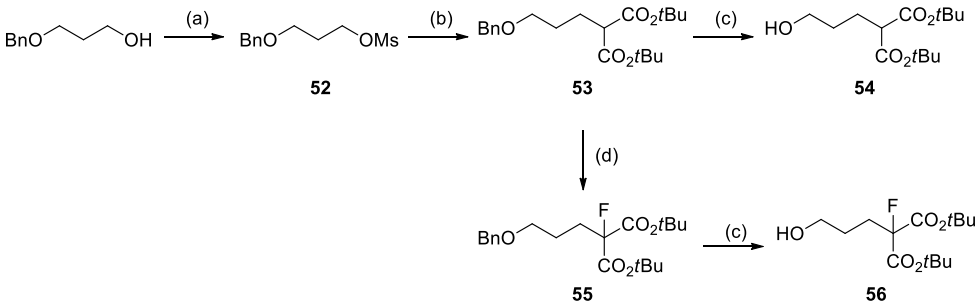

Reagents and conditions: (a) Mesyl chloride, triethylamine, DCM, 0ºC to rt, 1 h, 99%; (b) di-*tert*-butyl malonate, NaH, NaI, DMF:THF, 0ºC to 80ºC, 17 h, 66%; (c) H_2, 10% Pd(C), EtOH, 60ºC, 99%; (d) Selectfluor®, NaH, DMF:THF, 0ºC to rt, 48 h, 99%.

Scheme 8

Once the glycerol moieties were synthesized, acylation with oleoyl chloride followed by hydrolysis with TFA of the resulting intermediates **57** and **58** allowed to obtain final compounds **1e** and **1f** in good yields (Scheme 9).

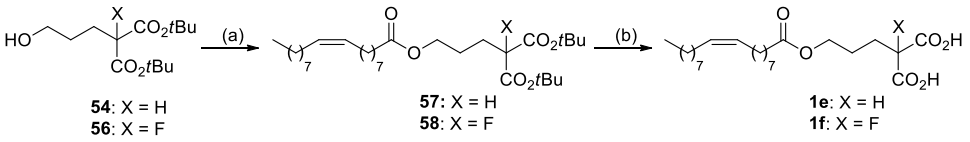

Reagents and conditions: (a) Oleoyl chloride, 2,4,6-collidine, DCM, -78ºC to rt, 24 h, 59-70%; (b) TFA, DCM, rt, 16-17 h, 59-90%.

Scheme 9

Synthesis of final compound **1g** started from derivative **49**, which by reaction with trimethylsilyldiazomethane followed by hydrolysis of the *tert*-butyl ester groups led to the desired compound (Scheme 10).

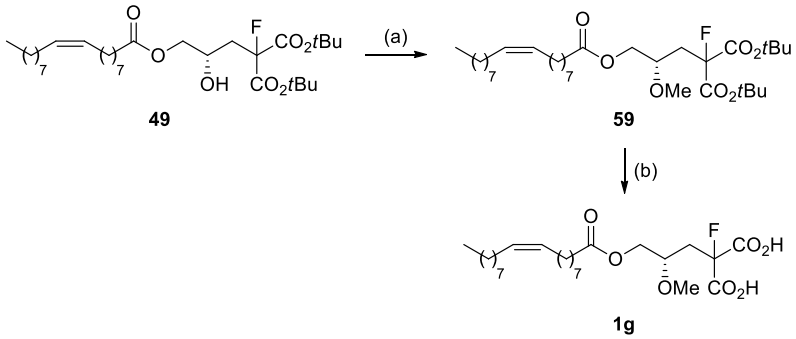

49 **59** **1g**

Reagents and conditions: (a) Trimethylsilyldiazomethane, HBF_4, DCM, 0ºC, 90 min, 38%; (b) TFA, DCM, rt, 17 h, 95%.

Scheme 10

The capacity of compounds **1e**-**g** to activate LPA_1 receptor was determined and the results are shown in Table 4. Taking together all the data obtained for series **I**, the necessity of an acidic polar group seems clear. However, it is not the only requirement, as **1f**, with a pK_a value similar to compound **1g**, is completely inactive. This suggests the importance of the oxygen atom of the hydroxy group in the spacer that separates the fatty acid chain and the polar head group.

Table 4. Agonist activities of compounds **1e-g** at LPA_1 receptor

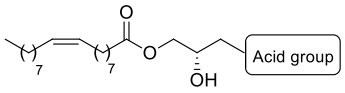

Compound	Acid group	E_{max} (%)[a]	EC_{50} (μM)[b]	pK_a[c]
1e	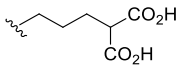	N.E.[d]	-	3.2 ± 0.2
1f	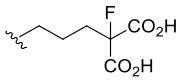	N.E.	-	1.1 ± 0.4
1g	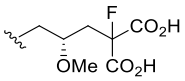	74 ± 14	6 ± 1	0.9 ± 0.4
LPA	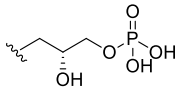	100	0.83 ± 0.02	1.8 ± 0.1

[a]E_{max} = maximal efficacy of the drug/maximal efficacy of LPA, expressed as the percentage. [b]For E_{max} > 30%, EC_{50} values are expressed as mean ± s.e.m, from a minimum of two independent experiments, performed in triplicate. [c]Values estimated with ACDLabs program. [d]No effect was observed at the highest concentration of compound tested (10 μM).

In conclusion, this initial series of compounds allowed to identify two LPA_1 receptor agonists, **1c** (E_{max} = 33%; EC_{50} = 1.7 μM) and **1g** (E_{max} = 74%; EC_{50} = 6 μM), which confirms that it is possible to mimic the phosphate group of LPA with other polar moieties. However, these two agonists are still less potent than LPA so, in order to optimize the structure, the study of the influence of the hydrophobic chain of LPA was addressed.

*2.1.3 Design and synthesis of series **II***

During the last years, several studies have been carried out trying to establish the structural requirements needed for the hydrophobic moiety. Although no definitive conclusions have been reached yet, it seems clear that modifications on this part of the molecule are less critical for activity at LPA_1 receptor, probably because its flexible disposition facilitates its fitting into the receptor pocket. In fact, it must be noted that LPA_1 receptor admits the presence of either saturated or insaturated moieties, even though most of the agonist compounds reported (see

Introduction) bear an oleic acid chain in their structure, and show preference for this length when compared to the shorter palmitoleic acid chain.

Thus, for series **II**, a comprehensive study of the influence of the hydrophobic moeity was carried out, including modifications on the overall length of the fatty acid chain as well as the incorporation of aromatic rings (Figure 20).

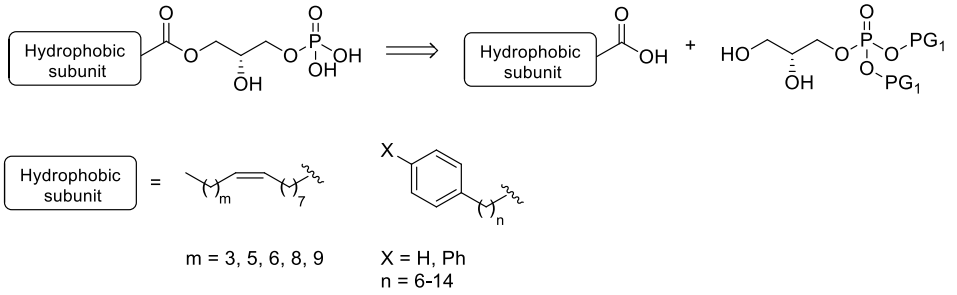

Figure 20. Design of compounds of series **II**.

2.1.3.1 Derivatives of series **II** containing aliphatic chains

Modifications of the length of the fatty acid chain implied the synthesis of the corresponding alkynylcarboxylic acids, followed by their partial hydrogenation to obtain the *Z*-alkenes. Regarding the phosphorylated glycerol protecting groups, the compatibility between the deprotection conditions of the phosphate group (PG_1) and the existence of double bonds in the molecule had to be considered, and so, *tert*-butyl group was chosen, as its hydrolysis takes place in acid media, which should not affect the double bond. Furthermore, the deprotection conditions of the diol PG should be orthogonal with PG_1, so benzyl group was selected as the most appropriate option (Figure 21).

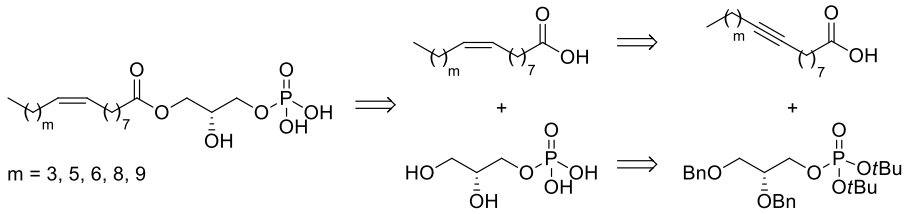

Figure 21. Retrosynthetic analysis for aliphatic derivatives of series **II**.

Alkynyl derivatives **61**-**63** were achieved by a Sonogashira coupling of methyl 8-bromooctanoate (**60**) and the corresponding commercially available alkynes using a carbene ligand suitable for unactivated alkyl bromides[100] (Scheme 11). The

subsequent hydrogenation of the alkynes **61**-**63** turned out to be extremely challenging. A variety of conditions was tried, including hydrogenation in the H-Cube continuous flow hydrogenation reactor using different catalysts, conventional hydrogenation in a Parr instrument with Lindlar catalyst ($Pd/CaCO_3/Pb$)/quinoline system, and also a transfer hydrogenation reaction with $Pd(OAc)_2$ as catalyst and DMF/KOH as hydrogen source. Time, solvent, and temperature were modified (Tables 5-7) searching for a complete conversion of the starting material to the alkene, as mixtures of saturated and insaturated products cannot be separated by chromatography.

In our hands, all the conditions tested in the H-Cube flow reactor (Table 5) gave a mixture of products. In the case of the Parr apparatus (Table 6), conditions for the obtention of the *Z*-alkene were found by using but-2-yne-1,4-diol as model substrate. However, when these conditions (2.5% w Lindlar catalyst, 3% mol quinoline, 5:1 toluene:methanol, 20 psi, rt, 2 h) were used with the alkynylcarboxylic acids, only starting material was recovered. A possible explanation could be the poisoning of the Lindlar catalyst with remaining traces of the catalyst from the previous Sonogashira reaction. Transfer hydrogenation with $Pd(OAc)_2$ was also tried (Table 7), but a mixture of alkyne and alkene was obtained.

Table 5. Hydrogenation conditions with H-Cube reactor

Substrate	Catalyst	Conditions	Result
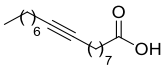	$Pd/CaCO_3/Pb$	10 bar, rt, ethanol	Alkyne+alkene
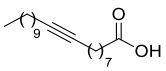	$Pd/CaCO_3/Pb$	20 bar, rt, ethanol	Alkyne+alkene
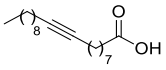	Pd/C 1%	30 bar, rt, ethanol	Alkyne+alkene+alkane

Table 6. Hydrogenation conditions with Parr instrument

Substrate	Catalyst	Conditions		Result
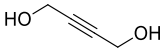	Lindlar cat. (5% w) Quinoline (3% mol)	Toluene:methanol 5:1, 20 psi, rt	1 h	Alkene+alkane
			2 h	Alkene+alkane
	Lindlar cat. (2.5% w) Quinoline (3% mol)	Toluene:methanol 5:1, 20 psi, rt	15 min	Alkyne
			30 min	Alkyne+alkene
			1 h	Alkyne+alkene
			2 h	Alkene
			3 h	Alkene+alkane
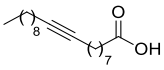	Lindlar cat. (2.5% w) Quinoline (3% mol)	Toluene:methanol 5:1, 20 psi, rt	1 h	Alkyne
			2 h	Alkyne
	Lindlar cat. (5% w) Quinoline (3% mol)	Toluene: methanol 5:1, rt	20 psi, 1 h	Alkyne
			20 psi, 2 h	Alkyne
			40 psi, 2 h	Alkyne
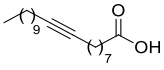	Lindlar cat. (10% w) Quinoline (3% mol)	Toluene:methanol 5:1, 40 psi, 6 h, rt		Alkyne
	Lindlar cat. (10% w)	Toluene, 40 psi, 6 h, rt		Alkyne
		Ethyl acetate, 40 psi, 4 h, rt		Alkyne
	Lindlar cat. (20% w)	Ethyl acetate, 40 psi, overnight, rt		Alkyne

Table 7. Other conditions

Substrate	Reaction conditions		Result
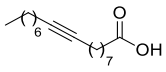	$Pd(OAc)_2$, KOH, DMF, H_2O, 145ºC, overnight		Alkyne+alkene
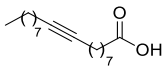	$Ni(OAc)_2 \cdot 4H_2O$, $NaBH_4$, ethylenediamine, H_2 (balloon), ethanol, rt	30 min	Alkyne+alkene
		1 h	Alkyne+alkene
		2 h	Alkene

Finally, Brown hydrogenation reaction[101] (optimization of the reaction in Table 7) allowed to obtain the desired alkenes **64**-**66** with total conversion employing nickel acetate tetrahydrate and sodium borohydride as the catalytic system, in the presence of ethylendiamine and under hydrogen atmosphere. Then, the alkenes were hydrolyzed to their corresponding carboxylic acids **67**-**69** (Scheme 11).

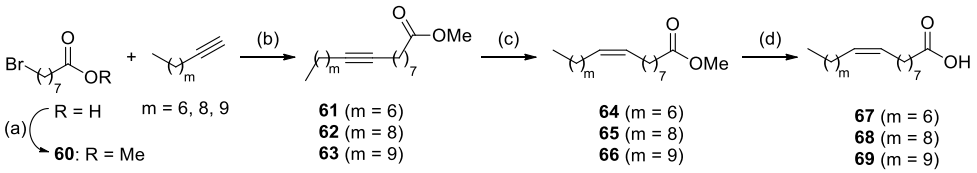

Reagents and conditions: (a) *p*TsOH, CH_3OH, reflux, 18 h, 95%; (b) $[(\pi\text{-allyl})PdCl]_2$, 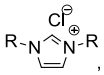 , R = 1-adamantyl, CuI, Cs_2CO_3, DMF:Et_2O, 55ºC, 16 h, 36-44%; (c) $Ni(OAc)_2 \cdot 4H_2O$, $NaBH_4$, ethylenediamine, H_2 (1 atm), EtOH, rt, 2 h, 89-92%; (d) $LiOH \cdot H_2O$, THF:H_2O, rt, 16-18 h, 99%.

Scheme 11

Next, phosphate moieties were prepared following a synthetic methodology previously set up in the laboratory consisting on a phosphoramidite reaction and oxidation of the intermediate phosphite formed.[102] Thus, one-pot reaction of (*S*)-(-)-2,3-bis(bencyloxy)propan-1-ol with di-*tert*-butyl *N*,*N*-diisopropylphosphoramidite, followed by oxidation with *m*-chloroperbenzoic acid (*m*CPBA) led to derivative **70**. Removal of the benzyl groups by catalytic hydrogenation yielded diol **71** (Scheme 12).

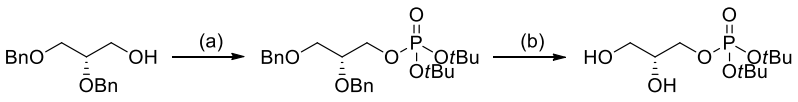

70 **71**

Reagents and conditions: (a) i) iPr$_2$NP(OtBu)$_2$, 1*H*-tetrazole, DCM, rt, 2 h; ii) *m*CPBA, DCM, -30ºC, 90 min, 38%; (b) H_2, 10% Pd(C), EtOH, 60ºC, 99%.

Scheme 12

Finally, the esterification reaction between myristoleic or palmitoleic acid or the non-commercial carboxylic acids **67**-**69** and the phosphorylated diol **71** led to intermediates **72**-**76**, which were then deprotected to obtain the final products **2a-e** with good yields (Scheme 13).

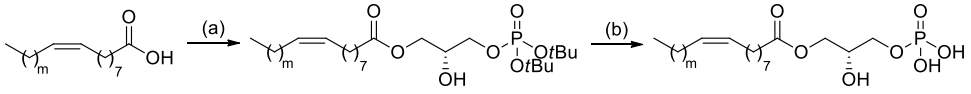

Myristoleic acid (m = 3)	**72** (m = 3)	**2a-e**
Palmitoleic acid (m = 5)	**73** (m = 5)	(m = 3, 5, 6, 8, 9)
67 (m = 6)	**74** (m = 6)	
68 (m = 8)	**75** (m = 8)	
69 (m = 9	**76** (m = 9)	

Reagents and conditions: (a) **71**, DCC, DMAP, DCM, -20ºC to rt, 16 h, 12-49%; (b) TFA, DCM, rt, 4-5 h, 90-99%.

Scheme 13

Synthesized compounds **2a**-**e** were tested for their activity at the LPA_1 receptor (Table 8). The most remarkable conclusion that can be drawn from the data obtained is the great influence on activity exerted by the length of the hydrophobic chain. As shown in Table 8, variations in just one methylene unit can turn a compound inactive (for example derivative **2d** shows an activity comparable to LPA whereas **2e** is inactive) or increase its activity almost two-fold, as shown by compounds **2d** (E_{max} = 88%; EC_{50} = 3.6 µM) and **2c** (E_{max} = 202%; EC_{50} = 2.1 µM). These data suggest that the optimal chain is the corresponding to (9*Z*)-hexadec-9-enoic acid, present in compound **2b** (E_{max} = 205%; EC_{50} = 0.45 µM), the most potent derivative within the series and better than the endogenous ligand LPA (E_{max} = 100%; EC_{50} = 0.83 µM).

Table 8. Agonist activities of compounds **2a**-**e** at LPA_1 receptor

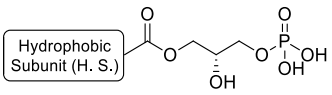

Compound	H. S. =	E_{max} (%)[a]	EC_{50} (μM)[b]
2a	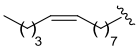	127± 1	2.8 ± 0.1
2b	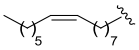	205 ± 9	0.45 ± 0.01
2c	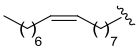	202 ± 1	2.1 ± 0.3
2d	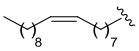	88 ± 2	3.6 ± 0.2
2e	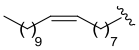	N.E.[c]	-
LPA	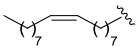	100	0.83 ± 0.02

[a]E_{max} = maximal efficacy of the drug/maximal efficacy of LPA, expressed as the percentage. [b]For E_{max} > 30%, EC_{50} values are expressed as mean ± s.e.m, from a minimum of two independent experiments, performed in triplicated. [c]No effect was observed at the highest concentration tested (10 μM).

2.1.3.2 Derivatives of series **II** containing aromatic rings

Previous results from our group indicate that phenyl and biphenyl groups can mimic unsaturated fatty acid chains.[103] Accordingly, the possibility of replacing the hydrophobic chain with other hydrophobic units containing aromatic rings was studied. In addition, and considering the importance of the length of the chain for activity, the influence of the distance between the aromatic rings and the ester group of the molecule (n) was screened in detail (Figure 22).

In this case, the synthesis involved the preparation of the non-commercial ω-phenylalkanoic carboxylic acids as well as the conveniently protected phosphorylated glycerol (Figure 22). Regarding the glycerol moiety and searching for synthetic simplicity and high yields, the phosphate group was protected with an

ethyl moiety (PG_1), whose removal should not interfere with the presence of an ester. As for the diol protecting group, the commercially available acetal was initially selected.

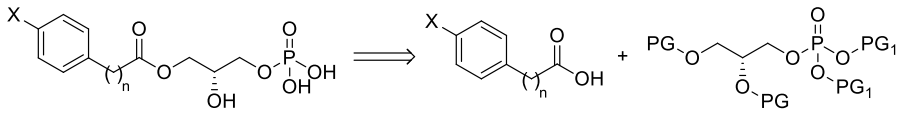

Figure 22. Retrosynthetic analysis for aromatic ring derivatives of series **II**.

Non-commercially available carboxylic acids (X = H, n = 7-9) were synthesized as depicted in Scheme 14, either by oxidation of the corresponding alcohol, in the case of acid **77**, or by Wittig reaction between the appropriate bromoacid and benzaldehyde, followed by catalytic hydrogenation, in the case of acids **80** and **81**.

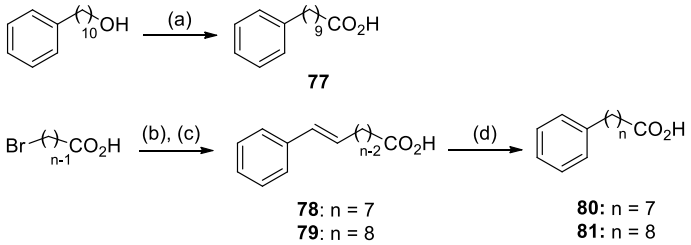

Reagents and conditions: (a) PDC, DMF, rt, 16 h, 52%; (b) PPh_3, toluene, reflux, 24 h, 99%; (c) benzaldehyde, lithium bis(trimethylsilyl)amide, THF, -20ºC to rt, 18 h, 61-70%; (d) H_2, 10% Pd(C), EtOH, rt, 81-97%.

Scheme 14

The protected glycerol was reacted with diethyl chlorophosphate in the presence of a base to yield intermediate **82**, which after cleavage of the acetal group afforded the phosphorylated glycerol **83** (Scheme 15).

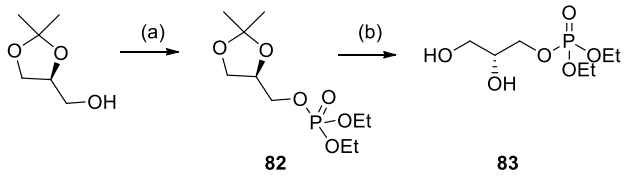

Reagents and conditions: (a) $ClP(O)(OEt)_2$, KO*t*Bu, DCM, rt, 48 h, 92%; (b) PS-*p*TsOH, CH_3OH, rt, 16 h, 50%.

Scheme 15

Once the phosphorylated glycerol **83** and the carboxylic acids **77**, **80** and **81** were prepared, the coupling reaction between **83** and **77** was carried out and the resulting ester **84** was treated with TMSBr as generally described[104] to remove the ethyl groups from the phosphate. However, instead of the expected product, the brominated derivative **3a** was obtained (Scheme 16). The formation of this product could be explained by migration of the acyl chain to the secondary hydroxy group, and substitution of the primary hydroxy group by the bromide present in the reaction media. This *sn*-1/*sn*-2 migration has been observed in other LPA derivatives.[105]

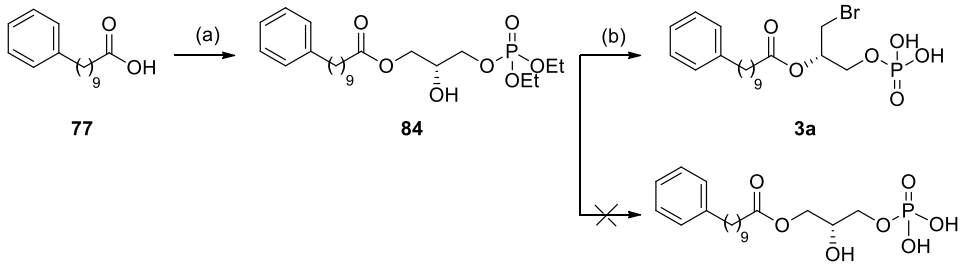

Reagents and conditions: (a) **83**, DCC, DMAP, -20ºC to rt, 18 h, 30%; (b) TMSBr, DCM, rt, 4 h, 90%.

Scheme 16

Although different deprotection conditions were assayed for compound **84**, it was not possible to isolate the desired product. Starting material was used thoroughly dried, *N*,*O*-bis(trimethylsilyl)trifluoroacetamide was employed as additive, and the reaction times were reduced, but it was observed that the migration occurred prior to the deprotection of the phosphate group, and a mixture of starting material, desired product and brominated product was obtained in all cases.

Hence, to obtain the phosphorylated diol, the phosphate group was introduced using the methodology previously used based on the employment of a phosphoramidite reagent. In this case, the protecting group selected for the phosphate was the benzyl group (Scheme 17).

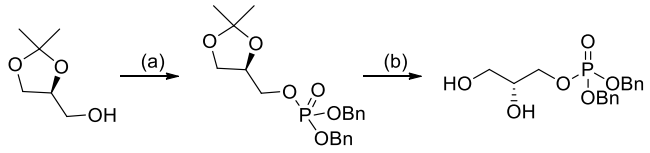

85 **86**

Reagents and conditions: (a) i) iPr$_2$NP(OBn)$_2$, 1*H*-tetrazole, DCM, rt, 2h; ii) *m*CPBA, DCM, -30ºC, 90 min, 76%; (b) PS-*p*TsOH, CH_3OH, rt, 16 h, 65%.

Scheme 17

The regioselective esterification reaction between diol **86** and the corresponding ω-phenylalkanoic acids (n = 6-9, 14) allowed to obtain the esters **87**-**91**, which after elimination of the benzyl groups by catalytic hydrogenation afforded the desired final compounds **2f-j** (Scheme 18).

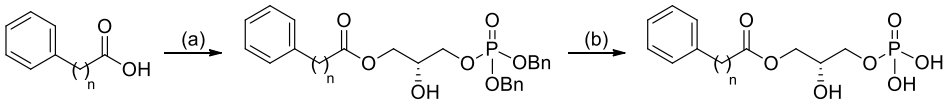

n = 6-9, 14

87: n = 6
88: n = 7
89: n = 8
90: n = 9
91: n =14

2f: n = 6
2g: n = 7
2h: n = 8
2i: n = 9
2j: n = 14

Reagents and conditions: (a) **86**, DCC, DMAP, DCM, -20ºC to rt, 16h, 18-58%; (b) H_2, 10% Pd(C), EtOH, rt, 80-99%.

Scheme 18

All the synthesized compounds **2f**-**j** were tested for activity at LPA_1 receptor and the results are shown in Table 9. Although compound **3a** bears a different phosphate scaffold, it was also tested, as a lack of regioselectivity between *sn*-1 and *sn*-2 positions has been reported for LPA_1 receptor. Furthermore, compounds containing a bromine in the polar head have been described as good agonists or antagonists for LPA receptors.[83]

Again, the obtained data (Table 9) point out the importance of the length of the hydrophobic chain of the compound in the activity at LPA_1 receptor, as small changes within the number of methylene units dramatically affects E_{max} and EC_{50} values. For example, compound **2g**, with n = 7, is inactive, whereas derivative **2h**, with n = 8, is almost as active as LPA. In addition, it must be highlighted that compound **3a**, with a different polar head group, exhibits a very good activity at

LPA_1 receptor. Among these derivatives, compounds **2i** and **3a**, with E_{max} > 100% and EC_{50} values of 0.5 and 0.24 µM, respectively, stand out.

Table 9. Agonist activities of compounds **2f-j** and **3a** at LPA_1 receptor

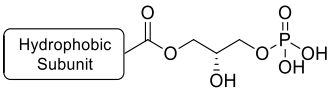

Compound	Hydrophobic Subunit	E_{max} (%)[a]	EC_{50} (µM)[b]
2f	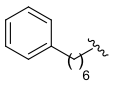	N. E.[c]	-
2g	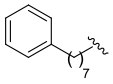	N. E.	-
2h	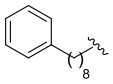	74 ± 4	2.1 ± 0.3
2i	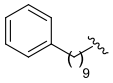	112 ± 3	0.5 ± 0.1
2j	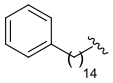	N. E.	-
3a	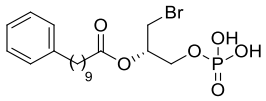	118 ± 24	0.24 ± 0.09
LPA	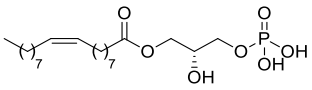	100	0.83 ± 0.02

[a]E_{max} = maximal efficacy of the drug/maximal efficacy of LPA, expressed as the percentage. [b]For E_{max} > 30%, EC_{50} values are expressed as mean ± s.e.m, from a minimum of two independent experiments, performed in triplicate. [c]No effect was observed at the highest concentration of compound tested (10 µM).

Regarding the fragments bearing a biphenyl ring (X = Ph, n = 6, 9, 12), the synthetic strategy employed was the same as for the phenyl ring derivatives, using a Wittig reaction to obtain the desired ω-biphenylalkanoic acids, and intermediate **86** to incorporate the phosphoglycerol moiety.

Thus, 9-bromononanoic acid **94** and 12-bromododecanoic acid **98** were first prepared by oxidation of 9-bromononan-1-ol and 12-bromododecan-1-ol **97**, respectively, with fuming nitric acid. Previously, alcohol **97** had been obtained from commercially available 1,12-dodecanodiol by selective bromination. The ω-bromoalkanoic acids reacted with triphenylphosphine in refluxing toluene to yield the corresponding phosphonium salts, which, by Wittig reaction with biphenyl-4-carbaldehyde, led to alkenes **92**, **95** and **99**. These intermediates were transformed into the desired carboxylic acids **93**, **96** and **100** by catalytic hydrogenation of the double bond (Scheme 19).

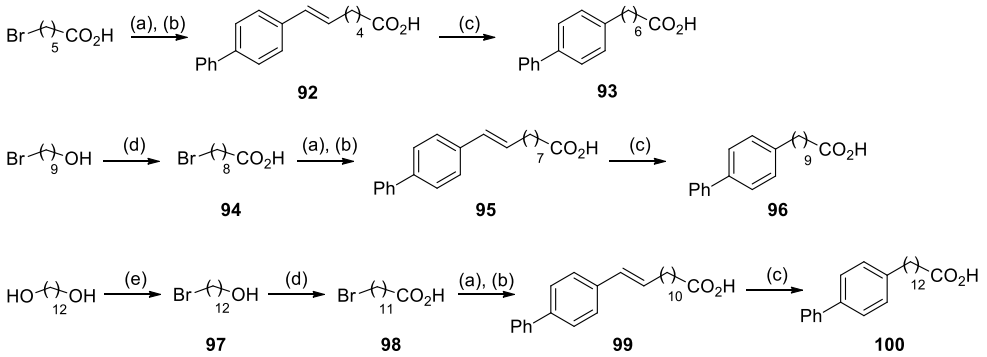

Reagents and conditions: (a) PPh_3, toluene, reflux, 24 h, 99%; (b) biphenyl-4-carbaldehyde, lithium bis(trimethylsilyl)amide, THF, -20ºC to rt, 18 h, 38-72%; (c) H_2, 10% Pd(C), EtOH, rt, 83-96%; (d) HNO_3, rt to 80ºC, 5 h, 43-61%; (e) 47% aq. HBr, cyclohexane, reflux, 6 h, 65%.

Scheme 19

Then, the carboxylic acids **93**, **96** and **100** were coupled with diol **86** to obtain the esters **101**-**103**. Final hydrogenation of these intermediates gave compounds **2k**-**m** in good yields (Scheme 20).

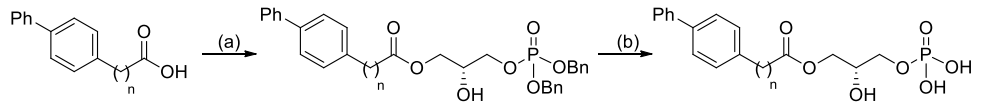

93: n = 6 **101**: n = 6 **2k**: n = 6
96: n = 9 **102**: n = 9 **2l**: n = 9
100: n =12 **103**: n =12 **2m**: n = 12

Reagents and conditions: (a) **86**, DCC, DMAP, DCM, -20ºC to rt, 16 h, 18-24%; (b) H_2, 10% Pd(C), EtOH, rt, 74-91%.

Scheme 20

Compounds **2k**-**m** were tested for LPA_1 activity, and the results are shown in Table 10. Once more, the exquisite influence of the length of the chain was

confirmed, with the compound bearing a nine carbon atom chain (**2l**) showing the highest activity (E_{max} = 127 %, EC_{50} = 3.3 µM).

Table 10. Agonist activities of compounds **2k-m** at LPA_1 receptor

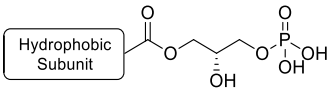

Compound	Hydrophobic Subunit	E_{max} (%)[a]	EC_{50} (µM)[b]
2k	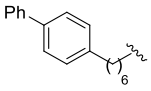	N. E.[c]	-
2l	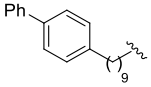	127 ± 9	3.3 ± 0.6
2m	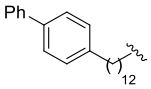	37 ± 1	19 ± 2
LPA	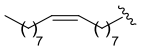	100	0.83 ± 0.02

[a]E_{max} = maximal efficacy of the drug/maximal efficacy of LPA, expressed as the percentage. [b]For E_{max} > 30%, EC_{50} values are expressed as mean ± s.e.m, from a minimum of two independent experiments, performed in triplicate. [c]No effect was observed at the highest concentration of compound tested (10 µM).

2.1.3.3 Analogues of **3a**

Considering the excellent activity of compound **3a**, which turned out to be the best LPA_1 receptor agonist among all the synthesized compounds so far (E_{max} = 118%, EC_{50} = 0.24 µM), additional structural exploration was extended around this scaffold. In particular, it was analysed whether changes in the length of the methylenic chain would affect its activity in the same degree observed for other compounds of series **I** and **II** (compounds **3b**, **c**). In addition, the replacement of the hydrophobic unit by the oleic acid chain was studied, in order to see if it would involve an increase in activity. Hence, compounds **3b**-**d** (Figure 23) were synthesized.

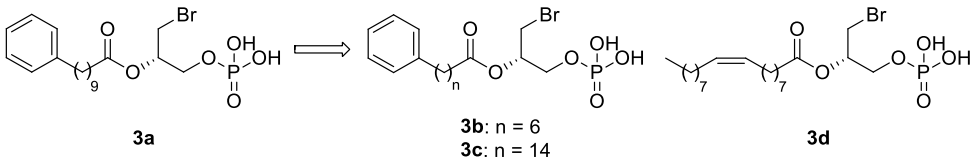

Figure 23. Designed derivatives of **3a**.

Phenyl-containing derivatives **3b** and **3c** were obtained from (*S*)-oxiran-2-ylmethanol, which was phosphorylated following the usual conditions. Then, opening of the oxirane ring of intermediate **104** with tetrabutylammonium bromide (TBABr) in the presence of TFA yielded derivative **105**, which was coupled with the corresponding ω-phenylalkanoic acids. Subsequent catalytic hydrogenation of the benzyl groups gave the desired final compounds **3b**, **c** (Scheme 21).

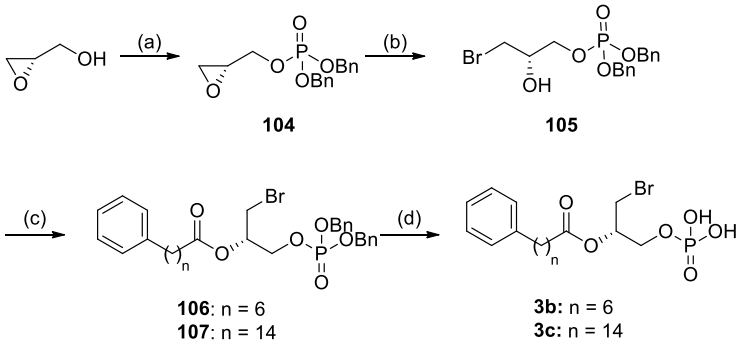

Reagents and conditions: (a) i) *i*$Pr_2NP(OBn)_2$, 1*H*-tetrazole, DCM, rt, 2h; ii) *m*CPBA, DCM, -30ºC, 90 min, 76%; (b) TBABr, TFA, $CHCl_3$, rt, 10 min, 89%; (c) $Ph(CH_2)_nCOOH$ (n = 6, 14), DCC, DMAP, DCM, rt, 16-18 h, 50-64%; (d) H_2, 10% Pd(C), EtOH, rt, 85-86%.

Scheme 21

A similar synthetic route, but employing *tert*-butyl instead of benzyl as protecting group for the phosphate, due to the presence of the double bond in the oleate moiety, allowed to obtain compound **3d** (Scheme 22).

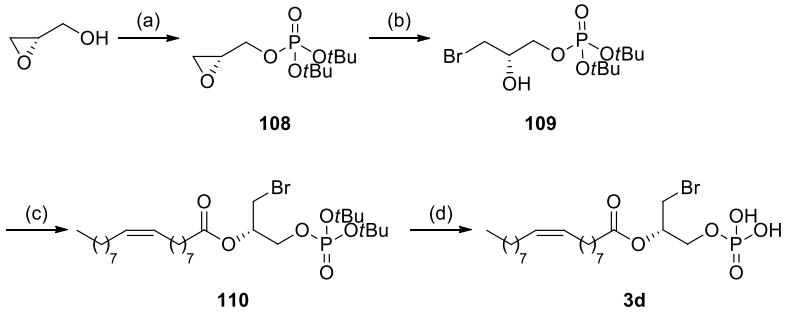

Reagents and conditions: (a) i) iPr$_2$NP(tBu)$_2$, 1H-tetrazole, DCM, rt, 2h; ii) mCPBA, DCM, -30ºC, 90 min, 52%; (b) TBABr, TFA, $CHCl_3$, rt, 10 min, 95%; (c) oleoyl chloride, pyridine, rt, 18 h, 15%; (d) TFA, DCM, rt, 5 h, 81%.

Scheme 22

Activity of these new compounds at the LPA_1 receptor was determined (Table 11). The obtained results showed that only the oleic acid chain derivative (**3d**) was able to activate the receptor, although it did not reach neither LPA nor **3a** values.

Table 11. Agonist activities of compounds **3a**-**d** at LPA_1 receptor

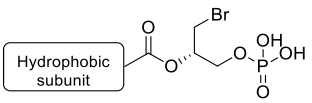

Compound	Hydrophobic subunit	E_{max} (%)[a]	EC_{50} (μM)[b]
3a	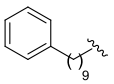	118 ± 24	0.24 ± 0.09
3b	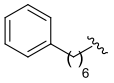	N. E.[c]	-
3c	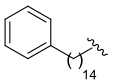	N. E.	-
3d	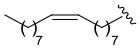	39 ± 3	3.2 ± 0.4
LPA	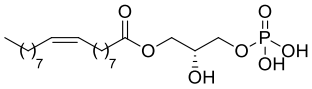	100	0.83 ± 0.02

[a]E_{max} = maximal efficacy of the drug/maximal efficacy of LPA, expressed as the percentage. [b]For E_{max} > 30%, EC_{50} values are expressed as mean ± s.e.m, from a minimum of two independent experiments, performed in triplicate. [c]No effect was observed at the highest concentration of compound tested (10 μM).

2.2 Combination of the acid and hydrophobic subunits

Among all the synthesized compounds, derivatives **1c**, **1g**, **2b**, **2i**, **2l**, **3a** and **3d** have shown the best activities at the LPA_1 receptor (Figure 24). They present EC_{50} values between 0.24 and 6 μM, comparable or even better than the endogenous ligand LPA (EC_{50} = 0.83 μM). This suggests that the phosphate glycerol of LPA can be mimicked by other acid moieties such as (5*S*)-3-fluoro-5-(hydroxymethyl)-2-oxotetrahydrofuran-3-carboxylic acid (present in **1c**), fluoro[(2*S*)-3-hydroxy-2-methoxypropyl]malonic acid (present in **1g**) and (2*S*)-3-bromo-2-hydroxypropyl dihydrogen phosphate (present in **3a** and **3d**). In addition to the oleic acid chain of LPA, the LPA_1 receptor recognizes shorter chains such as (9*Z*)-hexadec-9-enoic acid (present in **2b**), 10-phenyldecanoic acid (present in **2i** and **3a**) and 10-biphenyl-4-yldecanoic acid (present in **2l**) (Figure 24).

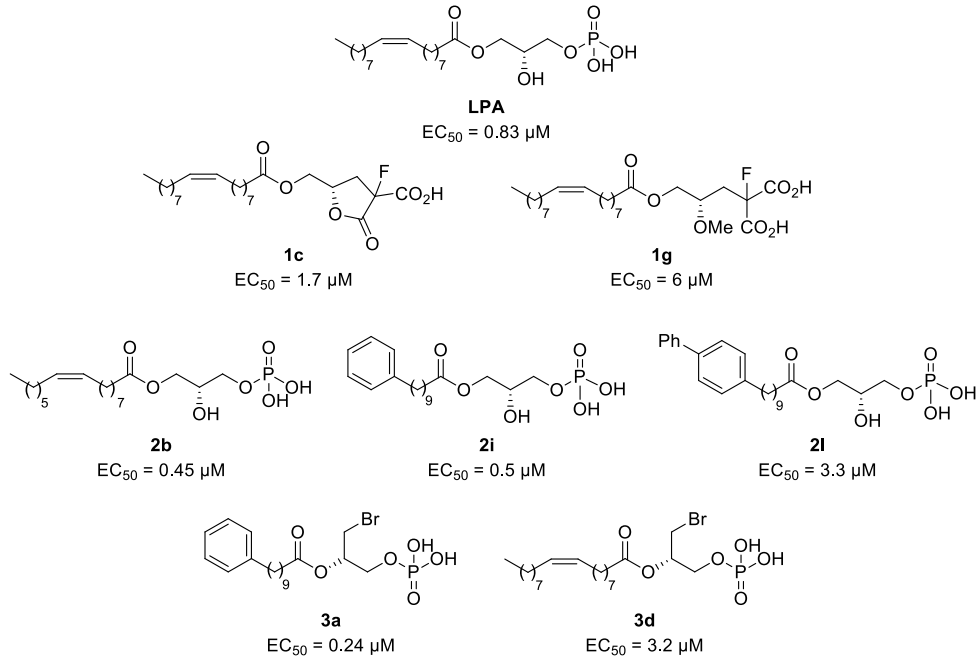

Figure 24. Compounds with activity at the LPA_1 receptor

With these results in hand, we combined some of the hydrophobic moieties present in these compounds with the polar heads that seem to be able to mimic the LPA phosphate group. Hence, the fluorinated lactone and the fluorinated malonic acid present in derivatives **1c** and **1g** were selected as polar heads. Regarding the hydrophobic moiety, palmitoleic acid chain present in **2b** and 10-phenyldecanoic

acid chain present in **2i** and **3a** were chosen. The combination of these moieties led to products **4a**-**c** which were synthesized and tested as agonists of the LPA_1 receptor (Figure 25).

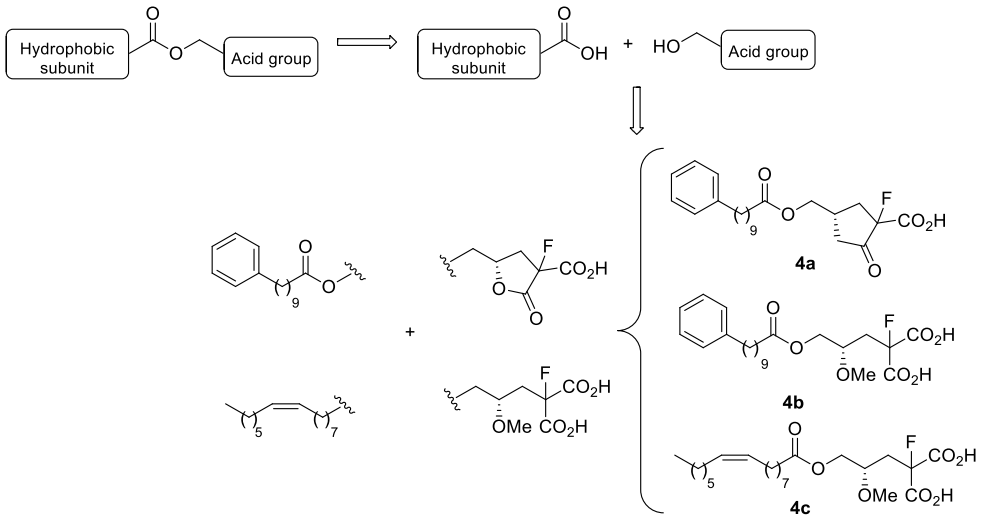

Figure 25. Combination of the acid and hydrophobic subunits.

The synthesis of lactone **4a** started with the benzylation of (*R*)-oxiran-2-ylmethanol, followed by oxirane opening with di-*tert*-butyl malonate in basic media and intramolecular cyclization to give lactone **112**. Fluorination in the usual conditions led to derivative **113**, whose catalytic hydrogenation yielded alcohol **114**. The esterification between **114** and 10-phenyldecanoic acid allowed to obtain ester **115**, which was treated with TFA to give final product **4a** as a mixture of diastereoisomers (Scheme 23).

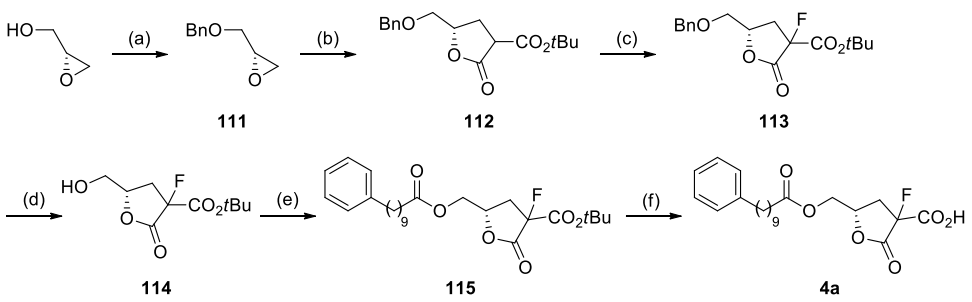

Reagents and conditions: (a) BnBr, NaH, DMF, 0ºC to rt, 18 h, 99%; (b) di-*tert*-butyl malonate, NaH, DMF:THF, 0ºC to 80ºC, 6 h, 62%; (c) Selectfluor®, NaH, DMF:THF, 0ºC to rt, 48 h, 99%; (d) H_2, 10% Pd(C), 60ºC, 90%; (e) **77**, DCC, DMAP, rt, 18 h, 35%; (f) TFA, DCM, rt, 17 h, 90%.

Scheme 23

Malonic acid derivatives **4b**, **c** were prepared by regioselective coupling of the corresponding carboxylic acid and diol **43**. Methylation of the hydroxy group present in the resulting esters **116** and **118** with trimethylsilyldiazomethane followed by removal of the *tert*-butyl groups yielded the desired compounds **4b**, **c** (Schemes 24 and 25).

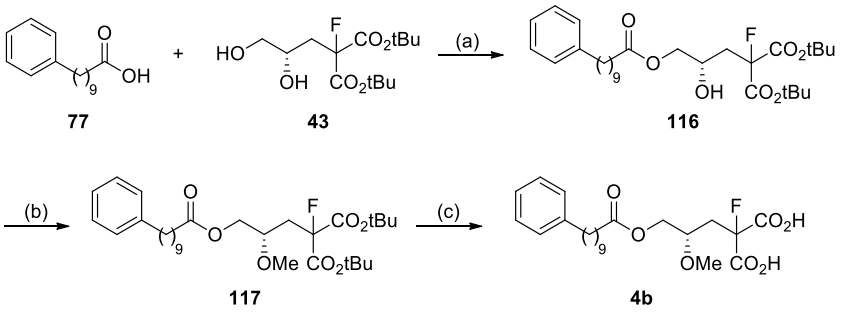

Reagents and conditions: (a) DCC, DMAP, DCM, -20ºC to rt, 17 h, 75%; (b) trimethylsilyldiazomethane, HBF_4, DCM, 0ºC, 90 min, 30%; (c) TFA, DCM, rt, 18 h, 68%.

Scheme 24

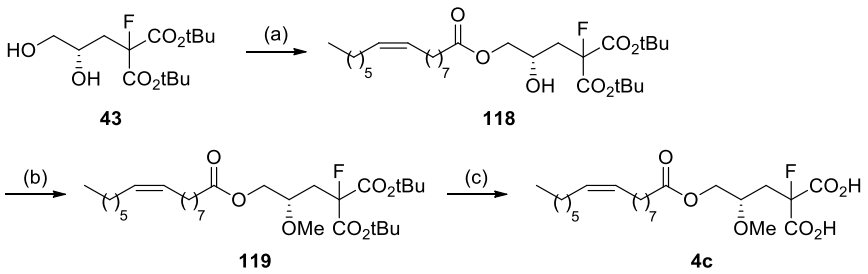

Reagents and conditions: (a) Palmitoleic acid, DCC, DMAP, DCM, -20ºC to rt, 18 h, 44%; (b) trimethylsilyldiazomethane, HBF_4, DCM, 0ºC, 90 min, 27%; (c) TFA, DCM, rt, 19 h, 93%.

Scheme 25

Compounds **4a**-**c** (Table 12) were tested for their activity at LPA_1 receptor. Unfortunately, the results obtained for compounds **4a**, **b** showed that replacement of the oleic acid chain by 10-phenyldecanoic acid is detrimental for activity. Instead, derivative **4c**, bearing a palmitoleic acid chain and malonic acid as polar head was able to activate LPA_1 receptor (E_{max} = 43%, EC_{50} = 1.4 µM).

Table 12. Agonist activities of compounds **4a**-**c** at LPA_1 receptor

Compound	Structure	E_{max} (%)[a]	EC_{50} (µM)[b]
4a	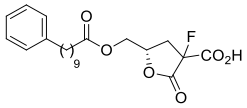	N. E.[c]	-
4b	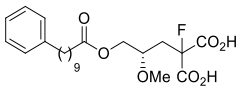	N. E.	-
4c	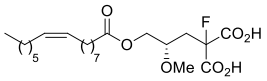	43 ± 6	1.4 ± 0.4
LPA	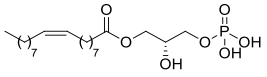	100	0.83 ± 0.02

[a]E_{max} = maximal efficacy of the drug/maximal efficacy of LPA, expressed as the percentage. [b]For E_{max} > 30%, EC_{50} values are expressed as mean ± s.e.m, from a minimum of two independent experiments, performed in triplicate. [c]No effect was observed at the highest concentration of compound tested (10 µM).

In summary, up to this moment we have successfully identified novel agonists with activity at LPA_1 receptor. The two series proposed for mimicking the hydrophobic chain and the polar head of the endogenous ligand LPA have yielded new scaffolds capable to activate the receptor. Regarding the combination process, the identification of compound **4c**, with good activity values, paves the way for further optimization processes.

From all the compounds synthesized so far, derivative **3a** stands out as the first agonist structurally different from the endogenous ligand LPA, with excellent activity values, which was selected for further biological characterization.

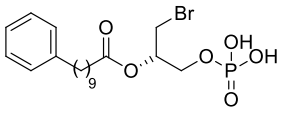

3a

EC_{50} = 0.24 µM

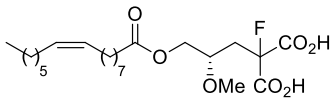

4c

EC_{50} = 1.4 µM

Figure 26

2.3 Determination of the antagonist activity at LPA_1 receptor

The involvement of LPA_1 receptor in diverse biological and pathological processes highlights the need of potent and selective antagonists as useful tools for evaluating these roles. Taking into account the fact that the structural requirements for agonism and antagonism at LPA_1 receptor have not been rationalized yet and that small changes in structure can turn agonists into antagonists and viceversa, all the synthesized compounds which were inactive as agonists at the LPA_1 receptor were screened for their antagonist capacity.

Hence, to determine the antagonist activity of the compounds, RH7777 cells stably transfected with the receptor were preloaded with Fluo 4-NW and then incubated with the compound under study at a fixed dose of 10 µM, followed by the addition of 10 µM LPA. The antagonism was measured as the capacity of the compound to decrease the intensity of LPA response. None of the compounds tested presented antagonist activity over 30% so their dose-response curves were not performed. Positive and negative controls were identical to those employed in previous experiments.

2.4 Selectivity over other LPA receptors

The high sequence homology among the LPA receptors, especially LPA_{1-3}, has hampered the development of high affinity and selective ligands for LPA_1 receptor, also slowing down the elucidation of its biological roles. Therefore, the characterization of the synthesized agonists in this work at each of the LPA receptors is crucial to define their role as tools to be used for the validation of LPA_1 receptor as a therapeutic target.

Towards this aim, cell lines stably overexpressing each of the five LPA receptor subtypes were generated. A B103 neuroblastoma cell line, which does not express LPA receptors intrinsically,[17] was chosen for its transfection with the corresponding plasmid containing LPA_{1-5} receptors fused with the enhanced green fluorescent protein (EGFP). B103 cells expressing high levels of EGFP, and thus of the desired receptor, were isolated by fluorescence-activated cell sorting (FACS). The generation of these cell lines was carried out during a predoctoral stay at Prof. Jerold Chun Lab, at The Scripps Research Institute (La Jolla, California).

Up to this moment, the screening of all the synthesized compounds at the LPA_2 receptor has been completed, being the characterization at the rest of the receptors currently under way in our laboratory. Table 13 shows the compounds active at any of the LPA receptors analysed.

Table 13. Agonist activities of compounds at LPA_1 and LPA_2 receptor

		LPA_1 receptor		LPA_2 receptor	
	Compound	**E_{max} (%)**[a]	**EC_{50} (µM)**[b]	**E_{max} (%)**	**EC_{50} (µM)**
1c	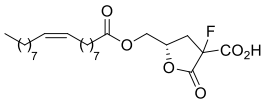	33 ± 5	1.7 ± 0.2	N. E.[c]	-
1g	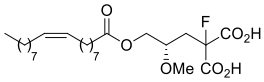	74 ± 14	6 ± 1	N. E.	-
2a	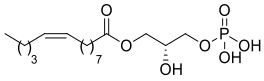	127 ± 1	2.8 ± 0.1	42 ± 5	8.1 ± 0.8
2b	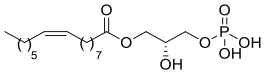	205 ± 9	0.45 ± 0.01	N. E.	-
2c	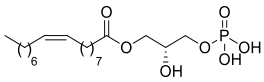	202 ± 1	2.1 ± 0.3	N. E.	-
2d	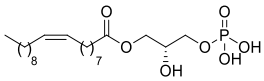	88 ± 2	3.6 ± 0.2	N. E.	-
2h	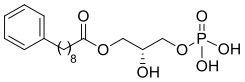	74 ± 4	2.1 ± 0.3	59 ± 2	12 ± 2
2i	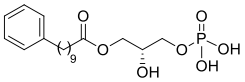	112 ± 3	0.5 ± 0.1	74 ± 6	5.3 ± 0.6
2l	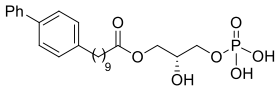	127 ± 9	3.3 ± 0.6	N. E.	-

Table 13 (cont.). Agonist activities of compounds at LPA_1 and LPA_2 receptor

Compound		LPA_1 receptor		LPA_2 receptor	
		E_{max} (%)[a]	EC_{50} (μM)[b]	E_{max} (%)[a]	EC_{50} (μM)[b]
2m	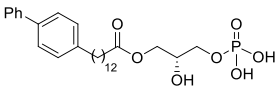	37 ± 1	19 ± 2	N. E.	-
3a	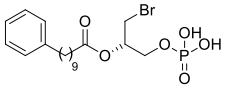	118 ± 24	0.24 ± 0.09	N. E.	-
3c	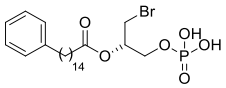	N. E.	-	57 ± 7	5 ± 1
3d	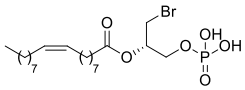	39 ± 3	3.2 ± 0.4	67 ± 8	4.9 ± 0.2
4b	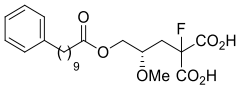	N. E.	-	55 ± 10	4.8 ± 0.1
4c	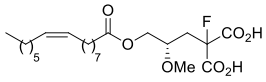	43 ± 6	1.4 ± 0.4	81 ± 1	10.8 ± 0.8

[a]E_{max} = maximal efficacy of the drug/maximal efficacy of LPA, expressed as the percentage. [b]For E_{max} > 30%, EC_{50} values are expressed as mean ± s.e.m, from a minimum of two independent experiments, performed in triplicate. [c]No effect was observed at the highest concentration of compound tested (10 μM).

Among the tested compounds, seven derivatives were able to activate LPA_2 receptor. Compounds **2a**, **2h**, **2i**, **3d**, and **4c** are dual agonists at LPA_{1-2} receptors, and compounds **3c** and **4b** show no activity at LPA_1 receptor. It must be remarked that compounds **1c**, **1g**, **2b**-**d**, **2l**, **2m**, and especially **3a**, are inactive at LPA_2 receptor.

These results indicate that slight differences in structure can render important changes in activity, also between receptors, fact that highlights the difficulty to obtain selective ligands for a particular LPA receptor subtype.

2.5 Biological characterization of compound 3a

In order to verify whether compound **3a**, which has been identified as a good LPA_1 agonist by calcium mobilization assay, and which is selective over LPA_2 receptor, is really acting at the LPA_1 receptor, a set of additional cellular experiments was performed. Compound **1c**, with moderate activity at LPA_1 and selective over LPA_2, was also tested for comparison. The existence of a correlation between the *in vitro* agonism and the cellular effects is the first and necessary step towards a complete biological characterization that would continue with diverse *in vivo* studies in the target validation process.

LPA_1 activation induces a range of well known cellular responses, from which cell migration[106] or cytoskeletal changes[17] stand out as they are implicated in diverse processes such as cancer, angiogenesis, fibrosis or neurodegenerative disorders. In B103 neuroblastoma cells, LPA induces neurite retraction with cells acquiring a rounded shape. Receptor internalization after stimulation with an agonist, characteristic of GPCRs, was also measured.[107]

2.5.1 Neurite retraction

B103 neuroblastoma cells overexpressing LPA_1 receptor and tagged with EGFP were exposed to different concentrations of compounds **1c** and **3a**. Then, they were fixed and stained with phalloydin and DAPI (4',6-diamidino-2-phenylindole) for cell morphology and the number of cells with retracted neurites and the number of total cells were counted. 1 µM LPA was employed as positive control, and 0.1% fatty acid free bovine serum albumin (FAF BSA) as negative control (Figure 27).

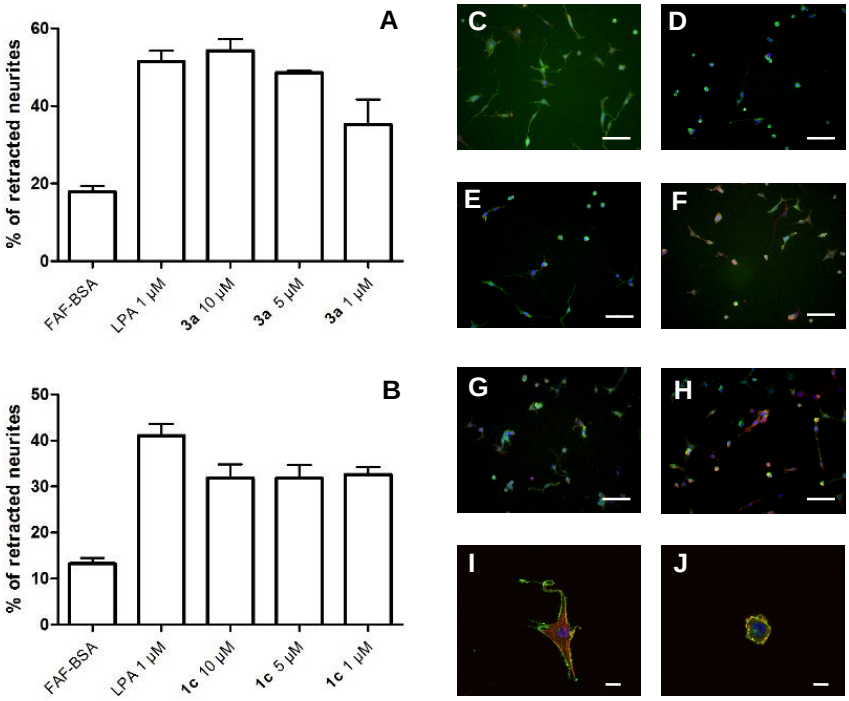

Figure 27. Neurite retraction induced by **3a** and **1c**. Percentage of retracted neurites at 10, 5 or 1 µM for compound **3a** (A) and **1c** (B). Visualization of neurite retraction: control 0.1% FAF BSA (C), 1 µM LPA (D), 10 µM **3a** (E), 1 µM **3a** (F), 10 µM **1c** (G), 1 µM **1c** (H). Representative images of neurite retraction: 0.1% FAF BSA (I), 10 µM **3a** (J). Samples were imaged under the same conditions by using a Zeiss fluorescence microscope (C-H, bars 100 µm) or Zeiss fluorescence confocal microscope (I-J, bars 10 µm).

Figures 27 A and 27 B show the percentage of retracted neurites for each of the compounds tested, with derivative **3a** exhibiting similar response to LPA at a 10 µM concentration, and also a dose-dependent response at the different concentrations assayed. As expected from its lower agonist activity, derivative **1c** does not reach LPA effects even at the highest dose tested (10 µM).

2.5.2 Cell migration

B103 neuroblastoma cells overexpressing LPA_1 receptor were seeded into the upper chamber of a permeable membrane, and compounds **1c** and **3a** and controls were placed in the lower chamber. After 5 h of incubation, migrated cells were stained and quantified under a microscope (Figures 28 and 29).

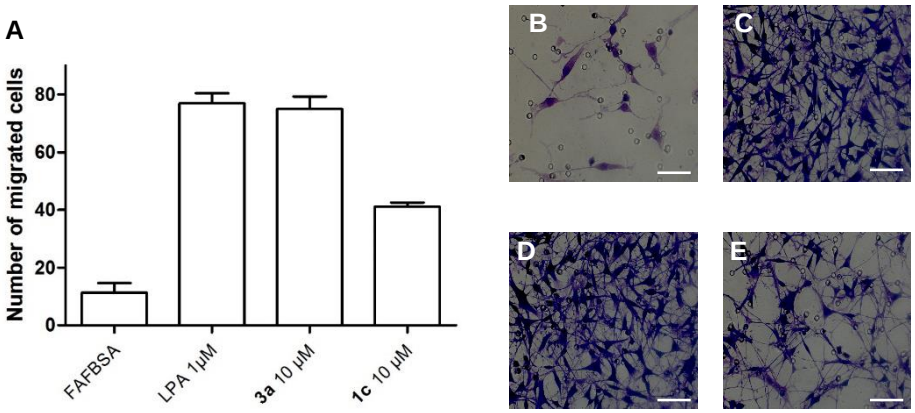

Figure 28. Migration experiment for compounds **3a** and **1c** at 10 µM. Number of migrated cells (A). Visualization of migrated cells (B-E): 0.1% FAF BSA (B), 1 µM LPA (C), 10 µM **3a** (D), 10 µM **1c** (E). Samples were imaged under the same conditions by using a Zeiss microscope (bars 50 µm). Cells were stained with 0.1% crystal violet solution.

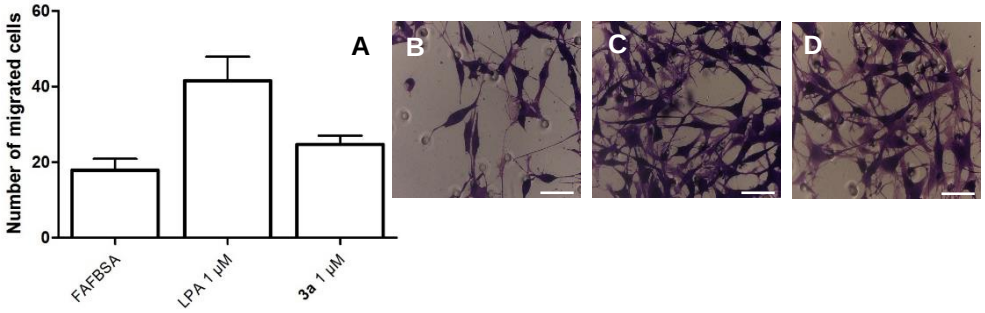

Figure 29. Migration experiment for compound **3a** at 1 µM. Number of migrated cells (A). Visualization of migrated cells (B-D): 0.1% FAF BSA (B), 1 µM LPA (C), 1 µM **3a** (D). Samples were imaged under the same conditions by using a Zeiss microscope (bars 50 µm). Cells were stained with 0.1% crystal violet solution.

Again, it was verified that, at the highest concentration tested, compound **3a** response is similar to LPA whereas derivative **1c** does not reach the same levels, according to their EC_{50} values. **3a** was also tested at 1 µM, and a decrease in the response was observed, in accordance with a dose-dependent behaviour.

2.5.3 Receptor internalization

B103 neuroblastoma cells overexpressing LPA_1 receptor were exposed to compounds **3a** or **1c** at concentrations ranging from 0.1 µM to 10 µM. LPA (1 µM) was employed as positive control and 0.1% FAF BSA as negative control. After fixing and staining the cells, their images were acquired with a confocal microscope. Both derivatives were able to induce internalization of the receptor at all the concentrations assayed. Figure 30 shows representative examples.

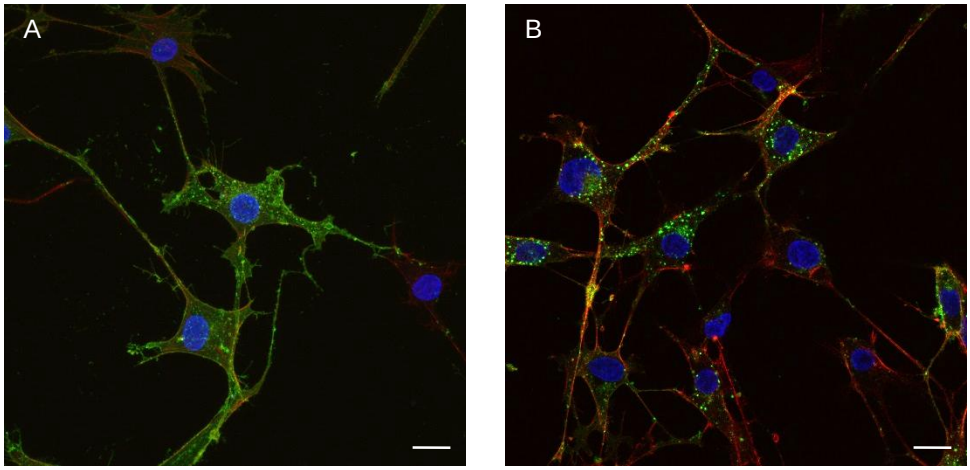

Figure 30. Visualization of receptor internalization. Compound **3a**, 1 µM (A). LPA, 1 µM (B). Cells were stained with DAPI and phalloydin for cell morphology. Samples were imaged under the same conditions by using a Zeiss fluorescence confocal microscope (bars 10 µm).

All in sum, these assays have helped to confirm the action of derivative **3a** at the LPA_1 receptor, not only *in vitro* but also at the cellular level, underscoring its significance as a promising hit with good activity and selectivity values.

3. CONCLUSIONS

1. In this work we have carried out the design and synthesis of new ligands for the LPA_1 receptor using as starting point the endogenous ligand, LPA. Both the polar head and the hydrophobic chain of LPA have been successfully mimicked by other moieties, thus paving the way for the development of structurally novel LPA_1 receptor ligands.

2. Five cell lines overexpressing the different LPA receptor subtypes LPA_{1-5} have been generated to enable the study of the complete selectivity profile within the LPA receptor family.

3. All the synthesized compounds have been evaluated for their functional activity at the LPA_1 receptor as well as for their selectivity at the LPA receptor family. Among all of them, compound **3a** stands out as a LPA_1 receptor agonist more potent than LPA. In addition, **3a** is selective against other LPA receptor subtypes such as LPA_2, and it is active in cellular assays, where it induces similar effects to LPA.

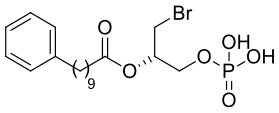

3a

E_{max} (LPA_1) = 118%; EC_{50} (LPA_1) = 0.24 µM
EC_{50} (LPA_2) > 10 µM

EXPERIMENTAL SECTION

4. EXPERIMENTAL SECTION

4.1 Synthesis

Unless otherwise stated, the starting materials, reagents, and solvents used were high-grade commercial products from Sigma-Aldrich, ABCR, Acros, Biotage, Fluka, Lancaster, Scharlab, or Panreac. Dichloromethane, diethyl ether and tetrahydrofuran (THF), were dried using a Pure Solv™ Micro 100 Liter solvent purification system. Triethylamine and pyridine were dried over CaH_2 and distilled prior to its use. Alcohol-free chloroform was obtained by washing with water, drying over $MgSO_4$, filtration and distillation over P_2O_5. Ethylenediamine was dried over 4Å molecular sieves, distilled and used immediately. All non-aqueous reactions were performed under an argon atmosphere in oven-dried glassware.

Analytical thin-layer chromatography (TLC) was run on Merck silica gel plates (Kieselgel 60 F-254), with detection by UV light (λ = 254 nm), ninhydrin solution, or 10% phosphomolybdic acid solution in ethanol. Flash chromatography was performed on glass column using Merck silica gel type 60 (particle size 230-400 mesh), or on a Varian 971-FP flash purification system, using silica gel cartridges (Varian, particle size 50 µm).

All compounds were obtained as oils, except for those whose melting points (m.p.) are indicated, which were solids. M.p. were determined on a Stuart Scientific electrothermal apparatus. Infrared (IR) spectra were measured on a Bruker Tensor 27 instrument equipped with a Specac ATR accessory of 5200-650 cm^{-1} transmission range; frequencies (ν) are expressed in cm^{-1}. Optical rotation [α] was measured on a Perkin Elmer 241 polarimeter using a sodium lamp (λ = 589 nm) with a 1 dm path length; concentrations are given as g/100 mL. ^{1}H, ^{13}C and ^{31}P Nuclear Magnetic Resonance (NMR) spectra were recorded on a Bruker Avance III 700MHz (^{1}H, 700 MHz; ^{13}C, 175 MHz), Bruker Avance 500MHz (^{1}H, 500 MHz; ^{13}C,

125 MHz, ^{31}P, 202 MHz) or Bruker DPX 300MHz (^{1}H, 300 MHz; ^{13}C, 75 MHz, ^{31}P, 121 MHz) instrument at room temperature at the UCM's NMR core facility. Chemical shifts (δ) are expressed in parts per million relative to internal tetramethylsilane; coupling constants (*J*) are in hertz (Hz). The following abbreviations are used to describe peak patterns when appropriate: s (singlet), d (doublet), t (triplet), q (quartet), qt (quintuplet), m (multiplet), dd (double doublet), dt (double triplet), td (triple doublet), app (apparent) and br (broad). 2D NMR experiments (COSY, HMQC and HMBC) of representative compounds were carried out to assign protons and carbons of the new structures. High resolution mass spectrometry (HRMS) was carried out on a FTMS Bruker APEX Q IV spectrometer in electrospray ionization (ESI) or matrix-assisted laser desorption/ionization (MALDI) mode at UCM's mass spectrometry core facility. For all final compounds, purity was determined by high-performance liquid chromatography coupled to mass spectrometry (HPLC-MS), and satisfactory chromatograms confirmed a purity of at least 95% for all tested compounds. HPLC-MS analysis was performed using an Agilent 1200LC-MSD VL instrument. LC separation was achieved with a Zorbax Eclipse XDB-C18 column (5 μm, 4.6 mm x 150 mm) or Zorbax SB-C3 (5 μm, 2.1 mm x 50 mm) together with a guard column (5 μm, 4.6 mm x 12.5 mm). The gradient mobile phases consisted of A (95:5 water/acetonitrile or water/methanol) and B (5:95 water/acetonitrile or water/methanol) with 0.1% ammonium hydroxide and 0.1% formic acid as the solvent modifiers, and the gradients are indicated in Table 15. MS analysis was performed with an ESI source. The capillary voltage was set to 3.0 kV and the fragmentor voltage was set at 25 eV. The drying gas temperature was 350 ºC, the drying gas flow was 10 L/min, and the nebulizer pressure was 20 psi.

Table 14. HPLC gradients

Method A		**Method B**	
Column SB-C3 Buffers water/acetonitrile		Column XDB-C18 Buffers water/methanol	
t (min)	**% B**	**t (min)**	**% B**
0	0	0	0
2	0	2	0
8	60	10	50
20	100	20	100
25	100	50	100
30	0	60	0

4.1.1 General procedures

4.1.1.1 Hydrogenation of alkenes and deprotection of dibenzyl phosphates and benzyl ethers

The corresponding alkene or benzylated derivative was dissolved in ethanol (0.2 mL/mg) and the solution was pumped through a H-Cube® continuous-flow hydrogenation reactor using a 10% Pd/C CatCart® cartridge, under full-H_2 mode at a flow-rate of 1 mL/min at room temperature (for alkenes and dibenzyl phosphates) or 60°C (for benzyl ethers). Solvent was then removed under reduced pressure to afford the corresponding compound in quantitative yield that was used without further purification.

4.1.1.2 Mesylation of alcohols

To a cooled (0°C) stirred solution of the corresponding alcohol (1 equiv) and triethylamine (3 equiv) in anhydrous dichloromethane (3.5 mL/mmol), methanesulfonyl chloride (1.5 equiv) was added dropwise. The reaction mixture was stirred at 0°C for 10 minutes and then at room temperature for 1 h. Afterward, the mixture was partitioned between ethyl acetate and brine. The organic layer was separated, washed with a saturated aqueous solution of $NaHCO_3$ and with brine, dried over Na_2SO_4, filtered and concentrated under reduced pressure to yield the corresponding mesylate, which was used in the next step without further purification.

4.1.1.3 Alkylation with di-*tert*-butyl malonate

Di-*tert*-butyl malonate (1.5 equiv) was added dropwise to a stirred suspension of NaH (1.5 equiv, 60% dispersion in oil) in a 2:1 mixture of anhydrous DMF/THF (6 mL/mmol) at 0ºC, and the mixture was stirred at room temperature for 15 minutes. A solution of the corresponding mesylate (1 equiv) in anhydrous THF (3 mL/mmol) was added, followed by NaI (1.1 equiv), and the resulting mixture was heated at 80ºC overnight. Afterward, the reaction was cooled to room temperature and quenched by addition of a saturated aqueous solution of NH_4Cl. The mixture was then diluted with water, and extracted with ethyl acetate. The organic phase was washed with brine, dried over Na_2SO_4, filtered and evaporated under reduced pressure. The residue was purified by flash chromatography to afford the corresponding alkylated product.

4.1.1.4 α-Fluorination of malonate derivatives using Selectfluor®

The corresponding malonate derivative (1 equiv) was added to a suspension of NaH (2 equiv, 60% dispersion in oil) in anhydrous THF (4 mL/mmol) at 0ºC, and the reaction mixture was warmed up to room temperature and then stirred at 70°C for 12 h. The solution was cooled to room temperature and diluted with anhydrous THF (8 mL/mmol) and *N,N*-dimethylformamide (DMF) (8 mL/mmol). Afterward, Selectfluor® was added (2 equiv) at 0ºC and the solution was stirred at this temperature for 4h and at room temperature overnight. The reaction mixture was quenched by addition of water and extracted with diethyl ether. The organic layer was dried over Na_2SO_4, filtered and concentrated under reduced pressure. The residue was purified by flash chromatography to afford the corresponding fluorinated derivative.

4.1.1.5 Deprotection of acetals using polystyrene-supported *p*TsOH

The corresponding acetal (1 equiv) was dissolved in methanol (3 mL/g resin) and the polystyrene-supported *p*TsOH (PS-*p*TsOH) was added (0.3 equiv, 4.56 mmol *p*TsOH/g resin). The reaction was stirred at room temperature overnight. Afterward, the mixture was filtered and the solvent was evaporated under reduced pressure. The crude was purified by flash chromatography to afford the corresponding diol.

4.1.1.6 Regioselective esterification of oleoyl chloride with diols

To a stirred suspension of the corresponding alcohol (1.5 equiv) in anhydrous dichloromethane (12 mL/mmol alcohol) at -78°C, 2,4,6-collidine (2 equiv) and

oleoyl chloride (1 equiv) were added. The mixture was stirred for 24 h while gradually warming to room temperature. After this time, solvent was evaporated under reduced pressure and the residue was treated with ethyl acetate, removing the 2,4,6-collidine hydrochloride by filtration. The filtrate was concentrated and the crude was purified by flash chromatography to yield the corresponding ester.

4.1.1.7 Deprotection of *tert*-butyl esters and alkyl di-*tert*-butyl phosphates

TFA (25 or 75 equiv) was added to a solution of the corresponding *tert*-butyl derivative (1 equiv) in anhydrous dichloromethane (20 mL/mmol) and the reaction was stirred at room temperature until disappearance of the starting material. The mixture was then treated with brine and the aqueous phase was extracted with dichloromethane. The combined organic layers were washed with water and brine, dried over Na_2SO_4 and filtered. The solvent was evaporated under reduced pressure to afford the corresponding phosphate or carboxylic acid.

4.1.1.8 Methylation of alcohols with trimethylsilyldiazomethane

To a vigorously stirred mixture of the corresponding alcohol (1 equiv) and HBF_4 (1 equiv, 35% aqueous solution) in anhydrous dichloromethane (4 mL/mmol) at 0ºC, trimethylsilyldiazomethane (1 equiv, 2 M in diethyl ether) was added dropwise, waiting for the yellow colour to disappear before each addition. The stirring was continued at 0ºC and three further portions of trimethylsilyldiazomethane (0.5 equiv, 0.25 equiv and 0.25 equiv) were added dropwise at intervals of 20 min. Afterward, the mixture was stirred at 0ºC for further 30 min, poured into water and extracted with dichloromethane. The organic layer was washed with water, dried over $MgSO_4$, filtered and concentrated under reduced pressure. The residue was purified by flash chromatography to afford the pure compound.

4.1.1.9 Sonogashira coupling reaction of alkynes with methyl-8-bromooctanoate

1,3-bis(1-adamantyl)imidazolium chloride (0.15 equiv), CuI (0.225 equiv), $[(\pi\text{-allyl})PdCl]_2$ (0.075 equiv), and Cs_2CO_3 (1.4 equiv) were added in turn to a thoroughly dried vial. A mixture of anhydrous diethyl ether (1 mL/mmol ester) and DMF (0.5 mL/mmol ester) was added, followed by the alkyne (1.3 equiv) and methyl-8-bromooctanoate (1 equiv). The vial was sealed with a Teflon-lined cap and the heterogeneous reaction mixture was stirred vigorously at 55ºC for 16 hours. The solvents were then evaporated under reduced pressure and the residue was purified by flash chromatography to yield the corresponding alkyne.

4.1.1.10 Stereoselective *cis*-hydrogenation of alkenes with P-2 nickel catalyst

$Ni(OAc)_2 \cdot 4H_2O$ (0.2 equiv) was suspended in absolute ethanol (3 mL/mmol alkyne) at room temperature. $NaBH_4$ (0.2 equiv) was added and the mixture was stirred for 15 min. Then, argon atmosphere was replaced by H_2 (balloon). Freshly distilled ethylenediamine was added (1.5 equiv) and the reaction was stirred for 15 minutes. A solution of the corresponding alkyne (1 equiv) in absolute ethanol (3 mL/mmol) was then added, and the reaction was stirred under a H_2 atmosphere at room temperature for 2 h. After this time, the reaction mixture was filtered through a pad of Celite, and the solvent was removed under reduced pressure. The residue was redissolved in ethyl acetate and washed with water and brine. The organic layer was dried over Na_2SO_4, filtered and concentrated to afford the corresponding *Z*-alkene, which was used in the next step without further purification.

4.1.1.11 Hydrolysis of methyl esters

The corresponding methyl ester (1 equiv) was dissolved in THF (10 mL/mmol) and a solution of LiOH (2 equiv) in water (1.5 mL/mmol) was added. The reaction was stirred at room temperature overnight. Then, the mixture was acidified with a 20% aqueous solution of HCl and extracted with dichloromethane. The organic phase was dried over Na_2SO_4, filtered and concentrated, affording the corresponding carboxylic acid in quantitative yield.

4.1.1.12 Phosphorylation of alcohols using phosphoramidites

To a solution of the corresponding alcohol (1 equiv) in anhydrous dichloromethane (12 mL/mmol), 1*H*-tetrazole (3 equiv, 0.45 M in acetonitrile) and the corresponding phosphoramidite (2 equiv) were added at room temperature and the reaction mixture was stirred until disappearance of the alcohol. Then it was cooled to -30ºC, *m*CPBA (2 equiv) was added and the mixture was stirred at -30ºC for 90 min. The reaction was quenched by addition of a 10% aqueous solution of $Na_2S_2O_3$ (12 mL/mmol alcohol) and allowed to warm to room temperature. Then, the mixture was extracted with dichloromethane, the extracts were successively washed with a 20% aqueous solution of K_2CO_3 and brine, dried over $MgSO_4$, filtered and concentrated under reduced pressure. The residue was purified by flash chromatography to afford the corresponding pure phosphate.

4.1.1.13 Regioselective esterification of carboxylic acids with diols

To a solution of the corresponding carboxylic acid (1 equiv), DCC (1.1 equiv) and DMAP (0.2 equiv) in anhydrous dichloromethane (10 mL/mmol acid) at -20ºC,

a solution of the corresponding diol (2 equiv) in anhydrous dichloromethane (2 mL/mmol) was added and the reaction was warmed to room temperature and stirred overnight. Afterward, the mixture was concentrated under reduced pressure, and the residue was redissolved in CCl_4 and filtered to remove dicyclohexylurea. The filtrate was evaporated and purified by flash chromatography to afford the corresponding pure ester.

4.1.1.14 Oxidation of alcohols with nitric acid

To a cooled (0ºC) solution of fuming nitric acid (50 equiv), the corresponding bromoalcohol (1 equiv) was added over a period of 30 minutes, maintaining the reaction temperature at 25-30ºC. The solution was stirred at room temperature for 4 h and then at 80ºC for an additional hour. The reaction mixture was then cooled back to room temperature, diluted carefully with water, and extracted with ethyl acetate. The organic phase was dried over $MgSO_4$, filtered, and the solvent was evaporated under reduced pressure. Flash chromatography afforded the corresponding carboxylic acid.

4.1.1.15 Wittig reaction of ω-bromoacids and aromatic aldehydes

A mixture of the corresponding ω-bromoacid (1.2 equiv) and triphenylphosphine (6 equiv) in anhydrous toluene (2.4 mL/mmol) was refluxed for 24 h. Then, the mixture was allowed to cool to room temperature, the solvent was evaporated and the residue was washed with hexane to remove excess triphenylphosphine, and dried. The obtained phosphonium salt (1.2 equiv) was dissolved in anhydrous THF (4.2 mL/mmol), and lithium hexamethyldisilazane (2.7 equiv, 1 M in toluene) was added dropwise at -20ºC, turning the solution orange. The mixture was stirred for 30 min followed by addition of the corresponding aldehyde (1 equiv) at -20ºC and the stirring was continued overnight at room temperature. The reaction mixture was acidified with 1 M HCl and extracted with ethyl acetate. The organic layer was dried over Na_2SO_4, filtered and concentrated under reduced pressure. The crude was purified by flash chromatography to yield the corresponding alkene.

4.1.1.16 Ring-opening of epoxides with TBABr

To a solution of the corresponding oxirane (1 equiv) and TBABr (3 equiv) in freshly distilled alcohol-free chloroform (10 mL/mmol), TFA (1.5 equiv) was added and the reaction was stirred for 10 minutes at room temperature. Then, the reaction mixture was passed through a silica gel column (5 g/mmol) prepared in

chloroform and it was washed with the same solvent (100 mL/mmol). The solvent was evaporated under reduced pressure to give the corresponding bromoalcohol, which was used in the next step without further purification.

4.1.1.16 Esterification of carboxylic acids with bromoalcohols and primary alcohols

To a stirred solution of the corresponding carboxylic acid (1 equiv), DCC (1.1 equiv) and DMAP (0.2 equiv) in anhydrous dichloromethane (10 mL/mmol), a solution of the corresponding alcohol (1 equiv) in anhydrous dichloromethane (2 mL/mmol) was added at room temperature and the reaction was stirred overnight. Afterward, the mixture was concentrated under reduced pressure, and the residue was redissolved in CCl_4 and filtered to remove dicyclohexylurea. The filtrate was concentrated and it was purified by flash chromatography to yield the corresponding ester.

*4.1.2 Synthesis of final compounds **1a**-**f***

4.1.2.1 Synthesis of diol **38**

tert-Butyl {[(2*R*)-2,3-bis(benzyloxy)propyl]oxy}acetate, 37

(*S*)-(-)-2,3-bis(benzyloxy)propan-1-ol (0.56 mL, 2.20 mmol, 1 equiv) was added dropwise to a stirred suspension of NaH (176 mg, 4.40 mmol, 2 equiv, 60% dispersion in oil) in anhydrous THF (10 mL) at 0°C. After stirring the mixture at room temperature for 30 minutes, *tert*-butyl bromoacetate (0.49 mL, 3.31 mmol, 1.5 equiv) and TBAI (41 mg, 0.11 mmol, 0.05 equiv) were added, and the resulting mixture was heated at 50°C overnight. After cooling to room temperature, the reaction was quenched by addition of water and concentrated under reduced pressure. The residue was dissolved with dichloromethane, washed with brine, dried over Na_2SO_4, filtered and the solvents were removed under reduced pressure. Flash chromatography of the residue (hexane/ethyl acetate, 9:1 to 8:2) afforded pure compound **37** in 22% yield.

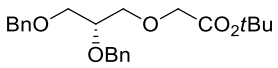

37

R_f: 0.52 (hexane/ethyl acetate, 8:2)
IR (ATR): 1738 (C=O)
^{1}H-NMR ($CDCl_3$, 300 MHz): δ 1.36 (s, 9H, $3CH_3$); 3.47-3.65 (m, 4H, $2CH_2$); 3.72 (qt, J = 4.7, 1H, CH); 3.88 (s, 2H, CH_2CO_2tBu); 4.44 (s, 2H, $PhCH_2$); 4.61 (s, 2H, $PhCH_2$); 7.11-7.29 (m, 10H, $10CH_{Ar}$)

^{13}C-NMR ($CDCl_3$, 75 MHz): δ 28.1 ($3CH_3$); 69.4 (CH_2); 70.4 (CH_2); 71.7 (CH_2); 72.3 (Ph$\underline{C}H_2$); 73.4 (Ph$\underline{C}H_2$); 77.4 (CH); 81.5 (C); 127.5 (CH_{Ar}); 127.6 (CH_{Ar}); 127.7 ($2CH_{Ar}$); 127.8 ($2CH_{Ar}$); 128.3 ($2CH_{Ar}$); 128.4 ($2CH_{Ar}$); 138.4; 138.8 ($2C_{Ar}$); 169.6 (CO)
MS (ESI, *m/z*): 387.7 $[M+H]^+$

***tert*-Butyl {[(2*R*)-2,3-dihydroxypropyl]oxy}acetate, 38**

Following the general procedure 4.1.1.1, diol **38** was obtained from **37** (190 mg, 0.49 mmol) at 60ºC in quantitative yield.

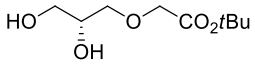

38

R_f: 0.11 (hexane/ethyl acetate, 8:2)
IR (ATR): 3376 (O-H); 1738 (C=O)
^{1}H-NMR (methanol-d_4, 300 MHz): δ 1.49 (s, 9H, $3CH_3$); 3.50-3.64 (m, 4H, $2CH_2$); 3.78 (qt, *J* = 5.3, 1H, CH); 4.87 (s, 2H, $C\underline{H}_2CO_2t$Bu)
^{13}C-NMR ($CDCl_3$, 75 MHz): δ 28.1 ($3CH_3$); 63.7 (CH_2OH); 68.8 ($\underline{C}H_2CO_2t$Bu); 70.5 (CH); 73.4 (CH_2O); 82.5 (C); 170.6 (CO)
MS (ESI, *m/z*): 229.1 $[M+Na]^+$

4.1.2.2 Synthesis of diols **41** and **43**

(2*R*)-2,3-Bis(benzyloxy)propyl methanesulfonate, 39

Following the general procedure 4.1.1.2, mesylate **39** was obtained from (*S*)-(-)-2,3-bis(benzyloxy)propan-1-ol (0.35 mL, 1.39 mmol) in 80% yield.

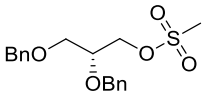

39

R_f: 0.51 (hexane/ethyl acetate, 7:3)
IR (ATR): 1354 (SO_2)
^{1}H-NMR ($CDCl_3$, 300 MHz): δ 2.95 (s, 3H, CH_3); 3.60 (dd, *J* = 4.8, 1.5, 2H, $C\underline{H}_2$OBn); 3.86 (m, 1H, CH); 4.31 (dd, *J* = 11.0, 5.6, 1H, ½$C\underline{H}_2$OMs); 4.43 (dd, *J* =11.0, 3.7, 1H, ½$C\underline{H}_2$OMs); 4.54 (s, 2H, Ph$C\underline{H}_2$); 4.66 (s, 2H, Ph$C\underline{H}_2$); 7.27-7.39 (m, 10H, $10CH_{Ar}$)

^{13}C-NMR ($CDCl_3$, 75 MHz): δ 37.5 (CH_3); 68.5 (CH_2); 69.4 (CH_2); 72.5 (PhCH_2); 73.6 (PhCH_2); 75.7 (CH); 127.8 (2CH_{Ar}); 127.9 (2CH_{Ar}); 127.91 (2CH_{Ar}); 128.0 (2CH_{Ar}); 128.5 (2CH_{Ar}); 137.7 (2C_{Ar})
MS (ESI, *m/z*): 368.2 $[M+NH_4]^+$

Di-*tert*-butyl [(2*S*)-2,3-bis(benzyloxy)propyl]malonate, 40

Following the general procedure 4.1.1.3, compound **40** was obtained from mesylate **39** (391 mg, 1.12 mmol) in 76% yield. Chromatography: hexane to hexane/ethyl acetate, 9:1.

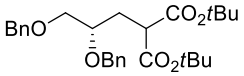

40

R_f: 0.65 (hexane/ethyl acetate, 9:1)
IR (ATR): 1727 (C=O)
^{1}H-NMR ($CDCl_3$, 300 MHz): δ 1.42 (s, 9H, 3CH_3); 1.45 (s, 9H, 3CH_3); 2.04-2.10 (m, 2H, CH_2CH(CO_2tBu)$_2$); 3.46 (dd, *J* = 8.9, 6.0, 1H, CH(CO_2tBu)$_2$); 3.55 (dd, *J* = 4.8, 0.8, 2H, CH_2OBn); 3.62-3.68 (m, 1H, CHOBn); 4.53 (d, *J* = 11.5, 1H, ½PhCH_2); 4.54 (s, 2H, PhCH_2); 4.69 (d, *J* = 11.5, 1H, ½PhCH_2); 7.31-7.38 (m, 10H, 10CH_{Ar})
^{13}C-NMR ($CDCl_3$, 75 MHz): δ 27.9 (3CH_3); 28.0 (3CH_3); 31.3 (CH_2CH(CO_2tBu)$_2$); 50.4 (CH(CO_2tBu)$_2$); 72.4 (PhCH_2); 72.8 (PhCH_2); 73.4 (CH_2OBn); 76.0 (CHOBn); 81.4 (2C); 127.55 (CH_{Ar}); 127.58 (CH_{Ar}); 127.6 (2CH_{Ar}); 127.9 (2CH_{Ar}); 128.3 (2CH_{Ar}); 128.4 (2CH_{Ar}); 138.6 (2C_{Ar}); 169.0 (2CO)
MS (ESI, *m/z*): 471.2 $[M+H]^+$

Di-*tert*-butyl [(2*S*)-2,3-dihydroxypropyl]malonate, 41

Following the general procedure 4.1.1.1, diol **41** was obtained from **40** (327 mg, 0.74 mmol) at 60ºC in quantitative yield.

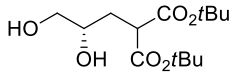

41

R_f: 0.37 (hexane/ethyl acetate, 8:2)
IR (ATR): 3408 (O-H); 1726 (C=O)
^{1}H-NMR (methanol-d_4, 300 MHz): δ 1.46 (s, 9H, 3CH_3); 1.47 (s, 9H, 3CH_3); 1.76 (ddd, *J* = 14.8, 9.6, 5.3, 1H, ½CH_2CH(CO_2tBu)$_2$); 2.02 (ddd, *J* = 14.8, 9.5, 3.3, 1H, ½CH_2CH(CO_2tBu)$_2$); 3.39-RN3.48 (m, 3H, CH_2OH, CH(CO_2tBu)$_2$); 3.52-3.63 (m, 1H, CHOH)

^{13}C-NMR (methanol-d_4, 75 MHz): δ 28.2 ($3CH_3$); 28.23 ($3CH_3$); 33.7 ($CH_2CH(CO_2tBu)_2$); 52.0 ($CH(CO_2tBu)_2$); 67.4 (CH_2OH); 70.9 (CHOH); 82.7 (2C); 170.4 (CO); 170.8 (CO)
MS (ESI, *m/z*): 289.1 $[M-H]^-$

Di-*tert*-butyl [(2*S*)-2,3-bis(benzyloxy)propyl](fluoro)malonate, 42

Following the general procedure 4.1.1.4, compound **42** was obtained from **40** (400 mg, 0.85 mmol) in 48% yield. Chromatography: hexane to hexane/ethyl acetate, 8:2.

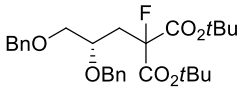

42

R_f: 0.53 (hexane/ethyl acetate, 8:2)
IR (ATR): 1736 (C=O); 1148 (C-F)
^{1}H-NMR ($CDCl_3$, 300 MHz): δ 1.35 (s, 9H, $3CH_3$); 1.45 (s, 9H, $3CH_3$); 2.24-2.38 (m, 2H, CH_2CF); 3.53 (d, *J* = 4.8, 2H, CH_2OBn); 3.85-3.93 (m, 1H, CH); 4.51 (d, *J* = 11.3, 1H, ½$PhCH_2$); 4.51 (s, 2H, $PhCH_2$); 4.60 (d, *J* = 11.3, 1H, ½$PhCH_2$); 7.28-7.33 (m, 10H, $10CH_{Ar}$)
^{13}C-NMR ($CDCl_3$, 75 MHz): δ 27.7 ($3CH_3$); 27.8 ($3CH_3$); 36.6 (CH_2CF); 72.6 ($PhCH_2$); 73.0 ($PhCH_2$); 73.3 (CH_2OBn); 74.7 (CH); 82.4; 82.8 ($2C(CH_3)_3$); 127.5 (CH_{Ar}); 127.5 (CH_{Ar}); 127.6 ($2CH_{Ar}$); 128.1 ($2CH_{Ar}$); 128.32 ($2CH_{Ar}$); 128.33 ($2CH_{Ar}$); 138.35 (C_{Ar}); 138.7 (C_{Ar}); 169.4 (CO); 170.1 (CO); (CF not observed)
MS (ESI, *m/z*): 506.3 $[M+NH_4]^+$

Di-*tert*-butyl [(2*S*)-2,3-dihydroxypropyl](fluoro)malonate, 43

Following the general procedure 4.1.1.1, diol **43** was obtained from **42** (211 mg, 0.43 mmol) at 60ºC in quantitative yield.

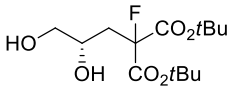

43

R_f: 0.14 (hexane/ethyl acetate, 8:2)
IR (ATR): 3407 (O-H); 1743 (C=O); 1154 (C-F)
^{1}H-NMR ($CDCl_3$, 300 MHz): δ 1.51 (s, 18H, $6CH_3$); 2.18 (dt, *J* = 15.3, 3.0, 1H, ½CH_2F); 2.34 (ddd, *J* = 15.3, 9.2, 9.0, 1H, ½CH_2F); 2.91-3.20 (br s, 2H, 2OH); 3.50 (dd, *J* = 11.3, 6.8, 1H, ½CH_2OH); 3.65 (dd, *J* = 11.3, 3.3, 1H, ½CH_2OH); 3.96-4.06 (m, 1H, CH)

^{13}C-NMR ($CDCl_3$, 75 MHz): δ 27.7 ($3CH_3$); 27.75 ($3CH_3$); 37.2 (d, *J* = 20.8, $\underline{C}H_2CF$); 66.5 (CH_2OH); 67.3 (d, *J* = 2.8, CH); 83.9 ($2\underline{C}(CH_3)_3$); 93.4 (d, *J* = 196.0, CF); 165.3 (d, *J* = 25.0, CO); 165.8 (d, *J* = 26.1, CO)

4.1.2.3 Synthesis of diol **46**

[(4*R*)-2,2-Dimethyl-1,3-dioxolan-4-yl]methyl 4-methylbenzenesulfonate, 44

To a solution of (*S*)-(2,2-dimethyl-1,3-dioxolan-4-yl)methanol (0.5 mL, 4.05 mmol, 1 equiv) in 5 mL of dry dichloromethane, pyridine (0.98 mL, 12.15 mmol, 3 equiv) was added. The reaction mixture was cooled to 0ºC, tosyl chloride (1.16 g, 6.07 mmol, 1.5 equiv) was added and the mixture was stirred overnight at room temperature. Afterward, brine was added and the organic phase was separated, dried over Na_2SO_4, filtered and concentrated under reduced pressure. The residue was purified by flash chromatography (hexane to hexane/ethyl acetate, 1:1), to afford pure compound **44** in 86% yield.

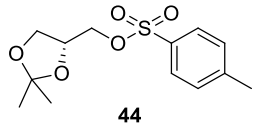

44

R_f: 0.28 (hexane/ethyl acetate, 5:1)
IR (ATR): 1364 (SO_2); 1179 (SO_2)
^{1}H-NMR ($CDCl_3$, 300 MHz): δ 1.31 (s, 3H, CH_3); 1.34 (s, 3H, CH_3); 2.45 (s, 3H, $PhC\underline{H}_3$); 3.77 (dd, *J* = 8.8, 5.1, 1H, ½CH_2O); 3.94-4.06 (m, 3H, CH_2OS, ½CH_2O); 4.24-4.31 (m, 1H, CH); 7.35 (d, *J* = 8.1, 2H, $2CH_{Ar}$); 7.80 (d, *J* = 8.3, 2H, $2CH_{Ar}$)
^{13}C-NMR ($CDCl_3$, 75 MHz): δ 21.8 ($Ph\underline{C}H_3$); 25.3 (CH_3); 26.8 (CH_3); 66.4 (CH_2O); 69.6 (CH_2OS); 73.1 (CH); 110.2 (C); 128.2 ($2CH_{Ar}$); 130.1 ($2CH_{Ar}$); 132.8; 145.2 ($2C_{Ar}$)
$[\alpha]_D^{20}$: -4.2 (c = 1.41, methanol)
MS (ESI, *m/z*): 287.1 $[M+H]^+$

2-(4-{[(4*S*)-2,2-Dimethyl-1,3-dioxolan-4-yl]methoxy}phenyl)-4,4,5,5-tetramethyl-1,3,2-dioxaborolane, 45

Compound **45** was synthesized following the experimental procedure previously described for the (*R*)-isomer.[108]

To a solution of tosylate **44** (343 mg, 1.2 mmol, 1.2 equiv) and 4-(4,4,5,5-tetramethyl-1,3,2-dioxaborolan-2-yl)phenol (220 mg, 1 mmol, 1 equiv) in anhydrous DMF (5 mL), Cs_2CO_3 (652 mg, 2 mmol, 2 equiv) was added. The mixture was heated at 90ºC for 16 h. Afterward, the mixture was partitioned between ethyl

acetate and water and the aqueous layer was extracted with ethyl acetate. The organic phase was washed with brine, dried over Na_2SO_4, filtered and concentrated under reduced pressure. The residue was purified by flash chromatography (hexane to hexane/ethyl acetate, 7:3) to afford pure compound **45** in 84% yield.

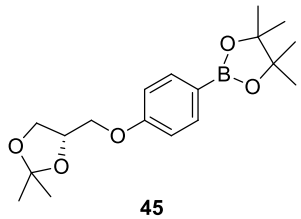

45

R_f: 0.63 (hexane/ethyl acetate, 8:2)
IR (ATR): 1362 (B-O)
^{1}H-NMR ($CDCl_3$, 300 MHz): δ 1.33 (s, 12H, $4CH_{3\ boronate}$); 1.40 (s, 3H, $CH_{3\ acetal}$); 1.46 (s, 3H, $CH_{3\ acetal}$); 3.90 (dd, *J* = 8.5, 5.8, 1H, ½CH_2O); 3.96 (dd, *J* = 9.6, 6.0, 1H, ½CH_2O); 4.08 (dd, *J* = 9.5, 5.4, 1H, ½CH_2O); 4.17 (dd, *J* = 8.5, 6.4, 1H, ½CH_2O); 4.48 (qt, *J* = 5.9, 1H, CH); 6.90 (d, *J* = 8.7, 2H, $2CH_{Ar}$); 7.74 (d, *J* = 8.6, 2H, $2CH_{Ar}$)
^{13}C-NMR ($CDCl_3$, 75 MHz): δ 25.0 ($4CH_{3\ boronate}$); 25.5; 26.9 ($2CH_{3\ acetal}$); 67.0 (CH_2); 68.7 (CH_2); 74.1 (CH); 83.7 ($2C_{boronate}$); 109.9 (C_{acetal}); 114.0 ($2CH_{Ar}$); 136.7 ($2CH_{Ar}$); 161.2 (C_{Ar}); (CB not observed)
$[\alpha]_D^{20}$: +9.2 (c = 0.6, $CHCl_3$)
MS (ESI, *m/z*): 335.2 $[M+H]^+$

(2*R*)-3-[4-(4,4,5,5-Tetramethyl-1,3,2-dioxaborolan-2-yl)phenoxy]propane-1,2-diol, 46

Following the general procedure 4.1.1.5, diol **46** was obtained from **45** (425 mg, 1.27 mmol) in 88% yield. Chromatography: hexane/ethyl acetate, 1:1 to 2:8.

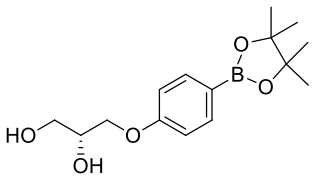

46

R_f: 0.05 (hexane/ethyl acetate, 7:3)
IR (ATR): 3372 (O-H); 1361 (B-O)

^{1}H-NMR ($CDCl_3$, 300 MHz): δ 1.33 (s, 12H, $4CH_3$); 2.76 (br s, 2H, OH); 3.72 (dd, *J* = 11.5, 5.5, 1H, ½CH_2OAr); 3.82 (dd, *J* = 11.5, 3.7, 1H, ½CH_2OAr); 4.02-4.04 (m, 2H, CH_2OH); 4.06-4.13 (m, 1H, CH); 6.88 (d, *J* = 8.7, 2H, $2CH_{Ar}$); 7.74 (d, *J* = 8.7, 2H, $2CH_{Ar}$)
^{13}C-NMR ($CDCl_3$, 75 MHz): δ 25.0 ($4CH_3$); 63.7 (CH_2OH); 69.0 (CH_2OAr); 70.5 (CH); 83.8 (2C); 114.0 ($2CH_{Ar}$); 136.7 ($2CH_{Ar}$); 161.1 (C_{Ar}); (CB not observed)
$[\alpha]_D^{20}$: +14.2 (c = 1.7, methanol)
MS (ESI, *m/z*): 295.1 $[M+H]^+$; 312.2 $[M+NH_4]^+$

4.1.2.4 Synthesis of alcohols **54** and **56**

3-(Benzyloxy)propyl methanesulfonate, 52

Following the general procedure 4.1.1.2, mesylate **52** was obtained from benzyloxypropan-1-ol (0.19 mL, 1.20 mmol) in 99% yield.

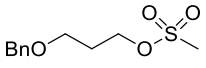

52

R_f: 0.4 (hexane/ethyl acetate, 5:1)
^{1}H-NMR (DMSO-d_6, 300 MHz): δ 2.04 (qt, *J* = 6.1, 2H, CH_2CH_2OMs); 2.96 (s, 3H, CH_3); 3.59 (t, *J* = 5.9, 2H, CH_2OBn); 4.36 (t, *J* = 6.2, 2H, CH_2OMs); 4.51 (s, 2H, PhCH_2); 7.27-7.39 (m, 5H, $5CH_{Ar}$)
^{13}C-NMR (DMSO-d_6, 75 MHz): δ 29.6 (CH_2CH_2OMs); 37.2 (CH_3); 65.5 (CH_2OMs); 67.4 (CH_2OBn); 73.2 (PhCH_2); 127.7 ($2CH_{Ar}$); 127.8 (CH_{Ar}); 128.5 ($2CH_{Ar}$); 138.1 (C_{Ar})
MS (ESI, *m/z*): 245.1 $[M+H]^+$; 267.0 $[M+Na]^+$

Di-*tert*-butyl [3-(benzyloxy)propyl]malonate, 53

Following the general procedure 4.1.1.3, compound **53** was obtained from mesylate **52** (270 mg, 1.11 mmol) in 66% yield. Chromatography: hexane to hexane/ethyl acetate, 7:3.

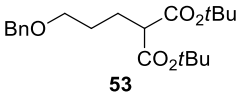

53

R_f: 0.49 (hexane/ethyl acetate, 8:2)
^{1}H-NMR (DMSO-d_6, 300 MHz): δ 1.45 (s, 18H, $6CH_3$); 1.60-1.70 (m, 2H, CH_2CH_2CH); 1.86-1.94 (m, 2H, CH_2CH); 3.14 (t, *J* = 7.5, 1H, CH); 3.49 (t, *J* = 6.4, 2H, CH_2OBn); 4.50 (s, 2H, PhCH_2); 7.24-7.37 (m, 5H, $5CH_{Ar}$)

^{13}C-NMR (DMSO-d_6, 75 MHz): δ 25.4 ($\underline{C}H_2CH$); 27.4 ($\underline{C}H_2CH_2CH$); 28.0 ($6CH_3$); 53.7 (CH); 69.8 ($\underline{C}H_2OBn$); 72.9 ($PhCH_2$); 81.3 (2C); 127.5 (CH_{Ar}); 127.6 ($2CH_{Ar}$); 128.4 ($2CH_{Ar}$); 138.5 (C_{Ar}); 168.9 (2CO)
MS (ESI, *m/z*): 365.3 $[M+H]^+$; 387.1 $[M+Na]^+$

Di-*tert*-butyl (3-hydroxypropyl)malonate, 54

Following the general procedure 4.1.1.1, alcohol **54** was obtained from **53** (260 mg, 0.68 mmol) at 60ºC in quantitative yield.

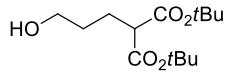

54

R_f: 0.63 (hexane/ethyl acetate, 1:1)
^{1}H-NMR (DMSO-d_6, 300 MHz): δ 1.46 (s, 18H, $6CH_3$); 1.56-1.67 (m, 2H, $C\underline{H}_2CH_2CH$); 1.86-1.93 (m, 2H, $C\underline{H}_2CH$); 3.16 (t, *J* = 7.4, 1H, CH); 3.65 (t, *J* = 6.3, 2H, $C\underline{H}_2OH$)
^{13}C-NMR (DMSO-d_6, 75 MHz): δ 24.8 ($\underline{C}H_2CH$); 27.9 ($6CH_3$); 30.4 ($\underline{C}H_2CH_2CH$); 53.6 (CH); 62.3 (CH_2OH); 81.5 (2C); 169.0 (2CO)
MS (ESI, *m/z*): 297.1 $[M+Na]^+$

Di-*tert*-butyl [3-(benzyloxy)propyl](fluoro)malonate, 55

Following the general procedure 4.1.1.4, compound **55** was obtained from **53** (250 mg, 0.71 mmol) in 99% yield, which was used in next step without further purification.

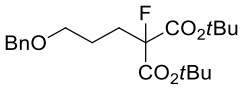

55

R_f: 0.82 (hexane/ethyl acetate, 8:2)
^{1}H-NMR (DMSO-d_6, 300 MHz): δ 1.49 (s, 18H, $6CH_3$); 1.59-1.77 (m, 2H, $C\underline{H}_2CH_2CF$); 2.00-2.24 (m, 2H, CH_2CF); 3.46-3.52 (m, 2H, $C\underline{H}_2OBn$); 4.49 (s, 2H, $PhC\underline{H}_2$); 7.28-7.37 (m, 5H, $5CH_{Ar}$)
^{13}C-NMR (DMSO-d_6, 75 MHz): δ 23.6 (d, *J* = 2.9, $\underline{C}H_2CH_2CF$); 28.2 ($6CH_3$); 31.2 (d, *J* = 21.8, $C\underline{H}_2CF$); 70.0 ($\underline{C}H_2OBn$); 73.1 ($PhC\underline{H}_2$); 83.8 ($2\underline{C}(CH_3)_3$); 100.9 (d, *J* = 165.6, CF); 127.9 (CH_{Ar}); 128.0 ($2CH_{Ar}$); 128.8 ($2CH_{Ar}$); 138.9 (C_{Ar}); 165.7 (d, *J* = 25.7, 2CO)
MS (ESI, *m/z*): 400.2 $[M+NH_4]^+$; 405.2 $[M+Na]^+$

Di-*tert*-butyl fluoro(3-hydroxypropyl)malonate, 56

Following the general procedure 4.1.1.1, alcohol **56** was obtained from **55** (329 mg, 0.86 mmol) at 60ºC in quantitative yield.

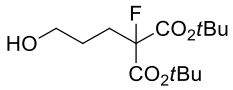

56

R_f: 0.31 (hexane/ethyl acetate, 4:1)
^{1}H-NMR (DMSO-d_6, 300 MHz): δ 1.50 (s, 18H, 6CH_3); 1.54-1.71 (m, 2H, C$H_2$$CH_2$CF); 1.91-2.20 (m, 2H, CH_2CF); 3.45-3.64 (m, 2H, CH_2OH)
^{13}C-NMR (DMSO-d_6, 75 MHz): δ 26.1 (d, *J* = 2.5, C$H_2$$CH_2$CF); 27.8 (6$CH_3$); 30.2 (d, *J* = 21.8, CH_2CF); 62.1 (CH_2OH); 83.5 (2C(CH_3)$_3$); 96.0 (d, *J* = 196.0, CF); 165.6 (d, *J* = 25.8, 2CO)
MS (ESI, *m/z*): 293.1 $[M+H]^+$

4.1.2.5 Synthesis of esters **47**-**51**, **57**, and **58**

(2*S*)-3-(2-*tert*-Butoxy-2-oxoethoxy)-2-hydroxypropyl (9*Z*)-octadec-9-enoate, 47

Method A (Scheme 4):

To a stirred suspension of diol **38** (50 mg, 0.24 mmol, 2 equiv) in dry dichloromethane (2 mL) at 0ºC, oleic acid (40 µL, 0.12 mmol, 1 equiv), DCC (25 mg, 0.12 mmol, 1 equiv) and DMAP (3 mg, 0.02 mmol, 0.2 equiv) were added. Then the reaction was allowed to reach room temperature and stirred overnight. Afterward, the mixture was treated with dichloromethane and the resulting precipitate was eliminated by filtration. The filtrate was washed with a saturated aqueous solution of $NaHCO_3$ and with brine, dried over Na_2SO_4 and filtered. The solvent was evaporated under reduced pressure and the residue was purified by flash chromatography (hexane to hexane/ethyl acetate, 8:2) to yield pure compound **47** in 15% yield.

Method B (Scheme 5):

Following the general procedure 4.1.1.6, ester **47** was obtained from diol **38** (82 mg, 0.49 mmol) in 36% yield. Chromatography: dichloromethane/ethyl acetate, 100:1 to 5:1.

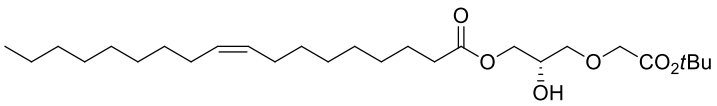

47

R_f: 0.52 (dichloromethane/ethyl acetate, 8:2)
IR (ATR): 3460 (O-H); 1739 (C=O)
^{1}H-NMR ($CDCl_3$, 300 MHz): δ 0.88 (t, *J* = 6.7, 3H, CH_3); 1.23-1.36 (m, 20H, $10CH_2$); 1.48 (s, 9H, $3CH_3$); 1.57-1.69 (m, 2H, CH_2CH_2CO); 1.95-2.06 (m, 4H, $2CH_2CH_{alkene}$); 2.34 (t, *J* = 7.6, 2H, CH_2CO); 3.56 (dd, *J* = 10.0, 6.4, 1H, ½$CHOHCH_2O$); 3.66 (dd, *J* = 10.0, 3.6, 1H, ½$CHOHCH_2O$); 3.95-4.07 (m, 3H, CH_2CO_2tBu, CH); 4.11-4.21 (m, 2H, CO_2CH_2); 5.29-5.40 (m, 2H, $2CH_{alkene}$)
^{13}C-NMR ($CDCl_3$, 75 MHz): δ 14.2 (CH_3); 22.8; 25.1 ($2CH_2$); 27.3; 27.4 ($2CH_2CH_{alkene}$); 28.3 ($3CH_3$); 29.3 ($2CH_2$); 29.32 (CH_2); 29.5 ($2CH_2$); 29.7; 29.8; 29.9; 32.1 ($4CH_2$); 34.3 (CH_2CO); 65.2 (CO_2CH_2); 69.0 (CH); 69.2 (CH_2CO_2tBu); 73.4 ($CHOHCH_2O$); 82.4 (C); 129.9; 130.2 ($2CH_{alkene}$); 170.4 (CO_2tBu); 174.0 (CO)
MS (ESI, *m/z*): 493.1 $[M+Na]^+$

Di-*tert*-butyl {(2*S*)-2-hydroxy-3-[(9*Z*)-octadec-9-enoyloxy]propyl}malonate, 48

Following the general procedure 4.1.1.6, ester **48** was obtained from diol **41** (190 mg, 0.72 mmol) in 99% yield. Chromatography: dichloromethane/ethyl acetate, 100:1 to 5:1.

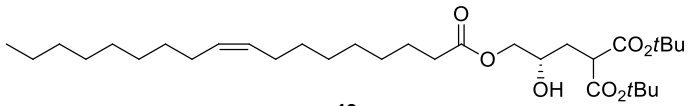

48

R_f: 0.60 (dichloromethane/ethyl acetate, 9:1)
^{1}H-NMR ($CDCl_3$, 300 MHz): δ 0.88 (t, *J* = 6.7, 3H, CH_3); 1.18-1.37 (m, 20H, $10CH_2$); 1.45 (s, 9H, $3CH_3$); 1.46 (s, 9H, $3CH_3$); 1.56-1.69 (m, 3H, CH_2CH_2CO, ½$CH_2CH(CO_2tBu)_2$); 1.89-2.08 (m, 5H, $2CH_2CH_{alkene}$, ½$CH_2CH(CO_2tBu)_2$); 2.34 (t, *J* = 7.5, 2H, CH_2CO); 3.44 (dd, *J* = 8.1, 6.2, 1H, $CH(CO_2tBu)_2$); 3.84-3.95 (m, 1H, CHOH); 4.01 (dd, *J* = 11.3, 6.7, 1H, ½CO_2CH_2); 4.12 (dd, *J* = 11.3, 3.7, 1H, ½CO_2CH_2); 5.31-5.36 (m, 2H, $2CH_{alkene}$)
^{13}C-NMR ($CDCl_3$, 75 MHz): δ 14.2 (CH_3); 22.8; 25.1 ($2CH_2$); 27.3; 27.4 ($2CH_2CH_{alkene}$); 28.0 ($3CH_3$); 28.1 ($3CH_3$); 29.2 ($2CH_2$); 29.3; 29.5; 29.7 ($3CH_2$); 29.8 ($2CH_2$); 29.9; 32.1; 32.4 ($3CH_2$); 34.3 (CH_2CO); 50.9 ($CH(CO_2tBu)_2$); 68.2 (CHOH); 68.3 (CO_2CH_2); 82.0 (2C); 129.9; 130.2 ($2CH_{alkene}$); 168.9; 169.2 ($2CO_2tBu$); 174.0 (CO)
MS (ESI, *m/z*): 555.2 $[M+H]^+$

Di-*tert*-butyl fluoro{(2S)-2-hydroxy-3-[(9*Z*)-octadec-9-enoyloxy]propyl} malonate, 49

Following the general procedure 4.1.1.6, ester **49** was obtained from diol **43** (116 mg, 0.38 mmol) in 60% yield. Chromatography: dichloromethane to dichloromethane/ethyl acetate, 9:1.

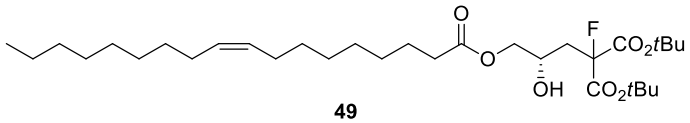

49

Rf: 0.56 (hexane/ethyl acetate, 8:2)
IR (ATR): 3513 (O-H); 1743 (C=O); 1164 (C-F)
^{1}H-NMR ($CDCl_3$, 300 MHz): δ 0.88 (t, *J* = 6.6, 3H, CH_3); 1.22-1.37 (m, 20H, $10CH_2$); 1.50 (s, 18H, $6CH_3$); 1.60-1.65 (m, 2H, CH_2CH_2CO); 1.97-2.03 (m, 4H, $2CH_2CH_{alkene}$); 2.23-2.44 (m, 4H, CH_2CO, CH_2CF); 3.99-4.21 (m, 3H, CO_2CH_2, CH); 5.32-5.36 (m, 2H, $2CH_{alkene}$)
^{13}C-NMR ($CDCl_3$, 75 MHz): δ 14.1 (CH_3); 22.7; 24.9 ($2CH_2$); 27.2; 27.24 ($2CH_2CH_{alkene}$); 27.7 ($3CH_3$); 27.78 ($3CH_3$); 29.1; 29.2 ($2CH_2$); 29.3 ($2CH_2$); 29.33; 29.5; 29.7; 29.8; 31.9 ($5CH_2$); 34.1 (CH_2CO); 37.4 (d, *J* = 20.4, CH_2CF); 65.3 (CH); 67.9 (CO_2CH_2); 83.8; 83.9 ($2C(CH_3)_3$); 129.8; 130.0 ($2CH_{alkene}$); 165.5 (d, *J* = 24.8, CO_2tBu); 166.0 (d, *J* = 25.7, CO_2tBu); 174.4 (CO); (CF not observed)
MS (ESI, *m/z*): 590.5 $[M+NH_4]^+$

(2*S*)-2-Hydroxy-3-[4-(4,4,5,5-tetramethyl-1,3,2-dioxaborolan-2-yl)phenoxy]propyl (9*Z*)-octadec-9-enoate, 50

Following the general procedure 4.1.1.6, ester **50** was obtained from diol **46** (130 mg, 0.44 mmol) in 40% yield. Chromatography: dichloromethane to dichloromethane/ethanol, 100:1.

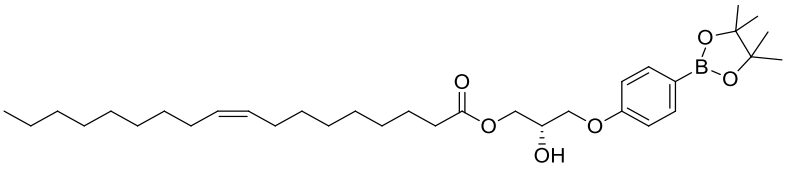

50

Rf: 0.46 (dichloromethane/ethanol, 20:1)
IR (ATR): 3459 (O-H); 1737 (C=O); 1362 (B-O)
^{1}H-NMR ($CDCl_3$, 300 MHz): δ 0.88 (t, *J* = 6.7, 3H, CH_3); 1.26-1.33 (m, 32H, $10CH_2$, $4CH_{3\ boronate}$); 1.56-1.68 (m, 2H, CH_2CH_2CO); 1.97-2.01 (m, 4H, $2CH_2CH_{alkene}$); 2.35

(t, *J* = 7.5, 2H, CH_2CO); 2.57 (br s, 1H, OH); 4.00-4.09 (m, 2H, CH_2OAr); 4.22-4.32 (m, 3H, CH, CO_2CH_2); 5.28-5.40 (m, 2H, $2CH_{alkene}$); 6.90 (d, *J* = 8.7, 2H, $2CH_{Ar}$); 7.75 (d, *J* = 8.6, 2H, $2CH_{Ar}$)

^{13}C-NMR ($CDCl_3$, 75 MHz): δ 14.3 (CH_3); 22.8 (CH_2); 25.0 ($4CH_3$); 25.04 (CH_2); 27.3; 27.4 (CH_2CH_{alkene}); 29.2 ($2CH_2$); 29.3 (CH_2); 29.5 ($2CH_2$); 29.7; 29.8; 29.9; 32.0 ($4CH_2$); 34.3 (CH_2CO); 65.3 (CO_2CH_2); 68.6 (CH_2OAr); 68.8 (CH); 83.8 (2C); 114.0 ($2CH_{Ar}$); 129.9; 130.2 ($2CH_{alkene}$); 136.7 ($2CH_{Ar}$); 161.0 (C_{Ar}); 174.1 (CO); (CB not observed)

$[\alpha]_D^{20}$: +1.5 (c = 1, $CHCl_3$)

MS (ESI, *m/z*): 557.8 $[M-H]^-$

Potassium [4-({(2*S*)-2-hydroxy-3-[(9*Z*)-octadec-9-enoyloxy]propyl}oxy)phenyl] trifluoroborate, 51

To a solution of boronate **50** (50 mg, 0.09 mmol, 1 equiv) in methanol (2 mL), potassium hydrogen fluoride was added (111 µL, 0.50 mmol, 5.6 equiv, 4.5 M in water) and the reaction was stirred at room temperature for 30 minutes. Then, solvent was evaporated under reduced pressure and the crude was redissolved in hot acetone and filtrated. The filtrate was concentrated under reduced pressure to afford intermediate **51** as a syrup in quantitative yield.

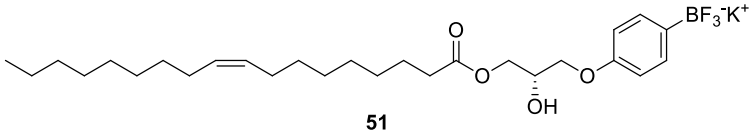

51

IR (ATR): 3500 (O-H); 1737 (C=O); 1237 (B-F); 1176 (B-C)

^{1}H-NMR (methanol-d_4, 300 MHz): δ 0.90 (t, *J* = 6.6, 3H, CH_3); 1.30-1.37 (m, 20H, $10CH_2$); 1.60-1.64 (m, 2H, CH_2CH_2CO); 2.02-2.04 (m, 4H, $2CH_2CH_{alkene}$); 2.36 (t, *J* = 7.4, 2H, CH_2CO); 3.94-4.02 (m, 2H, CH_2OAr); 4.09-4.28 (m, 3H, CH, CO_2CH_2); 5.29-5.40 (m, 2H, $2CH_{alkene}$); 6.79 (d, *J* = 8.0, 2H, $2CH_{Ar}$); 7.42 (d, *J* = 8.3, 2H, $2CH_{Ar}$)

^{13}C-NMR (methanol-d_4, 75 MHz): δ 14.5 (CH_3); 23.7; 26.0 ($2CH_2$); 28.1 ($2CH_2CH_{alkene}$); 30.2 ($2CH_2$); 30.3; 30.34; 30.5; 30.6; 30.8; 30.84; 33.1 ($7CH_2$); 34.9 (CH_2CO); 66.5 (CO_2CH_2); 69.2 (CH); 69.9 (CH_2OAr); 114.1 ($2CH_{Ar}$); 130.8; 130.9 ($2CH_{alkene}$); 133.6 ($2CH_{Ar}$); 158.8 (C_{Ar}); 175.4 (CO); (CB not observed)

$[\alpha]_D^{20}$: +2.4 (c = 0.9, methanol)

MS (ESI, *m/z*): 521.3 $[M-OH]^-$

Di-*tert*-butyl {3-[(9*Z*)-octadec-9-enoyloxy]propyl}malonate, 57

Following the general procedure 4.1.1.6, ester **57** was obtained from alcohol **54** (120 mg, 0.44 mmol) in 70% yield. Cromatography: dichloromethane.

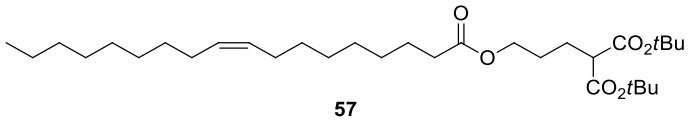

57

R_f: 0.44 (hexane/ethyl acetate, 1:1)

^{1}H-NMR (DMSO-d_6, 300 MHz): δ 0.88 (t, *J* = 6.7, 3H, CH_3); 1.25-1.29 (m, 20H, $10CH_2$); 1.46 (s, 18H, $6CH_3$); 1.54-1.72 (m, 4H, CH_2CH_2CO, $CH_2CH_2CH(CO_2tBu)_2$); 1.83-1.91 (m, 2H, $CH_2CH(CO_2tBu)_2$); 1.97-2.03 (m, 4H, $2CH_2CH_{alkene}$); 2.29 (t, *J* = 7.6, 2H, CH_2CO); 3.14 (t, *J* = 7.5, 1H, CH); 4.07 (t, *J* = 6.4, 2H, CO_2CH_2); 5.28-5.39 (m, 2H, $2CH_{alkene}$)

^{13}C-NMR (DMSO-d_6, 75 MHz): δ 14.2 (CH_3); 22.7; 25.0; 25.2; 26.4 ($4CH_2$); 27.2; 27.24 ($2CH_2CH_{alkene}$); 27.9 ($6CH_3$); 29.1; 29.18; 29.2 ($3CH_2$); 29.4 ($2CH_2$); 29.6; 29.7; 29.8; 31.9 ($4CH_2$); 34.3 (CH_2CO); 53.5 (CH); 63.7 (CO_2CH_2); 81.5 (2C); 129.9; 130.1 ($2CH_{alkene}$); 168.7 ($2CO_2tBu$); 173.9 (CO)

Di-*tert*-butyl fluoro{3-[(9*Z*)-octadec-9-enoyloxy]propyl}malonate, 58

Following the general procedure 4.1.1.6, ester **58** was obtained from alcohol **56** (199 mg, 0.68 mmol) in 59% yield. Chromatography: dichloromethane.

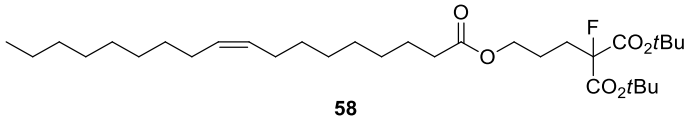

58

R_f: 0.69 (hexane/ethyl acetate, 1:1)

^{1}H-NMR (DMSO-d_6, 300 MHz): δ 0.88 (t, *J* = 6.8, 3H, CH_3); 1.23-1.37 (m, 20H, $10CH_2$); 1.46 (s, 3H, CH_3); 1.50 (s, 15H, $5CH_3$); 1.56-1.64 (m, 2H, CH_2CH_2CO); 1.69-1.79 (m, 2H, CH_2CH_2CF); 1.97-2.04 (m, 4H, $2CH_2CH_{alkene}$); 2.07-2.20 (m, 2H, CH_2CF); 2.29 (t, *J* = 7.6, 2H, CH_2CO); 4.08 (t, *J* = 6.3, 2H, CO_2CH_2); 5.29-5.40 (m, 2H, $2CH_{alkene}$)

^{13}C-NMR (DMSO-d_6, 75 MHz): δ 14.5 (CH_3); 22.7 (d, *J* = 3.2, CH_2CH_2CF); 23.1; 25.3 ($2CH_2$); 27.6; 27.61 ($2CH_2CH_{alkene}$); 28.2 ($6CH_3$); 28.3; 29.5; 29.54; 29.6; 29.7; 29.9; 30.1; 30.2 ($8CH_2$); 30.9 (d, *J* = 21.9, CH_2CF); 32.3 (CH_2); 34.7 (CH_2CO); 63.9 (CO_2CH_2); 84.0 ($2C(CH_3)_3$); 94.8 (d, *J* = 196.5, CF); 130.2; 130.4 ($2CH_{alkene}$); 165.7 (d, *J* = 25.4, $2CO_2tBu$); 174.2 (CO)

MS (ESI, *m/z*): 557.5 $[M+H]^+$

4.1.2.6 Synthesis of final compounds **1a**-**f**

({(2*S*)-2-Hydroxy-3-[(9*Z*)-octadec-9-enoyloxy]propyl}oxy)acetic acid, 1a

Following the general procedure 4.1.1.7, compound **1a** was obtained from *tert*-butyl ester **47** (48 mg, 84 µmol) and TFA (0.16 mL, 2.10 mmol) in 52% yield. Chromatography: ethyl acetate/ethanol, 20:1 to 1:5.

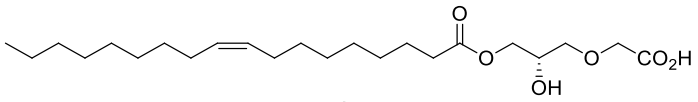

1a

R_f: 0.11 (ethyl acetate/ethanol, 8:2)

IR (ATR): 3301 (O-H); 1737 (C=O)

^{1}H-NMR ($CDCl_3$, 300 MHz): δ 0.88 (t, *J* = 6.6, 3H, CH_3); 1.26-1.29 (m, 20H, $10CH_2$); 1.52-1.65 (m, 2H, CH_2CH_2CO); 1.93-2.05 (m, 4H, $2CH_2CH_{alkene}$); 2.30 (t, *J* = 7.5, 2H, CH_2CO); 3.32-3.60 (m, 2H, $CHOHCH_2O$); 3.76-3.92 (br s, 2H, CH_2CO_2H); 3.95-4.19 (m, 3H, CO_2CH_2, CH); 5.26-5.35 (m, 2H, $2CH_{alkene}$)

^{13}C-NMR ($CDCl_3$, 75 MHz): δ 14.3 (CH_3); 22.9; 25.0 ($2CH_2$); 27.3; 27.4 ($2CH_2CH_{alkene}$); 29.2; 29.3; 29.4; 29.47; 29.48; 29.7; 29.8; 29.9; 32.1 ($9CH_2$); 34.2 (CH_2CO); 64.8 (CO_2CH_2); 65.8 (CH); 70.5 (CH_2CO_2H); 72.1 ($CHOHCH_2O$); 130.0; 130.2 ($2CH_{alkene}$); 173.4; 173.8 (2CO)

$[\alpha]_D^{20}$: -1.6 (c = 1, $CHCl_3$)

HRMS (ESI, *m/z*): calculated for $C_{23}H_{41}O_6$ ($[M-H]^-$): 413.2909; found: 413.2890

(5*S*)-5-{[(9*Z*)-octadec-9-enoyloxy]methyl}-2-oxotetrahydrofuran-3-carboxylic acid, 1b

Following the general procedure 4.1.1.7, compound **1b** was obtained from di-*tert*-butyl ester **48** (169 mg, 0.30 mmol) and TFA (0.58 mL, 7.53 mmol) in 88% yield. Chromatography: ethyl acetate/ethanol, 20:1 to 1:5.

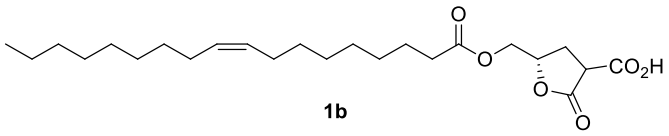

1b

R_f: 0.13 (ethyl acetate/ethanol, 8:2)

^{1}H-NMR ($CDCl_3$, 300 MHz): Mixture of diastereoisomers (1:1): δ 0.88 (t, *J* = 7.2, 3H, CH_3); 1.27-1.30 (m, 20H, $10CH_2$); 1.61-1.64 (m, 2H, CH_2CH_2CO); 1.97-2.03 (m, 4H, $2CH_2CH_{alkene}$); 2.33-2.37 (m, 2H, CH_2CO); 2.37-2.41 (m, 1H, $½CH_2CHCO_2H$); 2.47-2.54 (m, 1H, $½CH_2CHCO_2H$); 2.62-2.68 (m, 1H, $½CH_2CHCO_2H$); 2.78-2.84 (m, 1H, $½CH_2CHCO_2H$); 3.71-3.76 (m, 1H, $CHCO_2H$);

4.19 (dd, *J* = 12.6, 4.6) and 4.23 (dd, *J* = 12.5, 5.8, 1H, ½CO_2CH_2); 4.37 (m, 1H, ½CO_2CH_2); 4.74-4.79 (m, 1H, $CO_2CH_2C\underline{H}$); 4.89-4.94 (m, 1H, $CO_2CH_2C\underline{H}$); 5.30-5.38 (m, 2H, $2CH_{alkene}$)

^{13}C-NMR ($CDCl_3$, 75 MHz): Mixture of diastereoisomers (1:1): δ 14.3 (CH_3); 22.8 (CH_2); 24.9 and 24.94 (CH_2); 27.3; 27.37 ($2\underline{C}H_2CH_{alkene}$); 27.9; 29.2; 29.22; 29.3; 29.5; 29.7; 29.8; 29.9; 31.1 ($9CH_2$); 32.1 ($\underline{C}H_2CHCO_2H$); 34.0 and 34.1 ($\underline{C}H_2CO$); 46.0 and 46.2 ($\underline{C}HCO_2H$); 64.4 and 64.9 ($CO_2\underline{C}H_2$); 76.7 and 76.8 ($CO_2CH_2\underline{C}H$); 129.85 and 129.8 (CH_{alkene}); 130.17 and 130.19 (CH_{alkene}); 171.9; 172.1 (2CO); 173.4 and 173.6 (CO)

HRMS (ESI, *m/z*): calculated for $C_{23}H_{39}O_4$ ([M-CO_2H]$^-$): 379.2854, found: 379.2861

HPLC (method A, t_R, min): 14.37

(5*S*)-3-fluoro-5-{[(9*Z*)-octadec-9-enoyloxy]methyl}-2-oxotetrahydrofuran-3-carboxylic acid, 1c

Following the general procedure 4.1.1.7, compound **1c** was obtained from di-*tert*-butyl ester **49** (80 mg, 0.14 mmol) and TFA (0.27 mL, 3.50 mmol) without further purification in quantitative yield.

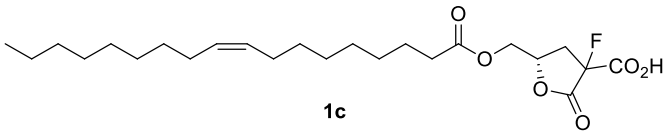

1c

IR (ATR): 3466 (O-H); 1795 (C=O); 1742 (C=O); 1163 (C-F)

^{1}H-NMR ($CDCl_3$, 500 MHz): Mixture of diastereoisomers (1:1): δ 0.88 (t, *J* = 6.9, 3H, CH_3); 1.20-1.37 (m, 20H, $10CH_2$); 1.58-1.67 (m, 2H, $C\underline{H}_2CH_2CO$); 1.97-2.05 (m, 4H, $2C\underline{H}_2CH_{alkene}$); 2.36-2.39 (m, 3H, CH_2CO, ½CH_2CF); 2.46-2.55 (m, 1H, ½CH_2CF); 2.76 (dd, *J* = 25.8, 7.2, 1H, ½CH_2CF); 2.95-3.05 (m, 1H, ½CH_2CF); 4.20 (dd, *J* = 15.5, 4.8) and 4.32 (dd, *J* = 15.5, 6.1, 1H, ½CO_2CH_2); 4.40-4.47 (m, 1H, ½CO_2CH_2); 4.90-5.01 (m, 1H, CH); 5.31-5.38 (m, 2H, $2CH_{alkene}$)

^{13}C-NMR ($CDCl_3$, 125 MHz): Mixture of diastereoisomers (1:1): δ 14.2 (CH_3); 22.8; 24.9 ($2CH_2$); 27.3; 27.4 ($2\underline{C}H_2CH_{alkene}$); 29.2; 29.22; 29.3; 29.5; 29.7; 29.81; 29.84; 29.9; 32.0 ($9CH_2$); 34.0 and 34.08 ($\underline{C}H_2CO$); 34.9 (d, *J* = 22.4) and 35.0 (d, *J* = 21.7, $\underline{C}H_2CF$); 63.6 and 63.9 ($CO_2\underline{C}H_2$); 75.7 (d, *J* = 2.9) and 76.5 (CH); 91.7 (d, *J* = 197.8) and 92.1 (d, *J* = 200.9, CF); 129.9 (CH_{alkene}); 130.16 and 130.18 (CH_{alkene}); 167.5 (d, *J* = 23.3, CO); 167.8 (d, *J* = 24.7, CO); 173.8 and 173.84 (CO)

HRMS (ESI, *m/z*): calculated for $C_{24}H_{38}FO_6$ ([M-H]$^-$): 441.2658, found 441.2667

HPLC (method A, t_R, min): 21.16

[4-({(2*S*)-2-Hydroxy-3-[(9*Z*)-octadec-9-enoyloxy]propyl}oxy)phenyl]boronic acid, 1d

To a solution of compound **51** (30 mg, 54 µmol, 1 equiv) in acetonitrile (0.5 mL), water (3 µL, 0.16 mmol, 3 equiv) and trimethylsilyl chloride (20 µL, 0.16 mmol, 3 equiv) were added and the mixture was stirred for 1 h at room temperature. Then, a saturated aqueous solution of $NaHCO_3$ was added, and the reaction mixture was extracted with dichloromethane. The organic layer was washed with brine, dried over Na_2SO_4, filtered and evaporated under reduced pressure. Flash chromatography of the residue (hexane/ethyl acetate, 10:1 to 1:1, followed by ethyl acetate/ethanol, 10:1 to 5:1) afforded compound **1d** in 60% yield.

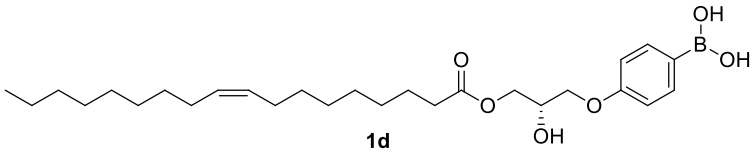

1d

R_f: 0.30 (hexane/ethyl acetate, 1:1)
IR (ATR): 1740 (C=O); 1368 (B-O); 1242 (B-C)
^{1}H-NMR ($CDCl_3$, 300 MHz): δ 0.87 (t, *J* = 6.5, 3H, CH_3); 1.26-1.30 (m, 20H, $10CH_2$); 1.63-1.67 (m, 2H, CH_2CH_2CO); 1.99-2.01 (m, 4H, $2CH_2CH_{alkene}$); 2.38 (t, *J* = 7.5, 2H, CH_2CO); 4.03-4.12 (m, 2H, CH_2OAr); 4.24-4.37 (m, 3H, CH, CO_2CH_2); 5.27-5.40 (m, 2H, $2CH_{alkene}$); 7.02 (d, *J* = 8.5, 2H, $2CH_{Ar}$); 8.16 (d, *J* = 8.4, 2H, $2CH_{Ar}$)
^{13}C-NMR ($CDCl_3$, 75 MHz): δ 14.3 (CH_3); 22.8; 25.1 ($2CH_2$); 27.3; 27.4 ($2CH_2CH_{alkene}$); 29.2 ($2CH_2$); 29.3 (CH_2); 29.5 ($2CH_2$); 29.7; 29.8; 29.9; 32.1 ($4CH_2$); 34.3 (CH_2CO); 65.4 (CO_2CH_2); 68.6 (CH_2OAr); 68.8 (CH); 114.2 ($2CH_{Ar}$); 129.9; 130.2 ($2CH_{alkene}$); 137.6 ($2CH_{Ar}$); 141.1 (C_{Ar}); 174.2 (CO); (CB not observed)
$[\alpha]_D^{20}$: limited solubility in DMSO
HRMS (ESI, *m/z*): calculated for $C_{27}H_{46}BO_6$ ($[M+H]^+$): 477.3387, found 477.3395
HPLC (method A, t_R, min): 22.85

{3-[(9*Z*)-Octadec-9-enoyloxy]propyl}malonic acid, 1e

Following the general procedure 4.1.1.7, compound **1e** was obtained from di-*tert*-butyl ester **57** (96 mg, 0.18 mmol) and TFA (0.34 mL, 4.45 mmol) without further purification in 90% yield.

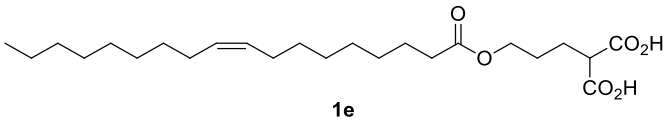

1e

IR (ATR): 3100 (O-H); 1735 (C=O)
^{1}H-NMR (DMSO-d_6, 300 MHz): δ 0.87 (t, J = 6.7, 3H, CH_3); 1.26-1.30 (m, 20H, $10CH_2$); 1.56-1.65 (m, 2H, $CH_2CH_2CH(CO_2H)_2$); 1.70-1.80 (m, 2H, CH_2CH_2CO); 1.93-2.07 (m, 6H, $2CH_2CH_{alkene}$, $CH_2CH(CO_2H)_2$); 2.30 (t, J = 7.6, 2H, CH_2CO); 3.48 (t, J = 7.4, 1H, CH); 4.11 (t, J = 6.1, 2H, CO_2CH_2); 5.28-5.39 (m, 2H, $2CH_{alkene}$)
^{13}C-NMR (DMSO-d_6, 75 MHz): δ 14.1 (CH_3); 22.7; 24.9; 25.3; 26.3 ($4CH_2$); 27.2; 27.24 ($2CH_2CH_{alkene}$); 27.9; 29.1; 29.2 ($3CH_2$); 29.3 ($2CH_2$); 29.6; 29.7; 29.8; 31.9 ($4CH_2$); 34.3 (CH_2CO); 51.0 (CH); 63.5 (CO_2CH_2); 129.8; 130.0 ($2CH_{alkene}$); 174.1 ($2CO_2H$); 174.3 (CO)
HRMS (ESI, *m/z*): calculated for $C_{24}H_{41}O_6$ ([M-H]$^-$): 425.2909, found 425.2898
HPLC (method A, t_R, min): 15.18

Fluoro{3-[(9*Z*)-octadec-9-enoyloxy]propyl}vmalonic acid, 1f

Following the general procedure 4.1.1.7, compound **1f** was obtained from di-*tert*-butyl ester **58** (61 mg, 0.11 mmol) and TFA (0.21 mL, 2.75 mmol) without further purification in 59% yield.

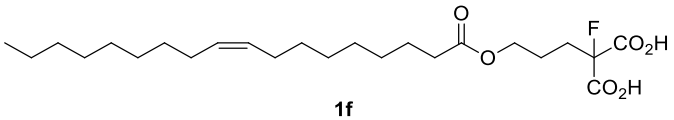

1f

IR (ATR): 1738 (C=O); 1166 (C-F)
^{1}H-NMR (DMSO-d_6, 300 MHz): δ 0.88 (t, J = 6.6, 3H, CH_3); 1.18-1.39 (m, 20H, $10CH_2$); 1.54-1.67 (m, 2H, CH_2CH_2CO); 1.70-1.85 (m, 2H, CH_2CH_2CF); 1.93-2.04 (m, 4H, $2CH_2CH_{alkene}$); 2.20-2.45 (m, 2H, CH_2CF); 2.41 (t, J = 7.6, 2H, CH_2CO); 4.02-4.18 (m, 2H, CO_2CH_2); 5.27-5.41 (m, 2H, $2CH_{alkene}$)
^{13}C-NMR (DMSO-d_6, 75 MHz): δ 14.1 (CH_3); 22.7; 24.9 ($2CH_2$); 24.93 (d, J = 2.8, CH_2CH_2CF); 27.2; 27.23 ($2CH_2CH_{alkene}$); 29.1; 29.2 ($2CH_2$); 29.3 ($2CH_2$); 29.5; 29.7; 29.74; 29.8 ($4CH_2$); 31.1 (d, J = 21.6, CH_2CF); 31.9 (CH_2); 34.3 (CH_2CO); 63.29 (CO_2CH_2); 129.7; 130.0 ($2CH_{alkene}$); 174.7 (CO); (CO_2H and CF not observed)
HRMS (ESI, *m/z*): calculated for $C_{24}H_{40}FO_6$ ([M-H]$^-$): 443.2814, found 443.2824
HPLC (method A, t_R, min): 16.75

*4.1.3 Synthesis of final compound **1g***

Di-*tert*-butyl fluoro{(2*S*)-2-methoxy-3-[(9*Z*)-octadec-9-enoyloxy]propyl} malonate, 59

Following the general procedure 4.1.1.8, compound **59** was obtained from **49** (90 mg, 0.16 mmol) in 38% yield. Chromatography: hexane/ethyl acetate, 30:1 to 5:1.

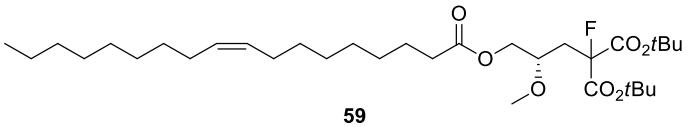

59

R_f: 0.41 (hexane/ethyl acetate, 8:2)
IR (ATR): 1769 (C=O); 1165 (C-F)
^{1}H-NMR ($CDCl_3$, 300 MHz): δ 0.87 (t, *J* = 6.5, 3H, CH_3); 1.26-1.29 (m, 20H, $10CH_2$); 1.48 (s, 9H, $3CH_3$); 1.48 (s, 9H, $3CH_3$); 1.59-1.64 (m, 2H, CH_2CH_2CO); 1.99-2.01 (m, 4H, $2CH_2CH_{alkene}$); 2.16-2.48 (m, 2H, CH_2CF); 2.32 (t, *J* = 7.5, 2H, CH_2CO); 3.29 (s, 3H, OCH_3); 3.57-3.64 (m, 1H, CH); 4.10 (AB system, *J* = 11.6, 4.7, 2H, CO_2CH_2); 5.28-5.39 (m, 2H, $2CH_{alkene}$)
^{13}C-NMR ($CDCl_3$, 75 MHz): δ 14.3 (CH_3); 22.8; 25.0 ($2CH_2$); 27.3; 27.34 ($2CH_2CH_{alkene}$); 27.8 ($3CH_3$); 27.9 ($3CH_3$); 29.2 ($2CH_2$); 29.3 (CH_2); 29.5 ($2CH_2$); 29.7; 29.8; 29.9; 32.0 ($4CH_2$); 34.3 (CH_2CO); 36.7 (d, *J* = 21.4, CH_2CF); 57.9 (OCH_3); 64.9 (CO_2CH_2); 73.9 (d, *J* = 3.3, CH); 83.2; 83.6 ($2C(CH_3)_3$); 92.5 (d, *J* = 195.3, CF); 129.9; 130.1 ($2CH_{alkene}$); 165.1 (d, *J* = 27.4, CO_2tBu); 165.2 (d, *J* = 23.8, CO_2tBu); 173.7 (CO)
$[\alpha]_D^{20}$: +4.1 (c = 0.75, $CDCl_3$)
MS (ESI, *m/z*): 609.4 $[M+Na]^+$

Fluoro{(2*S*)-2-methoxy-3-[(9*Z*)-octadec-9-enoyloxy]propyl}malonic acid, 1g

Following the general procedure 4.1.1.7, compound **1g** was obtained from di-*tert*-butyl ester **59** (10 mg, 17 µmol) and TFA (98 µL, 1.28 mmol) without further purification in 95% yield.

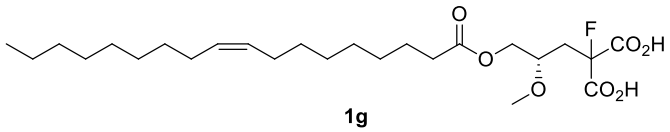

1g

IR (ATR): 3525 (O-H); 1742 (C=O); 1260 (C-F)

^{1}H-NMR (methanol-d_4, 700 MHz): δ 0.90 (t, *J* = 7.1, 3H, CH_3); 1.29-1.33 (m, 20H, $10CH_2$); 1.61-1.63 (m, 2H, CH_2CH_2CO); 2.02-2.05 (m, 4H, $2CH_2CH_{alkene}$), 2.24-2.30 (m, 1H, ½CH_2CF); 2.35 (t, *J* = 7.4, 2H, CH_2CO); 2.45-2.52 (m, 1H, ½CH_2CF); 3.33 (s, 3H, OCH_3); 3.63-3.65 (m, 1H, CH); 4.04 (dd, *J* = 11.7, 4.9, 1H, ½CO_2CH_2); 4.25 (dd, *J* = 11.7, 3.9, 1H, ½CO_2CH_2); 5.32-5.37 (m, 2H, $2CH_{alkene}$)
^{13}C-NMR (methanol-d_4, 175 MHz): δ 14.5 (CH_3); 23.8; 26.0 ($2CH_2$); 28.1 ($2CH_2CH_{alkene}$); 30.2 ($2CH_2$); 30.3; 30.4; 30.5; 30.6; 30.8; 30.9; 33.1 ($7CH_2$); 34.9 (CH_2CO); 38.4 (d, *J* = 20.1, CH_2CF); 58.1 (OCH_3); 65.9 (CO_2CH_2); 76.0 (CH); 94.4 (d, *J* = 192.5, CF); 130.8; 130.9 ($2CH_{alkene}$); 170.9 (br s, $2CO_2H$); 175.2 (CO)
$[\alpha]_D^{20}$: +29.5 (c = 0.2, methanol)
HRMS (ESI, *m/z*): calculated for $C_{25}H_{42}FO_7$ ($[M-H]^-$): 473.2915, found 473.2922
HPLC (method A, t_R, min): 14.51

*4.1.4 Synthesis of final compounds **2a-e***

4.1.4.1 Synthesis of non-commercial fatty acids **67-69**

Methyl 8-bromooctanoate, 60

8-bromooctanoic acid (2.0 g, 8.96 mmol, 1 equiv) was dissolved in methanol (10 mL), a catalytic amount of concentrated H_2SO_4 (0.2 mL) was added and the reaction mixture was refluxed overnight. Afterward, the solvent was evaporated and the crude was redissolved in ethyl acetate and washed with a saturated aqueous solution of NaHCO3 and brine. The residue was filtered and concentrated under reduced pressure to yield ester **60** in quantitative yield, which was used in the next step without further purification. The spectroscopic data correspond with those previously reported.[109]

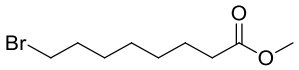

60

R_f: 0.23 (hexane/ethyl acetate, 20:1)
^{1}H-NMR ($CDCl_3$, 300 MHz): δ 1.30 (m, 4H, $2CH_2$); 1.40-1.45 (m, 2H, CH_2); 1.57-1.67 (m, 2H, CH_2); 1.84 (qt, J = 7.5, 2H, CH_2); 2.30 (t, J = 7.5, 2H, CH_2CO); 3.39 (t, J = 6.8, 2H, CH_2Br); 3.66 (s, 3H, CH_3)

Methyl heptadec-9-ynoate, 61

Following the general procedure 4.1.1.9, alkyne **61** was obtained from 1-nonyne (0.27 mL, 1.64 mmol) and methyl 8-bromooctanoate (300 mg, 1.26 mmol) in 36% yield. Chromatography: hexane.

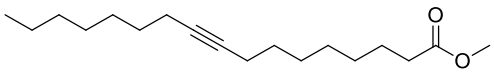

61

R_f: 0.32 (hexane/ethyl acetate, 20:1)
IR (ATR): 1740 (C=O)
^{1}H-NMR ($CDCl_3$, 300 MHz): δ 0.88 (t, *J* = 6.5, 3H, CH_3); 1.28-1.38 (m, 14H, $7CH_2$); 1.42-1.49 (m, 4H, $2CH_2$); 1.58-1.65 (m, 2H, CH_2CH_2CO); 2.13 (t, *J* = 6.9, 4H, $2CH_2C_{alkyne}$); 2.30 (t, *J* = 7.5, 2H; CH_2CO); 3.66 (s, 3H, OCH_3)
^{13}C-NMR ($CDCl_3$, 75 MHz): δ 14.2 (CH_3); 18.87; 18.9 ($2CH_2C_{alkyne}$); 22.8; 25.1; 28.8; 29.9 ($4CH_2$); 29.0 ($2CH_2$); 29.2; 29.22; 29.3; 31.9 ($4CH_2$); 34.2 (CH_2CO); 51.6 (OCH_3); 80.2; 80.5 ($2C_{alkyne}$); 174.4 (CO)

Methyl nonadec-9-ynoate, 62

Following the general procedure 4.1.1.9, alkyne **62** was obtained from 1-undecyne (0.33 mL, 1.64 mmol) and methyl 8-bromooctanoate (300 mg, 1.26 mmol) in 38% yield. Chromatography: hexane.

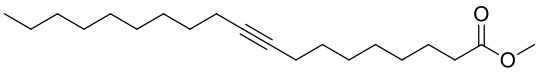

62

R_f: 0.36 (hexane/ethyl acetate, 20:1)
IR (ATR): 1742 (C=O)
^{1}H-NMR ($CDCl_3$, 300 MHz): δ 0.88 (t, *J* = 6.7, 3H, CH_3); 1.27-1.51 (m, 22H, $11CH_2$); 1.57-1.67 (m, 2H, CH_2CH_2CO); 2.11-2.16 (m, 4H, $2CH_2C_{alkyne}$); 2.30 (t, *J* = 7.5, 2H, CH_2CO), 3.66 (s, 3H, OCH_3)
^{13}C-NMR ($CDCl_3$, 75 MHz): δ 14.3 (CH_3); 18.88; 18.9 ($2CH_2C_{alkyne}$); 22.8; 25.1; 28.8; 28.9; 29.0; 29.2; 29.22 ($7CH_2$); 29.3 ($2CH_2$); 29.5; 29.7; 32.1 ($3CH_2$); 34.2 (CH_2CO); 51.6 (OCH_3); 80.2; 80.5 ($2C_{alkyne}$), 174.4 (CO)
MS (ESI, *m/z*): 309.3 $[M+H]^+$

Methyl icos-9-ynoate, 63

Following the general procedure 4.1.1.9, alkyne **63** was obtained from 1-dodecyne (0.32 mL, 1.64 mmol) and methyl 8-bromooctanoate (300 mg, 1.26 mmol) in 44% yield. Chromatography: hexane.

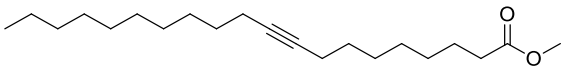

63

R_f: 0.48 (hexane/ethyl acetate, 20:1)
IR (ATR): 1740 (C=O)
^{1}H-NMR ($CDCl_3$, 300 MHz): δ 0.88 (t, *J* = 6.7, 3H, CH_3); 1.26-1.40 (m, 20H, $10CH_2$); 1.42-1.49 (m, 4H, $2CH_2$); 1.57-1.67 (m, 2H, CH_2CH_2CO); 2.13 (t, *J* = 6.9, 4H, $2CH_2C_{alkyne}$); 2.30 (t, *J* = 7.5, 2H, CH_2CO); 3.66 (s, 3H, OCH_3)
^{13}C-NMR ($CDCl_3$, 75 MHz): δ 14.3 (CH_3); 18.88; 18.9 ($2CH_2C_{alkyne}$); 22.8; 25.1; 28.8; 28.9; 29.0; 29.2; 29.22 ($7CH_2$); 29.3 ($2CH_2$); 29.5; 29.7; 29.74; 32.1 ($4CH_2$); 34.2 (CH_2CO); 51.6 (OCH_3); 80.2; 80.5 ($2C_{alkyne}$); 174.4 (CO)

Methyl (9*Z*)-heptadec-9-enoate, 64

Following the general procedure 4.1.1.10, alkene **64** was obtained from alkyne **61** (126 mg, 0.45 mmol) in 91% yield.

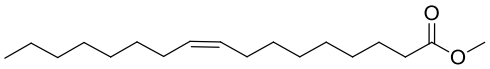

64

R_f: 0.32 (hexane/ethyl acetate, 20:1)
^{1}H-NMR ($CDCl_3$, 300 MHz): δ 0.87 (t, *J* = 6.6, 3H, CH_3); 1.27-1.29 (m, 18H, $9CH_2$); 1.59-1.63 (m, 2H, CH_2CH_2CO); 1.97-2.06 (m, 4H, $2CH_2CH_{alkene}$); 2.30 (t, *J* = 7.5, 2H, CH_2CO); 3.66 (s, 3H, OCH_3); 5.28-5.39 (m, 2H, $2CH_{alkene}$)
^{13}C-NMR ($CDCl_3$, 75 MHz): δ 14.3 (CH_3); 22.8; 25.1 ($2CH_2$); 27.3; 27.4 ($2CH_2CH_{alkene}$); 29.2; 29.26; 29.29; 29.3; 29.4; 29.8; 29.9; 32.0 ($8CH_2$); 34.2 (CH_2CO); 51.6 (OCH_3); 129.9; 130.1 ($2CH_{alkene}$); 174.5 (CO)

Methyl (9*Z*)-nonadec-9-enoate, 65

Following the general procedure 4.1.1.10, alkene **65** was obtained from alkyne **62** (120 mg, 0.39 mmol) in 92% yield.

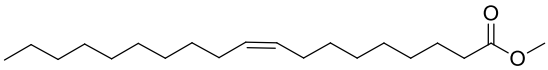

65

R_f: 0.36 (hexane/ethyl acetate, 20:1)
IR (ATR): 1742 (C=O)
^{1}H-NMR ($CDCl_3$, 300 MHz): δ 0.88 (t, *J* = 6.7, 3H, CH_3); 1.26-1.30 (m, 22H, $11CH_2$); 1.58-1.64 (m, 2H, CH_2CH_2CO); 1.97-2.01 (m, 4H, $2CH_2CH_{alkene}$); 2.30 (t, *J* = 7.5, 2H, CH_2CO); 3.66 (s, 3H, OCH_3); 5.29-5.40 (m, 2H, $2CH_{alkene}$)

^{13}C-NMR ($CDCl_3$, 75 MHz): δ 14.3 (CH_3); 22.8; 25.1 ($2CH_2$); 27.3; 27.4 ($2\underline{C}H_2CH_{alkene}$); 29.2; 29.3; 29.31; 29.4; 29.49; 29.7; 29.8; 29.84; 29.9; 32.1 ($10CH_2$); 34.3 ($\underline{C}H_2CO$); 51.6 (OCH_3); 129.9; 130.2 ($2CH_{alkene}$); 174.5 (CO)
MS (ESI, *m/z*): 311.3 $[M+H]^+$

Methyl (9*Z*)-icos-9-enoate, 66

Following the general procedure 4.1.1.10, alkene **66** was obtained from alkyne **63** (128 mg, 0.40 mmol) in 89% yield.

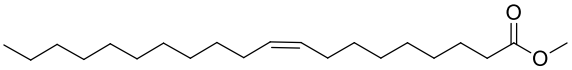

66

R_f: 0.48 (hexane/ethyl acetate, 20:1)
IR (ATR): 1743 (C=O)
^{1}H-NMR ($CDCl_3$, 300 MHz): δ 0.88 (t, *J* = 6.7 Hz, 3H, CH_3); 1.26-1.30 (m, 24H, $12CH_2$); 1.57-1.64 (m, 2H, $C\underline{H}_2CH_2CO$); 1.97-2.04 (m, 4H, $2C\underline{H}_2CH_{alkene}$); 2.30 (t, *J* = 7.5 Hz, 2H, CH_2CO); 3.66 (s, 3H, OCH_3); 5.29-5.40 (m, 2H, $2CH_{alkene}$)
^{13}C-NMR ($CDCl_3$, 75 MHz): δ 14.3 (CH_3); 22.8; 25.1 ($2CH_2$); 27.3; 27.4 ($2\underline{C}H_2CH_{alkene}$); 29.2; 29.28; 29.3; 29.4; 29.5; 29.7; 29.8; 29.81; 29.84; 29.9; 32.1 ($11CH_2$); 34.3 ($\underline{C}H_2CO$); 51.6 (OCH_3); 129.9; 130.2 ($2CH_{alkene}$); 174.5 (CO)

(9*Z*)-Heptadec-9-enoic acid, 67

Following the general procedure 4.1.1.11, carboxylic acid **67** was obtained from ester **64** (115 mg, 0.41 mmol) in quantitative yield.

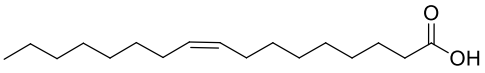

67

R_f: 0.43 (hexane/ethyl acetate, 1:1)
IR (ATR): 3252 (O-H); 1710 (C=O)
^{1}H-NMR ($CDCl_3$, 300 MHz): δ 0.88 (t, *J* = 6.7, 3H, CH_3); 1.27-1.31 (m, 18H, $9CH_2$); 1.58-1.66 (m, 2H, $C\underline{H}_2CH_2CO$); 1.98-2.04 (m, 4H, $2C\underline{H}_2CH_{alkene}$); 2.35 (t, *J* = 7.5, 2H, CH_2CO); 5.29-5.40 (m, 2H, $2CH_{alkene}$)
^{13}C-NMR ($CDCl_3$, 75 MHz): δ 14.3 (CH_3); 22.8; 24.8 ($2CH_2$); 27.3; 27.4 ($2\underline{C}H_2CH_{alkene}$); 29.2; 29.21; 29.3; 29.37; 29.4; 29.8; 29.9; 32.0 ($8CH_2$); 34.2 ($\underline{C}H_2CO$); 129.9; 130.2 ($2CH_{alkene}$); 180.0 (CO)
MS (ESI, *m/z*): 267.1 $[M-H]^-$

(9*Z*)-Nonadec-9-enoic acid, 68

Following the general procedure 4.1.1.11, carboxylic acid **68** was obtained from ester **65** (111 mg, 0.36 mmol) in quantitative yield.

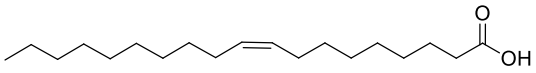

68

R_f: 0.45 (hexane/ethyl acetate, 1:1)
IR (ATR): 1710 (C=O)
^{1}H-NMR ($CDCl_3$, 300 MHz): δ 0.88 (t, *J* = 6.7, 3H, CH_3); 1.26-1.31 (m, 22H, $11CH_2$); 1.58-1.68 (m, 2H, CH_2CH_2CO); 1.98-2.04 (m, 4H, $2CH_2CH_{alkene}$); 2.35 (t, *J* = 7.5, 2H, CH_2CO); 5.29-5.40 (m, 2H, $2CH_{alkene}$)
^{13}C-NMR ($CDCl_3$, 75 MHz): δ 14.3 (CH_3); 22.8; 24.8 ($2CH_2$); 27.3; 27.4 ($2CH_2CH_{alkene}$); 29.2; 29.22; 29.3; 29.5; 29.51; 29.7; 29.8; 29.83; 29.9; 32.1 ($10CH_2$); 34.2 (CH_2CO); 129.9; 130.2 ($2CH_{alkene}$); 180.2 (CO)

(9*Z*)-Icos-9-enoic acid, 69

Following the general procedure 4.1.1.11, carboxylic acid **69** was obtained from ester **66** (114 mg, 0.35 mmol) in quantitative yield.

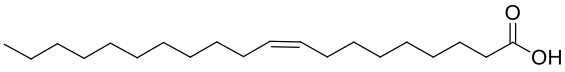

69

R_f: 0.46 (hexane/ethyl acetate, 1:1)
IR (ATR): 1711 (C=O)
^{1}H-NMR ($CDCl_3$, 300 MHz): δ 0.88 (t, *J* = 6.7, 3H, CH_3); 1.26-1.31 (m, 24H, $12CH_2$); 1.56-1.68 (m, 2H, CH_2CH_2CO); 1.94-2.04 (m, 4H, $2CH_2CH_{alkene}$); 2.35 (t, *J* = 7.5, 2H, CH_2CO); 5.29-5.40 (m, 2H, $2CH_{alkene}$)
^{13}C-NMR ($CDCl_3$, 75 MHz): δ 14.3 (CH_3); 22.9; 24.8 ($2CH_2$); 27.3; 27.4 ($2CH_2CH_{alkene}$); 29.2; 29.22; 29.3; 29.5; 29.51; 29.7; 29.8 ($7CH_2$); 29.82 ($2CH_2$); 29.9; 32.1 ($2CH_2$); 34.1 (CH_2CO); 129.9; 130.2 ($2CH_{alkene}$); 180.0 (CO)
MS (ESI, *m/z*): 309.2 $[M-H]^-$

4.1.4.2 Synthesis of phosphorylated diol **71**

(2*R*)-2,3-Bis(benzyloxy)propyl di-*tert*-butyl phosphate, 70

Following the general procedure 4.1.1.12, compound **70** was obtained from (*S*)-2,3-bis(benzyloxy)propan-1-ol (416 mg, 1.53 mmol) and di-*tert*-butyl *N*,*N*-

diisopropylphosphoramidite (0.85 mL, 3.06 mmol) in 38% yield. Chromatography: hexane to hexane/ethyl acetate, 1:1.

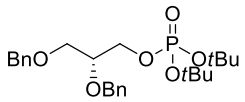

70

R_f: 0.36 (hexane/ethyl acetate, 1:1)
IR (ATR): 1265 (P=O); 996 (P-O)
^{1}H-NMR ($CDCl_3$, 300 MHz): δ 1.46 (s, 18H, $6CH_3$); 3.56-3.66 (m, 2H, CH_2OBn); 3.83 (qt, *J* = 5.1, 1H, CH); 4.00-4.15 (m, 2H, CH_2OP); 4.54 (s, 2H, $PhCH_2$); 4.69 (AB system, *J* = 11.9, 2.8, 2H, $PhCH_2$); 7.25-7.37 (m, 10H, $10CH_{Ar}$)
^{13}C-NMR ($CDCl_3$, 75 MHz): δ 29.9 ($3CH_3$); 30.0 ($3CH_3$); 66.1 (d, *J* = 6.4, CH_2OP); 69.8 (CH_2OBn); 72.4 ($PhCH_2$); 73.5 ($PhCH_2$); 76.9 (d, *J* = 8.6, CH); 82.4 (d, *J* = 7.5, C); 82.5 (d, *J* = 7.4, C); 127.7 ($4CH_{Ar}$); 127.9 ($2CH_{Ar}$); 128.4 ($2CH_{Ar}$); 128.5 ($2CH_{Ar}$); 138.3; 138.5 ($2C_{Ar}$)
^{31}P-NMR ($CDCl_3$, 121 MHz): δ -6.82
$[\alpha]_D^{20}$: +1.6 (c = 1, $CHCl_3$)
MS (ESI, *m/z*): 487.1 $[M+Na]^+$

Di-*tert*-butyl (2*R*)-2,3-dihydroxypropyl phosphate, 71

Following the general procedure 4.1.1.1, diol **71** was obtained from **70** (220 mg, 0.47 mmol) at 60ºC in quantitative yield.

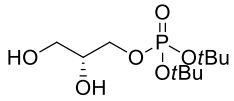

71

R_f: 0.06 (hexane/ethyl acetate, 1:1)
IR (ATR): 3345 (O-H); 1025 (P-O)
^{1}H-NMR ($CDCl_3$, 300 MHz): δ 1.47 (s, 18H, $6CH_3$); 3.60-3.73 (m, 2H, CH_2OH); 3.86-3.92 (m, 3H, CH, 2OH); 4.02 (dd, *J* = 9.1, 5.3, 2H, CH_2OP)
^{13}C-NMR (methanol-d_4, 75 MHz): δ 30.1 ($3CH_3$); 30.2 ($3CH_3$); 63.7 (CH_2OH); 69.2 (d, *J* = 6.8, CH_2OP); 71.9 (d, *J* = 10.1, CH); 84.5 (d, *J* = 7.7, 2C)
^{31}P-NMR ($CDCl_3$, 121 MHz): δ -6.03
$[\alpha]_D^{20}$: -1.5 (c = 1.7, methanol)
MS (ESI, *m/z*): 307.1 $[M+Na]^+$

4.1.4.3 Synthesis of esters **72**-**76**

(2*R*)-3-[(Di-*tert*-butoxyphosphoryl)oxy]-2-hydroxypropyl (9*Z*)-tetradec-9-enoate, 72

Following the general procedure 4.1.1.13, ester **72** was obtained from myristoleic acid (24 µL, 95 µmol) and diol **71** (54 mg, 0.19 mmol) in 28% yield. Chromatography: dichloromethane to dichloromethane/methanol, 95:5.

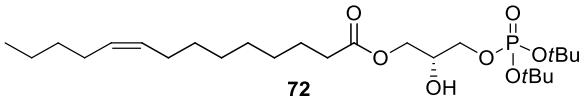

72

R_f: 0.88 (dichloromethane/methanol, 95:5)
IR (ATR): 3365 (O-H); 1739 (C=O); 1257 (P=O); 1000 (P-O)
^{1}H-NMR ($CDCl_3$, 300 MHz): δ 0.89 (t, *J* = 7.0, 3H, CH_3); 1.24-1.34 (m, 12H, $6CH_2$); 1.49 (s, 18H, $6CH_3$); 1.57-1.64 (m, 2H, CH_2CH_2CO); 1.94-2.02 (m, 4H, $2CH_2CH_{alkene}$); 2.33 (t, *J* = 7.6, 2H, CH_2CO); 3.95-4.13 (m, 3H, CH, CH_2OP); 4.15 (d, *J* = 4.7, 2H, CO_2CH_2); 5.27-5.40 (m, 2H, $2CH_{alkene}$)
^{13}C-NMR ($CDCl_3$, 75 MHz): δ 14.1 (CH_3); 22.5; 25.0 ($2CH_2$); 27.1; 27.3 ($2CH_2CH_{alkene}$); 29.2; 29.23; 29.3; 29.8 ($4CH_2$); 29.9 ($3CH_3$); 30.0 ($3CH_3$); 32.1 (CH_2); 34.3 (CH_2CO); 64.7 (CO_2CH_2); 68.3 (d, *J* = 5.8, CH_2OP); 69.1 (d, *J* = 5.0, CH); 83.4 (d, *J* = 7.5, 2C); 129.9; 130.1 ($2CH_{alkene}$); 173.9 (CO)
^{31}P-NMR (methanol-d_4, 121 MHz): δ -5.11
$[\alpha]_D^{20}$: +2.6 (c = 0.5, methanol)
MS (ESI, *m/z*): 515.2 $[M+Na]^+$

(2*R*)-3-[(Di-*tert*-butoxyphosphoryl)oxy]-2-hydroxypropyl (9*Z*)-hexadec-9-enoate, 73

Following the general procedure 4.1.1.13, ester **73** was obtained from palmitoleic acid (66 µL, 0.23 mmol) and diol **71** (133 mg, 0.47 mmol) in 49% yield. Chromatography: hexane/ethyl acetate, 40:1 to 1:1.

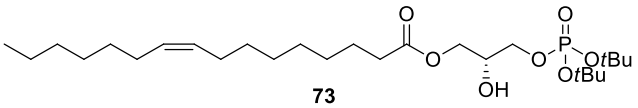

73

R_f: 0.38 (hexane/ethyl acetate, 1:1)
IR (ATR): 3363 (O-H); 1739 (C=O); 1251 (P=O); 1000 (P-O)
^{1}H-NMR ($CDCl_3$, 300 MHz): δ 0.87 (t, *J* = 6.7, 3H, CH_3); 1.28 (m, 16H, $8CH_2$); 1.48 (s, 18H, $6CH_3$); 1.56-1.69 (m, 2H, CH_2CH_2CO); 1.96-2.00 (m, 4H, $2CH_2CH_{alkene}$);

2.32 (t, *J* = 7.6, 2H, CH_2CO); 3.85 (br s, 1H, OH); 3.95-4.09 (m, 3H, CH, CH_2OP); 4.14 (app d, *J* = 4.6, 2H, CO_2CH_2); 5.27-5.38 (m, 2H, $2CH_{alkene}$)

^{13}C-NMR ($CDCl_3$, 75 MHz): δ 14.2 (CH_3); 22.8; 25.0 ($2CH_2$); 27.3; 27.33 ($2CH_2CH_{alkene}$); 29.1 (CH_2); 29.2 ($2CH_2$); 29.3; 29.8; 29.84 ($3CH_2$); 29.9 ($3CH_3$); 30.0 ($3CH_3$); 31.9 (CH_2); 34.2 (CH_2CO); 64.7 (CO_2CH_2); 68.3 (d, *J* = 6.0, CH_2OP); 69.0 (d, *J* = 5.2, CH); 83.4 (d, *J* = 7.5, 2C); 129.9; 130.1 ($2CH_{alkene}$); 173.9 (CO)

^{31}P-NMR ($CDCl_3$, 121 MHz): δ -5.23

$[\alpha]_D^{20}$: -1.9 (c = 1.21, $CHCl_3$)

MS (ESI, *m/z*): 543.3 $[M+Na]^+$

(2*R*)-3-[(Di-*tert*-butoxyphosphoryl)oxy]-2-hydroxypropyl (9*Z*)-heptadec-9-enoate, 74

Following the general procedure 4.1.1.13, ester **74** was obtained from carboxylic acid **67** (92 mg, 0.34 mmol) and diol **71** (195 mg, 0.69 mmol) in 40% yield. Chromatography: hexane/ethyl acetate, 20:1 to 2:1.

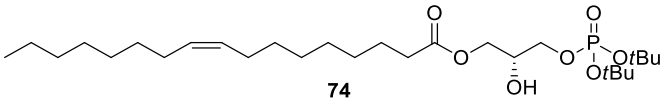

74

R_f: 0.36 (hexane/ethyl acetate, 1:1)

IR (ATR): 3366 (O-H); 1739 (C=O); 1647 (C=C); 1259 (P=O); 1007 (P-O)

^{1}H-NMR ($CDCl_3$, 300 MHz): δ 0.88 (t, *J* = 6.7, 3H, CH_3); 1.21-1.30 (m, 18H, $9CH_2$); 1.50 (s, 18H, $6CH_3$); 1.60-1.64 (m, 2H, CH_2CH_2CO); 1.97-2.01 (m, 4H, $2CH_2CH_{alkene}$); 2.34 (t, *J* = 7.6, 2H, CH_2CO); 3.71 (br s, 1H, OH); 3.98-4.11 (m, 3H, CH, CH_2OP); 4.16 (app d, *J* = 4.9, 2H, CO_2CH_2); 5.28-5.39 (m, 2H, $2CH_{alkene}$)

^{13}C-NMR ($CDCl_3$, 75 MHz): δ 14.1 (CH_3); 22.7; 24.9 ($2CH_2$); 27.2; 27.24 ($2CH_2CH_{alkene}$); 29.1 ($2CH_2$); 29.2; 29.25; 29.3 ($3CH_2$); 29.7 ($2CH_2$); 29.8 ($3CH_3$); 29.9 ($3CH_3$); 31.9 (CH_2); 34.1 (CH_2CO); 64.5 (CO_2CH_2); 68.3 (d, *J* = 5.4, CH_2OP); 69.1 (d, *J* = 4.8, CH); 83.3 (d, *J* = 7.8, 2C); 129.8; 130.0 ($2CH_{alkene}$); 173.8 (CO)

^{31}P-NMR ($CDCl_3$, 121 MHz): δ -5.01

$[\alpha]_D^{20}$: +3.5 (c = 0.77, methanol)

MS (ESI, *m/z*): 557.3 $[M+Na]^+$

(2*R*)-3-[(di-*tert*-butoxyphosphoryl)oxy]-2-hydroxypropyl (9*Z*)-nonadec-9-enoate, 75

Following the general procedure 4.1.1.13, ester **75** was obtained from carboxylic acid **68** (73 mg, 0.25 mmol) and diol **71** (140 mg, 0.49 mmol) in 17% yield. Chromatography: hexane/ethyl acetate, 20:1 to 2:1.

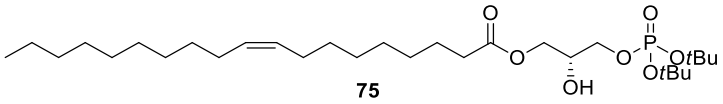

75

R_f: 0.37 (hexane/ethyl acetate, 1:1)
IR (ATR): 3359 (O-H); 1738 (C=O); 1650 (C=C); 1252 (P=O); 1010 (P-O)
^{1}H-NMR ($CDCl_3$, 300 MHz): δ 0.87 (t, *J* = 6.7, 3H, CH_3); 1.26-1.29 (m, 22H, $11CH_2$); 1.49 (s, 18H, $6CH_3$); 1.59-1.64 (m, 2H, CH_2CH_2CO); 1.97-2.01 (m, 4H, $2CH_2CH_{alkene}$); 2.33 (t, *J* = 7.6, 2H, CH_2CO); 3.76 (br s, 1H, OH); 3.95-4.10 (m, 3H, CH, CH_2OP); 4.15 (app d, *J* = 4.9, 2H, CO_2CH_2); 5.28-5.39 (m, 2H, $2CH_{alkene}$)
^{13}C-NMR ($CDCl_3$, 75 MHz): δ 14.3 (CH_3); 22.8; 25.1 ($2CH_2$); 27.3; 27.4 ($2CH_2CH_{alkene}$); 29.2 ($2CH_2$); 29.3; 29.4; 29.5; 29.7; 29.74; 29.8; 29.9 ($7CH_2$); 29.93 ($3CH_3$); 30.0 ($3CH_3$); 32.0 (CH_2); 34.1 (CH_2CO); 64.7 (CO_2CH_2); 68.3 (d, *J* = 6.0, CH_2OP); 69.1 (d, *J* = 5.0, CH); 83.4 (d, *J* = 7.5, 2C); 129.9; 130.1 ($2CH_{alkene}$); 173.9 (CO)
^{31}P-NMR ($CDCl_3$, 121 MHz): δ -5.15
$[\alpha]_D^{20}$: -1.7 (c = 1.18, $CHCl_3$)
MS (ESI, *m/z*): 449.4 $[M\text{-}2t\text{Bu}+H]^+$; 450.4 $[M\text{-}2t\text{Bu}+2H]^+$

(2*R*)-3-[(Di-*tert*-butoxyphosphoryl)oxy]-2-hydroxypropyl (9*Z*)-icos-9-enoate, 76

Following the general procedure 4.1.1.13, ester **76** was obtained from carboxylic acid **69** (65 mg, 0.21 mmol) and diol **71** (121 mg, 0.42 mmol) in 12% yield. Chromatography: hexane/ethyl acetate, 20:1 to 2:1.

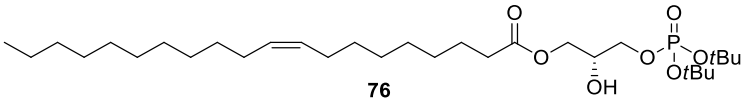

76

R_f: 0.43 (hexane/ethyl acetate, 1:1)
IR (ATR): 3370 (O-H); 1740 (C=O); 1258 (P=O); 1000 (P-O)
^{1}H-NMR ($CDCl_3$, 300 MHz): δ 0.87 (t, *J* = 6.7, 3H, CH_3); 1.26-1.30 (m, 24H, $12CH_2$); 1.50 (s, 18H, $6CH_3$); 1.60-1.65 (m, 2H, CH_2CH_2CO), 1.97-2.01 (m, 4H, $2CH_2CH_{alkene}$); 2.33 (t, *J* = 7.6, 2H, CH_2CO); 3.72 (d, *J* = 4.1, 1H, OH); 3.98-4.11 (m, 3H, CH, CH_2OP); 4.16 (app d, *J* = 4.9, 2H, CO_2CH_2); 5.28-5.39 (m, 2H, $2CH_{alkene}$)
^{13}C-NMR ($CDCl_3$, 75 MHz): δ 14.3 (CH_3); 22.8; 25.0 ($2CH_2$); 27.3; 27.4 ($2CH_2CH_{alkene}$); 29.2 ($2CH_2$); 29.3; 29.4; 29.5; 29.7; 29.78; 29.8; 29.84; 29.9 ($8CH_2$); 30.0 ($6CH_3$); 32.1 (CH_2); 34.3 (CH_2CO); 64.7 (CO_2CH_2); 68.4 (d, *J* = 5.5,

CH_2OP); 69.2 (d, *J* = 4.6, CH); 83.4 (d, *J* = 7.2, 2C); 129.9; 130.2 ($2CH_{alkene}$); 173.9 (CO)
^{31}P-NMR ($CDCl_3$, 121 MHz): δ -5.01
$[\alpha]_D^{20}$: +3.4 (c = 0.92, methanol)
MS (MALDI, *m/z*): 599.4 $[M+Na]^+$

4.1.4.4 Synthesis of final compounds **2a**-**e**

(2*R*)-2-Hydroxy-3-(phosphonooxy)propyl (9*Z*)-tetradec-9-enoate, 2a

Following the general procedure 4.1.1.7, compound **2a** was obtained from di-*tert*-butyl phosphate **72** (7 mg, 14 µmol) and TFA (27 µL, 0.35 mmol) without further purification in 99% yield.

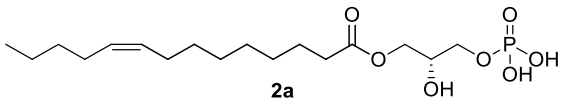

2a

IR (ATR): 3375 (O-H); 1737 (C=O); 1182 (P=O); 1058 (P-OH)
^{1}H-NMR (methanol-d_4, 500 MHz): δ 0.91 (t, *J* = 7.0, 3H, CH_3); 1.29-1.30 (m, 12H, $6CH_2$); 1.60-1.63 (m, 2H, CH_2CH_2CO); 2.02-2.04 (m, 4H, $2CH_2CH_{alkene}$); 2.36 (t, *J* = 7.4, 2H, CH_2CO); 3.96-3.98 (m, 3H, CH, CH_2OP); 4.07-4.17 (m, 2H, CO_2CH_2); 5.29-5.40 (m, 2H, $2CH_{alkene}$)
^{13}C-NMR (methanol-d_4, 125 MHz): δ 14.3 (CH_3); 23.4; 26.0 ($2CH_2$); 27.9; 28.1 ($2CH_2CH_{alkene}$); 30.1; 30.2; 30.3; 30.8; 33.1 ($5CH_2$); 34.9 (CH_2CO); 66.2 (CO_2CH_2); 67.6 (d, *J* = 5.2, CH_2OP); 69.8 (d, *J* = 6.9, CH); 130.8; 130.83 ($2CH_{alkene}$); 175.4 (CO)
^{31}P-NMR (methanol-d_4, 121 MHz): δ 3.23
$[\alpha]_D^{20}$: limited solubility in DMSO
HRMS (ESI, *m/z*): calculated for $C_{17}H_{32}O_7P$ ($[M-H]^-$): 379.2891, found: 379.2848
HPLC (method A, t_R, min): 9.81 min

(2*R*)-2-Hydroxy-3-(phosphonooxy)propyl (9*Z*)-hexadec-9-enoate, 2b

Following the general procedure 4.1.1.7, compound **2b** was obtained from di-*tert*-butyl phosphate **73** (24 mg, 46 µmol) and TFA (88 µL, 1.15 mmol) without further purification in 90% yield.

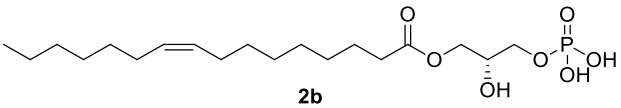

2b

IR (ATR): 3392 (O-H); 1737 (C=O); 1176 (=O); 1057 (P-OH)

^{1}H-NMR (methanol-d_4, 300 MHz): δ 0.90 (t, *J* = 6.7, 3H, CH_3); 1.29-1.33 (m, 16H, $8CH_2$); 1.60-1.64 (m, 2H, CH_2CH_2CO); 2.00-2.04 (m, 4H, $2CH_2CH_{alkene}$); 2.36 (t, *J* = 7.5, 2H, CH_2CO); 3.92-4.04 (m, 3H, CH, CH_2OP); 4.15 (AB system, *J* = 11.4, 4.8, 2H, CO_2CH_2); 5.29-5.40 (m, 2H, $2CH_{alkene}$)
^{13}C-NMR (methanol-d_4, 75 MHz): δ 14.5 (CH_3); 23.7; 26.0 ($2CH_2$); 28.1; 28.2 ($2CH_2CH_{alkene}$); 30.1 (CH_2); 30.2 ($2CH_2$); 30.3; 30.8; 30.84; 32.9 ($4CH_2$); 34.9 (CH_2CO); 66.2 (CO_2CH_2); 67.6 (d, *J* = 5.3, CH_2OP); 69.8 (d, *J* = 8.0, CH); 130.8; 130.9 ($2CH_{alkene}$); 175.4 (CO)
^{31}P-NMR (methanol-d_4, 121 MHz): δ 3.79
$[\alpha]_D^{20}$: limited solubility in DMSO
HRMS (MALDI, *m/z*): calculated for $C_{19}H_{37}NaO_7P$ ($[M+Na]^+$): 431.2175, found: 431.2169
HPLC (method A, t_R, min): 10.06

(2*R*)-2-Hydroxy-3-(phosphonooxy)propyl (9*Z*)-heptadec-9-enoate, 2c

Following the general procedure 4.1.1.7, compound **2c** was obtained from di-*tert*-butyl phosphate **74** (6 mg, 12 µmol) and TFA (22 µL, 0.30 mmol) without further purification in 99% yield.

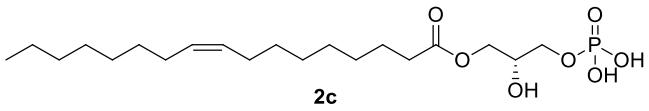

2c

IR (ATR): 3347 (O-H); 1737 (C=O); 1652 (C=C); 1186 (P=O); 1082 (P-OH)
^{1}H-NMR (methanol-d_4, 700 MHz): δ 0.90 (t, *J* = 6.7, 3H, CH_3); 1.29-1.33 (m, 18H, $9CH_2$); 1.60-1.64 (m, 2H, CH_2CH_2CO); 2.01-2.04 (m, 4H, $2CH_2CH_{alkene}$), 2.36 (t, *J* = 7.4, 2H, CH_2CO); 3.89-3.91 (m, 2H, CH_2OP); 3.95-3.98 (m, 1H, CH); 4.11 (dd, *J* = 11.4, 6.2, 1H, ½CO_2CH_2); 4.18 (dd, *J* = 11.4, 4.3, 1H, ½CO_2CH_2); 5.29-5.40 (m, 2H, $2CH_{alkene}$)
^{13}C-NMR (methanol-d_4, 175 MHz): δ 14.5 (CH_3); 23.7; 26.0 ($2CH_2$); 28.1 ($2CH_2CH_{alkene}$); 30.2; 30.22; 30.3; 30.34; 30.8; 30.82; 30.9; 33.1 ($8CH_2$); 34.9 (CH_2CO); 66.4 (CO_2CH_2); 67.2 (d, *J* = 5.2, CH_2OP); 70.1 (d, *J* = 7.9, CH); 130.8; 130.9 ($2CH_{alkene}$); 175.4 (CO)
^{31}P-NMR (methanol-d_4, 121 MHz): δ 4.34
$[\alpha]_D^{20}$: limited solubility in DMSO
HRMS (MALDI, *m/z*): calculated for $C_{20}H_{39}NaO_7P$ ($[M+Na]^+$): 445.2331, found: 445.2311
HPLC (method A, t_R, min): 10.42

(2*R*)-2-Hydroxy-3-(phosphonooxy)propyl (9*Z*)-nonadec-9-enoate, 2d

Following the general procedure 4.1.1.7, compound **2d** was obtained from di-*tert*-butyl phosphate **75** (24 mg, 43 µmol) and TFA (82 µL, 1.08 mmol) without further purification in 99% yield.

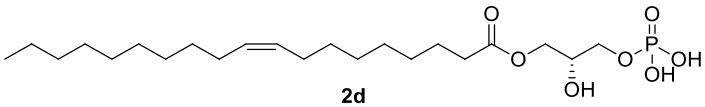

2d

IR (ATR): 3360 (O-H); 1738 (C=O); 1181 (P=O); 1060 (P-OH)

^{1}H-NMR (methanol-d_4, 300 MHz): δ 0.90 (t, *J* = 6.6, 3H, CH_3); 1.29-1.33 (m, 22H, $11CH_2$); 1.59-1.64 (m, 2H, CH_2CH_2CO); 2.02-2.04 (m, 4H, $2CH_2CH_{alkene}$); 2.35 (t, *J* = 7.5, 2H, CH_2CO); 3.91-4.05 (m, 3H, CH, CH_2OP); 4.15 (AB system, *J* = 11.3, 4.9, 2H, CO_2CH_2); 5.29-5.40 (m, 2H, $2CH_{alkene}$)

^{13}C-NMR (methanol-d_4, 75 MHz): δ 14.4 (CH_3); 23.7; 26.0 ($2CH_2$); 28.1 ($2CH_2CH_{alkene}$); 30.2 ($2CH_2$); 30.3 ($2CH_2$); 30.5; 30.6; 30.7 ($3CH_2$); 30.8 ($2CH_2$); 33.1 (CH_2); 34.9 (CH_2CO); 66.3 (CO_2CH_2); 67.5 (d, *J* = 4.8, CH_2OP); 69.9 (d, *J* = 7.7, CH); 130.8; 130.9 ($2CH_{alkene}$); 175.4 (CO)

^{31}P-NMR (methanol-d_4, 121 MHz): δ 3.88

$[\alpha]_D^{20}$: limited solubility in DMSO

HRMS (MALDI, *m/z*): calculated for $C_{22}H_{43}NaO_7P$ ($[M+Na]^+$): 473.2644, found: 473.2642

HPLC (method A, t_R, min): 11.30

(2*R*)-2-Hydroxy-3-(phosphonooxy)propyl (9*Z*)-icos-9-enoate, 2e

Following the general procedure 4.1.1.7, compound **2e** was obtained from di-*tert*-butyl phosphate **76** (9 mg, 16 µmol) and TFA (30 µL, 0.40 mmol) without further purification in 92% yield.

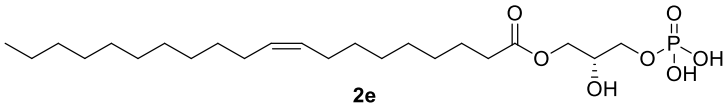

2e

IR (ATR): 3350 (O-H); 1738 (C=O); 1179 (P=O); 1059 (P-OH)

^{1}H-NMR (methanol-d_4, 700 MHz): δ 0.90 (t, *J* = 7.0, 3H, CH_3); 1.29-1.33 (m, 24H, $12CH_2$); 1.60-1.63 (m, 2H, CH_2CH_2CO); 2.02-2.05 (m, 4H, $2CH_2CH_{alkene}$); 2.35 (t, *J* = 7.5, 2H, CH_2CO); 3.94 (app t, *J* = 5.7, 2H, CH_2OP); 3.97-4.00 (m, 1H, CH); 4.11 (dd, *J* = 11.4, 6.0, 1H, ½CO_2CH_2); 4.18 (dd, *J* = 11.4, 4.3, 1H, ½CO_2CH_2); 5.32-5.37 (m, 2H, $2CH_{alkene}$)

^{13}C-NMR (methanol-d_4, 175 MHz): δ 14.5 (CH_3); 23.8; 26.0 ($2CH_2$); 28.1; 28.14 ($2\underline{C}H_2CH_{alkene}$); 30.2; 30.3; 30.5; 30.6 ($4CH_2$); 30.7 ($2CH_2$); 30.77 ($2CH_2$); 30.8 ($2CH_2$); 33.1 (CH_2); 34.9 ($\underline{C}H_2CO$); 66.1 ($CO_2\underline{C}H_2$); 67.6 (d, *J* = 5.3, CH_2OP); 69.7 (d, *J* = 7.6, CH); 130.8; 130.9 ($2CH_{alkene}$); 175.4 (CO)
^{31}P-NMR (methanol-d_4, 121 MHz): δ 3.16
$[\alpha]_D^{20}$: limited solubility in DMSO
HRMS (MALDI, *m/z*): calculated for $C_{23}H_{45}NaO_7P$ ($[M+Na]^+$): 487.2801, found: 487.2798
HPLC (method A, t_R, min): 12.35

*4.1.5 Synthesis of final compounds **3a** and **2f-j***

4.1.5.1 Synthesis of carboxylic acids **77**, **80**, and **81**

10-Phenyldecanoic acid, 77

To a stirred solution of 10-phenyldecanol (500 mg, 2.10 mmol, 1 equiv) in dry DMF (2 mL), pyridinium dichromate was added (2.92 g, 3.89 mmol, 3.7 equiv) and the reaction was stirred at room temperature overnight. Then, solvent was evaporated under reduced pressure and the crude was purified by flash chromatography (dichloromethane to dichloromethane/methanol, 10:1), affording carboxylic acid **77** in 52% yield.

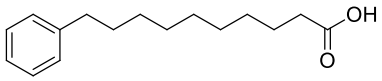

77

R_f: 0.6 (dichloromethane/methanol, 9:1)
^{1}H-NMR ($CDCl_3$, 300 MHz): δ 1.32 (m, 10H, $5CH_2$); 1.63-1.65 (m, 4H, $2CH_2$); 2.34 (t, *J* = 7.4, 2H, CH_2CO); 2.60 (t, *J* = 7.5, 2H, $PhC\underline{H}_2$); 7.18-7.22 (m, 3H, $3CH_{Ar}$); 7.27-7.33 (m, 2H, $2CH_{Ar}$)
^{13}C-NMR ($CDCl_3$, 75 MHz): δ 24.8; 29.2; 29.4; 29.41; 29.5; 29.6; 31.6 ($7CH_2$); 34.2 ($\underline{C}H_2CO$); 36.1 ($Ph\underline{C}H_2$); 125.7 (CH_{Ar}); 128.4 ($2CH_{Ar}$); 128.5 ($2CH_{Ar}$); 143.0 (C_{Ar}); 180.3 (CO)

(7*E,Z*)-8-Phenyloct-7-enoic acid, 78

Following the general procedure 4.1.1.15, alkene **78** was obtained from 7-bromoheptanoic acid (441 mg, 2.11 mmol) and benzaldehyde (103 µL, 1.00 mmol) in 61% yield. Chromatography: hexane to hexane/ethyl acetate, 1:1.

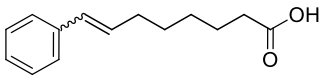

78

R_f: 0.61 (hexane/ethyl acetate, 8:2)
IR (ATR): 3057 (O-H); 1707 (C=O)
^{1}H-NMR ($CDCl_3$, 300 MHz): Mixture *E*:*Z* (2.3:1): δ 1.36-1.53 (m, 4H, $2CH_2$); 1.59-1.73 (m, 2H, CH_2); 2.23 (q, *J* = 6.8, 2H, $CH_2CH_{alkene(E)}$); 2.30-2.40 (m, 4H, $CH_2CH_{alkene(Z)}$, CH_2CO); 5.65 (dt, *J* = 11.7, 7.2, 1H, $CH_2CH_{alkene(Z)}$); 6.21 (dt, *J* = 15.8, 6.8, 1H, $CH_2CH_{alkene(E)}$); 6.39 (d, *J* = 15.6, 1H, $PhCH_{alkene(E)}$); 6.43 (d, *J* = 11.7, 1H, $PhCH_{alkene(Z)}$); 7.16-7.36 (m, 5H, $5CH_{Ar}$)
^{13}C-NMR ($CDCl_3$, 75 MHz): Mixture *E*:*Z* (2.3:1): δ 24.7 (CH_2); 28.5 ($CH_{2\ Z}$); 28.7 ($CH_{2\ E}$); 28.9 ($CH_{2\ Z}$); 29.1 ($CH_{2\ E}$); 32.9 (CH_2CH_{alkene}); 34.1 (CH_2CO); 126.1 ($2CH_{Ar\ E}$); 126.6 ($CH_{Ar\ Z}$); 127.0 ($CH_{Ar\ E}$); 128.3 ($2CH_{Ar\ Z}$); 128.6 ($2CH_{Ar\ E}$); 128.9 ($2CH_{Ar\ Z}$); 129.2 ($CH_{alkene(Z)}$); 130.2 ($CH_{alkene(E)}$); 130.8 ($CH_{alkene(E)}$); 132.8 ($CH_{alkene(Z)}$); 137.9 ($C_{Ar\ Z}$); 138.0 ($C_{Ar\ E}$); 179.9 (CO)
MS (ESI, *m/z*): 217.1 $[M-H]^-$

(8*E,Z*)-9-Phenylnon-8-enoic acid, 79

Following the general procedure 4.1.1.15, alkene **79** was obtained from 8-bromooctanoic acid (1g, 4.48 mmol) and benzaldehyde (0.36 mL, 3.58 mmol) in 70% yield. Chromatography: hexane to hexane/ethyl acetate, 1:1.

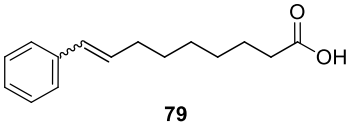

79

R_f: 0.52 (hexane/ethyl acetate, 8:2)
IR (ATR): 3024 (O-H); 1706 (C=O)
^{1}H-NMR ($CDCl_3$, 300 MHz): Mixture *E*:*Z* (1.5:1): δ 1.33-1.41 (m, 4H, $2CH_2$); 1.45-1.52 (m, 2H, CH_2); 1.59-1.72 (m, 2H, CH_2); 2.22 (q, *J* = 6.9, 2H, $CH_2CH_{alkene(E)}$); 2.37 (app q, *J* = 7.6, 4H, $CH_2CH_{alkene(Z)}$, CH_2CO); 5.66 (dt, *J* = 11.7, 7.3, 1H, $CH_2CH_{alkene(Z)}$); 6.23 (dt, *J* = 15.8, 6.8, 1H, $CH_2CH_{alkene(E)}$); 6.39 (d, *J* = 15.5, 1H, $PhCH_{alkene(E)}$); 6.44 (d, *J* = 11.5, 1H, $PhCH_{alkene(Z)}$); 7.17-7.37 (m, 5H, $5CH_{Ar}$)
^{13}C-NMR ($CDCl_3$, 75 MHz): Mixture *E*:*Z* (1.5:1): δ 24.7 and 24.75 (CH_2); 28.6; 28.9; 29.0; 29.3 and 29.9 ($3CH_{2\ Z,E}$); 33.1 (CH_2CH_{alkene}); 34.1 and 34.14 (CH_2CO); 126.0 ($2CH_{Ar\ E}$); 126.6 ($CH_{Ar\ Z}$); 126.9 ($CH_{Ar\ E}$); 128.2 ($2CH_{Ar\ Z}$); 128.6 ($2CH_{Ar\ E}$); 128.9 ($2CH_{Ar\ Z}$); 129.0 ($CH_{alkene(Z)}$); 130.0 ($CH_{alkene(E)}$); 131.06 ($CH_{alkene(E)}$); 133.10 ($CH_{alkene(Z)}$); 137.9 ($C_{Ar\ Z}$); 138.0 ($C_{Ar\ E}$); 180.1 (CO)

MS (ESI, *m/z*): 231.1 $[M-H]^-$

8-Phenyloctanoic acid, 80

Following the general procedure 4.1.1.1, carboxylic acid **80** was obtained from alkene **78** (60 mg, 0.27 mmol) at room temperature in 97% yield. The spectroscopic data correspond with those previously reported.[110]

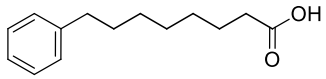

80

R_f: 0.60 (hexane/ethyl acetate, 8:2)
^{1}H-NMR ($CDCl_3$, 300 MHz): δ 1.41 (app s, 6H, $3CH_2$); 1.70 (br s, 4H, $2CH_2$); 2.42 (t, *J* = 7.5, 2H, CH_2CO); 2.67 (t, *J* = 7.7, 2H, $PhCH_2$); 7.23-7.26 (m, 3H, $3CH_{Ar}$); 7.32-7.37 (m, 2H, $2CH_{Ar}$)

9-Phenylnonanoic acid, 81

Following the general procedure 4.1.1.1, carboxylic acid **81** was obtained from alkene **79** (300 mg, 1.29 mmol) at room temperature in 81% yield.

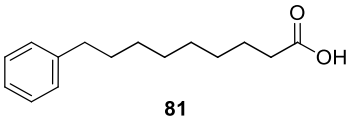

81

R_f: 0.61 (hexane/ethyl acetate, 8:2)
IR (ATR): 3063 (O-H); 1707 (C=O)
^{1}H-NMR ($CDCl_3$, 300 MHz): δ 1.32 (app s, 8H, $4CH_2$); 1.56-1.65 (m, 4H, $2CH_2$); 2.35 (t, *J* = 7.5, 2H, CH_2CO); 2.60 (t, *J* = 7.7, 2H, $PhCH_2$); 7.16-7.19 (m, 3H, $3CH_{Ar}$); 7.25-7.30 (m, 2H, $2CH_{Ar}$)
^{13}C-NMR ($CDCl_3$, 75 MHz): δ 24.8; 29.2; 29.3; 29.35; 29.4; 31.6 ($6CH_2$); 34.2 (CH_2CO); 36.1 ($PhCH_2$); 125.7 (CH_{Ar}); 128.4 ($2CH_{Ar}$); 128.5 ($2CH_{Ar}$); 143.0 (C_{Ar}); 180.5 (CO)
MS (ESI, *m/z*): 233.1 $[M-H]^-$

4.1.5.2 Synthesis of the phosphorylated diols **83** and **86**

[(4*R*)-2,2-Dimethyl-1,3-dioxolan-4-yl]methyl diethyl phosphate, 82

To a solution of (*S*)-(2,2-dimethyl-1,3-dioxolan-4-yl)methanol (0.3 mL, 2.43 mmol, 1 equiv) in 8 mL of anhydrous dichloromethane, diethyl chlorophosphate (0.44 mL, 3.04 mmol, 1.25 equiv) and potassium *tert*-butoxide (408 mg, 3.64 mmol, 1.5 equiv) were added and the mixture was stirred at room temperature for 48 h.

Then, the reaction was quenched with a saturated aqueous solution of NH_4Cl (3.5 mL/mmol of base) and stirred for 10 additional minutes. The mixture was extracted with dichloromethane and the organic phase was dried over Na_2SO_4, filtered and concentrated under reduced pressure. The residue was purified by flash chromatography (dichloromethane/ethyl acetate, 10:1 to 1:1), to afford pure product **82** in 92% yield.

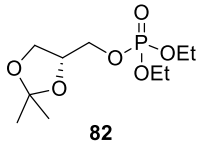

82

R_f: 0.26 (dichloromethane/ethyl acetate, 8:2)
IR (ATR): 1021 (P-O)
^{1}H-NMR ($CDCl_3$, 300 MHz): δ 1.31 (td, *J* = 7.1, 0.9, 6H, $2CH_2CH_3$); 1.33 (s, 3H, $CH_{3\ acetal}$); 1.39 (s, 3H, $CH_{3\ acetal}$); 3.81 (dd, *J* = 8.6, 5.5, 1H, ½CH_2O); 3.92-4.05 (m, 3H, ½CH_2O, CH_2OP); 4.07-4.16 (m, 4H, $2CH_2CH_3$): 4.24-4.33 (m, 1H, CH)
^{13}C-NMR ($CDCl_3$, 75 MHz): δ 16.2 (d, *J* = 6.7, $2CH_2CH_3$); 25.4 ($CH_{3\ acetal}$); 26.8 ($CH_{3\ acetal}$); 64.1 (d, *J* = 5.7, $2CH_2CH_3$); 66.3 (CH_2O); 67.4 (d, *J* = 5.8, CH_2OP); 74.2 (d, *J* = 8.2, CH); 109.9 (C)

(2*R*)-2,3-Dihydroxypropyl diethyl phosphate, 83

Following the general procedure 4.1.1.5, diol **83** was obtained from **82** (600 mg, 2.24 mmol) in 50% yield. Chromatography: dichloromethane/methanol, 50:1 to 10:1.

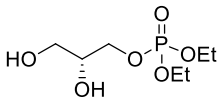

83

R_f: 0.11 (dichloromethane/methanol, 10:1)
IR (ATR): 3405 (O-H); 1256 (P=O); 1027 (P-O)
^{1}H-NMR ($CDCl_3$, 300 MHz): δ 1.34 (t, *J* = 7.1, 6H, $2CH_3$); 3.21 (br s, 2H, 2OH); 3.60-3.73 (m, 2H, CH_2OP); 3.75-3.83 (m, 1H, ½CH_2OH); 3.86-3.94 (m, 1H, CH); 4.06-4.18 (m, 5H, ½CH_2OH, $2CH_2CH_3$)
^{13}C-NMR ($CDCl_3$, 75 MHz): δ 16.2 (d, *J* = 6.7, $2CH_3$); 62.9 (CH_2OH); 64.5 (d, *J* = 6.0, $2CH_2CH_3$); 68.5 (d, *J* = 5.8, CH_2OP); 70.8 (d, *J* = 5.5, CH)
$[\alpha]_D^{20}$: -6.5 (c = 1.11, methanol)

Dibenzyl [(4*R*)-2,2-dimethyl-1,3-dioxolan-4-yl]methyl phosphate, 85

Following the general procedure 4.1.1.12, compound **85** was obtained from (*S*)-(2,2-dimethyl-1,3-dioxolan-4-yl)methanol (0.2 mL, 1.62 mmol) and dibenzyl *N*,*N*-diisopropylphosphoramidite (0.97 mL, 2.91 mmol) in 76% yield. Chromatography: hexane to hexane/ethyl acetate, 1:1.

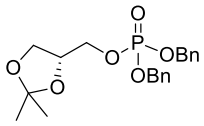

85

R_f: 0.4 (hexane/ethyl acetate, 1:1)
IR (ATR): 1255 (P=O); 991 (P-O)
^{1}H-NMR ($CDCl_3$, 300 MHz): δ 1.32 (s, 3H, CH_3); 1.38 (s, 3H, CH_3); 3.72 (dd, *J* = 8.6, 5.5, 1H, ½CH_2O); 3.87-4.04 (m, 3H, ½CH_2O, CH_2OP); 4.20 (qt, *J* = 5.7, 1H, CH); 4.97-5.13 (m, 4H, 2PhCH_2); 7.34 (app s, 10H, 10CH_{Ar})
^{13}C-NMR ($CDCl_3$, 75 MHz): δ 25.3; 26.8 (2CH_3); 66.2 (CH_2O); 67.5 (d, *J* = 5.9, CH_2OP); 69.5 (d, *J* = 5.6, 2PhCH_2); 74.0 (d, *J* = 8.3, CH); 109.9 (C); 128.1 (4CH_{Ar}); 128.7 (6CH_{Ar}); 135.8 (d, *J* = 6.6, 2C_{Ar})
^{31}P-NMR ($CDCl_3$, 121 MHz): δ 2.03
$[\alpha]_D^{20}$: +1.6 (c = 1, methanol)
MS (ESI, *m/z*): 393.1 $[M+H]^+$

Dibenzyl (2*R*)-2,3-dihydroxypropyl phosphate, 86

Following the general procedure 4.1.1.5, diol **86** was obtained from **85** (390 mg, 0.99 mmol) in 65% yield. Chromatography: ethyl acetate to ethyl acetate/ethanol, 7:3.

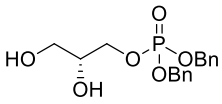

86

R_f: 0.56 (ethyl acetate)
IR (ATR): 3368 (O-H); 1255 (P=O); 1013 (P-O)
^{1}H-NMR ($CDCl_3$, 300 MHz): δ 2.53 (br s, 2H, OH); 3.52-3.65 (m, 2H, CH_2OP); 3.78-3.85 (m, 1H, CH); 4.03 (dd, *J* = 9.5, 5.0, 2H, CH_2OH); 4.98-5.11 (m, 4H, 2PhCH_2); 7.35 (app s, 10H, 10CH_{Ar})

^{13}C-NMR ($CDCl_3$, 75 MHz): δ 62.7 (CH_2OH); 68.8 (d, *J* = 5.9, CH_2OP); 69.9 (d, *J* = 5.8, 2Ph$\underline{C}H_2$); 70.7 (d, *J* = 5.2, CH); 128.2 ($4CH_{Ar}$); 128.8 ($4CH_{Ar}$); 128.9 ($2CH_{Ar}$); 135.60 (d, *J* = 6.6, $2C_{Ar}$)
^{31}P-NMR ($CDCl_3$, 121 MHz): δ 3.19
$[\alpha]_D^{20}$: -4.6 (c = 0.99, methanol)
MS (ESI, *m/z*): 353.0 $[M+H]^+$

4.1.5.3 Synthesis of carboxylic acids **93**, **96**, and **100**

(6*E*)-7-Biphenyl-4-ylhept-6-enoic acid, 92

Following the general procedure 4.1.1.15, alkene **92** was obtained from 6-bromohexanoic acid (1 g, 5.13 mmol) and biphenyl-4-carbaldehyde (540 mg, 2.96 mmol) in 72% yield. Chromatography: dichloromethane to dichoromethane/ethyl acetate, 5:1.

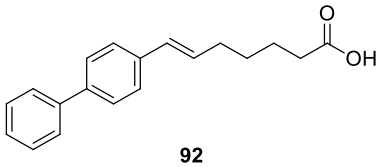

92

R_f: 0.39 (dichoromethane/ethyl acetate, 8:2)
IR (ATR): 3026 (O-H); 1700 (C=O)
^{1}H-NMR ($CDCl_3$, 300 MHz): δ 1.51-1.61 (m, 2H, CH_2); 1.67-1.78 (m, 2H, CH_2); 2.27 (q, *J* = 6.7, 2H, $C\underline{H}_2CH_{alkene}$); 2.41 (t, *J* = 7.4, 2H, CH_2CO); 6.25 (dt, *J* = 15.8, 6.8, 1H, $C\underline{H}CH_2$); 6.44 (d, *J* = 15.9, 1H, Ar$C\underline{H}$); 7.33 (t, *J* = 7.3, 1H, CH_{Ar}); 7.40-7.46 (m, 4H, $4CH_{Ar}$); 7.53-7.62 (m, 4H, $4CH_{Ar}$)
^{13}C-NMR ($CDCl_3$, 75 MHz): δ 24.4; 28.9 ($2CH_2$); 32.8 ($\underline{C}H_2CH_{alkene}$); 33.9 ($\underline{C}H_2CO$); 126.5 ($2CH_{Ar}$); 127.0 ($2CH_{Ar}$); 127.30 ($CH_{Ar}$); 127.34 ($2CH_{Ar}$); 128.9 ($2CH_{Ar}$); 130.0; 130.5 ($2CH_{alkene}$); 136.9; 139.8; 141.0 ($3C_{Ar}$); 179.5 (CO)
MS (ESI, *m/z*): 279.1 $[M-H]^-$

7-Biphenyl-4-ylheptanoic acid, 93

Following the general procedure 4.1.1.1, carboxylic acid **93** was obtained from alkene **92** (300 mg, 1.07 mmol) at room temperature as a white solid in 95% yield. The spectroscopic data correspond with those previously reported.[103]

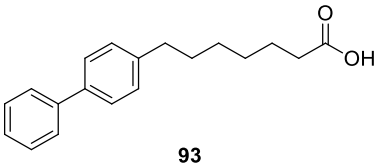

93

Rf: 0.43 (dichloromethane/ethyl acetate, 8:2)
m.p.: 70-71ºC (lit.[103] m.p.: 69-70ºC)
^{1}H-NMR ($CDCl_3$, 300 MHz): δ 1.37-1.42 (m, 4H, $2CH_2$); 1.61-1.71 (m, 4H, $2CH_2$); 2.36 (t, *J* = 7.5, 2H, CH_2CO); 2.65 (t, *J* = 7.5, 2H, $ArCH_2$); 7.25 (d, *J* = 8.7, 2H, $2CH_{Ar}$); 7.32 (t, *J* = 7.3, 1H, CH_{Ar}); 7.43 (t, *J* = 7.4, 2H, $2CH_{Ar}$); 7.51 (d, *J* = 8.2, 2H, $2CH_{Ar}$); 7.56-7.60 (m, 2H, $2CH_{Ar}$)
MS (ESI, *m/z*): 281.1 $[M-H]^-$

9-Bromononanoic acid, 94

Following the general procedure 4.1.1.14, carboxylic acid **94** was obtained from 9-bromononanol (1 g, 4.48 mmol) in 61% yield. Chromatography: dichloromethane to dichloromethane/ethyl acetate 5:1. The spectroscopic data correspond with those previously reported.[111]

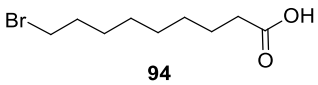

94

Rf: 0.67 (dichloromethane/ethyl acetate, 8:2)
^{1}H-NMR ($CDCl_3$, 300 MHz): δ 1.32-1.37 (m, 6H, $3CH_2$); 1.40-1.44 (m, 2H, CH_2); 1.58-1.69 (m, 2H, CH_2); 1.80-1.90 (m, 2H, CH_2); 2.36 (t, *J* = 7.5, 2H, CH_2CO); 3.40 (t, *J* = 6.8, 2H, CH_2Br); 8.81 (br s, 1H, OH)

(9*E,Z*)-10-Biphenyl-4-yldec-9-enoic acid, 95

Following the general procedure 4.1.1.15, alkene **95** was obtained from **94** (650 mg, 5.13 mmol) and biphenyl-4-carbaldehyde (400 mg, 2.19 mmol) in 51% yield. Chromatography: dichloromethane to dichloromethane/ethyl acetate, 5:1.

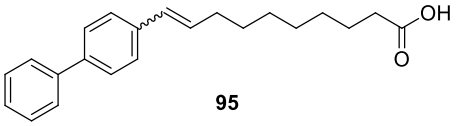

95

Rf: 0.5 (dichloromethane/ethyl acetate, 8:2)
IR (ATR): 3030 (O-H); 1705 (C=O)
^{1}H-NMR ($CDCl_3$, 300 MHz): Mixture *E*:*Z* (1.5:1): δ 1.36-1.39 (m, 6H, $3CH_2$); 1.48 (m, 2H, CH_2); 1.59-1.66 (m, 2H, CH_2); 2.23 (q, *J* = 6.7, 2H, $CH_2CH_{alkene(E)}$); 2.32-

2.42 (m, 4H, $C\underline{H}_2CH_{alkene(Z)}$, CH_2CO); 5.69 (dt, *J* = 11.8, 7.3, 1H, $CH_2C\underline{H}_{alkene(Z)}$); 6.27 (dt, *J* = 15.8, 6.7, 1H, $CH_2C\underline{H}_{alkene(E)}$); 6.42 (d, *J* = 15.9, 1H, $ArC\underline{H}_{alkene(E)}$); 6.44 (d, *J* = 11.5, 1H, $ArC\underline{H}_{alkene(Z)}$); 7.31-7.47 (m, 5H, $5CH_{Ar}$); 7.53-7.63 (m, 4H, $4CH_{Ar}$)

^{13}C-NMR ($CDCl_3$, 75 MHz): Mixture *E*:*Z* (1.5:1): δ 24.7 and 24.8 (CH_2); 28.9; 28.93; 29.0; 29.1; 29.2; 29.4 and 30.0 ($4CH_{2\ E,Z}$); 33.1 and 33.2 ($\underline{C}H_2CH_{alkene}$); 34.2 (br s, $\underline{C}H_2CO$); 126.4 ($2CH_{Ar\ E}$); 126.9 ($2CH_{Ar\ Z}$); 127.0 ($2CH_{Ar\ E}$); 127.1 ($2CH_{Ar\ Z}$); 127.3 ($CH_{Ar\ E}$); 127.31 ($2CH_{Ar\ E}$); 128.5 ($CH_{Ar\ Z}$); 128.8 ($2CH_{Ar\ E}$); 128.9 ($2CH_{Ar\ Z}$); 129.3 ($2CH_{Ar\ Z}$); 129.5 ($CH_{alkene(Z)}$); 131.3 ($CH_{alkene(E)}$); 132.3 ($CH_{alkene(E)}$); 133.4 ($CH_{alkene(Z)}$); 137.0 and 137.1 (C_{Ar}); 139.3 and 139.6 (C_{Ar}); 140.9 and 141.0 (C_{Ar}); 180.3 (CO)

MS (ESI, *m/z*): 321.1 $[M-H]^-$

10-Biphenyl-4-yldecanoic acid, 96

Following the general procedure 4.1.1.1, carboxylic acid **96** was obtained from alkene **95** (240 mg, 0.75 mmol) at room temperature as a white solid in 83% yield.

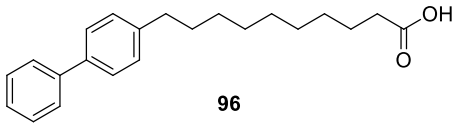

96

R_f: 0.5 (dichloromethane/ethyl acetate, 8:2)

m.p.: 92-95ºC

IR (ATR): 3032 (O-H); 1696 (C=O)

^{1}H-NMR ($CDCl_3$, 300 MHz): δ 1.31-1.39 (m, 10H, $5CH_2$); 1.68 (m, 4H, $2CH_2$); 2.40 (t, *J* = 7.5, 2H, CH_2CO); 2.69 (t, *J* = 7.5, 2H, $ArC\underline{H}_2$); 7.31 (d, *J* = 8.1, 2H, $2CH_{Ar}$); 7.37 (t, *J* = 7.3, 1H, CH_{Ar}); 7.48 (t, *J* = 7.5, 2H, $2CH_{Ar}$); 7.56 (d, *J* = 8.1, 2H, $2CH_{Ar}$); 7.62-7.65 (m, 2H, $2CH_{Ar}$)

^{13}C-NMR ($CDCl_3$, 75 MHz): δ 24.8; 29.2; 29.3; 29.4; 29.5; 29.6; 31.6 ($7CH_2$); 34.2 ($\underline{C}H_2CO$); 35.7 ($Ar\underline{C}H_2$); 127.1 (CH_{Ar}); 127.12 ($4CH_{Ar}$); 128.8 ($2CH_{Ar}$); 129.0 ($2CH_{Ar}$); 138.7; 141.3; 142.2 ($3C_{Ar}$), 180.2 (CO)

MS (ESI, *m/z*): 323.3 $[M-H]^-$

12-Bromododecan-1-ol, 97

To a suspension of 1,12-dodecanodiol (1.00 g, 4.94 mmol, 1 equiv) in cyclohexane (15 mL), 47% aq. HBr (15 mL) was added and the reaction was refluxed for 6 h. Then, the mixture was extracted with hexane and the organic phase was washed with a saturated aqueous solution of $NaHCO_3$ and with brine, dried over Na_2SO_4, filtered and evaporated under reduced pressure. The crude was purified by flash cromatography (hexane to dichloromethane) to afford

bromoalcohol **97** as in 65% yield. The spectroscopic data correspond with those previously reported.[112]

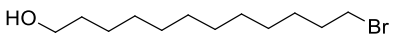

97

R_f: 0.71 (dichloromethane/ethyl acetate, 8:2)
^{1}H-NMR ($CDCl_3$, 300 MHz): δ 1.27-1.44 (m, 16H, $8CH_2$); 1.52-1.61 (m, 2H, CH_2); 1.80-1.90 (m, 2H, CH_2); 3.40 (t, *J* = 6.9, 2H, CH_2Br); 3.64 (t, *J* = 6.6, 2H, CH_2OH)

12-Bromododecanoic acid, 98

Following the general procedure 4.1.1.14, carboxylic acid **98** was obtained from bromoalcohol **97** (850 mg, 3.2 mmol) in 43% yield. Chromatography: dichloromethane to dichloromethane/ethyl acetate, 5:1. The spectroscopic data correspond with those previously reported.[112]

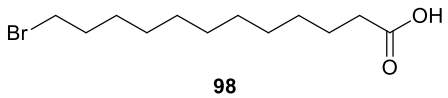

98

R_f: 0.51 (dichloromethane/ethyl acetate, 8:2)
^{1}H-NMR ($CDCl_3$, 300 MHz): δ 1.28 (app s, 12H, $6CH_2$); 1.39-1.44 (m, 2H, CH_2); 1.58-1.65 (m, 2H, CH_2); 1.80-1.89 (m, 2H, CH_2); 2.35 (t, *J* = 7.5, 2H, CH_2CO); 3.40 (t, *J* = 6.8, 2H, CH_2Br)

(12*E,Z*)-13-Biphenyl-4-yltridec-12-enoic acid, 99

Following the general procedure 4.1.1.15, alkene **99** was obtained from **98** (800 mg, 2.87 mmol) and biphenyl-4-carbaldehyde (422 mg, 2.32 mmol) in 38% yield. Chromatography: dichloromethane to dichloromethane/ethyl acetate, 5:1.

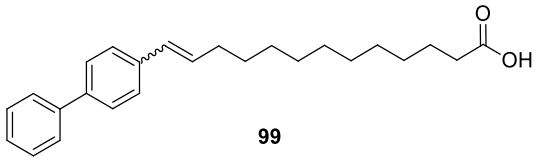

99

R_f: 0.46 (dichoromethane/ethyl acetate, 8:2)
IR (ATR): 3030 (O-H); 1703 (C=O)
^{1}H-NMR ($CDCl_3$, 300 MHz): Mixture *E*:*Z* (1:1): δ 1.26-1.29 (m, 10H, $5CH_2$); 1.45-1.50 (m, 2H, CH_2); 1.60-1.66 (m, 4H, $2CH_2$); 2.23 (q, *J* = 6.9, 2H, $CH_2CH_{alkene(Z)}$); 2.32-2.39 (m, 4H, $CH_2CH_{alkene(E)}$, CH_2CO); 5.70 (dt, *J* = 11.7, 7.2, 1H, $CH_2CH_{alkene(Z)}$); 6.27 (dt, *J* = 15.8, 6.7, 1H, $CH_2CH_{alkene(E)}$); 6.43 (d, *J* = 11.6, 1H,

ArC<u>H</u>$_{alkene(Z)}$); 6.47 (d, *J* = 15.2, 1H, ArC<u>H</u>$_{alkene(E)}$); 7.33-7.47 (m, 5H, 5CH_{Ar}); 7.52-7.63 (m, 4H, 4CH_{Ar})

<u>^{13}C-NMR ($CDCl_3$, 75 MHz)</u>: Mixture *E*:*Z* (1:1): δ 24.8 (CH_2); 28.9; 29.2; 29.4; 29.5; 29.53; 29.6; 29.7 and 30.1 (7$CH_{2\ Z,E}$); 31.7 and 33.3 (<u>C</u>H_2CH_{alkene}); 34.1 (<u>C</u>H_2CO); 126.4; 126.9; 127.0; 127.1; 127.2; 127.3; 128.4; 128.8 and 128.9 (7$CH_{Ar\ Z,E}$); 129.0 ($CH_{alkene\ Z/E}$); 129.3 (2$CH_{Ar\ Z/E}$); 129.4 ($CH_{alkene\ Z/E}$); 131.6 and 133.7 ($CH_{alkene\ Z,E}$); 137.0 and 137.2 (C_{Ar}); 138.8 and 139.3 (C_{Ar}); 140.2 and 141.0 (C_{Ar}); 179.7 (CO)

<u>MS (ESI, *m/z*)</u>: 363.2 $[M-H]^-$

13-Biphenyl-4-yltridecanoic acid, 100

Following the general procedure 4.1.1.1, carboxylic acid **100** was obtained from alkene **99** (300 mg, 0.82 mmol) at room temperature as a white solid in 96% yield.

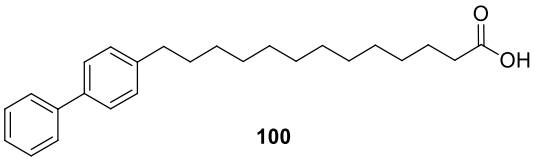

100

<u>R_f</u>: 0.46 (dichoromethane/ethyl acetate, 8:2)

<u>m.p.</u>: 103-105ºC

<u>IR (ATR)</u>: 3027 (O-H); 1696 (C=O)

<u>^{1}H-NMR ($CDCl_3$, 300 MHz)</u>: δ 1.22-1.46 (m, 16H, 8CH_2); 1.57-1.73 (m, 4H, 2CH_2); 2.35 (t, *J* = 7.5, 2H, CH_2CO); 2.65 (t, *J* = 7.5, 2H, ArC<u>H</u>$_2$); 7.26 (d, *J* = 8.0, 2H, 2CH_{Ar}); 7.32 (t, *J* = 7.3, 1H, CH_{Ar}); 7.43 (t, *J* = 7.5, 2H, 2CH_{Ar}); 7.52 (d, *J* = 8.1, 2H, 2CH_{Ar}); 7.59 (d, *J* = 7.6, 2H, 2CH_{Ar})

<u>^{13}C-NMR ($CDCl_3$, 75 MHz)</u>: δ 24.8; 29.2; 29.4; 29.5; 29.6; 29.7 (6CH_2); 29.72 (2CH_2); 29.8; 31.7 (2CH_2); 34.2 (<u>C</u>H_2CO); 35.8 (Ar<u>C</u>H_2); 127.1 (CH_{Ar}); 127.12 (4CH_{Ar}); 128.8 (2CH_{Ar}); 129.0 (2CH_{Ar}); 138.7; 141.3; 142.3 (3C_{Ar}); 180.0 (CO)

<u>MS (ESI, *m/z*)</u>: 365.2 $[M-H]^-$

4.1.5.4 <u>Synthesis of esters **84**, **87**-**91** and **101**-**103**</u>

(2*R*)-3-[(Diethoxyphosphoryl)oxy]-2-hydroxypropyl 10-phenyldecanoate, 84

Following the general procedure 4.1.1.13, ester **84** was obtained from carboxylic acid **77** (136 mg, 0.55 mmol) and diol **83** (250 mg, 1.10 mmol) in 30% yield. Chromatography: dichloromethane/methanol, 200:1 to 50:1.

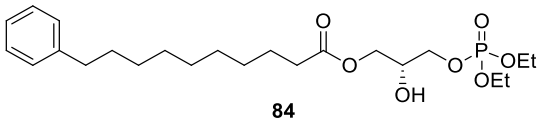

84

R_f: 0.45 (dichloromethane/methanol, 10:1)
^{1}H-NMR ($CDCl_3$, 300 MHz): δ 1.28 (app s, 10H, $5CH_2$); 1.35 (td, *J* = 7.1, 0.9, 6H, $2CH_3$); 1.55-1-62 (m, 4H, $2CH_2$); 2.33 (t, *J* = 7.6, 2H, CH_2CO); 2.59 (t, *J* = 7.7, 2H, $PhCH_2$); 4.02 – 4.26 (m, 9H, CH, $2CH_2CH_3$, CH_2OP, CH_2CO_2); 7.14-7.18 (m, 3H, $3CH_{Ar}$); 7.24-7.30 (m, 2H, $2CH_{Ar}$)
^{13}C-NMR ($CDCl_3$, 75 MHz): δ 16.2 (d, *J* = 6.6, $2CH_3$); 25.0; 29.2; 29.4; 29.41; 29.5; 29.6; 31.6 ($7CH_2$); 34.2 (CH_2CO); 36.1 ($PhCH_2$); 64.4 (d, *J* = 1.9, $2CH_2CH_3$); 64.5 (CO_2CH_2); 68.8 (d, *J* = 5.7, CH_2OP); 69.0 (d, *J* = 5.5, CH); 125.7 (CH_{Ar}); 128.3 ($2CH_{Ar}$); 128.5 ($2CH_{Ar}$); 143.0 (C_{Ar}); 174.0 (CO)
MS (ESI, *m/z*): 459.2 $[M+H]^+$

(2*R*)-3-{[Bis(benzyloxy)phosphoryl]oxy}-2-hydroxypropyl 7-phenylheptanoate 87

Following the general procedure 4.1.1.13, ester **87** was obtained from 7-phenylheptanoic acid (35 mg, 0.17 mmol) and diol **86** (120 mg, 0.34 mmol) in 39% yield. Chromatography: dichloromethane/ethyl acetate, 100:1 to 7:3.

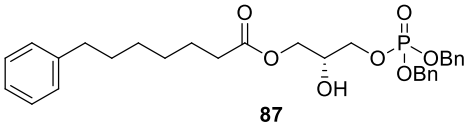

87

R_f: 0.32 (dichloromethane/ethyl acetate, 8:2)
IR (ATR): 3384 (O-H); 1736 (C=O); 1253 (P=O); 1007 (P-O)
^{1}H-NMR (C_6D_6, 300 MHz): δ 1.22-1.27 (m, 4H, $2CH_2$); 1.53-1.63 (m, 4H, $2CH_2$); 2.20 (t, *J* = 7.5, 2H, CH_2CO); 2.57 (t, *J* = 7.5, 2H, $PhCH_2$); 4.11-4.21 (m, 3H, CH, CH_2OP); 4.27-4.38 (m, 2H, CO_2CH_2); 4.47 (br s, 1H, OH); 5.00-5.14 (m, 4H, $2OCH_2Ph$); 7.13-7.24 (m, 9H, $9CH_{Ar}$); 7.29-7.35 (m, 6H, $6CH_{Ar}$)
^{13}C-NMR (C_6D_6, 75 MHz): δ 25.1; 29.2; 29.22; 31.6 ($4CH_2$); 34.1 (CH_2CO); 36.2 ($PhCH_2$); 64.6 (CO_2CH_2); 69.0 (d, *J* = 5.5, CH); 69.4 (d, *J* = 5.8, CH_2OP); 69.7 (d, *J* = 4.9, OCH_2Ph); 69.74 (d, *J* = 5.1, OCH_2Ph); 126.0 (CH_{Ar}); 128.4 ($2CH_{Ar}$); 128.41 ($2CH_{Ar}$); 128.6 ($2CH_{Ar}$); 128.7 ($2CH_{Ar}$); 128.76 ($2CH_{Ar}$); 128.78 ($4CH_{Ar}$); 136.4 (d, *J* = 6.7, $2C_{Ar}$); 142.9 (C_{Ar}); 173.1 (CO)
^{31}P-NMR (C_6D_6, 121 MHz): δ 3.65
MS (ESI, *m/z*): 523.2 $[M-H_2O+H]^+$; 541.3 $[M+H]^+$

(2*R*)-3-{[Bis(benzyloxy)phosphoryl]oxy}-2-hydroxypropyl 8-phenyloctanoate, 88

Following the general procedure 4.1.1.13, ester **88** was obtained from carboxylic acid **80** (37 mg, 0.17 mmol) and diol **86** (120 mg, 0.34 mmol) in 53% yield. Chromatography: dichloromethane to dichloromethane/methanol, 95:5.

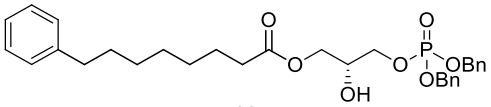

88

R_f: 0.44 (dichloromethane/methanol, 95:5)

IR (ATR): 3382 (O-H); 1738 (C=O); 1265 (P=O); 1016 (P-O)

^{1}H-NMR (methanol-d_4, 300 MHz): δ 1.22-1.35 (m, 6H, $3CH_2$); 1.48-1.64 (m, 4H, $2CH_2$); 2.19-2.32 (m, 2H, CH_2CO); 2.52-2.59 (m, 2H, $PhCH_2$); 3.42-4.70 (m, 1H, ½CH_2OP); 3.91-4.36 (m, 4H, CH, ½CH_2OP, CO_2CH_2); 5.01-5.10 (m, 4H, $2OCH_2Ph$); 7.09-7.14 (m, 3H, $3CH_{Ar}$); 7.20-7.25 (m, 2H, $2CH_{Ar}$); 7.30-7.39 (m, 10H, $10CH_{Ar}$)

^{13}C-NMR (methanol-d_4, 75 MHz): δ 26.0; 30.07; 30.1; 30.2; 32.6 ($5CH_2$); 34.7 (CH_2CO); 36.9 ($PhCH_2$); 65.4 (CO_2CH_2); 68.9 (d, J = 7.9, CH); 69.5 (d, J = 6.1, CH_2OP); 70.9 (d, J = 5.9, $2OCH_2Ph$); 126.6 (CH_{Ar}); 129.2 ($2CH_{Ar}$); 129.24 ($2CH_{Ar}$); 129.4 ($4CH_{Ar}$); 129.7 ($4CH_{Ar}$); 129.8 ($2CH_{Ar}$); 137.1 (d, J = 6.4, $2C_{Ar}$); 143.9 (C_{Ar}); 175.1 (CO)

^{31}P-NMR (methanol-d_4, 121 MHz): δ 1.54

$[\alpha]_D^{20}$: +1.6 (c = 1.19, methanol)

MS (ESI, *m/z*): 537.2 $[M-H_2O+H]^+$; 555.2 $[M+H]^+$

(2*R*)-3-{[Bis(benzyloxy)phosphoryl]oxy}-2-hydroxypropyl 9-phenylnonanoate, 89

Following the general procedure 4.1.1.13, ester **89** was obtained from carboxylic acid **81** (90 mg, 0.38 mmol) and diol **86** (271 mg, 0.76 mmol) in 58% yield. Chromatography: dichloromethane to dichloromethane/methanol, 95:5.

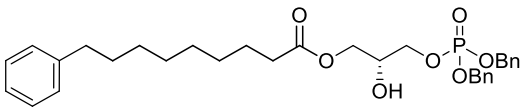

89

R_f: 0.44 (dichloromethane/methanol, 95:5)

IR (ATR): 3325 (O-H); 1736 (C=O); 1245 (P=O); 1013 (P-O)

^{1}H-NMR (methanol-d_4, 300 MHz): δ 1.25-1.35 (m, 8H, 4CH_2); 1.55-1.64 (m, 4H, 2CH_2); 2.30 (t, *J* = 7.4, 2H, CH_2CO); 2.58 (t, *J* = 7.7, 2H, PhCH_2); 3.91-3.98 (m, 1H, CH); 3.98-4.03 (m, 2H, CH_2OP); 4.07 (dd, *J* = 5.1, 1.5, 2H, CO_2CH_2); 5.05 (s, 2H, OCH_2Ph); 5.08 (s, 2H, OCH_2Ph); 7.10-7.16 (m, 3H, 3CH_{Ar}); 7.21-7.26 (m, 2H, 2CH_{Ar}); 7.36 (app s, 10H, 10CH_{Ar})

^{13}C-NMR (methanol-d_4, 75 MHz): δ 26.8; 30.1; 30.2; 30.3; 30.4; 32.7 (6CH_2); 34.9 (CH_2CO); 36.9 (PhCH_2); 65.4 (CO_2CH_2); 68.9 (d, *J* = 8.0, CH); 69.6 (d, *J* = 6.4, CH_2OP); 70.9 (d, *J* = 5.8, 2OCH_2Ph); 126.6 (CH_{Ar}); 129.20 (4CH_{Ar}); 129.24 (2CH_{Ar}); 129.4 (2CH_{Ar}); 129.7 (4CH_{Ar}); 129.8 (2CH_{Ar}); 137.2 (d, *J* = 6.5, 2C_{Ar}); 144.0 (C_{Ar}); 175.2 (CO)

^{31}P-NMR (methanol-d_4, 121 MHz): δ 1.61

$[\alpha]_D^{20}$: +0.02 (c = 0.65, methanol)

MS (ESI, *m/z*): 551.2 $[M\text{-}H_2O+H]^+$; 569.3 $[M+H]^+$

(2*R*)-3-{[Bis(benzyloxy)phosphoryl]oxy}-2-hydroxypropyl 10-phenyl decanoate, 90

Following the general procedure 4.1.1.13, ester **90** was obtained from carboxylic acid **77** (82 mg, 0.33 mmol) and diol **86** (233 mg, 0.66 mmol) in 16% yield. Chromatography: dichloromethane/ethyl acetate, 100:1 to 1:1.

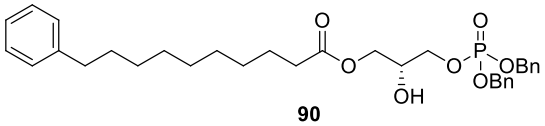

90

R_f: 0.43 (dichloromethane/ethyl acetate, 8:2)

IR (ATR): 3028 (O-H); 1738 (C=O); 1022 (P-O)

^{1}H-NMR (C_6D_6, 300 MHz): δ 1.15-1.20 (m, 10H, 5CH_2); 1.49-1.58 (m, 4H, 2CH_2); 2.11 (t, *J* = 7.5, 2H, CH_2CO); 2.51 (t, *J* = 7.5, 2H, PhCH_2); 3.95-4.06 (m, 3H, CH, CH_2OP); 4.12-4.24 (m, 2H, CO_2CH_2); 4.86-5.00 (m, 4H, 2OCH_2Ph); 7.03-7.12 (m, 9H, 9CH_{Ar}); 7.16-7.22 (m, 6H, 6CH_{Ar})

^{13}C-NMR (C_6D_6, 75 MHz): δ 25.2; 29.4; 29.6; 29.7; 29.8; 29.9; 31.9 (7CH_2); 34.2 (CH_2CO); 36.4 (PhCH_2); 64.6 (CO_2CH_2); 69.0 (d, *J* = 5.4, CH); 69.4 (d, *J* = 5.9, CH_2OP); 69.7 (d, *J* = 5.0, OCH_2Ph); 69.8 (d, *J* = 5.1, OCH_2Ph); 126.0 (CH_{Ar}); 128.5 (2CH_{Ar}); 128.6 (2CH_{Ar}); 128.8 (2CH_{Ar}); 128.83 (2CH_{Ar}); 128.9 (6CH_{Ar}); 136.4 (d, *J* = 6.7, 2C_{Ar}), 143.0 (C_{Ar}); 173.2 (CO)

^{31}P-NMR (C_6D_6, 121 MHz): δ 3.92

MS (ESI, *m/z*): 565.2 $[M\text{-}H_2O+H]^+$; 583.3 $[M+H]^+$

(2*R*)-3-{[Bis(benzyloxy)phosphoryl]oxy}-2-hydroxypropyl 15-phenyl pentadecanoate, 91

Following the general procedure 4.1.1.13, ester **91** was obtained from 15-phenylpentadecanoic acid (80 mg, 0.25 mmol) and diol **86** (177 mg, 0.50 mmol) in 18% yield. Chromatography: dichloromethane/ethyl acetate, 100:1 to 1:1.

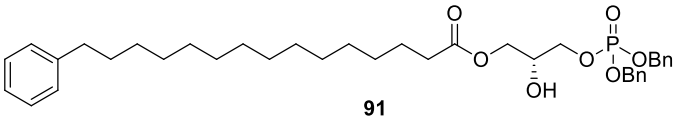

91

R_f: 0.55 (dichloromethane/ethyl acetate, 8:2)
IR (ATR): 3334 (O-H); 1740 (C=O); 1259 (P=O); 1017 (P-O)
^{1}H-NMR (C_6D_6, 500 MHz): δ 1.20-1.36 (m, 20H, 10CH_2); 1.54-1.58 (m, 4H, 2CH_2); 2.10 (t, *J* = 7.5, 2H, CH_2CO); 2.52 (t, *J* = 7.5, 2H, PhCH_2); 3.84-3.89 (m, 1H, CH); 3.91-3.99 (m, 2H, CH_2OP); 4.07 (dd, *J* = 11.4, 5.3, 1H, ½CO_2CH_2); 4.11 (dd, *J* = 11.4, 5.7, 1H, ½CO_2CH_2); 4.85-4.96 (m, 4H, 2OCH_2Ph); 7.04-7.12 (m, 8H, 8CH_{Ar}); 7.15-7.22 (m, 7H, 7CH_{Ar})
^{13}C-NMR (C_6D_6, 125 MHz): δ 25.3; 29.5; 29.7; 29.72; 29.9; 30.0; 30.08; 30.1; 30.14 (9CH_2); 30.2 (2CH_2); 32.0 (CH_2); 34.2 (CH_2CO); 36.4 (PhCH_2); 64.5 ($CO_2C H_2$); 69.2 (d, *J* = 4.8, CH); 69.4 (d, *J* = 5.6, CH_2OP); 69.7 (d, *J* = 5.5, OCH_2Ph); 69.74 (d, *J* = 5.5, OCH_2Ph); 126.2 (CH_{Ar}); 128.5 (4CH_{Ar}); 128.54 (2CH_{Ar}); 128.8 (2CH_{Ar}); 128.84 (2CH_{Ar}); 128.9 (4CH_{Ar}); 136.4 (d, *J* = 6.5, 2C_{Ar}); 143.1 (C_{Ar}); 173.1 (CO)
^{31}P-NMR (C_6D_6, 121 MHz): δ 4.60
MS (ESI, *m/z*): 653.4 $[M+H]^+$

(2*R*)-3-{[Bis(benzyloxy)phosphoryl]oxy}-2-hydroxypropyl 7-biphenyl-4-yl heptanoate, 101

Following the general procedure 4.1.1.13, ester **101** was obtained from carboxylic acid **93** (100 mg, 0.35 mmol) and diol **86** (249 mg, 0.71 mmol) in 17% yield. Chromatography: dichloromethane/ethyl acetate, 100:1 to 1:1.

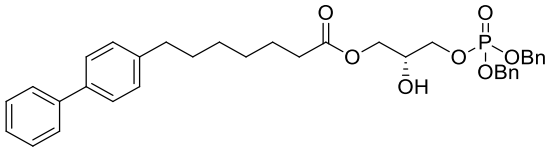

101

R_f: 0.54 (dichloromethane/ethyl acetate, 8:2)
IR (ATR): 3385 (O-H); 1736 (C=O); 1259 (P=O); 1017 (P-O)

^{1}H-NMR (C_6D_6, 300 MHz): δ 1.25-1.29 (m, 4H, 2CH_2); 1.58-1.64 (m, 4H, 2CH_2); 2.21 (t, *J* = 7.5, 2H, CH_2CO); 2.59 (t, *J* = 7.5, 2H, ArCH_2); 4.11-4.19 (m, 3H, CH, CH_2OP); 4.25-4.36 (m, 2H, CO_2CH_2); 4.41 (br s, 1H, OH); 4.97-5.11 (m, 4H, 2OCH_2Ph); 7.11-7.37 (m, 15H, 15CH_{Ar}); 7.58-7.65 (m, 4H, 4CH_{Ar})

^{13}C-NMR (C_6D_6, 75 MHz): δ 25.1; 29.16; 29.2; 31.6 (4CH_2); 34.1 (CH_2CO); 35.8 (ArCH_2); 64.6 (CO_2CH_2); 68.9 (d, *J* = 5.6, CH); 69.3 (d, *J* = 5.7, CH_2OP); 69.6 (d, *J* = 4.9, OCH_2Ph); 69.7 (d, *J* = 5.1, OCH_2Ph); 127.2 (CH_{Ar}); 127.3 (2CH_{Ar}); 127.4 (2CH_{Ar}); 128.3 (2CH_{Ar}); 128.5 (2CH_{Ar}); 128.6 (2CH_{Ar}); 128.7 (4CH_{Ar}); 129.0 (2CH_{Ar}); 129.2 (2CH_{Ar}); 136.3 (d, *J* = 6.7, 2C_{Ar}); 139.2; 141.7; 142.0 (3C_{Ar}); 173.1 (CO)

^{31}P-NMR (C_6D_6, 121 MHz): δ 3.77

MS (ESI, *m/z*): 599.7 $[M-H_2O+H]^+$; 617.7 $[M+H]^+$

(2*R*)-3-{[Bis(benzyloxy)phosphoryl]oxy}-2-hydroxypropyl 10-biphenyl-4-yl decanoate, 102

Following the general procedure 4.1.1.13, ester **102** was obtained from carboxylic acid **96** (92 mg, 0.28 mmol) and diol **86** (200 mg, 0.57 mmol) in 24% yield. Chromatography: dichloromethane to dichloromethane/ethyl acetate, 6:4.

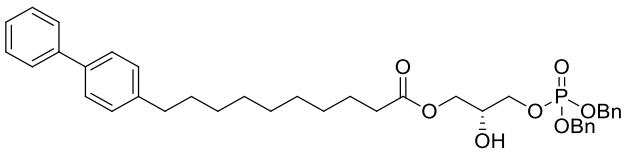

102

R_f: 0.51 (dichloromethane/ethyl acetate, 8:2)

IR (ATR): 3384 (O-H); 1738 (C=O); 1259 (P=O); 1016 (P-O)

^{1}H-NMR (C_6D_6, 300 MHz): δ 1.17-1.24 (m, 10H, 5CH_2); 1.54-1.62 (m, 4H, 2CH_2); 2.12 (t, *J* = 7.4, 2H, CH_2CO); 2.51-2.58 (m, 2H, ArCH_2); 4.00-4.07 (m, 3H, CH, CH_2OP); 4.13-4.24 (m, 3H, CO_2CH_2, OH); 4.86-5.00 (m, 4H, 2OCH_2Ph); 7.01-7.26 (m, 15H, 15CH_{Ar}); 7.48-7.54 (m, 4H, 4CH_{Ar})

^{13}C-NMR (C_6D_6, 75 MHz): δ 25.2; 29.5; 29.6; 29.7; 29.8; 29.9; 31.9 (7CH_2); 34.2 (CH_2CO); 36.0 (ArCH_2); 64.6 (CO_2CH_2); 69.0 (d, *J* = 5.4, CH); 69.4 (d, *J* = 5.9, CH_2OP); 69.7 (d, *J* = 5.0, OCH_2Ph); 69.74 (d, *J* = 5.0, OCH_2Ph); 127.3 (CH_{Ar}); 127.4 (2CH_{Ar}); 127.5 (2CH_{Ar}); 128.4 (2CH_{Ar}); 128.42 (2CH_{Ar}); 128.7 (2CH_{Ar}); 128.8 (4CH_{Ar}); 129.1 (2CH_{Ar}); 129.3 (2CH_{Ar}); 136.4 (d, *J* = 6.7, 2C_{Ar},); 139.3; 141.7; 142.1 (3C_{Ar}); 173.2 (CO)

^{31}P-NMR (C_6D_6, 121 MHz): δ 3.93

$[\alpha]_D^{20}$: +0.7 (c = 1.5, methanol)

MS (ESI, *m/z*): 641.7 $[M-H_2O+H]^+$; 659.7 $[M+H]^+$

(2*R*)-3-{[Bis(benzyloxy)phosphoryl]oxy}-2-hydroxypropyl 13-biphenyl-4-yl tridecanoate, 103

Following the general procedure 4.1.1.13, ester **103** was obtained from carboxylic acid **100** (104 mg, 0.28 mmol) and diol **86** (200 mg, 0.57 mmol) in 10% yield. Chromatography: dichloromethane/ethyl acetate, 100:1 to 1:1.

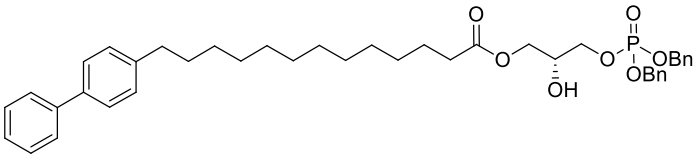

103

R_f: 0.42 (dichloromethane/ethyl acetate, 8:2)
IR (ATR): 1738 (C=O); 1260 (P=O); 1018 (P-O)
^{1}H-NMR (C_6D_6, 300 MHz): δ 1.14-1.30 (m, 16H, $8CH_2$); 1.54-1.64 (m, 4H, $2CH_2$); 2.11 (t, *J* = 7.5, 2H, CH_2CO); 2.57 (t, *J* = 7.5, 2H, $ArCH_2$); 3.92 (br s, 2H, CH, OH); 3.99 (dd, *J* = 10.0, 3.3, 2H, CH_2OP); 4.15 (AB system, *J* = 11.3, 4.5, 2H, CO_2CH_2); 4.84-5.00 (m, 4H, $2OCH_2Ph$); 7.03-7.27 (m, 15H, $15CH_{Ar}$); 7.48-7.55 (m, 4H, $4CH_{Ar}$)
^{13}C-NMR (C_6D_6, 75 MHz): δ 25.3; 29.5 ($2CH_2$); 29.7 ($2CH_2$); 29.9; 30.0 ($2CH_2$); 30.1 ($2CH_2$); 30.13; 32.0 ($2CH_2$); 34.2 (CH_2CO); 36.0 ($ArCH_2$); 64.6 (CO_2CH_2); 69.1 (d, *J* = 5.0, CH); 69.4 (d, *J* = 5.8, CH_2OP); 69.7 (d, *J* = 5.0, OCH_2Ph); 69.74 (d, *J* = 5.1, OCH_2Ph); 127.3 (CH_{Ar}); 127.4 ($2CH_{Ar}$); 127.5 ($2CH_{Ar}$); 128.4 ($2CH_{Ar}$); 128.41 ($2CH_{Ar}$); 128.7 ($2CH_{Ar}$); 128.8 ($4CH_{Ar}$); 129.1 ($2CH_{Ar}$); 129.3 ($2CH_{Ar}$); 136.4 (d, *J* = 6.8, $2C_{Ar}$); 139.3; 141.8; 142.1 ($3C_{Ar}$); 173.1 (CO)
^{31}P-NMR (C_6D_6, 121 MHz): δ 4.61
MS (ESI, *m/z*): 683.4 $[M-H_2O+H]^+$; 701.4 $[M+H]^+$

4.1.5.5 Synthesis of final compounds **3a** and **2f-j**

(1*S*)-2-Bromo-1-[(phosphonooxy)methyl]ethyl 10-phenyldecanoate, 3a

Thoroughly dried diethyl phosphate **84** (76 mg, 0.17 mmol, 1 equiv) was dissolved in anhydrous dichloromethane (2 mL) and TMSBr (0.22 mL, 1.66 mmol, 10 equiv) was added dropwise at room temperature. The reaction mixture was stirred for 4 h at room temperature, after which the solvent was evaporated at reduced pressure and the crude was redissolved in methanol (5 mL) and stirred for an additional hour. Evaporation of the solvent afforded compound **3a** in 90% yield.

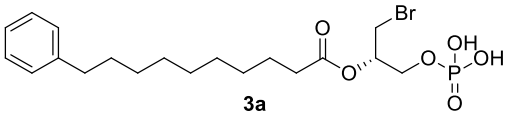

3a

IR (ATR): 3360 (O-H); 1738 (C=O), 1199 (P=O); 1025 (P-OH)
^{1}H-NMR (methanol-d_4, 500 MHz): δ 1.32 (m, 10H, 5CH_2); 1.60-1.65 (m, 4H, 2CH_2); 2.37 (t, *J* = 7.3, 2H, CH_2CO); 2.59 (t, *J* = 7.6, 2H, PhCH_2); 3.58 (dd, *J* = 10.9, 5.9, 1H, ½CH_2Br); 3.66 (dd, *J* = 10.9, 4.9, 1H, ½CH_2Br); 4.12-4.18 (m, 2H, CH_2OP); 5.14-5.19 (m, 1H, CH); 7.11-7.17 (m, 3H, 3CH_{Ar}); 7.23 (t, *J* = 7.5, 2H, 2CH_{Ar})
^{13}C-NMR (methanol-d_4, 125 MHz): δ 26.0; 30.1; 30.3; 30.31 (4CH_2); 30.5 (2CH_2); 30.8 (CH_2Br); 32.7 (CH_2); 34.9 (CH_2CO); 36.9 (PhCH_2); 66.3 (d, *J* = 5.0, CH_2OP); 72.5 (d, *J* = 8.3, CH); 126.6 (CH_{Ar}); 129.2 (2CH_{Ar}); 129.4 (2CH_{Ar}); 144.0 (C_{Ar}); 174.3 (CO)
^{31}P-NMR (methanol-d_4, 121 MHz): δ 3.10
$[\alpha]_D^{20}$: +1.6 (c = 0.5, methanol)
HRMS (ESI, *m/z*): calculated for $C_{19}H_{29}{}^{79}BrO_6P$ ([M(^{79}Br)-H]$^-$: 463.0891, found: 463.0902; calculated for $C_{19}H_{29}{}^{81}BrO_6P$ ([M(^{81}Br)-H]$^-$: 465.0870, found: 465.0880
HPLC (method B, t_R, min): 26.05

(2*R*)-2-Hydroxy-3-(phosphonooxy)propyl 7-phenylheptanoate, 2f

Following the general procedure 4.1.1.1, compound **2f** was obtained from dibenzyl phosphate **87** (30 mg, 56 µmol) at room temperature in 85% yield.

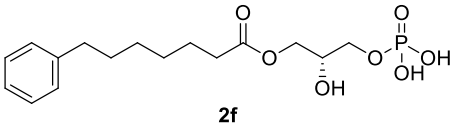

2f

IR (ATR): 1737 (C=O); 1258 (P=O); 1025 (P-OH)
^{1}H-NMR (methanol-d_4, 300 MHz): δ 1.33-1.36 (m, 4H, 2CH_2); 1.56-1.67 (m, 4H, 2CH_2); 2.35 (t, *J* = 7.4, 2H, CH_2CO); 2.60 (t, *J* = 7.5, 2H, PhCH_2); 3.95-4.01 (m, 3H, CH, CH_2OP); 4.10 (dd, *J* = 11.3, 5.4, 1H, ½CO_2CH_2); 4.17 (dd, *J* = 11.3, 4.3, 1H, ½CO_2CH_2); 7.10-7.17 (m, 3H, 3CH_{Ar}); 7.21-7.26 (m, 2H, 2CH_{Ar})
^{13}C-NMR (methanol-d_4, 75 MHz): δ 25.9; 29.9; 30.0; 32.6 (4CH_2); 34.8 (CH_2CO); 36.8 (PhCH_2); 65.9 (CO_2CH_2); 68.1 (d, *J* = 5.7, CH_2OP); 69.3 (d, *J* = 8.3, CH); 126.6 (CH_{Ar}); 129.3 (2CH_{Ar}); 129.4 (2CH_{Ar}); 143.9 (C_{Ar}); 175.3 (CO)
^{31}P-NMR (methanol-d_4, 121 MHz): δ 3.09
$[\alpha]_D^{20}$: +5.3 (c = 0.47, methanol)
HRMS (ESI, *m/z*): calculated for $C_{16}H_{24}O_7P$ ([M-H]$^-$): 359.1265, found: 359.1273
HPLC (method B, t_R, min): 21.72

(2*R*)-2-Hydroxy-3-(phosphonooxy)propyl 8-phenyloctanoate, 2g

Following the general procedure 4.1.1.1, compound **2g** was obtained from dibenzyl phosphate **88** (63 mg, 0.11 mmol) at room temperature in 80% yield.

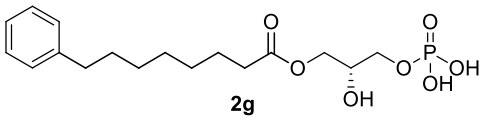

2g

IR (ATR): 1737 (C=O); 1027 (P-O)

^{1}H-NMR (methanol-d_4, 300 MHz): δ 1.33 (app s, 6H, 3CH_2); 1.58-1.60 (m, 4H, 2CH_2); 2.27-2.37 (m, 2H, CH_2CO); 2.59 (t, *J* = 7.5, 2H, PhCH_2); 3.59-3.61 (m, 3H, CH, CH_2OP); 3.99-4.41 (m, 2H, CO_2CH_2); 7.10-7.16 (m, 3H, 3CH_{Ar}); 7.21-7.26 (m, 2H, 2CH_{Ar})

^{13}C-NMR (methanol-d_4, 75 MHz): δ 25.9; 30.07; 30.1; 30.2; 32.6 (5CH_2); 34.8 (CH_2CO); 36.9 (PhCH_2); 65.8 (CO_2CH_2); 68.1 (d, *J* = 5.0, CH_2OP); 69.3 (br s, CH); 126.6 (CH_{Ar}); 129.2 (2CH_{Ar}); 129.4 (2CH_{Ar}); 143.9 (C_{Ar}); 175.3 (CO)

^{31}P-NMR (methanol-d_4, 121 MHz): δ 3.04

$[\alpha]_D^{20}$: +2.8 (c = 1.58, methanol)

HRMS (ESI, *m/z*): calculated for $C_{17}H_{26}O_7P$ ($[M-H]^-$): 373.1422, found: 373.1432

HPLC (method A, t_R, min): 8.07

(2*R*)-2-Hydroxy-3-(phosphonooxy)propyl 9-phenylnonanoate, 2h

Following the general procedure 4.1.1.1, compound **2h** was obtained from dibenzyl phosphate **89** (90 mg, 0.16 mmol) at room temperature in 99% yield.

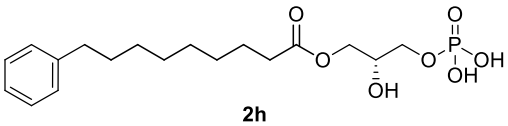

2h

IR (ATR): 3355 (O-H); 1737 (C=O); 1259 (P=O); 1029 (P-O)

^{1}H-NMR (methanol-d_4, 300 MHz): δ 1.32 (app s, 8H, 4CH_2); 1.60 (br s, 4H, 2CH_2); 2.34 (t, *J* = 7.4, 2H, CH_2CO); 2.59 (t, *J* = 7.8, 2H, PhCH_2); 3.67-3.79 (m, 1H, CH); 3.98-4.00 (m, 2H, CH_2OP); 4.07-4.21 (m, 2H, CO_2CH_2); 7.09-7.17 (m, 3H, 3CH_{Ar}); 7.21-7.26 (m, 2H, 2CH_{Ar})

^{13}C-NMR (methanol-d_4, 75 MHz): δ 25.9; 30.1; 30.2; 30.3; 30.4; 32.7 (6CH_2); 34.8 (CH_2CO); 36.9 (PhCH_2); 65.8 (CO_2CH_2); 68.1 (d, *J* = 6.0, CH_2OP); 69.3 (d, *J* = 8.3, CH); 126.6 (CH_{Ar}); 129.2 (2CH_{Ar}); 129.4 (2CH_{Ar}); 143.9 (C_{Ar}); 175.3 (CO)

^{31}P-NMR (methanol-d_4, 121 MHz): δ 3.05

$[\alpha]_D^{20}$: +2.5 (c = 1.13, methanol)

HRMS (ESI, *m/z*): calculated for $C_{18}H_{28}O_7P$ ($[M-H]^-$): 387.1578, found: 387.1591
HPLC (method A, t_R, min): 8.34

(2*R*)-2-Hydroxy-3-(phosphonooxy)propyl 10-phenyldecanoate, 2i

Following the general procedure 4.1.1.1, compound **2i** was obtained from dibenzyl phosphate **90** (20 mg, 34 µmol) at room temperature in 80% yield.

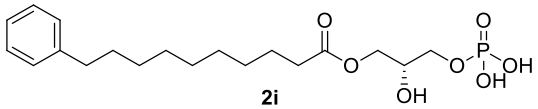

2i

IR (ATR): 1739 (C=O); 1051 (P-OH)
^{1}H-NMR (methanol-d_4, 500 MHz): δ 1.29-1.32 (m, 10H, 5CH_2); 1.61 (m, 4H, 2CH_2); 2.35 (t, *J* = 7.5, 2H, CH_2CO); 2.59 (t, *J* = 7.6, 2H, PhCH_2); 3.96-4.01 (m, 3H, CH, CH_2OP); 4.11 (dd, *J* = 11.3, 5.3, 1H, ½CO_2CH_2); 4.17 (dd, *J* = 11.3, 4.1, 1H, ½CO_2CH_2); 7.11-7.16 (m, 3H, 3CH_{Ar}); 7.23 (t, *J* = 7.5, 2H, 2CH_{Ar})
^{13}C-NMR (methanol-d_4, 125 MHz): δ 26.0; 30.2; 30.3; 30.34 (4CH_2); 30.5 (2CH_2); 32.7 (CH_2); 34.9 (CH_2CO); 36.9 (PhCH_2); 65.9 (CO_2CH_2); 68.1 (d, *J* = 5.7, CH_2OP); 69.4 (d, *J* = 8.1, CH); 126.6 (CH_{Ar}); 129.2 (2CH_{Ar}); 129.4 (2CH_{Ar}); 144.0 (C_{Ar}); 175.4 (CO)
^{31}P-NMR (methanol-d_4, 202 MHz): δ 3.14
$[\alpha]_D^{20}$: +2.3 (c = 0.4, methanol)
HRMS (ESI, *m/z*): calculated for $C_{19}H_{30}O_7P$ ($[M-H]^-$): 401.1735, found: 401.1734
HPLC (method B, t_R, min): 24.37

(2*R*)-2-Hydroxy-3-(phosphonooxy)propyl 15-phenylpentadecanoate, 2j

Following the general procedure 4.1.1.1, compound **2j** was obtained from dibenzyl phosphate **91** (20 mg, 31 µmol) at room temperature in 90% yield.

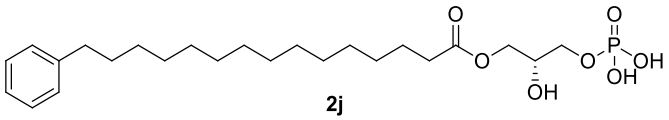

2j

IR (ATR): 1738 (C=O); 1259 (P=O); 1083 (P-OH)
^{1}H-NMR (methanol-d_4, 300 MHz): δ 1.28-1.32 (m, 20H, 10CH_2); 1.57-1.64 (m, 4H, 2CH_2); 2.35 (t, *J* = 7.4, 2H, CH_2CO); 2.59 (t, *J* = 7.5, 2H, PhCH_2); 3.97-4.35 (m, 5H, CO_2CH_2, CH, CH_2OP); 7.08-7.16 (m, 3H, 3CH_{Ar}); 7.21-7.26 (m, 2H, 2CH_{Ar})
^{13}C-NMR (methanol-d_4, 75 MHz): δ 26.0; 30.2; 30.3; 30.4; 30.59; 30.6; 30.7 (7CH_2); 30.73 (2CH_2); 30.75 (2CH_2); 32.8 (CH_2); 34.9 (CH_2CO); 36.9 (PhCH_2); 64.9

($CO_2\underline{C}H_2$); 67.1 (d, *J* = 5.3, CH_2OP); 68.3 (d, *J* = 8.3, CH); 126.6 (CH_{Ar}); 129.2 ($2CH_{Ar}$); 129.4 ($2CH_{Ar}$); 144.0 (C_{Ar}); 175.4 (CO)

^{31}P-NMR (methanol-d_4, 121 MHz): δ 3.11

$[\alpha]_D^{20}$: +4.2 (c = 0.4, methanol)

HRMS (ESI, *m/z*): calculated for $C_{24}H_{40}O_7P$ ($[M-H]^-$): 471.2517, found: 471.2520

HPLC (method B, t_R, min): 33.42

(2*R*)-2-Hydroxy-3-(phosphonooxy)propyl 7-biphenyl-4-ylheptanoate, 2k

Following the general procedure 4.1.1.1, compound **2k** was obtained from dibenzyl phosphate **101** (27 mg, 43 µmol) at room temperature in 74% yield.

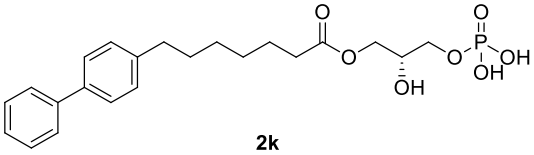

2k

IR (ATR): 1720 (C=O); 1058 (P-OH)

^{1}H-NMR (methanol-d_4, 300 MHz): δ 1.36-1.40 (m, 4H, $2CH_2$); 1.60-1.70 (m, 4H, $2CH_2$); 2.36 (t, *J* = 7.4, 2H, CH_2CO); 2.64 (t, *J* = 7.5, 2H, $ArC\underline{H}_2$); 3.97-4.01 (m, 3H, CH, CH_2OP); 4.11 (dd, *J* = 11.3, 5.3, 1H, ½CO_2CH_2); 4.17 (dd, *J* = 11.3, 4.1, 1H, ½CO_2CH_2); 7.24 (d, *J* = 8.1, 2H, $2CH_{Ar}$); 7.30 (t, *J* = 7.5, 1H, CH_{Ar}); 7.40 (t, *J* = 7.6, 2H, $2CH_{Ar}$); 7.51 (d, *J* = 8.2, 2H, $2CH_{Ar}$); 7.58 (d, *J* = 7.7, 2H, $2CH_{Ar}$)

^{13}C-NMR (methanol-d_4, 125 MHz): δ 25.9; 29.9; 30.0; 32.5 ($4CH_2$); 34.9 ($\underline{C}H_2CO$); 36.4 ($Ar\underline{C}H_2$); 65.9 ($CO_2\underline{C}H_2$); 68.1 (d, *J* = 5.4, CH_2OP); 69.3 (d, *J* = 8.3, CH); 127.8 ($2CH_{Ar}$); 127.84 ($2CH_{Ar}$); 128.0 (CH_{Ar}); 129.8 ($2CH_{Ar}$); 129.9 ($2CH_{Ar}$); 139.9; 142.4; 143.1 ($3C_{Ar}$); 175.3 (CO)

^{31}P-NMR (methanol-d_4, 121 MHz): δ 3.11

$[\alpha]_D^{20}$: +7.6 (c = 0.67, methanol)

HRMS (ESI, *m/z*): calculated for $C_{22}H_{28}O_7P$ ($[M-H]^-$): 435.1578, found: 435.1562

HPLC (method B, t_R, min): 26.61

(2*R*)-2-Hydroxy-3-(phosphonooxy)propyl 10-biphenyl-4-yldecanoate, 2l

Following the general procedure 4.1.1.1, compound **2l** was obtained from dibenzyl phosphate **102** (20 mg, 30 µmol) at room temperature in 85% yield.

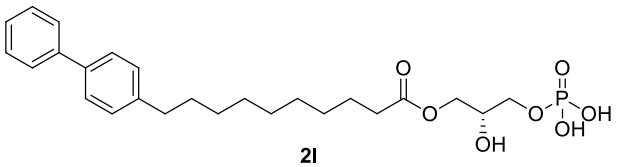

2l

IR (ATR): 3314 (O-H); 1654 (C=O); 1015 (P-O)
^{1}H-NMR (methanol-d_4, 500 MHz,): δ 1.28-1.35 (m, 10H, 5CH_2); 1.58-1.66 (m, 4H, 2CH_2); 2.35 (t, *J* = 7.4, 2H, CH_2CO); 2.64 (t, *J* = 7.5, 2H, ArCH_2); 3.96-4.00 (m, 3H, CH, CH_2OP); 4.11 (dd, *J* = 11.4, 5.4, 1H, ½CO_2CH_2); 4.17 (dd, *J* = 11.4, 4.2, 1H, ½CO_2CH_2); 7.24 (d, *J* = 8.1, 2H, 2CH_{Ar}); 7.29 (t, *J* = 7.4, 1H, CH_{Ar}); 7.40 (t, *J* = 7.7, 2H, 2CH_{Ar}); 7.51 (d, *J* = 8.2, 2H, 2CH_{Ar}); 7.58 (dd, *J* = 8.3, 1.1, 2H, 2CH_{Ar})
^{13}C-NMR (methanol-d_4, 125 MHz): δ 26.0; 30.2; 30.3; 30.4; 30.5; 30.52; 32.7 (7CH_2); 34.9 (CH_2CO); 36.5 (ArCH_2); 65.9 (CO_2CH_2); 68.1 (d, *J* = 5.6, CH_2OP); 69.3 (d, *J* = 8.2, CH); 127.8 (2CH_{Ar}); 127.83 (2CH_{Ar}); 128.0 (CH_{Ar}); 129.8 (2CH_{Ar}); 129.9 (2CH_{Ar}); 139.9; 142.5; 143.2 (3C_{Ar}); 175.4 (CO)
^{31}P-NMR (methanol-d_4, 121 MHz): δ 3.11
HRMS (ESI, *m/z*): calculated for $C_{25}H_{34}O_7P$ ([M-H]$^-$): 477.2048, found: 477.2029
HPLC (method A, t_R, min): 10.49

(2*R*)-2-Hydroxy-3-(phosphonooxy)propyl 13-biphenyl-4-yltridecanoate, 2m

Following the general procedure 4.1.1.1, compound **2m** was obtained from dibenzyl phosphate **103** (37 mg, 53 µmol) at room temperature as a white solid in 91% yield.

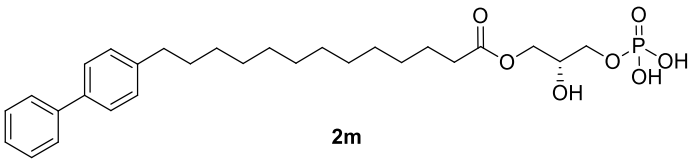

2m

m.p.: 95-97ºC
IR (ATR): 1730 (C=O); 1258 (P=O); 1027 (P-O)
^{1}H-NMR (DMSO-d_6, 500 MHz): δ 1.23-1.29 (m, 16H, 8CH_2); 1.49-1.52 (m, 2H, CH_2); 1.57-1.60 (m, 2H, CH_2); 2.28 (t, *J* = 7.4, 2H, CH_2CO); 2.60 (t, *J* = 7.6, 2H, ArCH_2); 3.35 (br s, 1H, OH); 3.73-3.76 (m, 2H, CH_2OP); 3.79-3.85 (m, 1H, CH); 3.94 (dd, *J* = 11.2, 6.0, 1H, ½CO_2CH_2); 4.02 (dd, *J* = 11.2, 4.3, 1H, ½CO_2CH_2); 7.27 (d, *J* = 8.1, 2H, 2CH_{Ar}); 7.33 (t, *J* = 7.3, 1H, CH_{Ar}); 7.44 (t, *J* = 7.7, 2H, 2CH_{Ar}); 7.56 (d, *J* = 8.1, 2H, 2CH_{Ar}); 7.63 (d, *J* = 7.3, 2H, 2CH_{Ar})
^{13}C-NMR (DMSO-d_6, 126 MHz): δ 26.4; 28.5; 28.6; 28.7; 28.8; 28.9 (6CH_2); 28.98 (2CH_2); 29.0; 30.9 (2CH_2); 33.4 (CH_2CO); 34.7 (ArCH_2); 64.9 (CO_2CH_2); 66.1 (d, *J* = 5.3, CH_2OP); 67.3 (d, *J* = 7.8, CH); 126.4 (2CH_{Ar}); 126.5 (2CH_{Ar}); 127.1 (CH_{Ar}); 128.85 (2CH_{Ar}); 128.87 (2CH_{Ar}); 137.5; 140.1; 141.6 (3C_{Ar}); 172.9 (CO)
^{31}P-NMR (DMSO-d_6, 121 MHz): δ 2.16
$[\alpha]_D^{20}$: limited solubility in DMSO

HRMS (ESI, *m/z*): calculated for $C_{28}H_{40}O_7P$ ([M-H]$^-$): 519.2517, found: 519.2508
HPLC (method A, t_R, min): 12.15

*4.1.6 Synthesis of final compounds **3b-d***

4.1.6.1 Synthesis of bromoalcohols **105** and **109**

Dibenzyl (2*R*)-oxiran-2-ylmethyl phosphate, 104

Following the general procedure 4.1.1.12, compound **104** was obtained from (2*S*)-oxiran-2-ylmethanol (0.3 mL, 4.52 mmol) and dibenzyl *N*,*N*-diisopropylphosphoramidite (3.04 mL, 9.04 mmol) in 76% yield. Chromatography: dichloromethane to dichloromethane/ethyl acetate, 20:1.

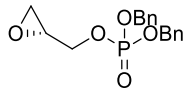

104

R_f: 0.35 (hexane/ethyl acetate, 1:1)
IR (ATR): 1275 (P=O); 1013 (P-O)
^{1}H-NMR ($CDCl_3$, 300 MHz): δ 2.59 (dd, *J* = 4.8, 2.6, 1H, ½$CH_{2\ epox}$); 2.78 (t, *J* = 4.7, 1H, ½$CH_{2\ epox}$); 3.04-3.25 (m, 1H, CH); 3.89 (ddd, *J* = 11.7, 8.5, 5.9, 1H, ½CH_2OP); 4.12-4.27 (m, 1H, ½CH_2OP); 4.97-5.15 (m, 4H, 2PhCH_2); 7.35 (app s, 10H, 10CH_{Ar})
^{13}C-NMR ($CDCl_3$, 75 MHz): δ 44.7 ($CH_{2\ epox}$); 50.0 (d, *J* = 8.0, CH); 68.1 (d, *J* = 5.5, CH_2OP); 69.6 (d, *J* = 5.3, PhCH_2); 69.61 (d, *J* = 5.5, PhCH_2); 128.1 (4CH_{Ar}); 128.7 (6CH_{Ar}); 135.8 (d, *J* = 6.8, 2C_{Ar})
^{31}P-NMR ($CDCl_3$, 121 MHz): δ 2.03
$[\alpha]_D^{20}$: -8.8 (c = 1, methanol)
MS (ESI, *m/z*): 335.9 $[M+H]^+$

Dibenzyl (2*S*)-3-bromo-2-hydroxypropyl phosphate, 105

Following the general procedure 4.1.1.16, bromoalcohol **105** was obtained from oxirane **104** (990 mg, 2.96 mmol) in 89% yield.

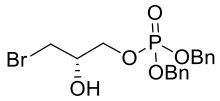

105

R_f: 0.41 (dichloromethane/ethyl acetate, 10:1)

IR (ATR): 3371 (O-H); 1009 (P=O)
^{1}H-NMR ($CDCl_3$, 300 MHz): δ 2.96 (br s, 1H, OH); 3.36 (d, *J* = 5.7, 2H, CH_2Br); 3.88-3.95 (m, 1H, CH); 4.06-4.12 (m, 2H, CH_2OP); 5.00-5.12 (m, 4H, 2PhCH_2); 7.36 (app s, 10H, 10CH_{Ar})
^{13}C-NMR ($CDCl_3$, 75 MHz): δ 33.3 (CH_2Br); 69.2 (d, *J* = 6.0, CH_2OP); 69.7 (d, *J* = 6.6, CH); 70.3 (d, *J* = 5.8, PhCH_2); 70.4 (d, *J* = 5.6, PhCH_2); 128.3 (4CH_{Ar}); 128.9 (4CH_{Ar}); 129.1 (2CH_{Ar}); 135.3 (d, *J* = 6.3, 2C_{Ar})
^{31}P-NMR ($CDCl_3$, 121 MHz): δ 2.48
$[\alpha]_D^{20}$: -2.1 (c = 1.44, methanol)
MS (ESI, *m/z*): 414.8 [M(^{79}Br)+H]$^+$; 416.8 [M(^{81}Br)+H]$^+$

Di-*tert*-butyl (2*R*)-oxiran-2-ylmethyl phosphate, 108

Following the general procedure 4.1.1.12, compound **108** was obtained from (2*S*)-oxiran-2-ylmethanol (0.18 mL, 2.69 mmol) and di-*tert*-butyl *N*,*N*-diisopropylphosphoramidite (1.7 mL, 5.39 mmol) in 52% yield. Chromatography: hexane to ethyl acetate.

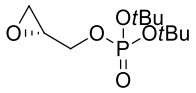

108

R_f: 0.5 (hexane/ethyl acetate, 1:1)
IR (ATR): 1263 (P=O and ring st); 999 (P-O)
^{1}H-NMR ($CDCl_3$, 300 MHz): δ 1.48 (s, 9H, 3CH_3); 1.49 (s, 9H, 3CH_3); 2.66 (dd, *J* = 4.7, 2.6, 1H, ½$CH_{2\ epox}$); 2.83 (t, *J* = 4.7, 1H, ½$CH_{2\ epox}$); 3.21-3.27 (m, 1H, CH); 3.85-3.94 (m, 1H, ½CH_2OP); 4.10-4.18 (m, 1H, ½CH_2OP)
^{13}C-NMR ($CDCl_3$, 75 MHz): δ 29.9 (3CH_3); 30.0 (3CH_3); 44.9 ($CH_{2\ epox}$); 50.3 (d, *J* = 9.0, CH); 67.4 (d, *J* = 5.8, CH_2OP); 82.8 (d, *J* = 7.4, C); 82.83 (d, *J* = 7.4, C)
^{31}P-NMR ($CDCl_3$, 121 MHz): δ -6.90
$[\alpha]_D^{20}$: -9.2 (c = 1.02, methanol)
MS (ESI, *m/z*): 289.0 [M+Na]$^+$

(2*S*)-3-Bromo-2-hydroxypropyl di-*tert*-butyl phosphate, 109

Following the general procedure 4.1.1.16, bromoalcohol **109** was obtained from oxirane **108** (210 mg, 0.79 mmol) in 95% yield.

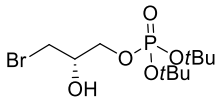

109

R_f: 0.37 (hexane/ethyl acetate, 1:1)
IR (ATR): 3342 (O-H); 1251 (P=O); 996 (P-O)
^{1}H-NMR ($CDCl_3$, 300 MHz): δ 1.50 (s, 18H, $6CH_3$); 3.49 (d, *J* = 6.0, 2H, CH_2Br); 4.00-4.06 (m, 1H, CH); 4.12-4.17 (m, 2H, CH_2OP); 6.34 (br s, 1H, OH)
^{13}C-NMR ($CDCl_3$, 75 MHz): δ 29.9 ($3CH_3$); 30.0 ($3CH_3$); 33.4 (CH_2Br); 68.5 (d, *J* = 6.3, CH_2OP); 70.1 (d, *J* = 6.2, CH); 84.5 (d, *J* = 7.4, C); 84.53 (d, *J* = 7.4, C)
^{31}P-NMR ($CDCl_3$, 121 MHz): δ -7.05
$[\alpha]_D^{20}$: +3.2 (c = 1.11, methanol)
MS (ESI, *m/z*): 369.0 $[M(^{79}Br)+Na)]^+$; 371.0 $[M(^{81}Br)+Na)]^+$

4.1.6.2 Synthesis of esters **106**, **107** and **110**

(1*S*)-2-{[Bis(benzyloxy)phosphoryl]oxy}-1-(bromomethyl)ethyl 7-phenyl heptanoate, 106

Following the general procedure 4.1.1.17, ester **106** was obtained from 7-phenylheptanoic acid (80 mg, 0.39 mmol) and bromoalcohol **105** (161 mg, 0.39 mmol) in 64% yield. Chromatography: dichloromethane to dichloromethane/ethyl acetate, 5:1.

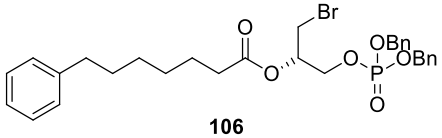

106

R_f: 0.79 (dichloromethane/ethyl acetate, 10:1)
IR (ATR): 1741 (C=O); 1276 (P=O); 1015 (P-O)
^{1}H-NMR (C_6D_6, 300 MHz): δ 1.08-1.13 (m, 4H, $2CH_2$); 1.40-1.52 (m, 4H, $2CH_2$); 2.08 (t, *J* = 7.5, 2H, CH_2CO); 2.44 (t, *J* = 7.5, 2H, $PhCH_2$); 3.04 (AB system, *J* = 11.0, 5.5, 2H, CH_2Br); 3.95-4.12 (m, 2H, CH_2OP); 4.83-5.00 (m, 4H, $2OCH_2Ph$); 5.01-5.08 (m, 1H, CH); 7.00-7.11 (m, 9H, $9CH_{Ar}$); 7.15-7.23 (m, 6H, $6CH_{Ar}$)
^{13}C-NMR (C_6D_6, 75 MHz): δ 25.0 (CH_2); 29.1 ($2CH_2$); 30.0 (CH_2Br); 31.6 (CH_2); 34.1 (CH_2CO); 36.2 ($PhCH_2$); 66.3 (d, *J* = 5.3, CH_2OP); 69.5 (d, *J* = 5.3, $2OCH_2Ph$); 70.8 (d, *J* = 7.5, CH); 126.0 (CH_{Ar}); 128.4 ($4CH_{Ar}$); 128.6 ($2CH_{Ar}$); 128.7 ($2CH_{Ar}$); 128.76 ($2CH_{Ar}$); 128.79 ($4CH_{Ar}$); 136.4 (d, *J* = 6.5, C_{Ar}); 136.5 (d, *J* = 6.5, C_{Ar}); 142.9 (C_{Ar}); 172.3 (CO)

^{31}P-NMR ($CDCl_3$, 121 MHz): δ 1.94
MS (ESI, *m/z*): 602.8 [M(^{79}Br)+h]$^+$; 604.8 [M(^{81}Br)+H]$^+$

(1*S*)-2-{[Bis(benzyloxy)phosphoryl]oxy}-1-(bromomethyl)ethyl 15-phenyl pentadecanoate, 107

Following the general procedure 4.1.1.17, ester **107** was obtained from 15-phenylpentadecanoic acid (80 mg, 0.25 mmol) and bromoalcohol **105** (104 mg, 0.25 mmol) in 50% yield. Chromatography: dichloromethane to dichloromethane/ethyl acetate, 5:1.

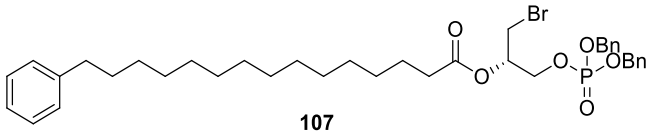

107

R_f: 0.83 (dichloromethane/ethyl acetate, 10:1)
IR (ATR): 1742 (C=O); 1263 (P=O); 1015 (P-O)
^{1}H-NMR (C_6D_6, δ)(300 MHz): δ 1.12-1.35 (m, 20H, 10CH_2); 1.50-1.65 (m, 4H, 2CH_2); 2.13 (t, *J* = 7.5, 2H, CH_2CO); 2.52 (t, *J* = 7.5, 2H, PhCH_2); 3.06 (AB system, *J* = 11.0, 5.5, 2H, CH_2Br); 3.95-4.13 (m, 2H, CH_2OP); 4.84-5.00 (m, 4H, 2OCH_2Ph); 5.02-5.09 (m, 1H, CH); 7.01-7.24 (m, 15H, 15CH_{Ar})
^{13}C-NMR (C_6D_6, δ)(75 MHz): δ 25.1; 29.3 (2CH_2); 29.6 (2CH_2); 29.9; 29.91; 29.95 (3CH_2); 30.0 (2CH_2); 30.08 (CH_2); 30.1 (2CH_2); 32.0 (CH_2); 34.1 (CH_2CO); 36.3 (PhCH_2); 66.2 (d, *J* = 5.2, CH_2OP); 69.4 (d, *J* = 5.4, 2OCH_2Ph); 70.7 (d, *J* = 7.3, CH); 126.0 (CH_{Ar}); 128.3 (4CH_{Ar}); 128.6 (2CH_{Ar}); 128.63 (2CH_{Ar}); 128.7 (6CH_{Ar}); 136.4 (d, *J* = 6.2, C_{Ar}); 136.5 (d, *J* = 6.3, C_{Ar}); 143.0 (C_{Ar}); 172.3 (CO)
^{31}P-NMR ($CDCl_3$, 121 MHz): δ 3.24
MS (MALDI, *m/z*): 737.2 [M(^{79}Br)+Na]$^+$; 739.2 [M(^{81}Br)+Na]$^+$

(1*S*)-2-Bromo-1-{[(di-*tert*-butoxyphosphoryl)oxy]methyl}ethyl (9*Z*)-octadec-9-enoate, 110

To a stirred solution of bromoalcohol **109** (80 mg, 0.23 mmol, 1.1 equiv) in 1.5 mL of anhydrous dichloromethane at room temperature, pyridine (34 µL, 0.42 mmol, 2 equiv) was added, followed by oleoyl chloride (69 µL, 0.21 mmol, 1 equiv). The reaction mixture was stirred overnight at room temperature. Afterward, the reaction mixture was concentrated under reduced pressure and purified by flash chromatography (alumina, hexane to hexane/ethyl acetate, 10:1) to afford pure ester **110** in 15% yield.

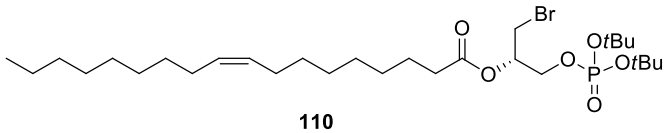

110

R_f: 0.64 (dichloromethane/ethyl acetate, 20:1)
IR (ATR): 1744 (C=O); 1002 (P-O)
^{1}H-NMR ($CDCl_3$, 300 MHz): δ 0.88 (t, *J* = 6.5, 3H, CH_3); 1.18-1.39 (m, 20H, $10CH_2$); 1.49 (s, 18H, $6CH_3$); 1.57-1.71 (m, 2H, CH_2); 1.95-2.06 (m, 4H, $2CH_2CH_{alkene}$); 2.35 (t, *J* = 7.7, 2H, CH_2CO); 3.52 (dd, *J* = 10.9, 5.2, 1H, ½CH_2Br); 3.61 (dd, *J* = 10.9, 5.4, 1H, ½CH_2Br); 4.05-4.20 (m, 2H, CH_2OP); 5.15 (qt, *J* = 5.2, 1H, CH); 5.27-5.43 (m, 2H, $2CH_{alkene}$)
^{13}C-NMR ($CDCl_3$, 75 MHz): δ 14.3 (CH_3); 22.8; 25.0 ($2CH_2$); 27.3; 27.4 ($2CH_2CH_{alkene}$); 29.2; 29.24; 29.3 ($3CH_2$); 29.5 ($2CH_2$); 29.7; 29.8; 29.9 ($3CH_2$); 29.95 ($3CH_3$); 30.0 ($3CH_3$); 30.1 (CH_2Br); 32.1 (CH_2); 34.3 (CH_2CO); 65.1 (d, *J* = 5.9, CH_2OP); 70.7 (d, *J* = 9.3, CH); 83.0 (d, *J* = 7.4, C); 83.05 (d, *J* = 7.4, C); 129.9; 130.2 ($2CH_{alkene}$); 172.9 (CO)
^{31}P-NMR ($CDCl_3$, 121 MHz): δ -7.14
$[\alpha]_D^{20}$: +4.9 (c = 0.66, methanol)
MS (ESI, *m/z*): 633.3 [M(^{79}Br)+Na]$^+$; 635.3 [M(^{81}Br)+Na]$^+$

4.1.6.3 Synthesis of final compounds **3b**-**d**

(1*S*)-2-Bromo-1-[(phosphonooxy)methyl]ethyl 7-phenylheptanoate, 3b

Following the general procedure 4.1.1.1, compound **3b** was obtained from dibenzyl phosphate **106** (114 mg, 0.19 mmol) at room temperature in 85% yield.

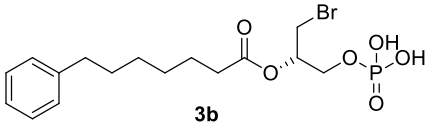

3b

IR (ATR): 1740 (C=O); 1026 (P-O)
^{1}H-NMR (methanol-d_4, 300 MHz): δ 1.28-1.41 (m, 4H, $2CH_2$); 1.57-1.68 (m, 4H, $2CH_2$); 2.37 (t, *J* = 7.3, 2H, CH_2CO); 2.60 (t, *J* = 7.5, 2H, $PhCH_2$); 3.55-3.68 (m, 2H, CH_2Br); 4.10-4.18 (m, 2H, CH_2OP); 5.12-5.21 (m, 1H, CH); 7.10-7.26 (m, 5H, $5CH_{Ar}$)
^{13}C-NMR (methanol-d_4, 75 MHz): δ 25.9; 29.9; 29.94 ($3CH_2$); 30.7 (CH_2Br); 32.6 (CH_2); 34.9 (CH_2CO); 36.8 ($PhCH_2$); 66.3 (d, *J* = 5.1, CH_2OP); 72.5 (d, *J* = 8.3, CH); 126.6 (CH_{Ar}); 129.3 ($2CH_{Ar}$); 129.4 ($2CH_{Ar}$); 143.9 (C_{Ar}); 174.3 (CO)

^{31}P-NMR (methanol-d_4, 121 MHz): δ 2.77
$[\alpha]_D^{20}$: +4.8 (c = 0.75, methanol)
HRMS (ESI, *m/z*): calculated for $C_{16}H_{23}{}^{79}BrO_6P$ ([M(^{79}Br)-H]$^-$): 421.0421, found: 421.0435; calculated for $C_{16}H_{23}{}^{81}BrO_6P$ ([M(^{81}Br)-H]$^-$): 423.0401, found: 423.0414
HPLC (method B, t_R, min): 24.23

(1*S*)-2-Bromo-1-[(phosphonooxy)methyl]ethyl 15-phenylpentadecanoate, 3c

Following the general procedure 4.1.1.1, compound **3c** was obtained from dibenzyl phosphate **107** (70 mg, 98 µmol) at room temperature in 86% yield.

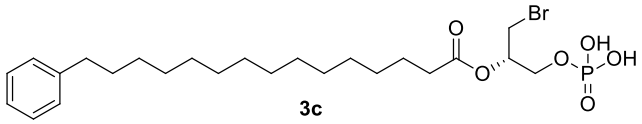

3c

IR (ATR): 1740 (C=O); 1027 (P-OH)
^{1}H-NMR (methanol-d_4, 300 MHz): δ 1.21-1.43 (m, 20H, 10CH_2); 1.52-1.71 (m, 4H, 2CH_2); 2.37 (t, *J* = 7.3, 2H, CH_2CO); 2.59 (t, *J* = 7.5, 2H, PhCH_2); 3.62 (AB system, *J* = 11.0, 5.5, 2H, CH_2Br); 4.11-4.17 (m, 2H, CH_2OP); 5.17 (qt, *J* = 5.0, 1H, CH); 7.09-7.17 (m, 3H, 3CH_{Ar}); 7.20-7.27 (m, 2H, 2CH_{Ar})
^{13}C-NMR (methanol-d_4, 75 MHz): δ 26.0; 30.2; 30.3; 30.4 (4CH_2); 30.6 (2CH_2); 30.7 (3CH_2); 30.74 (3CH_2); 32.8 (CH_2); 34.9 (CH_2CO); 36.9 (PhCH_2); 66.3 (d, *J* = 5.0, CH_2OP); 72.5 (d, *J* = 8.3, CH); 126.6 (CH_{Ar}); 129.2 (2CH_{Ar}); 129.4 (2CH_{Ar}); 144.0 (C_{Ar}); 174.3 (CO)
^{31}P-NMR (methanol-d_4, 121 MHz): δ 2.76
$[\alpha]_D^{20}$: +1.2 (c = 1.03, methanol)
HRMS (ESI, *m/z*): calculated for $C_{24}H_{39}{}^{79}BrO_6P$ ([M(^{79}Br)-H]$^-$): 533.1673, found: 533.1694; calculated for $C_{24}H_{39}{}^{81}BrO_6P$ ([M(^{81}Br)-H]$^-$): 535.1654, found: 533.1673

(1*S*)-2-Bromo-1-[(phosphonooxy)methyl]ethyl (9*Z*)-octadec-9-enoate, 3d

Following the general procedure 4.1.1.7, compound **3d** was obtained from di-*tert*-butyl phosphate **110** (5 mg, 8.17 µmol) and TFA (15 µL, 204 µmol) without further purification in 81% yield.

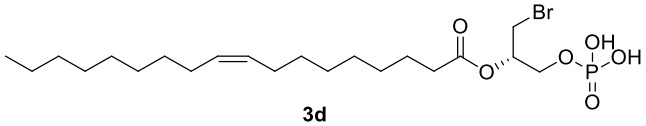

3d

IR (ATR): 1739 (C=O); 1666 (C=C); 1071 (P-O)

^{1}H-NMR (methanol-d_4, 700 MHz): δ 0.90 (t, *J* = 7.0, 3H, CH_3); 1.28-1.35 (m, 20H, $10CH_2$); 1.62-1.65 (m, 2H, CH_2CH_2CO); 2.02-2.05 (m, 4H, $2CH_2CH_{alkene}$); 2.37 (td, *J* = 7.4, 3.2, 2H, CH_2CO); 3.60 (dd, *J* = 11.0, 6.1, 1H, ½CH_2Br); 3.68 (dd, *J* = 11.0, 4.6, 1H, ½CH_2Br); 4.07-4.12 (m, 2H, CH_2OP); 5.14-5.18 (m, 1H, CH); 5.32-5.37 (m, 2H, $2CH_{alkene}$)

^{13}C-NMR (methanol-d_4, 175 MHz): δ 14.5 (CH_3); 23.8; 26.0 ($2CH_2$); 28.1 ($2CH_2CH_{alkene}$); 30.1; 30.2; 30.3; 30.4; 30.5; 30.6; 30.8; 30.9; 31.1; 33.1 ($10CH_2$); 35.0 (CH_2CO); 66.0 (d, *J* = 3.1, CH_2OP); 72.8 (d, *J* = 5.5, CH) 130.8; 130.9 ($2CH_{alkene}$); 174.4 (CO)

^{31}P-NMR (methanol-d_4, 202 MHz): δ 3.36

$[\alpha]_D^{20}$: +3.3 (c = 0.33, methanol)

HRMS (ESI, *m/z*): calculated for $C_{21}H_{39}{}^{79}BrO_6P$ ([M(^{79}Br)-H]$^-$): 497.1673, found: 497.1664; calculated for $C_{21}H_{39}{}^{81}BrO_6P$ ([M(^{81}Br)-H]$^-$): 499.1653, found: 499.1642

HPLC (method B, t_R, min): 25.58

*4.1.7 Synthesis of final compounds **4a-c***

4.1.7.1 Synthesis of final compound **4a**

(2*S*)-2-[(Benzyloxy)methyl]oxirane, 111

To a suspension of NaH (65 mg, 1.62 mmol, 1.2 equiv, 60% dispersion in oil) in DMF (3 mL) at 0ºC, (2*R*)-oxiran-2-ylmethanol (100 mg, 1.35 mmol, 1 equiv) was added, followed by benzyl bromide (0.21 mL, 1.76 mmol, 1.3 equiv). The reaction was allowed to warm up to room temperature and stirred overnight. Afterward, water was added and the mixture was extracted with dichloromethane. The organic layer was washed with water and brine, dried over Na_2SO_4 and filtered. The solvent was evaporated under reduced pressure to afford product **111** in quantitative yield, which was used in the next step without further purification. Spectroscopic data correspond with those previously reported.[113]

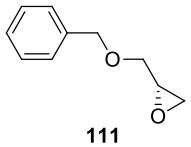

111

^{1}H-NMR ($CDCl_3$, 300 MHz): δ 2.62 (dd, *J* = 5.0, 2.7, 1H, ½$CH_{2\ epox}$); 2.81 (dd, *J* = 4.9, 4.1, 1H, ½$CH_{2\ epox}$); 3.17-3.22 (m, 1H, CH); 3.45 (dd, *J* = 11.4, 5.8, 1H, ½CH_2O); 3.77 (dd, *J* = 11.4, 3.0, 1H, ½CH_2O); 4.59 (dd, *J* = 19.4, 11.9, 2H, OCH_2Ph); 7.27-7.39 (m, 5H, $5CH_{Ar}$)

tert-Butyl (5*S*)-5-((benzyloxy)methyl)-2-oxotetrahydrofuran-3-carboxylate, 112

Di-*tert*-butyl malonate (0.97 mL, 1.58 mmol, 2 equiv) was added dropwise to a stirred suspension of NaH (63 mg, 1.58 mmol, 2 equiv, 60% dispersion in oil) in a 2:1 mixture of anhydrous DMF:THF (6 mL) at 0°C, and the mixture was stirred at room temperature for 30 minutes. A solution of **111** (130 mg, 0.79 mmol, 1 equiv) in dry THF (2 mL) was then added, and the resulting mixture was stirred at 80°C for 6 hours. After cooling to room temperature, the reaction was quenched by addition of a saturated aqueous solution of NH_4Cl, diluted with water, and extracted with ethyl acetate. The organic phase was washed with brine, dried over Na_2SO_4, filtered and the solvents were removed under reduced pressure. The residue was purified by flash chromatography (dichloromethane) to afford lactone **112** in 62% yield.

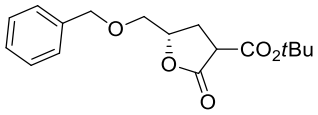

112

R_f: 0.36 (hexane/ethyl acetate, 9:1)

IR (ATR): 1777 (C=O); 1729 (C=O); 1147 (C-O)

^{1}H-NMR ($CDCl_3$, 300 MHz): Mixture of diastereoisomers A:B (3:2): δ 1.48 (s, 9H, $3CH_{3\ B}$); 1.49 (s, 9H, $3CH_{3\ A}$); 2.36 (ddd, *J* = 13.0, 9.7, 4.7, 2H, $CH_2CHCO_2tBu_B$); 2.42-2.49 (m, 1H, ½$CH_2CHCO_2tBu_A$); 2.60-2.70 (m, 1H, ½$CH_2CHCO_2tBu_A$); 3.47-3.71 (m, 3H, $CHCO_2tBu$, OCH_2CH); 4.50-4.65 (m, 3H, $PhCH_2$, OCH_2CH_B); 4.71-4.78 (m, 1H, OCH_2CH_A); 7.26-7.38 (m, 5H, $5CH_{Ar}$)

^{13}C-NMR ($CDCl_3$, 75 MHz): δ 28.0 ($3CH_3$); 28.3 ($CH_2CHCO_2tBu_B$); 28.5 ($CH_2CHCO_2tBu_A$); 47.6 ($CHCO_2tBu_B$); 47.8 ($CHCO_2tBu_A$); 71.2 ($PhCH_2$); 73.6 (OCH_2CH_B); 73.7 (OCH_2CH_A); 77.7 (OCH_2CH_B); 77.8 (OCH_2CH_A); 82.8 (C_A); 82.9 (C_B); 127.7 ($2CH_{Ar\ A}$); 127.8 ($2CH_{Ar\ B}$); 127.9 ($CH_{Ar\ B}$); 128.0 ($CH_{Ar\ A}$); 128.6 ($2CH_{Ar\ B}$); 128.62 ($2CH_{Ar\ A}$); 137.6 ($C_{Ar\ A}$); 137.7 ($C_{Ar\ B}$); 166.8 (CO_2tBu_B); 167.3 (CO_2tBu_A); 171.9 ($CO_{lactone\ B}$); 172.6 ($CO_{lactone\ A}$)

tert-Butyl (5*S*)-5-[(benzyloxy)methyl]-3-fluoro-2-oxotetrahydrofuran-3-carboxylate, 113

Following the general procedure 4.1.1.4, compound **113** was obtained from lactone **112** (1.70 g, 5.54 mmol) in 99% yield, which was used in the next step without further purification.

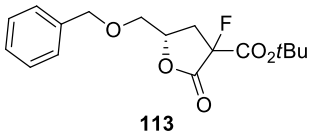

113

R_f: 0.80 (dichloromethane)
IR (ATR): 1794 (C=O); 1756 (C=O); 1157 (C-F)
^{1}H-NMR ($CDCl_3$, 300 MHz): Mixture of diastereoisomers A:B (2.3:1): δ 1.48 (s, 9H, $3CH_{3\ B}$); 1.50 (s, 9H, $3CH_{3\ A}$); 2.48-2.81 (m, 2H, CH_2CF); 3.60-3.76 (m, 2H, OCH_2CH); 4.59 (s, 2H, $PhCH_2$); 4.69-4.78 (m, 1H, CH_A); 4.81-4.89 (m, 1H, CH_B); 7.29-7.38 (m, 5H, $5CH_{Ar}$)
^{13}C-NMR ($CDCl_3$, 75 MHz): δ 27.8 ($3CH_{3\ B}$); 27.9 ($3CH_{3\ A}$); 35.1 (d, *J* = 21.9, CH_2CF_B); 35.2 (d, *J* = 22.4, CH_2CF_A); 69.8 ($PhCH_2$); 73.7 (OCH_2CH_B); 73.8 (OCH_2CH_A); 76.5 (d, *J* = 4.9, CH_A); 76.6 (CH_B); 85.3 ($C(CH_3)_{3\ B}$); 85.6 ($C(CH_3)_{3\ A}$); 127.7 ($2CH_{Ar\ B}$); 127.8 ($2CH_{Ar\ A}$); 128.0 ($CH_{Ar\ B}$); 128.1 ($CH_{Ar\ A}$); 128.56 ($2CH_{Ar\ B}$); 128.59 ($2CH_{Ar\ A}$); 137.2 ($C_{Ar\ A}$); 137.5 ($C_{Ar\ B}$); 168.5 (d, *J* = 24.8, $CO_{lactone}$); (CF and CO_2tBu not observed)
MS (ESI, *m/z*): 342.1 $[M+NH_4]^+$

***tert*-Butyl (5*S*)-3-fluoro-5-(hydroxymethyl)-2-oxotetrahydrofuran-3-carboxylate, 114**

Following the general procedure 4.1.1.1, alcohol **114** was obtained from **113** (480 mg, 1.48 mmol) at 60ºC in quantitative yield.

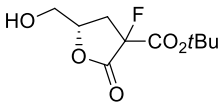

114

R_f: 0.25 (dichloromethane)
IR (ATR): 3318 (O-H); 1689 (C=O)
^{1}H-NMR ($CDCl_3$, 300 MHz): Mixture of diastereoisomers A:B (1.2:1): δ 1.52 (s, 9H, $3CH_3$); 2.51-2.95 (m, 2H, CH_2CF); 3.66-3.75 (m, 1H, ½CH_2OH); 3.96-4.03 (m, 1H, ½CH_2OH); 4.67-4.75 (m, 1H, CH_B); 4.78-4.86 (m, 1H, CH_A)
^{13}C-NMR ($CDCl_3$, 75 MHz): δ 27.9 ($3CH_3$); 34.2 (d, *J* = 22.4) and 34.3 (d, *J* = 21.9) (CH_2CF); 62.5 and 62.8 (CH_2OH); 78.2 (d, *J* = 4.7) and 78.9 (CH); 85.5 and 85.7 ($C(CH_3)_3$); 92.2 (d, *J* = 198) and 92.4 (d, *J* = 199, CF); 164.5 (d, *J* = 26.9, CO_2tBu); 168.7 (d, *J* = 25.0, $CO_{lactone}$)
MS (ESI, *m/z*): 177.9 $[M-tBu]^+$; 159.9 $[M-F-tBu]^+$

tert-Butyl (5*S*)-3-fluoro-2-oxo-5-{[(10-phenyldecanoyl)oxy]methyl} tetrahydrofuran-3-carboxylate, 115

Following the general procedure 4.1.1.17, ester **115** was obtained from carboxylic acid **77** (64 mg, 0.26 mmol) and alcohol **114** (60 mg, 0.26 mmol) in 35% yield. Chromatography: dichloromethane.

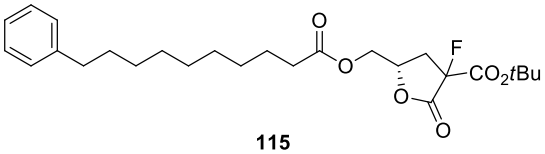

115

R_f: 0.85 (dichloromethane)

IR (ATR): 1743 (C=O); 1156 (C-F)

^{1}H-NMR ($CDCl_3$, 300 MHz): Mixture of diastereoisomers A:B (1.7:1): δ 1.28-1.29 (m, 10H, $5CH_2$); 1.53 (s, 9H, $3CH_{3\ B}$); 1.54 (s, 9H, $3CH_{3\ A}$); 1.58-1.63 (m, 4H, $2CH_2$); 2.36 (t, *J* = 7.6, 2H, CH_2CO); 2.41-2.91 (m, 2H, CH_2CF); 2.59 (t, *J* = 7.8, 2H, $PhCH_2$); 4.17-4.28 (m, 1H, $½CO_2CH_{2\ B}$); 4.24 (dd, *J* = 11.4, 5.4, 1H, $½CO_2CH_{2\ A}$); 4.39 (app t, *J* = 3.6, 1H, $½CO_2CH_{2\ A}$); 4.43 (app t, *J* = 3.7, 1H, $½CO_2CH_{2\ B}$); 4.79-4.86 (m, 1H, CH_B); 4.87-4.96 (m, 1H, CH_A); 7.16-7.18 (m, 3H, $3CH_{Ar}$); 7.24-7.30 (m, 2H, $2CH_{Ar}$)

^{13}C-NMR ($CDCl_3$, 75 MHz): δ 24.9 (CH_2); 28.0 ($3CH_3$); 29.2; 29.3; 29.4; 29.5; 29.6; 31.6 ($6CH_2$); 34.1 (CH_2CO); 35.1 (d, *J* = 22.8) and 35.14 (d, *J* = 21.8, CH_2CF); 36.1 ($PhCH_2$); 63.6 and 63.9 (CO_2CH_2); 75.1 (d, *J* = 4.6) and 75.7 (CH); 85.7 and 85.9 ($C(CH_3)_3$); 125.7 (CH_{Ar}); 128.4 ($2CH_{Ar}$); 128.5 ($2CH_{Ar}$); 143.02 and 143.04 (C_{Ar}); 164.3 (CO_2*t*Bu); 167.8 (d, *J* = 23.8, $CO_{lactone}$); 173.4 and 173.45 (CO); (CF not observed)

MS (ESI, *m/z*): 482.3 $[M+NH_4]^+$

(5*S*)-3-Fluoro-2-oxo-5-{[(10-phenyldecanoyl)oxy]methyl}tetrahydrofuran-3-carboxylic acid, 4a

Following the general procedure 4.1.1.7, compound **4a** was obtained from *tert*-butyl ester **115** (30 mg, 65 µmol) and TFA (0.37 mL, 4.84 mmol) in 90% yield.

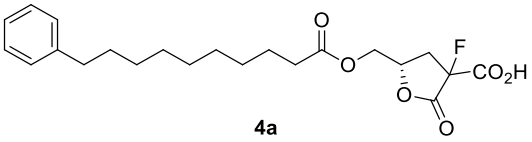

4a

IR (ATR): 3506 (O-H); 1795 (C=O); 1795 (C=O); 1741 (C=O)

^{1}H-NMR ($CDCl_3$, 500 MHz): Mixture of diastereoisomers: δ 1.26-1.30 (m, 10H, $5CH_2$); 1.59-1.62 (m, 4H, $2CH_2$); 2.36 (t, *J* = 7.3, 2H, CH_2CO); 2.49-3.06 (m, 2H, CH_2CF); 2.59 (t, *J* = 7.7, 2H, $PhCH_2$); 4.28-4.30 (m, 1H, ½CO_2CH_2); 4.42 (m, 1H, ½CO_2CH_2); 4.95 (m, 1H, CH); 7.16-7.18 (m, 3H, $3CH_{Ar}$); 7.25-7.28 (m, 2H, $2CH_{Ar}$)
^{13}C-NMR ($CDCl_3$, 125 MHz): δ 24.9; 29.2; 29.3; 29.4; 29.5; 29.6; 31.6 ($7CH_2$); 34.0 and 34.1 (CH_2CO); 35.1 (br d, *J* = 25.0, CH_2CF); 36.1 ($PhCH_2$); 63.5 and 63.9 (CO_2CH_2); 75.6 (br s) and 76.3 (CH); 125.6 and 125.7 (CH_{Ar}); 128.4 ($2CH_{Ar}$); 128.5 ($2CH_{Ar}$); 143.0 and 143.1 (C_{Ar}); 168.0 (br s, CO_2H and $CO_{lactone}$); 173.6 and 173.8 (CO); (CF not observed)
HRMS (ESI, *m/z*): calculated for $C_{22}H_{28}FO_6$ ($[M-H]^-$): 407.1875, found: 407.1875
HPLC (method A, t_R, min): 10.31

4.1.7.2 Synthesis of final compound **4b**

Di-*tert*-butyl fluoro{(2*S*)-2-hydroxy-3-[(10-phenyldecanoyl)oxy]propyl} malonate, 116

Following the general procedure 4.1.1.13, ester **116** was obtained from carboxylic acid **77** (65 mg, 0.26 mmol) and diol **43** (161 mg, 0.52 mmol) in 75% yield. Chromatography: dichloromethane to dichloromethane/methanol, 99:1.

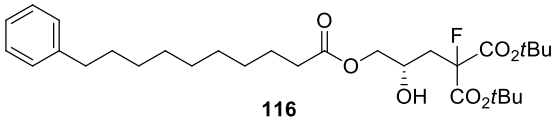

116

R_f: 0.43 (hexane/ethyl acetate, 8:2)
IR (ATR): 3387 (O-H); 1743 (C=O); 1154 (C-F)
^{1}H-NMR ($CDCl_3$, 300 MHz): δ 1.29 (m, 10H, $5CH_2$); 1.50 (s, 18H, $6CH_3$); 1.56-1.62 (m, 4H, $2CH_2$); 2.17-2.44 (m, 2H, CH_2CF); 2.33 (t, *J* = 7.5, 2H, CH_2CO); 2.59 (t, *J* = 7.8, 2H, $PhCH_2$); 4.00-4.20 (m, 3H, CH, CO_2CH_2); 7.17 (d, *J* = 6.5, 3H, $3CH_{Ar}$); 7.24-7.27 (m, 2H, $2CH_{Ar}$)
^{13}C-NMR ($CDCl_3$, 75 MHz): δ 25.0 (CH_2); 27.9 ($3CH_3$); 28.0 ($3CH_3$); 29.2; 29.4; 29.41; 29.5; 29.6; 31.6 ($6CH_2$); 34.3 (CH_2CO); 36.1 ($PhCH_2$); 37.5 (d, *J* = 20.8, CH_2CF); 65.4 (d, *J* = 3.5, CH); 68.0 (CO_2CH_2); 83.9; 84.0 ($2C(CH_3)_3$); 93.2 (d, *J* = 196.7, CF); 125.7 (CH_{Ar}); 128.3 ($2CH_{Ar}$); 128.5 ($2CH_{Ar}$); 143.0 (C_{Ar}); 165.2 (d, *J* = 24.6, CO_2tBu); 165.6 (d, *J* = 25.9, CO_2tBu); 173.9 (CO)

Di-*tert*-butyl fluoro{(2*S*)-2-methoxy-3-[(10-phenyldecanoyl)oxy]propyl} malonate, 117

Following the general procedure 4.1.1.8, compound **117** was obtained from **116** (100 mg, 0.19 mmol) in 30% yield. Chromatography: hexane to hexane/ethyl acetate, 8:2.

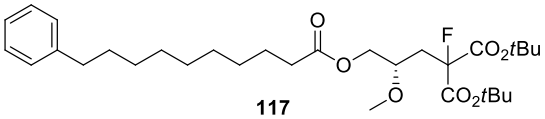

117

R_f: 0.73 (hexane/ethyl acetate, 8:2)
IR (ATR): 1707 (C=O); 1163 (C-F)
^{1}H-NMR ($CDCl_3$, 300 MHz): δ 1.25-1.29 (m, 10H, $5CH_2$); 1.48 (s, 9H, $3CH_3$); 1.49 (s, 9H, $3CH_3$); 1.58-1.62 (m, 4H, $2CH_2$); 2.16-2.50 (m, 2H, CH_2CF); 2.32 (t, *J* = 7.5, 2H, CH_2CO); 2.59 (t, *J* = 7.7, 2H, $PhCH_2$); 3.30 (s, 3H, OCH_3); 3.57-3.65 (m, 1H, CH); 4.05 (dd, *J* = 11.7, 4.8, 1H, $½CO_2CH_2$); 4.17 (dd, *J* = 11.7, 4.6, 1H, $½CO_2CH_2$); 7.14-7.19 (m, 3H, $3CH_{Ar}$); 7.24-7.29 (m, 2H, $2CH_{Ar}$)
^{13}C-NMR ($CDCl_3$, 75 MHz): δ 25.0 (CH_2); 27.9 ($3CH_3$); 27.92 ($3CH_3$); 29.3; 29.4; 29.42; 29.5; 29.6; 31.6 ($6CH_2$); 34.3 (CH_2CO); 36.1 ($PhCH_2$); 36.7 (d, *J* = 21.4, CH_2CF); 57.8 (OCH_3); 64.9 (CO_2CH_2); 74.0 (d, *J* = 3.4, CH); 83.4; 83.6 ($2C(CH_3)_3$); 92.6 (d, *J* = 195.4, CF); 125.7 (CH_{Ar}); 128.4 ($2CH_{Ar}$); 128.5 ($2CH_{Ar}$); 143.0 (C_{Ar}); 165.2 (d, *J* = 27.5, CO_2tBu); 165.24 (d, *J* = 23.9, CO_2tBu); 173.7 (CO)
$[\alpha]_D^{20}$: +3.0 (c = 1.69, methanol)
MS (MALDI, *m/z*): 570.9 $[M+NH_4]^+$

Fluoro{(2*S*)-2-methoxy-3-[(10-phenyldecanoyl)oxy]propyl}malonic acid, 4b

Following the general procedure 4.1.1.7, compound **4b** was obtained from di-*tert*-butyl ester **117** (44 mg, 80 µmol) and TFA (0.46 mL, 5.97 mmol) without further purification in 68% yield.

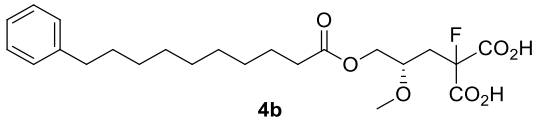

4b

IR (ATR): 3342 (O-H); 1736 (C=O)
^{1}H-NMR (methanol-d_4, 300 MHz): δ 1.28-1.31 (m, 10H, $5CH_2$); 1.58-1.62 (m, 4H, $2CH_2$); 2.22-2.54 (m, 2H, CH_2CF); 2.34 (t, *J* = 7.4, 2H, CH_2CO); 2.59 (t, *J* = 7.7, 2H, $PhCH_2$); 3.32 (s, 3H, OCH_3); 3.60-3.65 (m, 1H, CH); 4.04 (dd, *J* = 11.8, 4.8,

1H, ½CO_2CH_2); 4.25 (dd, *J* = 11.7, 4.1, 1H, ½CO_2CH_2); 7.09-7.16 (m, 3H, 3CH_{Ar}); 7.21-7.26 (m, 2H, 2CH_{Ar})

^{13}C-NMR (CDCl$_3$, 75 MHz): δ 26.0; 30.1; 30.2; 30.3 (4CH_2); 30.5 (2CH_2); 32.7 (CH_2); 34.9 (CH_2CO); 36.9 (PhCH_2); 38.1 (d, *J* = 21.3, CH_2CF); 58.1 (OCH_3); 65.8 (CO_2CH_2); 75.8 (d, *J* = 3.4, CH); 126.6 (CH_{Ar}); 129.2 (2CH_{Ar}); 129.4 (2CH_{Ar}); 144.0 (C_{Ar}); 175.2 (CO); (CF and CO_2H not observed)

$[\alpha]_D^{20}$: limited solubility in DMSO

HRMS (ESI, *m/z*): calculated for $C_{23}H_{32}FO_6$ ([M-H]$^-$): 439.2138, found: 439.2119

HPLC (method A, t_R, min): 10.25

4.1.7.3 Synthesis of final compound **4c**

Di-*tert*-butyl fluoro{(2*S*)-3-[(9*Z*)-hexadec-9-enoyloxy]-2-hydroxypropyl} malonate, 118

Following the general procedure 4.1.1.13, ester **118** was obtained from palmitoleic acid (95 mg, 0.37 mmol) and diol **43** (230 mg, 0.75 mmol) in 44% yield. Chromatography: dichloromethane to dichloromethane/methanol, 8:2.

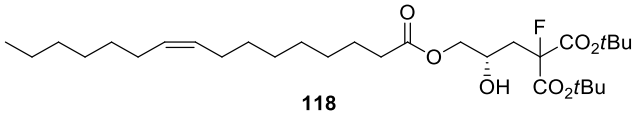

118

R_f: 0.61 (hexane/ethyl acetate, 8:2)

IR (ATR): 3401 (O-H); 1744 (C=O); 1150 (C-F)

^{1}H-NMR (CDCl$_3$, 300 MHz): δ 0.86 (t, *J* = 6.6, 3H, CH_3); 1.28 (m, 16H, 8CH_2); 1.48 (s, 18H, 6CH_3); 1.58-1.63 (m, 2H, CH_2CH_2CO); 1.96-2.02 (m, 4H, 2CH_2CH_{alkene}); 2.16-2.49 (m, 2H, CH_2CF); 2.32 (t, *J* = 7.5, 2H, CH_2CO); 3.97-4.18 (m, 3H, CH, CO_2CH_2); 5.27-5.38 (m, 2H, 2CH_{alkene})

^{13}C-NMR (CDCl$_3$, 75 MHz): δ 14.2 (CH_3); 22.8; 25.0 (2CH_2); 27.2; 27.3 (2CH_2CH_{alkene}); 27.8 (3CH_3); 27.9 (3CH_3); 29.1; 29.19; 29.2; 29.3; 29.8; 29.83; 31.9 (7CH_2); 34.2 (CH_2CO); 37.5 (d, *J* = 20.7, CH_2CF); 65.3 (d, *J* = 3.5, CH); 68.0 (CO_2CH_2); 83.9; 84.0 (2$C(CH_3)_3$); 93.1 (d, *J* = 198.2, CF); 129.8; 130.1 (2CH_{alkene}); 165.3 (d, *J* = 24.6, CO_2*t*Bu); 165.7 (d, *J* = 25.8, CO_2*t*Bu); 173.9 (CO)

$[\alpha]_D^{20}$: +6.7 (c = 1.04, methanol)

MS (ESI, *m/z*): 562.4 [M+NH_4]$^+$; 567.4 [M+Na]$^+$

Di-*tert*-butyl fluoro{(2*S*)-3-[(9*Z*)-hexadec-9-enoyloxy]-2-methoxypropyl} malonate, 119

Following the general procedure 4.1.1.8, compound **119** was obtained from **118** (86 mg, 0.16 mmol) in 27% yield. Chromatography: hexane to hexane/ethyl acetate, 8:2.

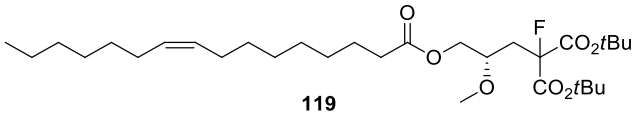

119

R_f: 0.81 (hexane/ethyl acetate, 8:2)

^{1}H-NMR ($CDCl_3$, 300 MHz): δ 0.88 (t, *J* = 6.7, 3H, CH_3); 1.29 (m, 16H, $8CH_2$); 1.48 (s, 9H, $3CH_3$); 1.49 (s, 9H, $3CH_3$); 1.60-1.64 (m, 2H, CH_2CH_2CO); 1.97-2.01 (m, 4H, $2CH_2CH_{alkene}$); 2.17-2.50 (m, 2H, CH_2CF); 2.33 (t, *J* = 7.6, 2H, CH_2CO); 3.30 (s, 3H, OCH_3); 3.57-3.64 (m, 1H, CH); 4.05 (dd, *J* = 11.6, 4.9, 1H, $½CO_2CH_2$); 4.17 (dd, *J* = 11.6, 4.7, 1H, $½CO_2CH_2$); 5.28-5.39 (m, 2H, $2CH_{alkene}$)

^{13}C-NMR ($CDCl_3$, 75 MHz): δ 14.2 (CH_3); 22.8; 25.0 ($2CH_2$); 27.3; 27.4 ($2CH_2CH_{alkene}$); 27.9 ($3CH_3$); 27.91 ($3CH_3$); 29.1 (CH_2); 29.2 ($2CH_2$); 29.3; 29.8; 29.9; 31.9 ($4CH_2$); 34.3 (CH_2CO); 36.7 (d, *J* = 21.2, CH_2CF); 57.8 (OCH_3); 64.9 (CO_2CH_2); 74.0 (d, *J* = 3.4, CH); 83.2; 83.6 ($2C(CH_3)_3$); 92.6 (d, *J* = 195.3, CF); 129.9; 130.1 ($2CH_{alkene}$); 165.2 (d, *J* = 27.3, CO_2tBu); 165.2 (d, *J* = 24.0, CO_2tBu); 173.7 (CO)

Fluoro{(2*S*)-3-[(9*Z*)-hexadec-9-enoyloxy]-2-methoxypropylmalonic acid, 4c

Following the general procedure 4.1.1.7, compound **4c** was obtained from di-*tert*-butyl ester **119** (20 mg, 36 µmol) and TFA (0.21 mL, 2.68 mmol) without further purification in 93% yield.

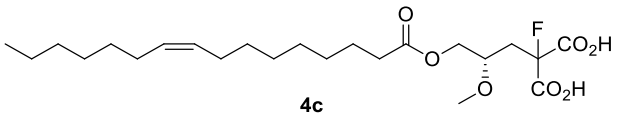

4c

IR (ATR): 1740 (C=O); 1164 (C-F)

^{1}H-NMR (methanol-d_4, 300 MHz): δ 0.90 (t, *J* = 6.3, 3H, CH_3); 1.29-1.32 (m, 16H, $8CH_2$); 1.57-1.64 (m, 2H, CH_2CH_2CO); 2.02-2.04 (m, 4H, $2CH_2CH_{alkene}$), 2.10-2.59 (m, 2H, CH_2CF); 2.35 (t, *J* = 7.4, 2H, CH_2CO); 3.32 (s, 3H, OCH_3); 3.60-3.67 (m, 1H, CH), 4.04 (dd, *J* = 11.8, 4.8, 1H, $½CO_2CH_2$); 4.25 (dd, *J* = 11.7, 4.1, 1H, $½CO_2CH_2$); 5.29-5.39 (m, 2H, $2CH_{alkene}$)

^{13}C-NMR (methanol-d_4, 75 MHz): δ 14.4 (CH_3); 23.7; 26.0 ($2CH_2$); 28.1; 28.2 ($2CH_2CH_{alkene}$); 30.0 (CH_2); 30.1 ($2CH_2$); 30.2; 30.8; 30.82; 32.9 ($4CH_2$); 34.9 (CH_2CO); 38.3 (d, *J* = 21.3, CH_2CF); 58.1 (OCH_3); 65.9 (CO_2CH_2); 75.9 (br s, CH); 130.8; 130.9 ($2CH_{alkene}$); 175.2 (CO); (CF and CO_2H not seen)
$[\alpha]_D^{20}$: +14.1 (c = 0.79, methanol)
HRMS (ESI, *m/z*): calculated for $C_{23}H_{38}FO_7$ ($[M-H]^-$): 445.2607, found: 445.2618
HPLC (method A, t_R, min): 11.89

4.2 Biological assays

Collagen, poly-D-lysine, poly-L-lysine and LPA were purchased from Aldrich. Ionomycin was purchased from Cayman. RH7777 hepatoma cells stably expressing the LPA_1 receptor and their corresponding non-transfected controls were kindly provided by Prof. Gabor Tigyi (University of Tennessee Health Science Center, Memphis, Tennessee) and B103 neuroblastoma cells were provided by Prof. Jerold Chun (The Scripps Research Institute, La Jolla, California). Retrovirus expression vector (LZRS-EGFP) and Phoenix retrovirus producer cell lines were provided by Prof. Garry P. Nolan (Stanford University, Stanford, California).

4.2.1 Cell culture

All reagents were from Gibco. All cells were grown in Dulbecco's modified Eagle medium (DMEM) supplemented with 10% fetal bovine serum (FBS), 1% non-essential aminoacids, 1% sodium pyruvate, 100 U/mL penicillin, and 100 μg/mL streptomycin in a 5% CO_2 humidified atmosphere at 37 ºC. For passage, cells were rinsed with phosphate buffered saline (PBS) and incubated with 0.125% trypsin, 0.02% EDTA solution for 2 min at 37 ºC. Detached cells were resuspended in growth medium, counted if necessary and splitted onto fresh dishes.

4.2.2 Generation of LPA_{1-5} overexpressing cell lines

Cell lines stably expressing LPA_{1-5} receptors were generated by retroviral infection of B103 cells. Lipofectamine 2000 transfection reagent (Invitrogen) was used to transfect the Phoenix ecotropic packaging cell line with retroviral constructs expressing FLAG-tagged human LPA_{1-3} and LPA_5, and mouse LPA_4 cDNAs and EGFP. An internal ribosomal entry site (IRES) allowed dual expression of both the LPA_{1-5} receptors and EGFP. Retroviral supernatant was harvested 48 h post-transfection, filtered through a 0.45 μm filter and added to B103 cells in the presence of Polybrene (Sigma). Cells were centrifugued for 90 minutes at 28ºC, after which the retroviral supernatant was replaced by DMEM. B103 cells

expressing high levels of LPA_{1-5} and high levels of EGFP were isolated by FACS using a Vantage DiVa I instrument. Control B103 cells transfected with empty vector were also obtained and used as control throughout the experiments.

4.2.3 Evaluation of receptor activation by Ca^{2+} mobilization assay

Changes in intracellular calcium levels were measured by using the fluorescent calcium sensitive dye Fluo-4NW (Invitrogen). RH7777 cells or B103 cells were plated on poly-D-lysine or collagen-coated, respectively, black-wall clear-bottom 96-well plates (Corning) at a density of 50000 cells/well and cultured overnight. The culture medium was then replaced with Fluo-4 NW dye loading solution containing 2.5 µM of probenecid and incubated for 30 minutes at 37ºC followed by an additional 30 minutes at room temperature. Fluorescence changes were registered in a FluoStar Optima instrument (BMG Labtech) at 525 nm using an excitation wavelength of 494 nm. Each well was monitored for 240 s. 20 µL of the test compound from a 6x stock solution in assay buffer were added after 120 s of starting the measurement. Ca^{2+} transient increase was quantified by calculating the difference between maximum and baseline values for each well. As positive controls, 10 µM LPA and 10 µM ionomycin were included in every experiment. At this concentration, LPA induced a response about 30-33% of the one shown by ionomycin, which is in agreement with previously described results.[99]

The data presented are from two to four independent experiments carried out in triplicate or quadruplicate. Dose-response curves were generated and EC_{50} values calculated by nonlinear regression analysis using PRISM software version 5 (GraphPad Software Inc, San Diego, CA, USA).

4.2.4 Receptor internalization and neurite retraction assay

B103 neuroblastoma cells overexpressing LPA_1 receptor were plated on poly-L-lysine-coated glass coverslips in 24-well plates ($5 \cdot 10^4$ cells per well) and serum-starved overnight. For the experiment, media was replaced with 1 mL fresh serum-free DMEM, supplemented with 0.1% FAF BSA, 1 µM LPA, or compound. After 15 minutes, cells were fixed with 4% paraformaldehyde and permeabilized with 0.025% Triton X-100/PBS for 15 min. F-actin was detected with rhodamine-phalloidin (Sigma) in PBS and nuclei with DAPI (Sigma). For neurite retraction, samples were visualized on a fluorescence microscopy (Carl Zeiss). For receptor internalization cells were analysed using confocal fluorescence microscopy (Carl Zeiss).

4.2.5 Migration assay

Cell migration was measured in Transwell chambers (PET membrane with 8 µm pore size, Becton Dickinson). Bottom membrane of transwells was precoated overnight at 4 °C with 10 µg/ml of collagen solution in PBS. B103 neuroblastoma cells overexpressing LPA_1 receptor were serum-starved overnight, and then harvested with 0.125% trypsin containing 0.02% EDTA, washed once, counted and resuspended in serum-free DMEM. The cells were seeded into the upper chamber ($2.5 \cdot 10^5$ cells per transwell), and 0.1% FAF BSA, 1 µM LPA or compound under study were placed in the lower chamber. Cells were allowed to migrate for 5 h at 37°C. Non-migrated cells were removed from the top filter surface with a cotton swab. Migrated cells attached to the underside of the transwells were washed with PBS, stained with 0.1% crystal violet solution and counted under a microscope.

RESUMEN

5. RESUMEN

5.1 Introducción

La función biológica de los fosfolípidos ha estado tradicionalmente relacionada con un papel estructural, ya que son uno de los componentes mayoritarios de las membranas biológicas. Sin embargo, recientemente se ha descubierto la implicación de algunos de ellos en la regulación de procesos fisiológicos y patológicos de importancia.[1,2]

Los fosfolípidos se dividen en dos familias: (i) glicerofosfolípidos,[3] basados en el esqueleto de glicerol y (ii) esfingofosfolípidos, en el aminoalcohol esfingosina. Todos ellos presentan una cabeza polar con un grupo fosfato y dos cadenas hidrofóbicas. Cuando una de estas dos cadenas no está presente, las moléculas derivadas se denominan lisofosfolípidos. Estas moléculas, a pesar de su presencia minoritaria en el cuerpo humano, están ganando atención e importancia debido a su capacidad de señalizar a través de GPCRs. De entre ellas, destacan el ácido lisofosfatídico (LPA) y la esfingosina 1-fosfato (S1P), por su relevante papel en diversos procesos fisiológicos y patológicos.[4]

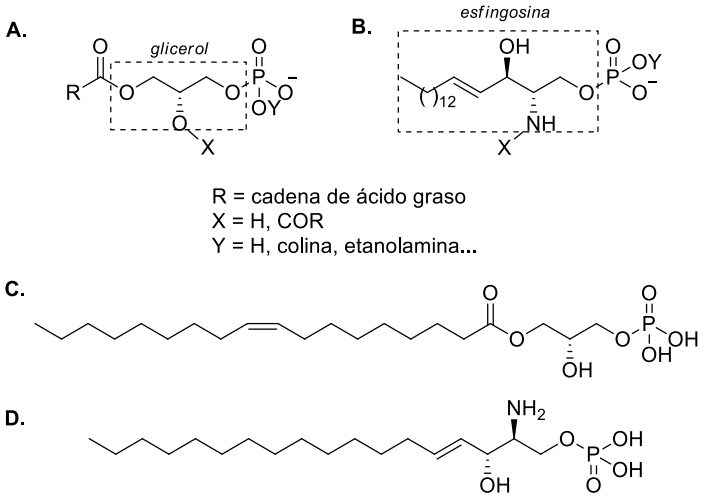

Figura 1. Estructura general de los glicerofosfolípidos (A) y esfingofosfolípidos (B). Estructura del LPA (C) y S1P (D).

En el caso del LPA, destacan sus efectos en el sistema nervioso central, los cuales parecen mediados fundamentalmente por el receptor LPA_1. Éste fue identificado como el primer receptor de LPA en 1996, y en la actualidad se han

identificado cinco subtipos adicionales de este receptor (LPA_2-LPA_6). Los subtipos LPA_1-LPA_3 comparten una elevada similitud entre sí, mientras que el LPA_4 y el LPA_5 presentan notables diferencias en cuanto a homología de secuencia.

El receptor LPA_1 (364 aminoácidos, masa molecular 41 kDa) está expresado principalmente en el sistema nervioso, y también se ha detectado en diversos tejidos tales como corazón, placenta, bazo, riñón, colon, intestino, próstata, testículo, ovario, páncreas, músculo esquelético y timo. El receptor LPA_1 está acoplado a tres tipos de proteínas G ($G_{i/o}$, G_q y $G_{12/13}$) y su activación induce un amplio número de respuestas celulares.

El LPA_1 está presente de forma mayoritaria en la mayoría de los tipos celulares del sistema nervioso tanto en condiciones fisiológicas como patológicas. En el cerebro, el LPA_1 se localiza de forma preferente en células progenitoras neuronales (*NPCs, neural progenitor cells*), jugando un papel importante en el desarrollo del cerebro embrionario, el cual está relacionado con la posterior aparición de enfermedades neuropsiquiátricas. Asimismo, su expresión en oligodendrocitos lo relaciona con el proceso de mielinización y el dolor neuropático.[34]

Además de su papel en el sistema nervioso, el receptor LPA_1 ha sido recientemente relacionado con el desarrollo de enfermedades tales como la fibrosis, la artritis reumatoide, la obesidad o el cáncer.

Dada la implicación del receptor LPA_1 en diversas patologías, el descubrimiento de ligandos potentes y selectivos es crucial para determinar su potencial como diana terapéutica. Sin embargo, hasta este momento no existe ningún fármaco en el mercado que actúe sobre los receptores de LPA. El único fármaco dirigido a un receptor lisofosfolipídico es Fingolimod (Gilenya®), un pan-agonista de S1P, comercializado para el tratamiento de la esclerosis múltiple.

Fingolimod

Aunque en los últimos años se han descrito una gran variedad ligandos agonistas y antagonistas para los receptores del LPA, todos ellos presentan una selectividad muy limitada y han sido escasamente validados *in vivo*. Estos compuestos pueden clasificarse dos grandes tipos: (i) miméticos del LPA y (ii) pequeñas moléculas no lipídicas identificadas mediante *high throughput screening*.

Entre los primeros, destaca el ligando NAEPA (2-[(9*Z*)-octadec-9-enoilamino]etil dihidrogeno fosfato), el primer agonista descrito para LPA, con actividad en los receptores LPA_1 y LPA_2.[68] Algunas de las modificaciones estructurales de este ligando han permitido mejorar la actividad, obteniéndose tanto agonistas como antagonistas. Como ejemplo, cabe destacar el ligando VPC51098, un antagonista dual de los receptores LPA_1 y LPA_3 con actividad nanomolar.[82] Otro importante análogo de LPA es el bromofosfonato denominado BrP-LPA, un pan-antagonista de los receptores LPA_{1-4} e inhibidor de autotaxina *in vitro*.[83] Ésta molécula ha contribuido a elucidar la implicación de los receptores de LPA en la inhibición del crecimiento tumoral, así como de la atenuación de la artritis en modelos animales.

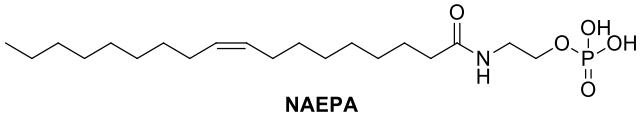

NAEPA

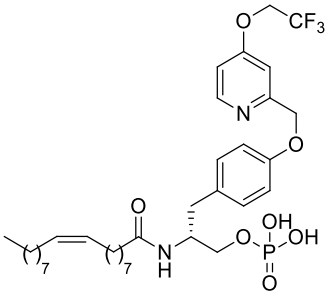

VPC51098

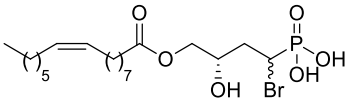

BrP-LPA

Entre las moléculas no lipídicas destaca Ki16425, un antagonista dual de $LPA_{1/3}$ que presenta actividad *in vivo*.[86] Las variaciones en el esqueleto de esta molécula han sido ampliamente estudiadas, destacando los antagonistas BMS-986020 y SAR100842, que actualmente están en fases clínicas para el tratamiento de la fibrosis y la esclerosis sistémica, respectivamente.[58,66]

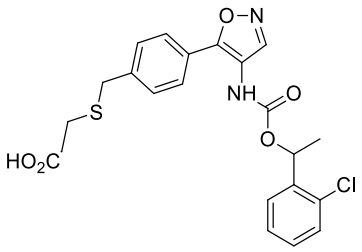

Ki16425

Por tanto, para contribuir a la elucidación de los roles del receptor LPA_1 tanto en condiciones fisiológicas como patológicas, es necesario desarrollar agonistas y antagonistas potentes y selectivos, lo que constituye el principal objetivo de este trabajo.

5.2 Objetivos

En este proyecto de Tesis Doctoral se pretende validar el receptor de ácido lisofosfatídico LPA_1 como diana terapéutica. Para ello, en primer lugar, se abordará el diseño de ligandos utilizando como punto de partida la estructura del LPA. Así, se han diseñado dos series de compuestos de estructura general **I** y **II**. Estos ligandos serán evaluados como agonistas del receptor LPA_1, estudiándose también su posible carácter antagonista así como su selectividad frente a los demás receptores de LPA. Asimismo, para los agonistas óptimos, se llevarán a cabo diversos ensayos celulares.

5.3 Resultados y discusión

En la etapa inicial de este proyecto, la información disponible acerca de los receptores de LPA era muy escasa, ya que no se conocía la estructura 3D de ninguno de ellos, ni se habían descrito ligandos potentes y selectivos. Por tanto, la búsqueda de nuevas moléculas con actividad en el receptor LPA_1 se basó en la modificación de la estructura del ligando endógeno LPA. Para ello, se diseñaron inicialmente dos series de compuestos: la serie **I**, en la que se modifica el grupo ácido, y la serie **II**, que incluye modificaciones en la subunidad hidrofóbica (Figura 2)

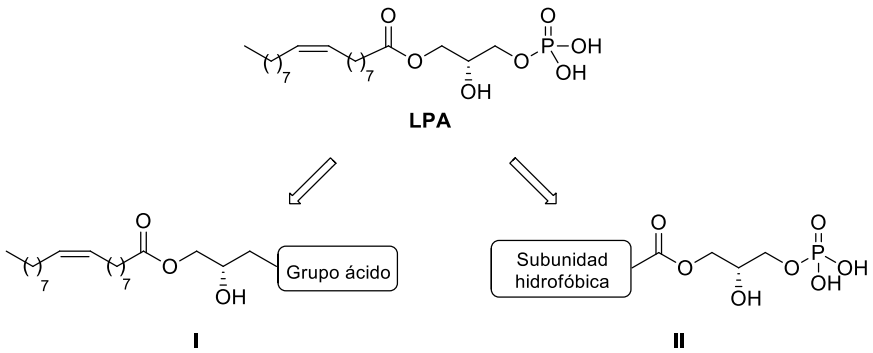

Figura 2. Diseño de nuevos ligandos para el receptor LPA_1.

*5.3.1 Diseño y síntesis de la serie **I***

Diversos estudios de relación estructura-actividad[40] destacan la dificultad de modificar el grupo fosfato del LPA para lograr ligandos con alta actividad, subrayando la importancia de la existencia de cargas negativas a pH fisiológico, así como de mantener un pK_a similar al del grupo fosfato. De hecho, esta parte de la molécula ha sido extensamente modificada sin haberse logrado resultados positivos hasta el momento. Por tanto, en la serie **I** se planteó la sustitución del grupo fosfato por otros fragmentos miméticos de éste, tales como ácidos carboxílicos y borónicos (Figura 3).[96]

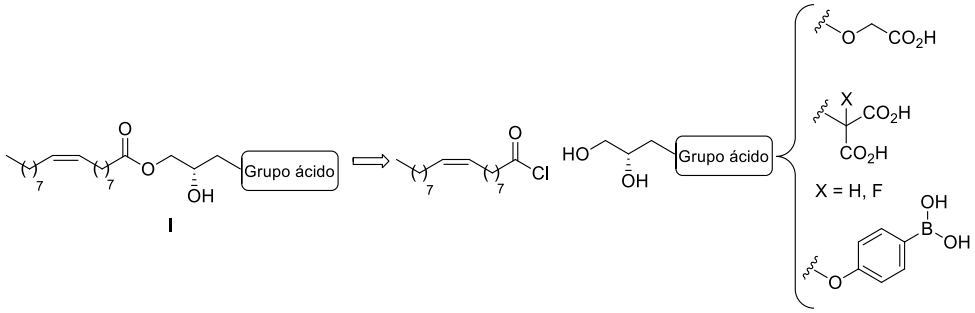

Figura 3. Grupos ácidos propuestos para la serie **I**.

Para ello, en primer lugar se sintetizaron los fragmentos de glicerol necesarios para su posterior reacción de esterificación regioselectiva con el cloruro del ácido oleico (Esquema 1). La desprotección del éster carboxílico con ácido trifluoroacético (TFA) permitió la obtención del producto final deseado **1a**. Sin embargo, en el caso de los ésteres malónicos, el tratamiento con TFA condujo

a la formación de las lactonas **1b** y **1c**, como mezcla de diastereoisómeros en proporción 1:1, por reacción de ciclación intramolecular del ácido carboxílico con el grupo hidroxilo en posición γ. Finalmente, el producto **1d** se obtuvo mediante la transformación del derivado de éster de pinacolboronato en la correspondiente sal de trifluoroborato, seguido de hidrólisis en presencia de cloruro de trimetilsilano para obtener el ácido borónico.

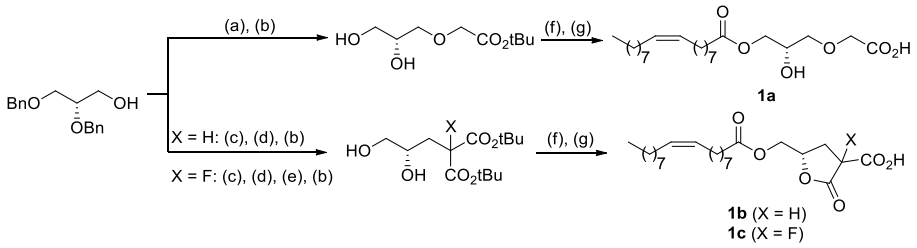

Reactivos y condiciones: (a) Bromoacetato de *terc*-butilo, NaH, TBAI, THF, 0ºC a 50ºC, 16 h, 22%; (b) H_2, Pd(C) 10%, EtOH, 60ºC, 99%; (c) cloruro de mesilo, trietilamina, DCM, 0ºC a ta, 1 h, 48%; (d) malonato de di-*terc*-butilo, NaH, NaI, DMF:THF, 0ºC a 80ºC, 17 h, 76%; (e) Selectfluor®, NaH, THF:DMF, 0ºC a ta, 48 h, 48%; (f) cloruro de oleoilo, 2,4,6-colidina, DCM, -78ºC a ta, 24 h, 36-99%; (g) TFA, DCM, ta, 17-18 h, 52-99%.

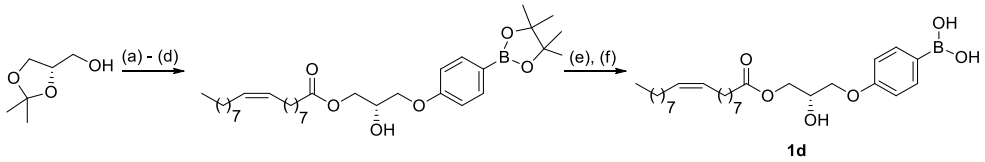

Reactivos y condiciones: (a) Cloruro de tosilo, piridina, DCM, 0ºC a ta, 16 h, 86%; (b) éster de pinacol del ácido 4-hidroxifenilborónico, Cs_2CO_3, DMF, 90ºC, 16 h, 84%; (c) PS-*p*TsOH, CH_3OH, ta, 18 h, 88%; (d) cloruro de oleoilo, 2,4,6-colidina, DCM, -78ºC a ta, 24 h, 40%; (e) KHF_2, CH_3OH:H_2O, ta, 30 min; 99%; (f) TMSCl, CH_3CN:H_2O, ta, 1 h, 60%.

Esquema 1

Los compuestos obtenidos **1a**-**d** se ensayaron como agonistas del receptor LPA_1, empleando para ello un ensayo de movilización de calcio en una línea celular que sobreexpresa dicho receptor.

*5.3.2 Determinación de la actividad agonista de los compuestos **1a**-**d** por el receptor LPA_1*

La capacidad para activar el receptor LPA_1 se determinó mediante experimentos de movilización de calcio en células RH7777 transfectadas de forma estable con este receptor, puesto que tanto el LPA como los ligandos agonistas producen un aumento en los niveles de calcio intracelular, y esta variación puede ser cuantificada mediante el empleo de sondas fluorescentes. Tras diversas optimizaciones experimentales, finalmente se seleccionó la sonda Fluo-4NW para monitorizar la concentración intracelular de calcio. Para ello, las

células se incubaron en presencia de dicha sonda y de los compuestos objeto de estudio y se midió la intensidad de fluorescencia (longitud de onda de excitación de 494 nm y de emisión de 516 nm). Como control positivo se empleó ionomicina 10 µM y como control negativo se realizó el experimento con células RH7777 no transfectadas con el receptor LPA_1.

Los compuestos se ensayaron a una dosis fija de 10 µM, expresándose la activación máxima del receptor (E_{max}) como porcentaje respecto a la respuesta inducida por el LPA a una concentración de 10 µM. La curva dosis-respuesta se determinó para aquellos compuestos con E_{max} mayor de 30%.

Este experimento permitió identificar al compuesto **1c** como agonista del receptor LPA_1, con un valor de activación máxima del receptor (E_{max}) del 33% y un valor de concentración efectiva 50 (EC_{50}) de 1.7 µM. Por tanto, con objeto de obtener los derivados del ácido malónico propuestos inicialmente y evitar el proceso de ciclación intramolecular, se sintetizaron los compuestos **1e**-**g**, siguiendo el procedimiento que se indica en el Esquema 2. De entre ellos, destaca el compuesto **1g** con EC_{50} = 6 µM.

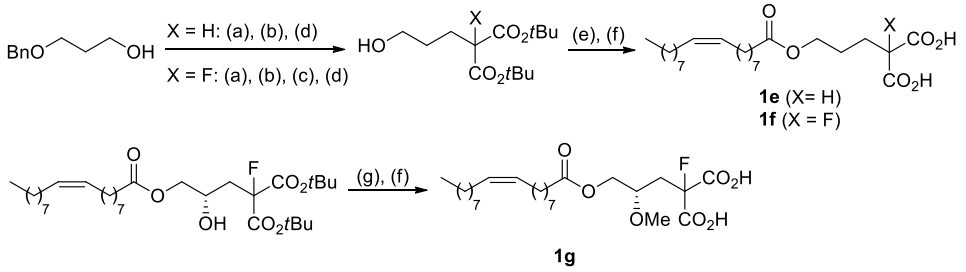

Reactivos y condiciones: (a) Cloruro de mesilo, trietilamina, DCM, 0ºC a ta, 1 h, 99%; (b) malonato de di-*terc*-butilo, NaH, NaI, DMF:THF, 0ºC a 80ºC, 17 h, 66%; (c) Selectfluor®, NaH, THF:DMF, 0ºC a ta, 48 h, 99%; (d) H_2, Pd(C) 10%, EtOH, 60ºC, 99%; (e) cloruro de oleoilo, 2,4,6-colidina, DCM, -78ºC a ta, 24 h, 59-70%; (f) TFA, DCM, ta, 16-17 h, 59-95%; (g) trimetilsilildiazometano, HBF_4, DCM, 0ºC, 90 min, 38%.

Esquema 2

En resumen, la modificación del grupo ácido del LPA ha permitido identificar dos agonistas del receptor LPA_1, **1c** (E_{max} = 33%; EC_{50} = 1.7 µM) y **1g** (E_{max} = 74%; EC_{50} = 6 µM), confirmando que es posible mimetizar el grupo fosfato presente en el ligando endógeno LPA con otras subunidades polares. Con objeto de seguir optimizando la estructura, se estudió a continuación la influencia de la cadena hidrofóbica.

*5.3.3 Diseño y síntesis de la serie **II***

Para la serie **II**, se estudió exhaustivamente la influencia de la subunidad hidrofóbica, incluyendo cambios en la longitud total de la cadena de ácido graso, así como la incorporación de anillos aromáticos, según se indica en la Figura 4.

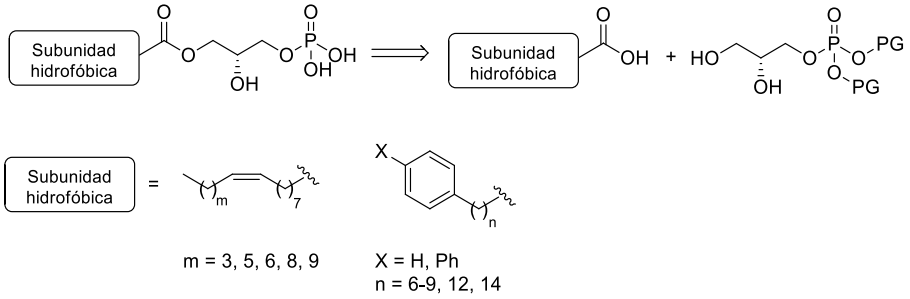

Figura 4. Diseño de los compuestos de la serie **II**.

5.3.3.1 Derivados de la serie **II** que contienen cadenas alifáticas

La modificación de la longitud total de la cadena hidrofóbica implicó la síntesis de los correspondientes ácidos alquinilcarboxílicos para su posterior semihidrogenación. El fragmento de glicerol fosforilado se sintetizó empleando el grupo *terc*-butilo como protector del grupo fosfato (Esquema 3).

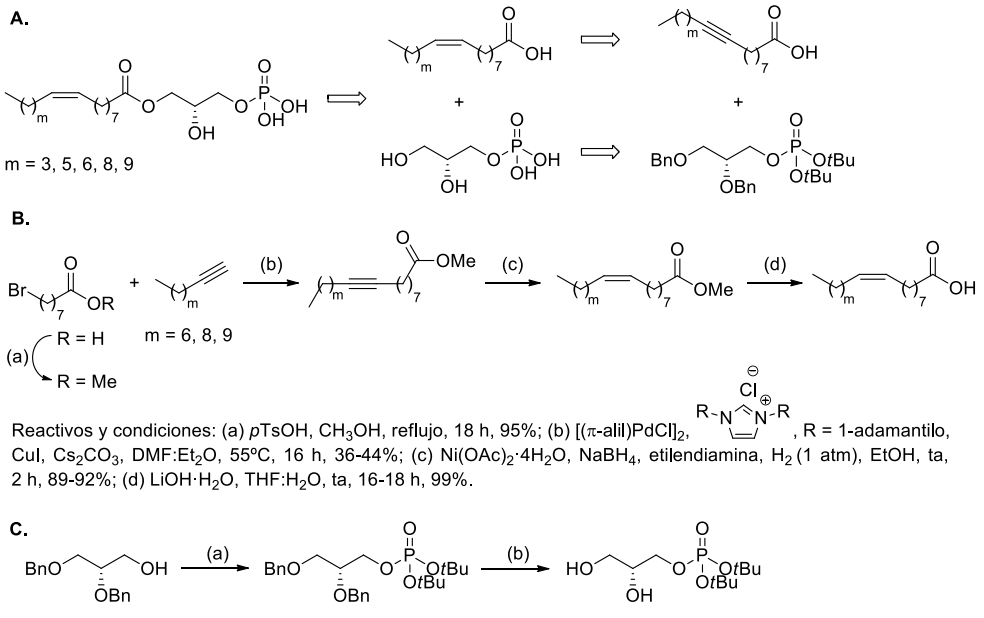

Esquema 3. (A) Esquema restrosintético. (B) Síntesis de las cadenas alifáticas. (C) Obtención del fragmento de glicerol fosforilado

Finalmente, los ácidos miristoleico (n = 3) y palmitoleico (n = 5) comerciales, así como los ácidos carboxílicos preparados previamente se esterificaron con el fragmento de glicerol, seguido de la desprotección del grupo fosfato por tratamiento con TFA, para obtener los productos finales **2a**-**e** (Esquema 4). Una vez sintetizados, se determinó la actividad agonista de los nuevos compuestos en el receptor LPA_1 (Tabla 1).

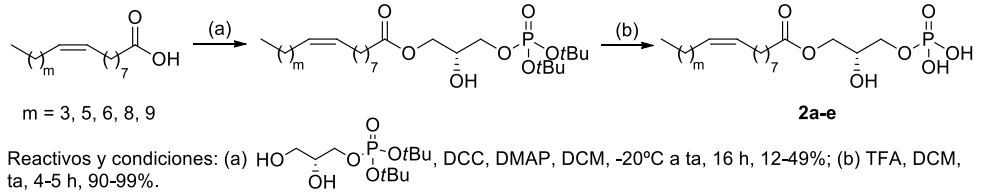

Esquema 4

Tabla 1. Actividad agonista de los compuestos **2a-e** en el receptor LPA_1

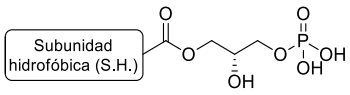

Compuesto	S. H. = 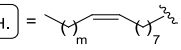	E_{max} (%)[a]	EC_{50} (μM)[b]
2a	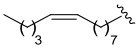	127± 1	2.8 ± 0.1
2b	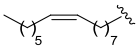	205 ± 9	0.45 ± 0.01
2c	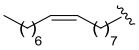	202 ± 1	2.1 ± 0.3
2d	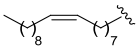	88 ± 2	3.63 ± 0.2
2e	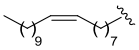	N.E.[c]	-
LPA	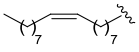	100	0.83 ± 0.02

[a]E_{max} = eficacia máxima del compuesto/eficacia máxima del LPA, expresado como porcentaje. [b]Para E_{max} > 30%, los valores de EC_{50} corresponden al valor medio ± E.E. obtenido en un mínimo de dos experimentos independientes realizados por triplicado. [c]No se observa efecto a la máxima concentración ensayada (10 μM).

La Tabla 1 muestra la gran influencia que ejerce la longitud de la cadena hidrofóbica en la actividad, con cambios apreciables incluso en variaciones de una única unidad metilénica. De estos datos se desprende que la cadena óptima es la correspondiente al ácido (9*Z*)-hexadec-9-enoico, presente en el derivado **2b** (E_{max} = 205%; EC_{50} = 0.45 μM), que es el compuesto más potente de la serie y con mejores valores de actividad que el propio LPA (E_{max} = 100%; EC_{50} = 0.83 μM).

5.3.3.2 Derivados de la serie **II** que contienen anillos aromáticos

La síntesis de estos derivados implicó la preparación de los ácidos carboxílicos no comerciales, así como la síntesis del fragmento de glicerol, empleando en este caso el grupo etilo como protector del grupo fosfato.

A.

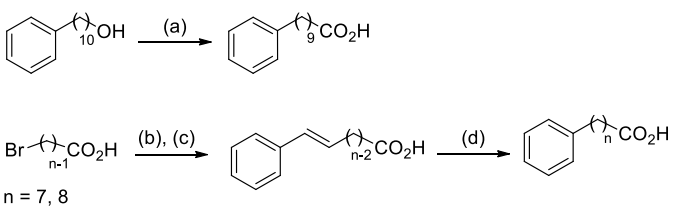

Reactivos y condiciones: (a) PDC, DMF, ta, 16 h, 52%; (b) PPh_3, tolueno, reflujo, 24 h, 99%; (c) benzaldehído, bis(trimetilsilil)amiduro de litio, THF, -20ºC a ta, 18 h, 61-70%; (d) H_2, Pd(C) 10%, EtOH, ta, 81-97%.

B.

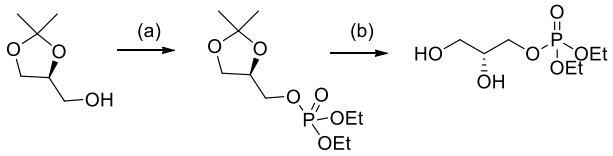

Reactivos y condiciones: (a) $ClP(O)(OEt)_2$, KO*t*Bu, DCM, ta, 48 h, 92%; (b) PS-*p*TsOH, CH_3OH, ta, 16 h, 50%.

Esquema 5. (A) Síntesis de los ácidos carboxílicos no comerciales. (B) Síntesis del fragmento de glicerol fosforilado.

Con el objeto de acceder a los productos finales diseñados, en primer lugar se llevó a cabo la reacción de esterificación entre el ácido 10-fenilcarboxílico y el glicerol fosforilado, obteniéndose el éster correspondiente. La desprotección del grupo fosfato de dicho éster se realizó empleando bromuro de trimetilsililo, lo que condujo al producto final bromado **3a** en lugar de al derivado deseado (Esquema 6). La formación de este derivado bromado a partir del correspondiente fosfato de dietilo se puede explicar considerando una migración de la cadena acilo al grupo hidroxilo secundario y la posterior sustitución nucleófila del grupo hidroxilo primario por bromuro.

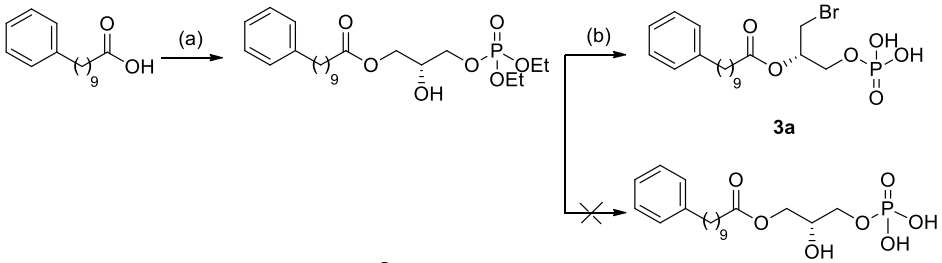

Reactivos y condiciones: (a) 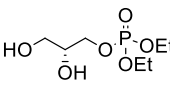 , DCC, DMAP, -20ºC a ta, 18 h, 30%; (b) TMSBr, DCM, ta, 4 h, 90%.

Esquema 6

A pesar de que se ensayaron distintas condiciones de reacción para la desprotección del fosfato de dietilo, en ningún caso fue posible aislar el producto deseado, por lo cual se modificó la ruta sintética prevista, empleándose en este caso el grupo bencilo como protector del grupo fosfato para la síntesis de los productos finales **2f**-**j** (Esquema 7).

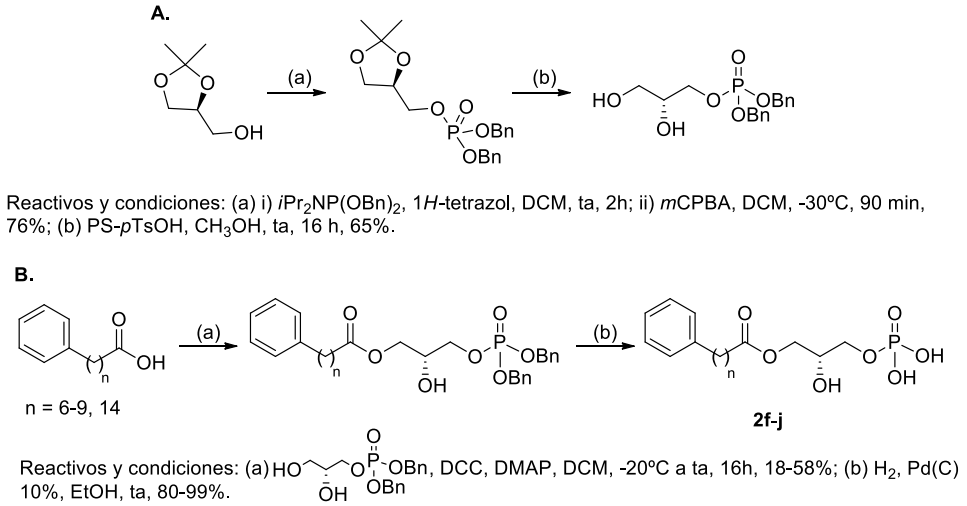

Reactivos y condiciones: (a) i) iPr$_2$NP(OBn)$_2$, 1*H*-tetrazol, DCM, ta, 2h; ii) *m*CPBA, DCM, -30ºC, 90 min, 76%; (b) PS-*p*TsOH, CH_3OH, ta, 16 h, 65%.

Reactivos y condiciones: (a) HO-(OH)-O-P(=O)(OBn)-OBn, DCC, DMAP, DCM, -20ºC a ta, 16h, 18-58%; (b) H_2, Pd(C) 10%, EtOH, ta, 80-99%.

Esquema 7

En el caso de los compuestos **2k**-**m**, que presentan un resto de bifenilo en su estructura, su obtención se detalla en el Esquema 8, siguiendo un planteamiento análogo al de los derivados de fenilo.

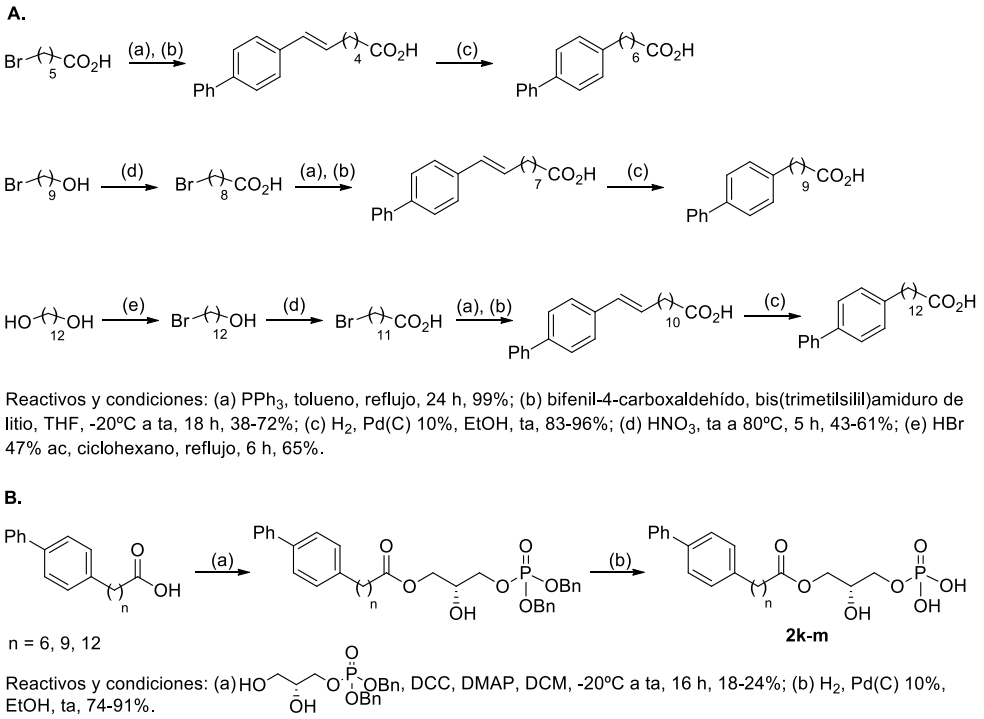

Esquema 8

Los nuevos compuestos **2f**-**m** y **3a** fueron ensayados como agonistas del receptor LPA_1. Los datos obtenidos sugieren de nuevo una estrecha relación entre actividad y longitud de la cadena (Tabla 2). En este caso, de entre todos los compuestos analizados, destacan los derivados **2i** y **3a**, que presentan nueve unidades metilénicas en su cadena, con E_{max} > 100% y valores de EC_{50} de 0.5 y 0.24 µM, respectivamente.

Tabla 2. Actividad agonista de los compuestos **2f-m** y **3a** en el receptor LPA_1

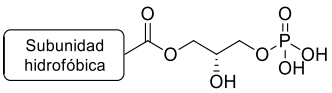

Compuesto	Subunidad hidrofóbica	E_{max} (%)[a]	EC_{50} (μM)[b]
2f	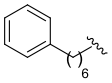	N. E.[c]	-
2g	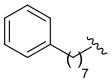	N. E.	-
2h	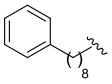	74 ± 4	2.1 ± 0.3
2i	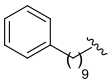	112 ± 3	0.5 ± 0.1
2j	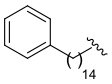	N. E.	-
2k	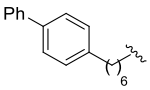	N. E.	-
2l	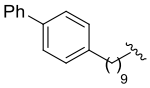	127 ± 9	3.3 ± 0.6
2m	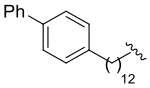	37 ± 1	19 ± 2
3a	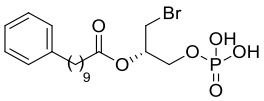	118 ± 24	0.24 ± 0.09
LPA	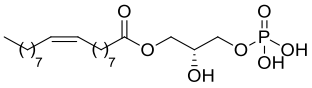	100	0.83 ± 0.02

[a]E_{max} = eficacia máxima del compuesto/eficacia máxima del LPA, expresado como porcentaje. [b]Para E_{max} > 30%, los valores de EC_{50} corresponden al valor medio ± E.E. obtenido en un mínimo de dos experimentos independientes realizados por triplicado. [c]No se observa efecto a la máxima concentración ensayada (10 μM).

5.3.3.3 Análogos de **3a**

Considerando la excelente actividad mostrada por el derivado **3a** (E_{max} = 118%, EC_{50} = 0.24 µM) se decidió extender el estudio de esta estructura, analizando tanto cambios en la longitud de la cadena alifática, como la introducción de la cadena de ácido oleico. Así, se sintetizaron los compuestos **3b-d** (Esquema 9)

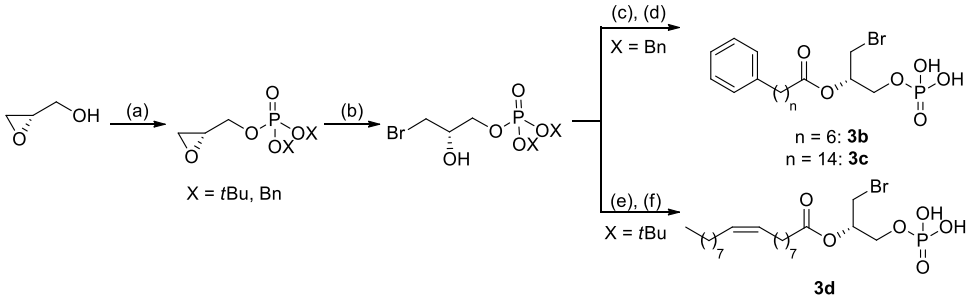

Reactivos y condiciones: (a) iPr$_2$NP(OX)$_2$, 1*H*-tetrazol, DCM, ta, 2 h; ii) *m*CPBA, DCM, -30ºC, 90 min, 52-76%; (b) TBABr, TFA, $CHCl_3$, ta, 10 min, 89-95%; (c) Ph(CH$_2$)$_n$COOH (n = 6, 14), DCC, DMAP, DCM, ta, 16-18 h, 50-64%; (d) H_2, Pd/C 10%, EtOH, ta, 85-86%; (e) cloruro de oleoilo, piridina, ta, 18 h, 15%; (f) TFA, DCM, ta, 5 h, 81%.

Esquema 9

De entre los compuestos sintetizados, únicamente el derivado **3d** presentó actividad agonista frente al receptor LPA_1 (E_{max} = 39%; EC_{50} = 3.2 µM)

5.3.4 Combinación de las subunidades ácidas e hidrofóbicas

La combinación de los fragmentos presentes en los compuestos que resultaron más activos en el receptor LPA_1 (**1c**, **1g**, **2b**, **2i**, **2l**, **3a** y **3d**, Figura 5A) sirvió como punto de partida para el comienzo del proceso de combinación (Figura 5B). Los derivados **4a**-**c** fueron sintetizados como se indica en los Esquemas 10-12 y evaluados como agonistas del receptor LPA_1. Únicamente el compuesto **4c** fue capaz de activar el receptor LPA_1 (E_{max} = 43 %, EC_{50} = 1.4 µM).

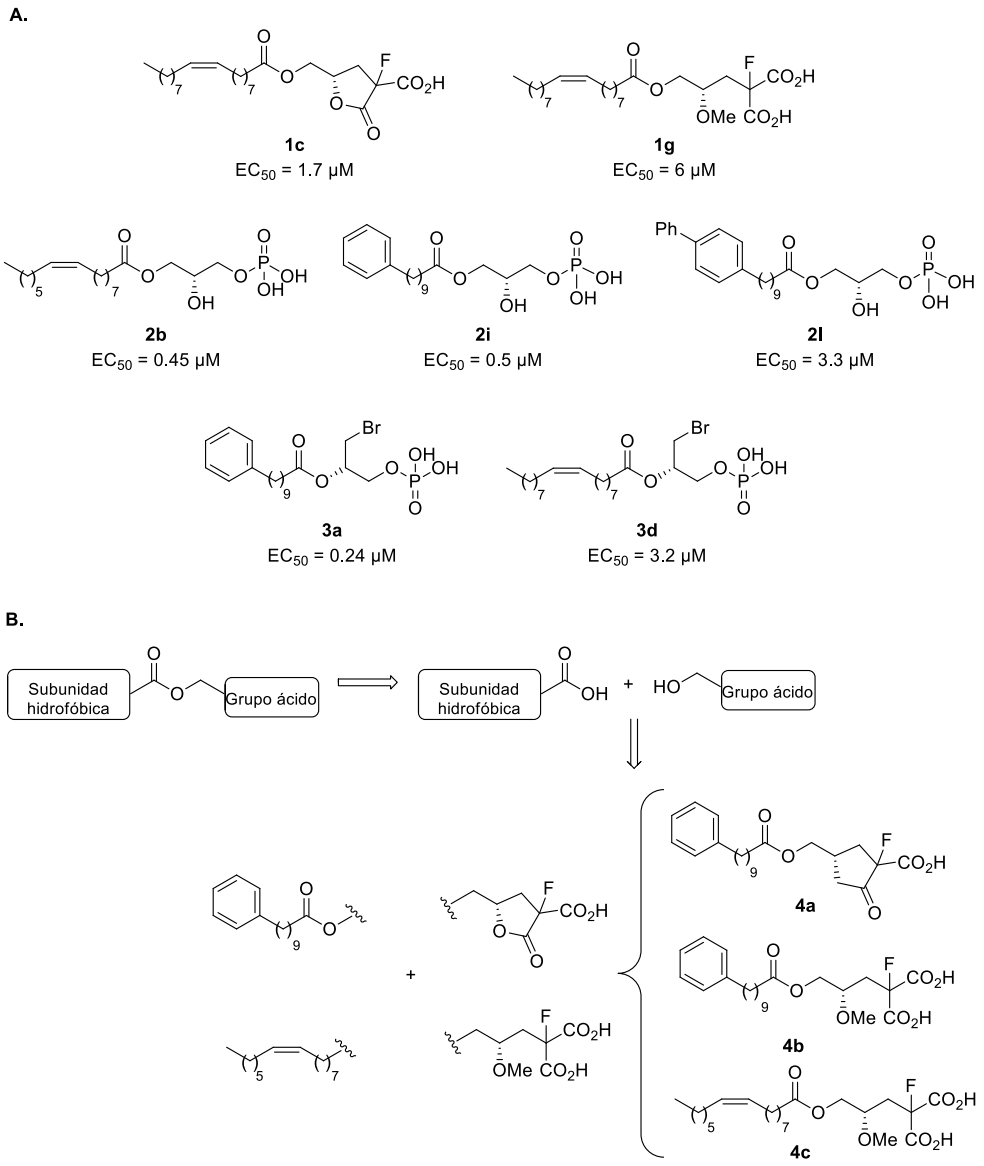

Figura 5. (A) Estructura de los compuestos **1c**, **1g**, **2b**, **2i**, **2l**, **3a** y **3d**. (B) Diseño de nuevos compuestos mediante combinación de las subunidades hidrofóbicas y los grupos ácidos óptimos.

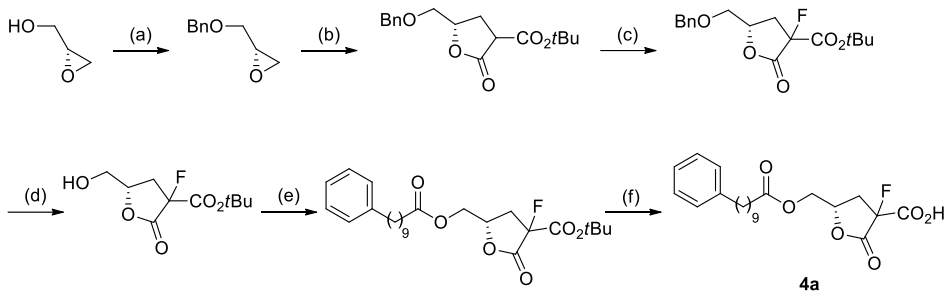

Reactivos y condiciones: (a) BnBr, NaH, DMF, 0ºC a ta, 18 h, 99%; (b) malonato de di-*terc*-butilo, NaH, DMF:THF, 0ºC a 80ºC, 6 h, 62%; (c) Selectfluor®, NaH, DMF:THF, 0ºC a ta, 48 h, 99%; (d) H_2, Pd(C) 10%, 60ºC, 99%; (e) $Ph(CH_2)_9COOH$, DCC, DMAP, ta, 18 h, 35%; (f) TFA, DCM, ta, 17 h, 90%.

Esquema 10

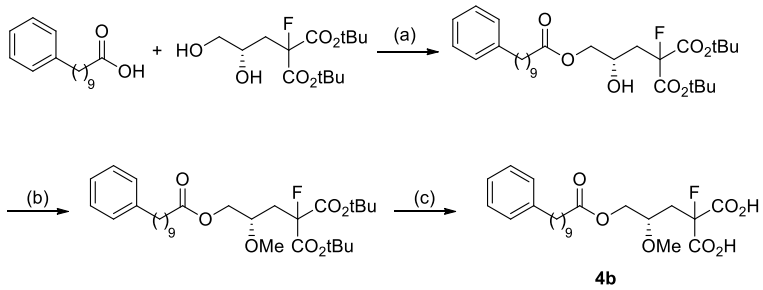

Reactivos y condiciones: (a) DCC, DMAP, DCM, -20ºC a ta, 17 h, 75%; (b) trimetilsilildiazometano, HBF_4, DCM, 0ºC, 90 min, 30%; (c) TFA, DCM, ta, 18 h, 68%.

Esquema 11

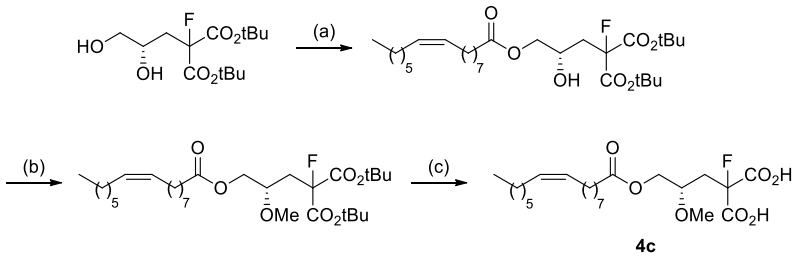

Reactivos y condiciones: (a) Ácido palmitoleico, DCC, DMAP, DCM, -20ºC a ta, 18h, 44%; (b) trimetilsilildiazometano, HBF_4, DCM, 0ºC, 90 min, 27%; (c) TFA, DCM, ta, 19 h, 93%.

Esquema 12

En resumen, en este trabajo de investigación se han identificado nuevos agonistas con actividad en el receptor LPA_1. A partir de las dos series propuestas

para mimetizar el grupo fosfato (serie **I**) y la cadena hidrofóbica (serie **II**) del ligando endógeno LPA se han identificado nuevos esqueletos capaces de activar el receptor. Estos resultados han permitido comenzar con el proceso *hit to lead*, el cual se encuentra actualmente en curso en nuestro grupo de investigación.

De entre todos los compuestos obtenidos hasta el momento, el derivado **3a** destaca como el primer agonista estructuralmente diferente al ligando LPA, con excelentes valores de actividad, por lo que fue seleccionado para una caracterización biológica más profunda.

5.3.5 Determinación de la actividad antagonista en el receptor LPA_1

La necesidad de antagonistas para el estudio del receptor LPA_1 en diversos procesos biológicos y patológicos es clara. Dado que pequeños cambios estructurales provocan cambios de actividad entre agonistas y antagonistas, todos los compuestos que resultaron inactivos como agonistas en el receptor LPA_1 fueron evaluados como antagonistas en dicho receptor.

Para ello, células RH7777 transfectadas de forma estable con el receptor LPA_1 se incubaron en presencia de la sonda Fluo 4-NW y de los compuestos objeto de estudio a una dosis fija de 10 µM. A continuación se añadió LPA 10 µM y la capacidad antagonista se determinó como la disminución en la intensidad de fluorescencia en la señal del LPA. Ninguno de los compuestos analizados presentó una actividad antagonista significativa.

5.3.6 Selectividad sobre otros receptores

Con objeto de determinar la selectividad de los compuestos sintetizados a lo largo de la presente Tesis Doctoral por los diferentes subtipos de los receptores de LPA (LPA_{1-5}) se generaron cinco líneas celulares que sobreexpresan de forma estable uno de los cinco subtipos de receptores de LPA (LPA_{1-5}) mediante transfección de células B103 con el plásmido correspondiente que contiene el receptor de interés LPA_{1-5} fusionado a la proteína verde fluorescente (*enhanced green fluorescent protein*, EGFP). Las células con mayor expresión de EGFP fueron seleccionadas mediante citometría de flujo. Este trabajo se llevó a cabo durante una estancia predoctoral en el laboratorio del Prof. Jerold Chun, en *The Scripps Research Institute* (La Jolla, California).

Hasta este momento, se ha completado el análisis de la actividad de todos los compuestos sintetizados en el receptor LPA_2. De entre los derivados analizados, siete compuestos presentaron actividad por este receptor. La Tabla 3 resume los

compuestos activos identificados hasta el momento. Cabe destacar que el compuesto **3a** no presenta actividad por el receptor LPA_2.

Tabla 3. Actividad agonista de los compuestos en los receptores LPA_1 y LPA_2

		LPA_1		**LPA_2**	
	Compuesto	**E_{max} (%)**[a]	**EC_{50} (μM)**[b]	**E_{max} (%)**	**EC_{50} (μM)**
1c	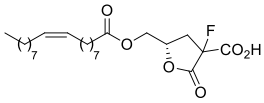	33 ± 5	1.7 ± 0.2	N. E.[c]	-
1g	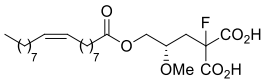	74 ± 14	6 ± 1	N. E.	-
2a	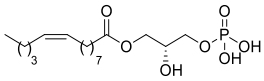	127 ± 1	2.8 ± 0.1	42 ± 5	8.1 ± 0.8
2b	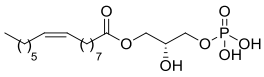	205 ± 9	0.45 ± 0.01	N. E.	-
2c	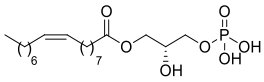	202 ± 1	2.1 ± 0.3	N. E.	-
2d	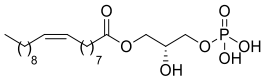	88 ± 2	3.6 ± 0.2	N. E.	-
2h	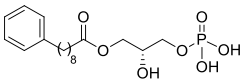	74 ± 4	2.1 ± 0.3	59 ± 2	12 ± 2
2i	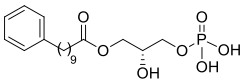	112 ± 3	0.5 ± 0.1	74 ± 6	5.3 ± 0.6

Tabla 3 (cont.). Actividad agonista de los compuestos en los receptores LPA_1 y LPA_2

		LPA_1		LPA_2	
	Compuesto	**E_{max} (%)[a]**	**EC_{50} (μM)[b]**	**E_{max} (%)[a]**	**EC_{50} (μM)[b]**
2l	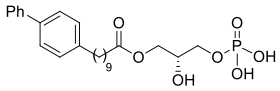	127 ± 9	3.3 ± 0.6	N. E.	-
2m	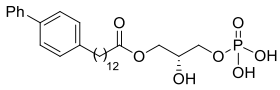	37 ± 1	19 ± 2	N. E.	-
3a	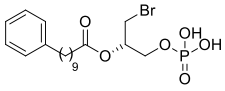	118 ± 24	0.24 ± 0.09	N. E.	-
3c	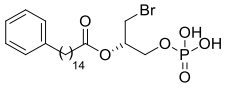	N. E.	-	57 ± 7	5 ± 1
3d	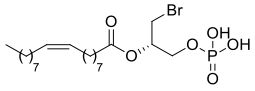	39 ± 3	3.2 ± 0.4	67 ± 8	4.9 ± 0.2
4b	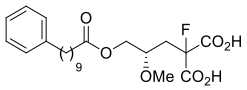	N. E.	-	55 ± 10	4.8 ± 0.1
4c	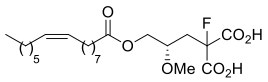	43 ± 6	1.4 ± 0.4	81 ± 1	10.8 ± 0.8

[a]E_{max} = eficacia máxima del compuesto/eficacia máxima del LPA, expresado como porcentaje. [b]Para E_{max} > 30%, los valores de EC_{50} corresponden al valor medio ± E.E. obtenido en un mínimo de dos experimentos independientes realizados por triplicado. [c]No se observa efecto a la máxima concentración ensayada (10 μM).

*5.3.7 Caracterización in vitro del compuesto **3a***

La activación del receptor LPA_1 a través de proteínas G provoca diversas respuestas celulares tales como cambios en la morfología de la célula, que en el caso de las células neuronales B103 consisten en la pérdida de las prolongaciones que exhiben en condiciones normales para adquirir una morfología esférica.[17] Otras de las respuestas estudiadas fueron la migración

celular[106] y la internalización del receptor tras su estimulación. De entre los compuestos ensayados, el compuesto **3a** presenta un comportamiento comparable al del ligando endógeno LPA en los ensayos de internalización, migración y redondeamiento celular. El compuesto **1c** se ensayó también con fines comparativos. Las Figuras 6, 7 y 8 muestran algunos ejemplos representativos.

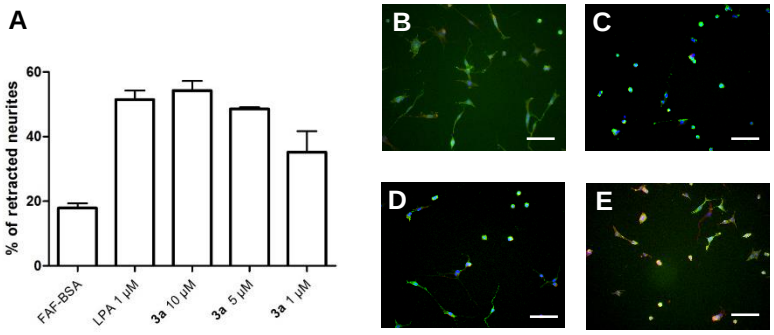

Figura 6. Redondeamiento celular ejercido por el compuesto **3a**. Porcentaje de células redondeadas (A). Imágenes representativas obtenidas tras el tratamiento con FAF BSA 0.1% (B), LPA 1 µM (C), **3a** 10 µM (D), **3a** 1 µM (E). Escala: 100 µm.

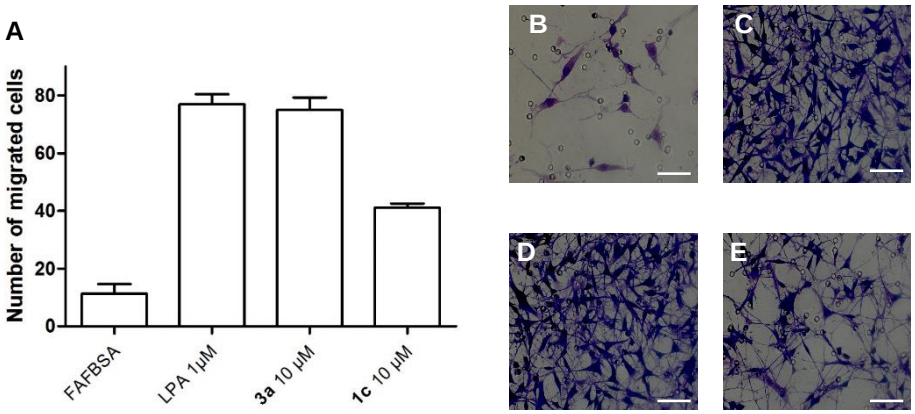

Figura 7. Experimento de migración celular para los compuestos **3a** y **1c** a 10 µM. Cuantificación de la migración celular (A). Imágenes representativas obtenidas tras el tratamiento con FAF BSA 0.1% (B), LPA 1 µM (C), **3a** 10 µM (D), **1c** 10 µM (E). Escala: 50 µm.

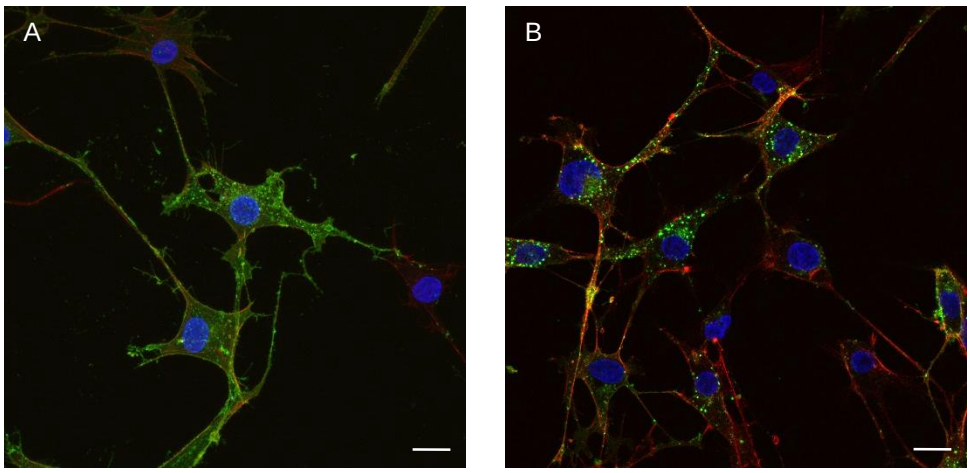

Figura 8. Internalización del receptor LPA_1 tras el tratamiento con **3a** 1 µM (A) o LPA 1 µM (B). Las células se tiñeron con DAPI y faloidina para observar su morfología y se visualizaron con un microscopio confocal Zeiss (escala 10 µm).

5.4 Conclusiones

En el presente trabajo de investigación se han identificado nuevos agonistas con actividad en el receptor LPA_1. A partir de las dos series propuestas para mimetizar el grupo ácido y la cadena hidrofóbica del ligando endógeno LPA se han obtenido nuevos esqueletos capaces de activar el receptor. En cuanto a la combinación de subestructuras, la identificación del compuesto **4c**, con buenos valores de actividad, es un punto de partida para continuar con el proceso de optimización.

De entre todos los compuestos sintetizados, el derivado **3a** destaca como el primer agonista estructuralmente diferente del ligando endógeno con una excelente capacidad para activar el receptor en sistemas celulares.

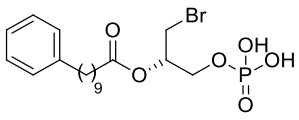

3a
EC_{50} = 0.24 µM

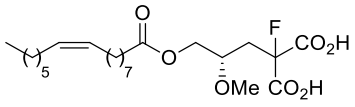

4c
EC_{50} = 1.4 µM

SUMMARY

6. SUMMARY

6.1 Background and aims

Lysophospholipids are lipid molecules that are receiving growing attention because, in addition to their structural function in the cell membrane, they are now regarded as important regulators for diverse biological functions through activation of specific receptors.[4] These receptors have been characterized during the last two decades as G protein-coupled receptors (GPCRs) and, among them, two families stand out: lysophosphatidic acid (LPA_{1-6}) and sphingosine 1-phoshate ($S1P_{1-5}$) receptors. Despite their interest, the high structural similarity between them has restrained the development of selective and high affinity ligands and therefore the elucidation of the role of these receptors in the central nervous system (CNS). This work will focus on the LPA receptors and, in particular, on the LPA_1 subtype, considering its prominent expression in the CNS[34] and the lack of potent and selective agonists and antagonists that allow for the elucidation of its (patho)physiological roles.

6.2 Results and discussion

6.2.1 Synthesis of new ligands for the LPA_1 receptor

At the moment of starting this project, little information about this novel signalling system was available. No receptor 3D structures had been elucidated and, although several structure-activity relationship (SAR) studies had been carried out,[40] no potent ligands for the LPA_1 receptor had been described, especially in the agonist field. In this context, we focused our efforts on finding molecular entities with activity at this receptor, using as starting point the structure of the endogenous ligand, LPA. Initially, two series of compounds were designed: series **I**, which comprised changes in the acid group, and series **II**, which included modifications in the hydrophobic unit.

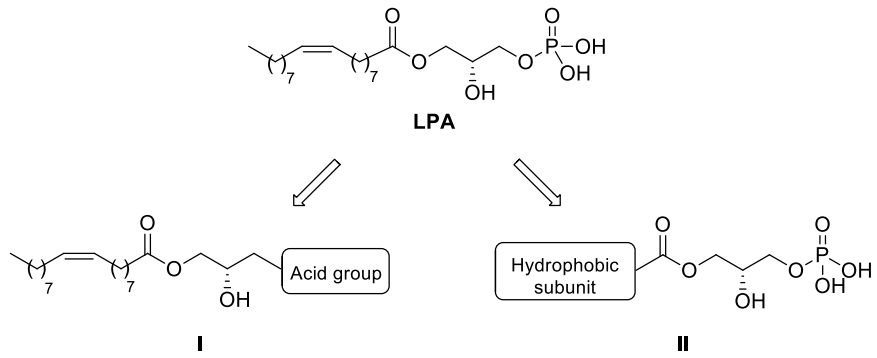

Figure 31. Design of new LPA_1 ligands.

It has been shown that changes in the polar head of LPA are poorly tolerated which is confirmed by the few potent agonists described for this receptor despite the variety of phosphate replacements tried. Thus, phosphorous-free isosters, specifically carboxylic and boronic acids were chosen as acidic replacements.[96] Compounds belonging to series **I** were synthesized according to Scheme 1. It must be noted that the reaction conditions employed for the obtention of these derivatives led to the formation of lactones **1b** and **1c** instead of the expected malonic acids.

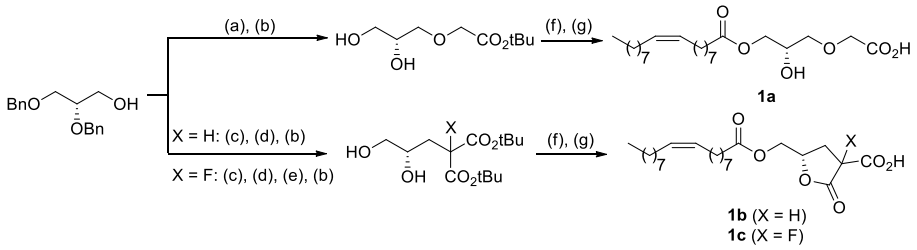

Reagents and conditions: (a) *tert*-Butyl bromoacetate, NaH, TBAI, THF, 0ºC to 50ºC, 16 h, 22%; (b) H_2, 10% Pd(C), EtOH, 60ºC, 89-95%; (c) mesyl chloride, triethylamine, DCM, 0ºC to rt, 1 h, 80%; (d) di-*tert*-butyl malonate, NaH, NaI, DMF:THF, 0ºC to 80ºC, 17 h, 76%; (e) Selectfluor®, NaH, THF:DMF, 0ºC to rt, 48 h, 48%; (f) oleoyl chloride, 2,4,6-collidine, DCM, -78ºC to rt, 24 h, 36-99%; (g) TFA, DCM, rt, 17-18 h, 52-99%.

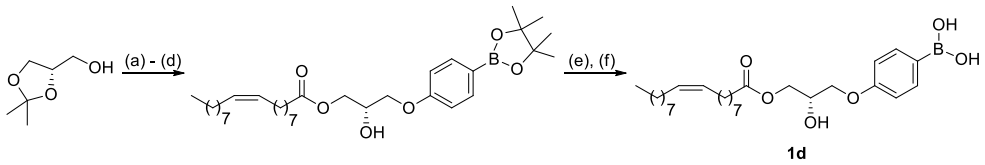

Reagents and conditions: (a) Tosyl chloride, pyridine, DCM, 0ºC to rt, 16 h, 86%; (b) 4-hydroxyphenylboronic acid pinacol ester, Cs_2CO_3, DMF, 90ºC, 16 h, 84%; (c) PS-*p*TsOH, CH_3OH, rt, 18 h, 88%; (d) oleoyl chloride, 2,4,6-collidine, DCM, -78ºC to rt, 24 h, 40%; (e) KHF_2, CH_3OH:H_2O, rt, 30 min; 99%; (f) TMSCl, CH_3CN:H_2O, rt, 1 h, 60%.

Scheme 1

In order to determine the agonist capacity of the synthesized compounds, calcium mobilization assays in RH7777 cells stably transfected with LPA_1R were carried out. Activation of LPA_1R induces a transient increase in the intracellular Ca^{2+} levels which was detected by fluorescence. Parallel experiments using vector-transfected cells were carried out in order to rule out non-LPA_1R mediated effects.

From this initial set of compounds only compound **1c** activated the receptor, with an E_{max} of 33% and an EC_{50} value of 1.7 µM. Accordingly, it was necessary to confirm if the non-cyclic malonic derivatives originally proposed, with two free carboxylic acids, would exhibit better activities at LPA_1 receptor. In order to avoid cyclization, compounds **1e**-**g** were prepared (Scheme 2). Among them, compound **1g** stands out, with an EC_{50} value of 6 µM.

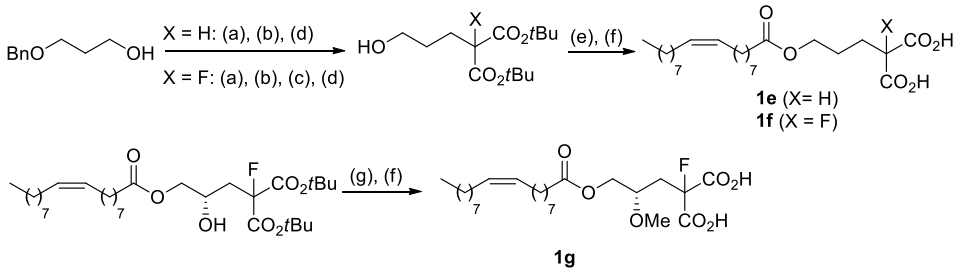

Reagents and conditions: (a) Mesyl chloride, triethylamine, DCM, 0ºC to rt, 1 h, 99%; (b) di-*tert* butyl malonate, NaH, NaI, DMF:THF, 0ºC to 80ºC, 17 h, 66%; (c) Selectfluor®, NaH, THF:DMF, 0ºC to rt, 48 h, 99%; (d) H_2, 10% Pd(C), EtOH, 60ºC, 99%; (e) oleoyl chloride, 2,4,6-collidine, DCM, -78ºC to rt, 24 h, 59-70%; (f) TFA, DCM, rt, 16-17 h, 59-95%; (g) trimethylsilyldiazomethane, HBF_4, DCM, 0ºC, 90 min, 38%.

Scheme 2

Regarding series **II**, several studies show that modifications on this part of the molecule are less critical for activity at LPA_1 receptor, probably because its flexible disposition facilitates its fitting into the LPA_1 receptor pocket. Thus, a comprehensive study of the influence of the hydrophobic moeity was carried out, including modifications on the overall length of the fatty acid chain as well as the incorporation of aromatic rings (Scheme 3).

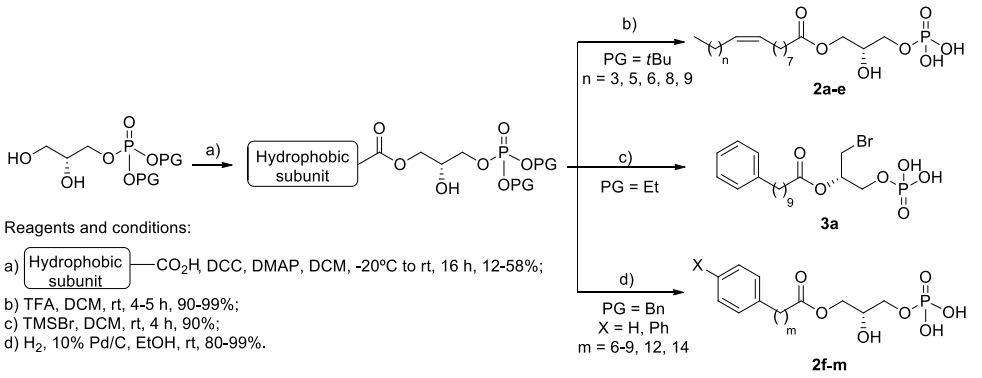

Scheme 3

Compounds **2a**-**m** and the unexpectedly obtained **3a** were tested for their agonist activity at the LPA_1 receptor. The most remarkable conclusion that can be drawn from the obtained data is the great influence on activity exerted by the length of the hydrophobic chain. From all the compounds tested, derivatives **2i** (X = H, m = 9) and **3a**, with E_{max} > 100% and EC_{50} values of 0.5 and 0.24 µM respectively, stand out. Considering the excellent activity of compound **3a**, additional structural exploration was extended around this scaffold (Scheme 4). The obtained results showed that only **3d** was able to activate the receptor (E_{max} = 39%, EC_{50} = 3.2 µM), although it did not reach neither LPA nor **3a** values.

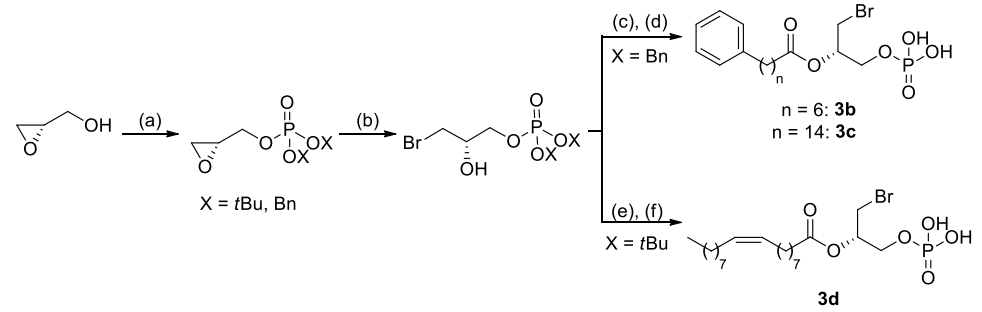

Reagents and conditions: (a) i) $iPr_2NP(OX)_2$, 1*H*-tetrazole, DCM, rt, 2 h; ii) *m*CPBA, -30ºC, 90 min, 52-76%; (b) TBABr, TFA, $CHCl_3$, rt, 10 min, 89-95%; (c) $Ph(CH_2)_nCOOH$ (n = 6, 14), DCC, DMAP, DCM, rt, 16-18 h 50-64%; (d) H_2, 10% Pd(C), EtOH, rt, 85-86%; (e) oleoyl chloride, pyridine, rt, 18 h, 15%; (f) TFA, DCM, rt, 5 h, 81%.

Scheme 4

The next step was the combination of some of the hydrophobic moieties present in these compounds with the polar heads that seem to be able to mimic the LPA phosphate group, leading to products **4a**-**c** (Figure 2) which were synthesized and tested as agonists of the LPA_1 receptor.

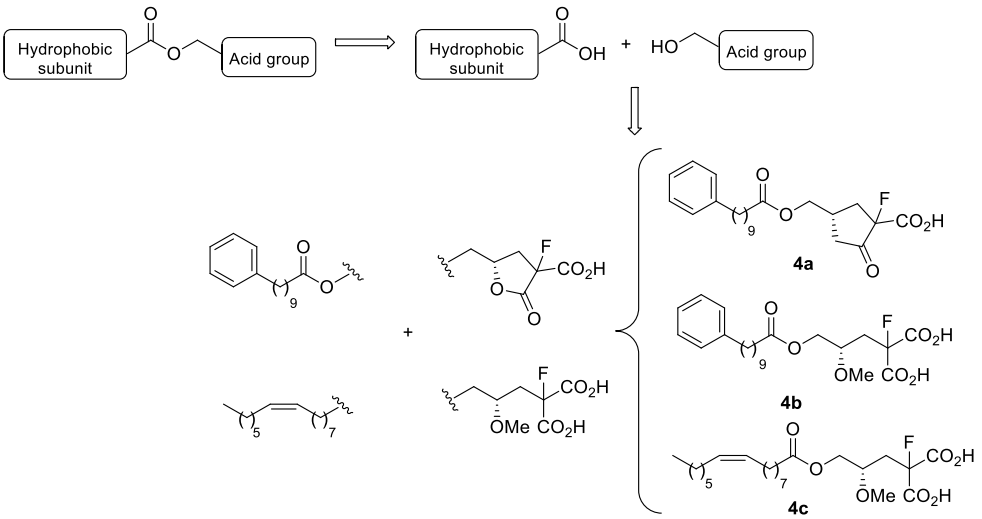

Figure 2

The results obtained for compounds **4a**, **b** showed that replacement of the oleic acid chain by 10-phenyldecanoic acid is detrimental for activity. Instead, derivative **4c**, bearing a palmitoleic acid chain and malonic acid as polar head was able to activate LPA_1 receptor (E_{max} = 43%, EC_{50} = 1.4 µM).

6.2.2 Additional biological characterization

All the synthesized compounds which were inactive as agonists at the LPA_1 receptor were screened for their antagonist capacity but none of the compounds tested presented significant antagonist activity.

In order to test the selectivity of all the synthesized compounds, cell lines stably overexpressing each of the five LPA receptor subtypes were generated during a predoctoral stay at Prof. Jerold Chun Lab, at The Scripps Research Institute (La Jolla, California). Up to this moment, the screening of all the synthesized compounds at the LPA_2 receptor has been completed, being the characterization at the rest of the receptors currently under way in our laboratory. From the results obtained for this receptor, it must be highlighted that compound **3a** does not present activity at LPA_2 receptor.

Finally, to verify whether compound **3a**, which has been identified as a good LPA_1 agonist by calcium mobilization assay, and which is selective over LPA_2 receptor, is really acting at the LPA_1 receptor, a set of additional cellular experiments was carried out. The existence of a correlation between the results

from these independent *in vitro* data is the first and necessary step towards a complete biological characterization that would continue with diverse *in vivo* studies in the drug discovery process. As expected for an agonist, compound **3a** induces neurite retraction,[17] cellular migration[106] and internalization of the LPA_1 receptor (Figures 3-5) in B103 cells stably transfected with LPA_1.

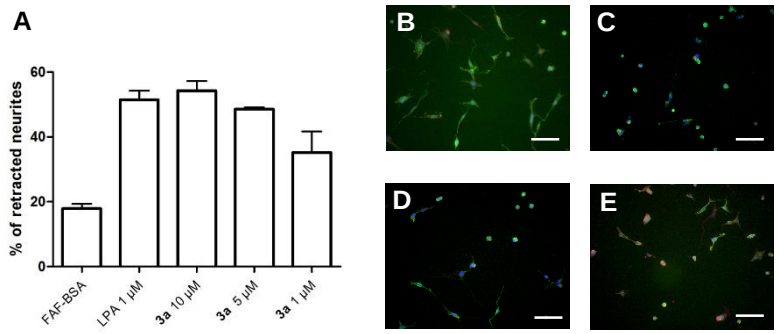

Figure 3. Neurite retraction induced by **3a** and **1c**. Percentage of retracted neurites at 10, 5 or 1 µM for compound **3a** (A). Visualization of neurite retraction: control 0.1% FAF BSA (B), 1 µM LPA (C), 10 µM **3a** (D), **3a** 1 µM (E). Samples were imaged under the same conditions by using a Zeiss fluorescence microscope (bars 100 µm).

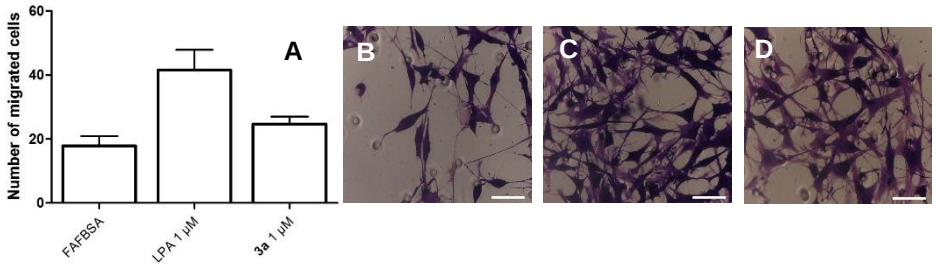

Figure 4. Migration experiment for compound **3a** at 1 µM. Number of migrated cells (A). Visualization of migrated cells (B-D): 0.1% FAF BSA (B), 1 µM LPA (C), 1 µM **3a** (D). Samples were imaged under the same conditions by using a Zeiss microscope (bars 50 µm). Cells were stained with 0.1% crystal violet solution.

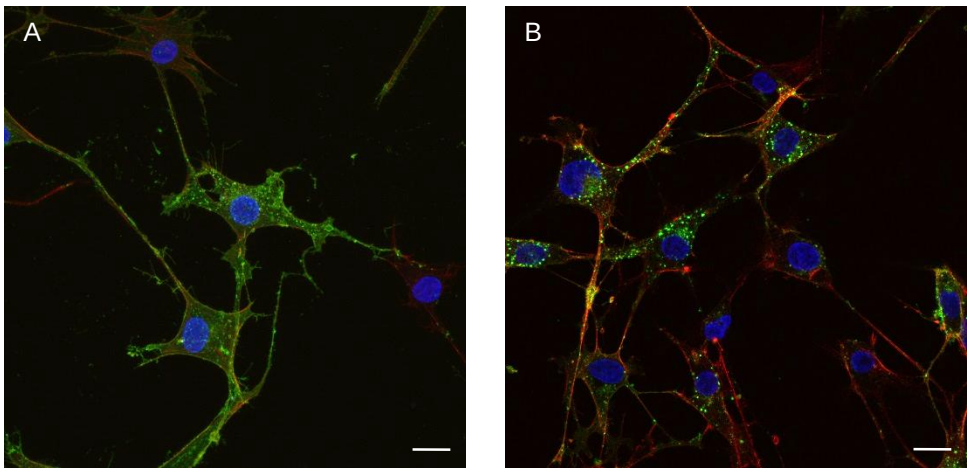

Figure 5. Visualization of receptor internalization. Compound **3a**, 1 µM (A). LPA, 1 µM (B). Cells were stained with DAPI and phalloydin for cell morphology. Samples were imaged under the same conditions by using a Zeiss fluorescence confocal microscope (bars 10 µm).

6.3 Conclusions

In summary, up to this moment we have successfully identified novel agonists with activity at LPA_1 receptor. The two series proposed for mimicking the polar head and the hydrophobic chain of the endogenous ligand LPA have yielded new scaffolds capable to activate the receptor. Regarding the combination of the optimal moieties, the identification of compound **4c**, with good activity values, paves the way for further optimization processes.

From all the compounds synthesized so far, derivative **3a** stands out as the first agonist structurally different from the endogenous ligand LPA, with excellent capacity to activate the LPA_1 receptor in cellular systems.

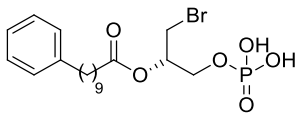

3a
EC_{50} = 0.24 µM

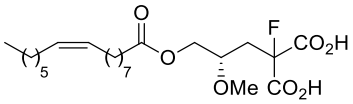

4c
EC_{50} = 1.4 µM

7. BIBLIOGRAPHY

1. Brown, H. A.; Marnett, L. J. Introduction to lipid biochemistry, metabolism, and signaling. *Chem. Rev.* **2011**, *111*, 5817-5820.

2. Musille, P. M.; Kohn, J. A.; Ortlund, E. A. Phospholipid - driven gene regulation. *FEBS Lett.* **2013**, *587*, 1238-1246.

3. Scott, S. A.; Mathews, T. P.; Ivanova, P. T.; Lindsley, C. W.; Brown, H. A. Chemical modulation of glycerolipid signaling and metabolic pathways. *Biochim. Biophys. Acta Mol. Cell Biol. Lipids* **2014**, *1841*, 1060-1084.

4. Mutoh, T.; Rivera, R.; Chun, J. Insights into the pharmacological relevance of lysophospholipid receptors. *Br. J. Pharmacol.* **2012**, *165*, 829-844.

5. Grzelczyk, A.; Gendaszewska-Darmach, E. Novel bioactive glycerol-based lysophospholipids: new data - new insight into their function. *Biochimie* **2013**, *95*, 667-679.

6. Vogt, W. Pharmacologically active acidic phospholipids and glycolipids. *Biochem. Pharmacol.* **1963**, *12*, 415-420.

7. van Corven, E. J.; Groenink, A.; Jalink, K.; Eichholtz, T.; Moolenaar, W. H. Lysophosphatidate-induced cell proliferation: identification and dissection of signaling pathways mediated by G proteins. *Cell* **1989**, *59*, 45-54.

8. Dyer, D.; Tigyi, G.; Miledi, R. The effect of active serum albumin on PC12 cells: I. Neurite retraction and activation of the phosphoinositide second messenger system. *Mol. Brain Res.* **1992**, *14*, 293-301.

9. Jalink, K.; Moolenaar, W. H. Thrombin receptor activation causes rapid neural cell rounding and neurite retraction independent of classic second messengers. *J. Cell Biol.* **1992**, *118*, 411-419.

10. Ridley, A. J.; Hall, A. The small GTP-binding protein rho regulates the assembly of focal adhesions and actin stress fibers in response to growth factors. *Cell* **1992**, *70*, 389-399.

11. Yamamura, S.; Yatomi, Y.; Ruan, F.; Sweeney, E. A.; Hakomori, S.; Igarashi, Y. Sphingosine 1-phosphate regulates melanoma cell motility through a receptor-coupled extracellular action and in a pertussis toxin-insensitive manner. *Biochemistry* **1997**, *36*, 10751-10759.

12. van der Bend, R. L.; Brunner, J.; Jalink, K.; van Corven, E. J.; Moolenaar, W. H.; van Blitterswijk, W. J. Identification of a putative membrane receptor for the bioactive phospholipid, lysophosphatidic acid. *EMBO J.* **1992**, *11*, 2495-2501.

13. Thomson, F. J.; Perkins, L.; Ahern, D.; Clark, M. Identification and characterization of a lysophosphatidic acid receptor. *Mol. Pharmacol.* **1994**, *45*, 718-723.

14. Hecht, J. H.; Weiner, J. A.; Chun, J. *Ventricular zone gene-1* (*vzg-1*) encodes a lysophosphatidic acid receptor expressed in neurogenic regions of the developing cerebral cortex. *J. Cell Biol.* **1996**, *83*, 1071-1083.

15. An, S.; Dickens, M. A.; Bleu, T.; Hallmark, O. G.; Goetzl, E. J. Molecular cloning of the human Edg2 protein and its identification as a functional cellular receptor for lysophosphatidic acid. *Biochem. Biophys. Res. Commun.* **1997**, *231*, 619-622.

16. Erickson, J. R.; Wu, J. J.; Goddard, J. G.; Tigyi, G.; Kawanishi, K.; Tomei, L. D.; Kiefer, M. C. Edg-2/Vzg-1 couples to the yeast pheromone response pathway selectively in response to lysophosphatidic acid. *J. Biol. Chem.* **1998**, *273*, 1506-1510.

17. Fukushima, N.; Kimura, Y.; Chun, J. A single receptor encoded by *vzg-1* / *lp*$_{A1}$ / *edg-2* couples to G proteins and mediates multiple cellular responses to lysophosphatidic acid. *Proc. Natl. Acad. Sci. USA* **1998**, *95*, 6151-6156.

18. Contos, J. J. A.; Fukushima, N.; Weiner, J. A.; Kaushal, D.; Chun, J. Requirement for the lp$_{A1}$ lysophosphatidic acid receptor gene in normal suckling behavior. *Proc. Natl. Acad. Sci. USA* **2000**, *97*, 13384-13389.

19. Zondag, G. C.; Postma, F. R.; Etten, I. V.; Verlaan, I.; Moolenaar, W. H. Sphingosine 1-phosphate signalling through the G protein-coupled receptor Edg-1. *Biochem. J.* **1998**, *330*, 605-609.

20. Lee, M. J.; Van Brocklyn, J. R.; Thangada, S.; Liu, C. H.; Hand, A. R.; Menzeleev, R.; Spiegel, S.; Hla, T. Sphingosine 1-phosphate as a ligand for the G protein-coupled receptor EDG-1. *Science* **1998**, *279*, 1552-1555.

21. An, S.; Bleu, T.; Hallmark, O. G.; Goetzl, E. J. Characterization of a novel subtype of human G protein-coupled receptor for lysophosphatidic acid. *J. Biol. Chem.* **1998**, *273*, 7906-7910.

22. Contos, J. J. A.; Chun, J. Genomic characterization of the lysophosphatidic acid receptor gene, *lp*$_{A2}$/*Edg4*, and identification of a frameshift mutation in a previously characterized cDNA. *Genomics* **2000**, *64*, 155-169.

23. Bandoh, K.; Aoki, J.; Hosono, H.; Kobayashi, S.; Kobayashi, T.; Murakami-Murofushi, K.; Tsujimoto, M.; Arai, H.; Inoue, K. Molecular cloning and characterization of a novel human G protein-coupled receptor, EDG7, for lysophosphatidic acid. *J. Biol. Chem.* **1999**, *274*, 27776-27785.

24. Van Brocklyn, J. R.; Gräler, M. H.; Bernhardt, G.; Hobson, J. P.; Lipp, M.; Spiegel, S. Sphingosine 1-phosphate is a ligand for the G protein-coupled receptor EDG-6. *Blood* **2000**, *95*, 2624-2629.

25. Im, D.-S.; Heise, C. E.; Ancellin, N.; O'Dowd, B. F.; Shei, G.; Heavens, R. P.; Rigby, M. R.; Hla, T.; Mandala, S.; McAllister, G.; George, S. R.; Lynch, K. R. Characterization of a novel sphingosine 1-phosphate receptor, Edg-8. *J. Biol. Chem.* **2000**, *275*, 14281-14286.

26. Noguchi, K.; Ishii, S.; Shimizu, T. Identification of p2y9/GPR23 as a novel G protein-coupled receptor for lysophosphatidic acid, structurally distant from the Edg family. *J. Biol. Chem.* **2003**, *278*, 25600-25606.

27. Lee, C.-W.; Rivera, R.; Dubin, A. E.; Chun, J. LPA_4/GPR23 is a lysophosphatidic acid (LPA) receptor utilizing G_s-, G_q/G_i-mediated calcium signaling and $G_{12/13}$-mediated Rho activation. *J. Biol. Chem.* **2007**, *282*, 4310-4317.

28. Lee, C.-W.; Rivera, R.; Gardell, S.; Dubin, A. E.; Chun, J. GPR92 as a new $G_{12/13}$- and G_q-coupled lysophosphatidic acid receptor that increases cAMP, LPA_5. *J. Biol. Chem.* **2006**, *281*, 23589-23597.

29. Kotarsky, K.; Boketoft, Å.; Bristulf, J.; Nilsson, N. E.; Norberg, Å.; Hansson, S.; Owman, C.; Sillard, R.; Leeb-Lundberg, L. M.; Olde, B. Lysophosphatidic acid binds to and activates GPR92, a G protein-coupled receptor highly expressed in gastrointestinal lymphocytes. *J. Pharmacol. Exp. Ther.* **2006**, *318*, 619-628.

30. Pasternack, S. M.; von Kugelgen, I.; Al Aboud, K.; Lee, Y. A.; Ruschendorf, F.; Voss, K.; Hillmer, A. M.; Molderings, G. J.; Franz, T.; Ramirez, A.; Nurnberg, P.; Nothen, M. M.; Betz, R. C. G protein-coupled receptor P2Y5 and its ligand LPA are involved in maintenance of human hair growth. *Nat. Genet.* **2008**, *40*, 329-334.

31. Yanagida, K.; Masago, K.; Nakanishi, H.; Kihara, Y.; Hamano, F.; Tajima, Y.; Taguchi, R.; Shimizu, T.; Ishii, S. Identification and characterization of a novel lysophosphatidic acid receptor, p2y5/LPA_6. *J. Biol. Chem.* **2009**, *284*, 17731-17741.

32. Choi, J. W.; Herr, D. R.; Noguchi, K.; Yung, Y. C.; Lee, C.-W.; Mutoh, T.; Lin, M. E.; Teo, S. T.; Park, K. E.; Mosley, A. N.; Chun, J. LPA receptors: subtypes and biological actions. *Annu. Rev. Pharmacol. Toxicol.* **2010**, *50*, 157-186.

33. Yung, Y. C.; Stoddard, N. C.; Chun, J. LPA receptor signaling: pharmacology, physiology, and pathophysiology. *J. Lipid Res.* **2014**, *55*, 1192-1214.

34. Choi, J. W.; Chun, J. Lysophospholipids and their receptors in the central nervous system. *Biochim. Biophys. Acta Mol. Cell Biol. Lipids* **2013**, *1831*, 20-32.

35. Contos, J. J. A.; Ishii, I.; Fukushima, N.; Kingsbury, M. A.; Ye, X.; Kawamura, S.; Brown, J. H.; Chun, J. Characterization of *lpa*$_2$ (*Edg4*) and *lpa*$_1$/*lpa*$_2$ (*Edg2*/*Edg4*) lysophosphatidic acid receptor knockout mice: signaling deficits without obvious phenotypic abnormality attributable to *lpa*$_2$. *Mol. Cell. Biol.* **2002**, *22*, 6921-6929.

36. Christiano, A. M. Methods for P2RY5 mediated regulation of hair growth and mutants thereof. WO2009089380A2, **2009**.

37. Davenport, A. P.; Alexander, S. P.; Sharman, J. L.; Pawson, A. J.; Benson, H. E.; Monaghan, A. E.; Liew, W. C.; Mpamhanga, C. P.; Bonner, T. I.; Neubig, R. R.; Pin, J. P.; Spedding, M.; Harmar, A. J. International Union of Basic and Clinical Pharmacology. LXXXVIII. G protein-coupled receptor list: recommendations for new pairings with cognate ligands. *Pharmacol. Rev.* **2013**, *65*, 967-986.

38. Hanson, M. A.; Roth, C. B.; Jo, E.; Griffith, M. T.; Scott, F. L.; Reinhart, G.; Desale, H.; Clemons, B.; Cahalan, S. M.; Schuerer, S. C.; Sanna, M. G.; Han, G. W.; Kuhn, P.; Rosen, H.; Stevens, R. C. Crystal structure of a lipid G protein-coupled receptor. *Science* **2012**, *335*, 851-855.

39. O'Sullivan, C.; Dev, K. K. The structure and function of the $S1P_1$ receptor. *Trends Pharmacol. Sci.* **2013**, *34*, 401-412.

40. Parrill, A. L.; Tigyi, G. Integrating the puzzle pieces: the current atomistic picture of phospholipid G protein-coupled receptor interactions. *Biochim. Biophys. Acta Mol. Cell Biol. Lipids* **2013**, *1831*, 2-12.

41. Fujiwara, Y.; Sardar, V.; Tokumura, A.; Baker, D.; Murakami-Murofushi, K.; Parrill, A.; Tigyi, G. Identification of residues responsible for ligand recognition and regioisomeric selectivity of lysophosphatidic acid receptors expressed in mammalian cells. *J. Biol. Chem.* **2005**, *280*, 35038-35050.

42. Valentine, W. J.; Fells, J. I.; Perygin, D. H.; Mujahid, S.; Yokoyama, K.; Fujiwara, Y.; Tsukahara, R.; Van Brocklyn, J. R.; Parrill, A. L.; Tigyi, G. Subtype-specific residues involved in ligand activation of the endothelial differentiation gene family lysophosphatidic acid receptors. *J. Biol. Chem.* **2008**, *283*, 12175-12187.

43. Archbold, J. K.; Martin, J. L.; Sweet, M. J. Towards selective lysophospholipid GPCR modulators. *Trends Pharmacol. Sci.* **2014**, *35*, 219-226.

44. Pages, C.; Simon, M. F.; Valet, P.; Saulnier-Blache, J. S. Lysophosphatidic acid synthesis and release. *Prostaglandins Other Lipid Mediat.* **2001**, *64*, 1-10.

45. Tabchy, A.; Tigyi, G.; Mills, G. B. Location, location, location: a crystal-clear view of autotaxin saturating LPA receptors. *Nat. Struct. Mol. Biol.* **2011**, *18*, 117-118.

46. Albers, H. M.; Ovaa, H. Chemical evolution of autotaxin inhibitors. *Chem. Rev.* **2012**, *112*, 2593-2603.

47. van Meeteren, L. A.; Ruurs, P.; Stortelers, C.; Bouwman, P.; van Rooijen, M. A.; Pradere, J. P.; Pettit, T. R.; Wakelam, M. J.; Saulnier-Blache, J. S.; Mummery, C. L.; Moolenaar, W. H.; Jonkers, J. Autotaxin, a secreted lysophospholipase D, is essential for blood vessel formation during development. *Mol. Cell. Biol.* **2006**, *26*, 5015-5022.

48. Gierse J; Thorarensen A; Beltey K; Bradshaw-Pierce E; Cortes-Burgos L; Hall T; Johnston A; Murphy M; Nemirovskiy O; Ogawa S; Pegg L; Pelc M; Prinsen M; Schnute M; Wendling J; Wene S; Weinberg R; Wittwer A; Zweifel B; Masferrer, J. A novel autotaxin inhibitor reduces lysophosphatidic acid levels in plasma and the site of inflammation. *J. Pharmacol. Exp. Ther.* **2010**, *334*, 310-317.

49. Blaho, V. A.; Hla, T. Regulation of mammalian physiology, development, and disease by the sphingosine 1-phosphate and lysophosphatidic acid receptors. *Chem. Rev.* **2011**, *111*, 6299-6320.

50. Yung, Y. C.; Mutoh, T.; Lin, M. E.; Noguchi, K.; Rivera, R. R.; Choi, J. W.; Kingsbury, M. A.; Chun, J. Lysophosphatidic acid signaling may initiate fetal hydrocephalus. *Sci. Transl. Med.* **2011**, *3*, 99ra87.

51. Herr, K. J.; Herr, D. H.; Lee, C.-W.; Noguchi, K.; Chun, J. Stereotyped fetal brain disorganization is induced by hypoxia and requires lysophosphatidic acid receptor 1 (LPA_1) signaling. *Proc. Natl. Acad. Sci. USA* **2011**, *108*, 15444-15449.

52. Anliker, B.; Choi, J. W.; Lin, M. E.; Gardell, S. E.; Rivera, R. R.; Kennedy, G.; Chun, J. Lysophosphatidic acid (LPA) and its receptor, LPA_1, influence embryonic Schwann cell migration, myelination, and cell-to-axon segregation. *Glia* **2013**, *61*, 2009-2022.

53. Ueda, H.; Matsunaga, H.; Olaposi, O. I.; Nagai, J. Lysophosphatidic acid: chemical signature of neuropathic pain. *Biochim. Biophys. Acta Mol. Cell Biol. Lipids* **2013**, *1831*, 61-73.

54. Lin, M. E.; Rivera, R. R.; Chun, J. Targeted deletion of LPA_5 identifies novel roles for lysophosphatidic acid signaling in development of neuropathic pain. *J. Biol. Chem.* **2012**, *287*, 17608-17617.

55. Schober, A.; Siess, W. Lysophosphatidic acid in atherosclerotic diseases. *Br. J. Pharmacol.* **2012**, *167*, 465-482.

56. Sevastou, I.; Kaffe, E.; Mouratis, M. A.; Aidinis, V. Lysoglycerophospholipids in chronic inflammatory disorders: the PLA_2/LPC and ATX/LPA axes. *Biochim. Biophys. Acta Mol. Cell Biol. Lipids* **2013**, *1831*, 42-60.

57. Budd, D. C.; Qian, Y. Development of lysophosphatidic acid pathway modulators as therapies for fibrosis. *Future Med. Chem.* **2013**, *5*, 1935-1952.

58. Safety and efficacy of a lysophosphatidic acid receptor antagonist in idiopathic pulmonary fibrosis. http://clinicaltrials.gov/ct2/show/NCT01766817?term=lysophosphatidic+acid&rank=2.

59. Angion Biomedica Pipeline. http://angion.com/products.asp.

60. Miyabe, Y.; Miyabe, C.; Iwai, Y.; Takayasu, A.; Fukuda, S.; Yokoyama, W.; Nagai, J.; Jona, M.; Tokuhara, Y.; Ohkawa, R.; Albers, H. M.; Ovaa, H.; Aoki, J.; Chun, J.; Yatomi, Y.; Ueda, H.; Miyasaka, M.; Miyasaka, N.; Nanki, T. Necessity of lysophosphatidic acid receptor 1 for development of arthritis. *Arthritis Rheum.* **2013**, *65*, 2037-2047.

61. Orosa, B.; Garcia, S.; Martinez, P.; Gonzalez, A.; Gomez-Reino, J. J.; Conde, C. Lysophosphatidic acid receptor inhibition as a new multipronged treatment for rheumatoid arthritis. *Ann. Rheum. Dis.* **2014**, *73*, 298-305.

62. Rancoule, C.; Dusaulcy, R.; Treguer, K.; Gres, S.; Attane, C.; Saulnier-Blache, J. S. Involvement of autotaxin/lysophosphatidic acid signaling in obesity and impaired glucose homeostasis. *Biochimie* **2014**, *96*, 140-143.

63. Gotoh, M.; Fujiwara, Y.; Yue, J.; Liu, J.; Lee, S.; Fells, J.; Uchiyama, A.; Murakami-Murofushi, K.; Kennel, S.; Wall, J.; Patil, R.; Gupte, R.; Balazs, L.; Miller, D. D.; Tigyi, G. J. Controlling cancer through the autotaxin-lysophosphatidic acid receptor axis. *Biochem. Soc. Trans.* **2012**, *40*, 31-36.

64. Brinkmann, V.; Billich, A.; Baumruker, T.; Heining, P.; Schmouder, R.; Francis, G.; Aradhye, S.; Burtin, P. Fingolimod (FTY720): discovery and development of an oral drug to treat multiple sclerosis. *Nat. Rev. Drug Discov.* **2010**, *9*, 883-897.

65. Absorption, distribution, metabolism and excretion (ADME) Study of BMS-986020. http://clinicaltrials.gov/ct2/show/NCT02068053?term=lysophosphatidic+acid&rank=4.

66. Proof of biological activity of SAR100842 in systemic sclerosis. http://clinicaltrials.gov/ct2/show/NCT01651143?term=lysophosphatidic+acid&rank=6.

67. Sugiura, T.; Tokumura, A.; Gregory, L.; Nouchi, T.; Weintraub, S. T.; Hanahan, D. J. Biochemical characterization of the interaction of lipid phosphoric acids with human platelets: comparison with platelet activating factor. *Arch. Biochem. Biophys.* **1994**, *311*, 358-368.

68. Lynch, K. R.; Hopper, D. W.; Carlisle, S. J.; Catalano, J. G.; Zhang, M.; MacDonald, T. L. Structure/activity relationships in lysophosphatidic acid: the 2-hydroxyl moiety. *Mol. Pharmacol.* **1997**, *52*, 75-81.

69. Heise, C. E.; Santos, W. L.; Schreihofer, A. M.; Heasley, B. H.; Mukhin, Y. V.; Macdonald, T. L.; Lynch, K. R. Activity of 2-substituted lysophosphatidic acid (LPA) analogs at LPA receptors: discovery of a LPA_1/LPA_3 receptor antagonist. *Mol. Pharmacol.* **2001**, *60*, 1173-1180.

70. Santos, W. L.; Heasley, B. H.; Jarosz, R.; Carter, K. M.; Lynch, K. R.; Macdonald, T. L. Synthesis and biological evaluation of phosphonic and thiophosphoric acid derivatives of lysophosphatidic acid. *Bioorg. Med. Chem. Lett.* **2004**, *14*, 3473-3476.

71. Xu, Y.; Aoki, J.; Shimizu, K.; Umezu-Goto, M.; Hama, K.; Takanezawa, Y.; Yu, S.; Mills, G. B.; Arai, H.; Qian, L.; Prestwich, G. D. Structure-activity relationships of fluorinated lysophosphatidic acid analogues. *J. Med. Chem.* **2005**, *48*, 3319-3327.

72. Hasegawa, Y.; Erickson, J. R.; Goddard, G. J.; Yu, S.; Liu, S.; Cheng, K. W.; Eder, A.; Bandoh, K.; Aoki, J.; Jarosz, R.; Schrier, A. D.; Lynch, K. R.; Mills, G. B.; Fang, X. Identification of a phosphothionate analogue of lysophosphatidic acid (LPA) as a selective agonist of the LPA_3 receptor. *J. Biol. Chem.* **2003**, *278*, 11962-11969.

73. Qian, L.; Xu, Y.; Simper, T.; Jiang, G.; Aoki, J.; Umezu-Goto, M.; Arai, H.; Yu, S.; Mills, G. B.; Tsukahara, R.; Makarova, N.; Fujiwara, Y.; Tigyi, G.; Prestwich, G. D. Phosphorothioate analogues of alkyl lysophosphatidic acid as LPA_3 receptor-selective agonists. *ChemMedChem* **2006**, *1*, 376-383.

74. Jiang, G.; Inoue, A.; Aoki, J.; Prestwich, G. D. Phosphorothioate analogs of *sn*-2 radyl lysophosphatidic acid (LPA): metabolically stabilized LPA receptor agonists. *Bioorg. Med. Chem. Lett.* **2013**, *23*, 1865-1869.

75. Xu, Y.; Prestwich, G. D. Concise synthesis of acyl migration-blocked 1,1-difluorinated analogues of lysophosphatidic acid. *J. Org. Chem.* **2002**, *67*, 7158-7161.

76. Xu, Y.; Qian, L.; Pontsler, A. V.; McIntyre, T. M.; Prestwich, G. D. Synthesis of difluoromethyl substituted lysophosphatidic acid analogues. *Tetrahedron* **2004**, *60*, 43-49.

77. Xu, Y.; Qian, L.; Prestwich, G. D. Synthesis of alpha-fluorinated phosphonates from alpha-fluorovinylphosphonates: a new route to analogues of lysophosphatidic acid. *Org. Lett.* **2003**, *5*, 2267-2270.

78. Xu, Y.; Jiang, G.; Tsukahara, R.; Fujiwara, Y.; Tigyi, G.; Prestwich, G. D. Phosphonothioate and fluoromethylene phosphonate analogues of cyclic phosphatidic acid: novel antagonists of lysophosphatidic acid receptors. *J. Med. Chem.* **2006**, *49*, 5309-5315.

79. Gududuru, V.; Zeng, K.; Tsukahara, R.; Makarova, N.; Fujiwara, Y.; Pigg, K. R.; Baker, D. L.; Tigyi, G.; Miller, D. D. Identification of Darmstoff analogs as selective agonists and antagonists of lysophosphatidic acid receptors. *Bioorg. Med. Chem. Lett.* **2006**, *16*, 451-456.

80. Gan, L.; Xue, J. X.; Li, X.; Liu, D. S.; Ge, Y.; Ni, P. Y.; Deng, L.; Lu, Y.; Jiang, W. Blockade of lysophosphatidic acid receptors $LPAR_{1/3}$ ameliorates lung fibrosis induced by irradiation. *Biochem. Biophys. Res. Commun.* **2011**, *409*, 7-13.

81. Heasley, B. H.; Jarosz, R.; Lynch, K. R.; Macdonald, T. L. Initial structure-activity relationships of lysophosphatidic acid receptor antagonists: discovery of a high-affinity LPA_1/LPA_3 receptor antagonist. *Bioorg. Med. Chem. Lett.* **2004**, *14*, 2735-2740.

82. East, J. E.; Carter, K. M.; Kennedy, P. C.; Schulte, N. A.; Toews, M. L.; Lynch, K. R.; Macdonald, T. L. Development of a phosphatase-resistant, L-tyrosine derived LPA_1/LPA_3 dual antagonist. *Med. Chem. Commun* **2011**, *2*, 325-330.

83. Jiang, G.; Xu, Y.; Fujiwara, Y.; Tsukahara, T.; Tsukahara, R.; Gajewiak, J.; Tigyi, G.; Prestwich, G. D. Alpha-substituted phosphonate analogues of lysophosphatidic acid (LPA) selectively inhibit production and action of LPA. *ChemMedChem* **2007**, *2*, 679-690.

84. Xu, X.; Prestwich, G. D. Inhibition of tumor growth and angiogenesis by a lysophosphatidic acid antagonist in an engineered three-dimensional lung cancer xenograft model. *Cancer* **2010**, *116*, 1739-1750.

85. Nikitopoulou, I.; Kaffe, E.; Sevastou, I.; Sirioti, I.; Samiotaki, M.; Madan, D.; Prestwich, G. D.; Aidinis, V. A metabolically-stabilized phosphonate analog of lysophosphatidic acid attenuates collagen-induced arthritis. *PLoS ONE* **2013**, *8*, e70941.

86. Ohta, H.; Sato, K.; Murata, N.; Damirin, A.; Malchinkhuu, E.; Kon, J.; Kimura, T.; Tobo, M.; Yamazaki, Y.; Watanabe, T.; Yagi, M.; Sato, M.; Suzuki, R.; Murooka, H.; Sakai, T.; Nishitoba, T.; Im, D. S.; Nochi, H.; Tamoto, K.; Tomura, H.; Okajima, F. Ki16425, a subtype-selective antagonist for EDG-family lysophosphatidic acid receptors. *Mol. Pharmacol.* **2003**, *64*, 994-1005.

87. Swaney, J. S.; Chapman, C.; Correa, L. D.; Stebbins, K. J.; Bundey, R. A.; Prodanovich, P. C.; Fagan, P.; Baccei, C. S.; Santini, A. M.; Hutchinson, J. H.; Seiders, T. J.; Parr, T. A.; Prasit, P.; Evans, J. F.; Lorrain, D. S. A novel, orally active LPA_1 receptor antagonist inhibits lung fibrosis in the mouse bleomycin model. *Br. J. Pharmacol.* **2010**, *160*, 1699-1713.

88. Castelino, F. V.; Seiders, J.; Bain, G.; Brooks, S. F.; King, C. D.; Swaney, J. S.; Lorrain, D. S.; Chun, J.; Luster, A. D.; Tager, A. M. Amelioration of dermal fibrosis by genetic deletion or pharmacologic antagonism of lysophosphatidic acid receptor 1 in a mouse model of scleroderma. *Arthritis Rheum.* **2011**, *63*, 1405-1415.

89. Swaney, J. S.; Chapman, C.; Correa, L. D.; Stebbins, K. J.; Broadhead, A. R.; Bain, G.; Santini, A. M.; Darlington, J.; King, C. D.; Baccei, C. S.; Lee, C.; Parr, T. A.; Roppe, J. R.; Seiders, T. J.; Ziff, J.; Prasit, P.; Hutchinson, J. H.; Evans, J. F.; Lorrain, D. S. Pharmacokinetic and pharmacodynamic characterization of an oral lysophosphatidic acid type 1 receptor-selective antagonist. *J. Pharmacol. Exp. Ther.* **2011**, *336*, 693-700.

90. Qian, Y.; Hamilton, M.; Sidduri, A.; Gabriel, S.; Ren, Y.; Peng, R.; Kondru, R.; Narayanan, A.; Truitt, T.; Hamid, R.; Chen, Y.; Zhang, L.; Fretland, A. J.; Sanchez, R. A.; Chang, K. C.; Lucas, M.; Schoenfeld, R. C.; Laine, D.; Fuentes, M. E.; Stevenson, C. S.; Budd, D. C. Discovery of highly selective and orally active lysophosphatidic acid receptor-1 antagonists with potent activity on human lung fibroblasts. *J. Med. Chem.* **2012**, *55*, 7920-7939.

91. Buckman, B. O.; Nicholas, J. B.; Emayan, K.; Seiwert, S. D. Lysophosphatidic acid receptor antagonists. WO2013025733, **2013**.

92. Kawaminami, E.; Takahashi, T.; Kanayama, T.; Kaizawa, H. Substituted amide compound. WO2011037192, **2011**.

93. Kawaminami, E.; Takahashi, T.; Kanayama, T.; Sakamoto, K. Substituted amide compound. WO2012039460, **2012**.

94. Tigyi, G.; Parrill, A. L. Molecular mechanisms of lysophosphatidic acid action. *Prog. Lipid Res.* **2003**, *42*, 498-526.

95. Burke, T. R.; Lee, K. Phosphotyrosyl mimetics in the development of signal transduction inhibitors. *Acc. Chem. Res.* **2003**, *36*, 426-433.

96. Meanwell, N. A. Synopsis of some recent tactical application of bioisosteres in drug design. *J. Med. Chem.* **2011**, *54*, 2529-2591.

97. Martín-Couce, L.; Martín-Fontecha, M.; Capolicchio, S.; López-Rodríguez, M. L.; Ortega-Gutiérrez, S. Development of endocannabinoid-based chemical probes for the study of cannabinoid receptors. *J. Med. Chem.* **2011**, *54*, 5265-5269.

98. An, S.; Bleu, T.; Zheng, Y.; Goetzl, E. J. Recombinant human G protein-coupled lysophosphatidic acid receptors mediate intracellular calcium mobilization. *Mol. Pharmacol.* **1998**, *54*, 881-888.

99. Hopper, D. W.; Ragan, S. P.; Hooks, S. B.; Lynch, K. R.; Macdonald, T. L. Structure-activity relationships of lysophosphatidic acid: conformationally restricted backbone mimetics. *J. Med. Chem.* **1999**, *42*, 963-970.

100. Eckhardt, M.; Fu, G. C. The first applications of carbene ligands in cross-couplings of alkyl electrophiles: Sonogashira reactions of unactivated alkyl bromides and iodides. *J. Am. Chem. Soc.* **2003**, *125*, 13642-13643.

101. Brown, C. A.; Ahuja, V. K. Catalytic hydrogenation. VI. Reaction of sodium borohydride with nickel salts in ethanol solution. P-2 Nickel, a highly convenient, new, selective hydrogenation catalyst with great sensitivity to substrate structure. *J. Org. Chem.* **1973**, *38*, 2226-2230.

102. Orcajo-Rincon, A. L.; Ortega-Gutierrez, S.; Serrano, P.; Torrecillas, I. R.; Wuthrich, K.; Campillo, M.; Pardo, L.; Viso, A.; Benhamu, B.; Lopez-Rodriguez, M. L. Development of non-peptide ligands of growth factor receptor-bound protein 2-SRC homology 2 domain using molecular modeling and NMR spectroscopy. *J. Med. Chem.* **2011**, *54*, 1096-1100.

103. Cisneros, J. A.; Bjorklund, E.; Gonzalez-Gil, I.; Hu, Y.; Canales, A.; Medrano, F. J.; Romero, A.; Ortega-Gutierrez, S.; Fowler, C. J.; Lopez-Rodriguez, M. L. Structure-activity relationship of a new series of reversible dual monoacylglycerol lipase/fatty acid amide hydrolase inhibitors. *J. Med. Chem.* **2012**, *55*, 824-836.

104. Durgam, G. G.; Virag, T.; Walker, M. D.; Tsukahara, R.; Yasuda, S.; Liliom, K.; van Meeteren, L. A.; Moolenaar, W. H.; Wilke, N.; Siess, W.; Tigyi, G.; Miller, D. D. Synthesis, structure-activity relationships, and biological evaluation of fatty alcohol phosphates as lysophosphatidic acid receptor ligands, activators of PPARgamma, and inhibitors of autotaxin. *J. Med. Chem.* **2005**, *48*, 4919-4930.

105. Plueckthun, A.; Dennis, E. A. Acyl and phosphoryl migration in lysophospholipids: importance in phospholipid synthesis and phospholipase specificity. *Biochemistry* **1982**, *21*, 1743-1750.

106. Fukushima, N. Lysophosphatidic acid influences the morphology and motility of young, postmitotic cortical neurons. *Mol. Cell. Neurosci.* **2002**, *20*, 271-282.

107. Ferguson, S. S. G. Evolving concepts in G Protein-Coupled Receptor endocytosis: the role in receptor desensitization and signaling. *Pharmacol. Rev.* **2001**, *53*, 1-24.

108. Hadida-Ruah, S.; Hamilton, M.; Miller, M.; Grootenhuis, P. D. J.; Bear, B.; McCartney, J.; Zhou, J.; Van Goor, F. Modulators of ATP-binding cassette transporters. US2008019915, **2008**.

109. Savariar, E. N.; Aathimanikandan, S. V.; Thayumanavan, S. Supramolecular assemblies from amphiphilic homopolymers: testing the scope. *J. Am. Chem. Soc.* **2006**, *128*, 16224-16230.

110. Iwasaki, T.; Higashikawa, K.; Reddy, V. P.; Ho, W. W. S.; Fujimoto, Y.; Fukase, K.; Terao, J.; Kuniyasu, H.; Kambe, N. Nickel·butadiene catalytic system for the cross-coupling of bromoalkanoic acids with alkyl grignard reagents: a practical and versatile method for preparing fatty acids. *Chemistry – A European Journal* **2013**, *19*, 2956-2960.

111. Duffy, P. E.; Quinn, S. M.; Roche, H. M.; Evans, P. Synthesis of *trans*-vaccenic acid and *cis*-9-*trans*-11-conjugated linoleic acid. *Tetrahedron* **2006**, *62*, 4838-4843.

112. Novotný, J.; Pospěchová, K.; Hrabálek, A.; Čáp, R.; Vávrová, K. Synthesis of fluorescent C24-ceramide: evidence for acyl chain length dependent differences in penetration of exogenous NBD-ceramides into human skin. *Bioorg. Med. Chem. Lett.* **2009**, *19*, 6975-6977.

113. Jeon, O.-Y.; Carreira, E. M. Differential interaction of an AmB analogue and ergosterol in enantiomeric membranes. *Org. Lett.* **2010**, *12*, 1772-1775.